

CORRELATIONS BETWEEN GROUND MOTION INTENSITY  
MEASURES AND STRUCTURAL RESPONSE PARAMETERS  
THROUGH NONLINEAR DYNAMIC ANALYSES

by

Ufuk Hancılar

B.S., Civil Engineering, İstanbul University, 1998

M.S., Earthquake Engineering, Boğaziçi University, 2002

Submitted to the Kandilli Observatory and  
Earthquake Research Institute in partial fulfillment of  
the requirements for the degree of  
Doctor of Philosophy

Graduate Program in Earthquake Engineering  
Boğaziçi University

2009

## ACKNOWLEDGEMENTS

I would like to express my deepest gratitude to my thesis supervisor Professor Eser Durukal for her enormous support and guidance whenever I need through my entire PhD studies. I am also grateful to Professor Mustafa Erdik for his invaluable support and guidance.

I would like to thank to Professor Erdal Şafak and Professor Nuray Aydınoglu for their kind support and valuable suggestions and comments on my work. I also would like to express my thanks to Professor Oguz Ozel for motivating and encouraging me.

I thank my friends, in Earthquake Engineering Department, Dr Can Zülfikar, Dr Karin Şeşetyan, Ms Mine B. Demircioğlu, Dr Göktürk Önem, Dr Cüneyt Tüzün, Ms Gökçe Tönük, Mr Yavuz Kaya and Mr Yaver Kamer for their invaluable friendship and simply for everything.

I also would like to express my thanks to Professor Stephen Mahin and Dr Yousef Bozorgnia for inviting me and allowing me to join in ground motion selection and modification (GMSM) workgroup of Pacific Earthquake Engineering Research (PEER) Center during the time that I spent at University of California, Berkeley. I am grateful to GMSM workgroup members, Dr Erol Kalkan, Professor Curt Haselton, Professor Jack Baker, Dr Nicolas Luco, Dr Jenny Watson-Lamprey, for sharing their knowledge, experience and studies. I am also very grateful to Dr Silvia Mazzoni for her support about OpenSees.

It is gratefully acknowledged that this thesis study was supported by *Bogazici University Research Fund* under Project No. 06T101D.

Finally a special “thank you” goes to my family.

## ABSTRACT

### **CORRELATIONS BETWEEN GROUND MOTION INTENSITY MEASURES AND STRUCTURAL RESPONSE PARAMETERS THROUGH NONLINEAR DYNAMIC ANALYSES**

The assessment of the structural response via nonlinear dynamic analyses requires some characterization of the correlations between ground motion intensity measures and structural response parameters. It gains more significance to understand which properties of a recorded ground motion are most strongly related to the response caused in the structure. The primary objective of this thesis is to investigate the correlations between ground motion intensity measures and structural response parameters through nonlinear dynamic analyses of multi-degree-of-freedom (MDOF) structures under real earthquake recordings.

For this purpose, a parametric investigation on reinforced concrete buildings is carried out. The building groups are five-, ten-, fifteen- and twenty-story reinforced concrete, code-conforming, regular moment-resisting frames. They are designed for different strength reduction factors,  $R=2, 4$  and  $6$ . Hence there are 12 buildings under consideration in total. Finite element modeling of the buildings is achieved by using line elements in *OpenSees* v2.0 (UC Berkeley, 2008) environment. The line elements are composed of fiber sections and utilize the distributed plasticity approach for columns and concentrated plasticity approach for beams.

Totally 8,808 nonlinear time-domain analyses are performed. The input ground motion dataset consist of 734 horizontal components of earthquake accelerograms whose magnitudes ( $M_w$ ) and source-to-site distances ( $R_{JB}$ ) vary between 5.5-7.62 and 0-100 km respectively. The recordings come from different soil conditions with the *NEHRP* site classes (B, C, D and E) based on the  $V_{s,30}$  values and faulting mechanisms (strike-slip, normal, reverse, reverse oblique and normal oblique). As the ground motion intensity

measures (IM), peak ground acceleration (*PGA*), peak ground velocity (*PGV*), peak ground displacement (*PGD*), spectral acceleration ( $S_a(T_I)$ ), spectral velocity ( $S_v(T_I)$ ) spectral displacement ( $S_d(T_I)$ ), Arias intensity (*AI*) and cumulative absolute velocity (*CAV*) are considered. The relative joint (one joint at each floor) accelerations and displacements as well as the plastic end rotations of beams at each floor are tracked in the nonlinear dynamic analyses. As the engineering demand parameters (EDP), maximum floor displacements (*MFD*), maximum inter-story drift ratios (*MIDR*), maximum plastic end rotations of beams (*MPR*) and maximum floor accelerations (*MFA*) are considered.

The best correlations between ground motion and structural response parameters are provided and the functions to predict the structural response via ground motion intensity measure are computed. This is done by non-parametric statistical approach, i.e. regression analysis. Then a parametric statistical evaluation procedure based on a log-normal distribution assumption is applied to the best correlations and median prediction functions are obtained. In order to make a cross-check, the prediction functions resulting from non-parametric evaluation are compared to the median prediction functions obtained from the parametric method. In addition, examples of three-dimensional structural response surfaces are provided in order to utilize in damage assessment of the buildings with similar characteristics.

The findings and observations should prudently be utilized in selection and scaling/modification of ground motion recordings as input for the nonlinear dynamic analyses. The provided correlations might also help in developing better intensity measures that sufficiently and efficiently incorporate the seismic hazard at the site and that also reduce the scatter in the nonlinear structural response when using a smaller number of records.

## ÖZET

### **YER HAREKETİ ŞİDDET ÖLÇÜTLERİ VE YAPISAL DAVRANIŞ PARAMETRELERİ ARASINDAKİ KORELASYONLARIN DOĞRUSAL OLMAYAN DİNAMİK ANALİZLER YARDIMIYLA BULUNMASI**

Yapısal davranışın doğrusal olmayan dinamik analizler ile değerlendirilmesi, yer hareketi şiddet ölçütleri ve yapısal davranış parametreleri arasındaki korelasyonların bir ölçüde karakterize edilmesini gerektirir. Kaydedilmiş bir yer hareketinin en çok hangi özellikleri ile yapıda meydana getirdiği tepki arasında ilişki olduğunun anlaşılması gittikçe önem kazanmaktadır. Bu tezin temel amacı, yer hareketi şiddet ölçütleri ve yapısal davranış parametreleri arasındaki korelasyonların, çok serbestlik dereceli yapıların gerçek deprem kayıtları altında doğrusal olmayan dinamik analizleri yardımıyla araştırılmasıdır.

Bu amaçla, betonarme binalar üzerinde parametrik bir araştırma gerçekleştirilir. Seçilen bina grupları beş, on, on beş ve yirmi katlı depreme dayanıklı olarak tasarlanmış, moment aktaran düzenli çerçevelerdir. Bu binalar,  $R=2, 4$  ve  $6$  olmak üzere farklı dayanım azaltma katsayılarına göre tasarlanmışlardır. Sonuçta on iki bina üzerinde çalışılmıştır. Binaların sonlu elemanlar ile modellenmesi *OpenSees v2.0* yazılım ortamında çubuk elemanlar kullanılarak yapılır. Bu çubuk elemanlar liflerden oluşur ve kolonlar için dağıtılmış plastisite yaklaşımı ve kirişler için konsantre plastisite yaklaşımından yararlanır.

Zaman-tanım alanında toplam 8.808 tane doğrusal olmayan analiz gerçekleştirilir. Kullanılan yer hareketi veri seti, manyitüdüleri 5,5 ila 7,62 arasında ve kaynak-saha uzaklıkları 0 ila 100 km arasında değişen depremlerin ivme kayıtlarının 734 tane yatay bileşenini içermektedir. Yer hareketi kayıtları, kayma dalgası yayılım hızına dayanan NEHRP zemin sınıflandırmasına göre farklı zeminlerden (B, C, D ve E gibi) ve farklı faylanma mekanizmalarından (doğrultu atımlı, yanal atımlı, ters atımlı gibi) gelmektedir.

Yer hareketi şiddet ölçütleri olarak en büyük yer ivmesi, en büyük yer hızı, en büyük yer deformasyonu, spektral ivme, spektral hız, spektral yerdeğiştirme, Arias şiddeti ve yığışımli mutlak hız gözönünde bulundurulmaktadır. Binaların her bir katında seçilen düğüm noktalarının görelivme ve yer değıştirmeleri ile her kattaki orta açıklık kirişlerinin uç plastik dönmeleri doğrusal olmayan dinamik analizler sırasında kaydedilir. Yapısal davranış (mühendislik talep) parametreleri olarak maksimum kat yerdeğiştirmeleri, katlar arası maksimum göreliv ötelenme oranları, maksimum kiriş uç plastik dönmeleri ve maksimum kat ivmeleri gözönünde bulundurulmaktadır.

Doğrusal olmayan dinamik analiz sonuçlarına göre, yer hareketi şiddet ölçütleri ve yapısal davranış parametreleri arasındaki en iyi korelasyonlar ve yapısal davranışı yer hareketi şiddet ölçütüne bağılı olarak tahmin etmeyi sağılayan fonksiyonlar hesaplanır. Bu iş, parametrik olmayan istatistiksel yaklaşım ile yani regresyon analizleri ile yapılır. Daha sonra, bulunan en iyi korelasyonlara log-normal dağılım esasına dayanan parametrik istatistiksel yaklaşım uygulanır ve medyan yapısal davranış tahmin fonksiyonları elde edilir. Parametrik yaklaşımla elde edilen tahmin fonksiyonları ile parametrik olmayan yaklaşımla elde edilen medyan tahmin fonksiyonları birbirleriyle kıyaslanarak kontrol edilirler. Bunlara ek olarak, bu çalışmada kullanılan binalara benzer yapıların hasar değlendirmelerinde yararlanmak üzere, üç boyutlu yapısal davranış yüzeyle de sunulmaktadır.

Bu çalışmada elde edilen bulgular ve gözlemler, doğrusal olmayan dinamik analizlerde kullanılacak yer hareketlerinin seçiminde ve oranlanmasında ihtiyatlı olarak kullanılabilir. Sunulan korelasyonlar, sözkonusu bir alandaki sismik tehlikenin yeterli bir şekilde ortaya konmasını sağılayacak daha iyi yer hareketi şiddet ölçütlerinin geliştirilmesinde ve ayrıca, daha az sayıda yer hareketi kullanıldığında ortaya çıkabilecek doğrusal olmayan yapısal davranış sonuçlarındaki saçılımlın azaltılmasında yararlanılabilir.

## TABLE OF CONTENTS

ACKNOWLEDGEMENTS .....	iii
ABSTRACT .....	iv
ÖZET .....	vi
LIST OF FIGURES .....	x
LIST OF TABLES .....	xviii
LIST OF SYMBOLS/ABBREVIATIONS .....	xx
1. INTRODUCTION .....	1
1.1. Objectives and Outline of the Thesis .....	2
2. ENGINEERING CHARACTERIZATION OF STRONG GROUND MOTION AND STRUCTURAL RESPONSE: INTENSITY MEASURES (IMs) and ENGINEERING DEMAND PARAMETERS (EDPs) .....	4
2.1. Introduction .....	4
2.2. Strong Ground Motion Records .....	4
2.2.1. Real Records .....	4
2.2.2. Artificial Records .....	5
2.2.3. Simulated (Synthetic) Records .....	5
2.3. Time Domain Parameters of Strong Ground Motions .....	6
2.4. Spectral Parameters of Strong Ground Motions .....	7
2.5. Energy-Related Parameters of Strong Ground Motions .....	9
2.6. Structural Response: Engineering Demand Parameters (EDP) .....	9
3. STRUCTURAL SYSTEMS, ANALYTICAL MODELING AND NONLINEAR DYNAMIC ANALYSES .....	11
3.1. Introduction .....	11
3.2. Generic Buildings Used in the Study .....	11
3.3. Analytical Modeling .....	15
3.4. Nonlinear Dynamic Analyses .....	22
3.4.1. Damping Modeling and Solution Algorithm .....	22
3.4.2. Input Ground Motions .....	23
3.4.3. Analyses Results .....	33

3.5. Effects of Magnitude, Source-to-Site Distance, Site Class and Faulting Mechanism on the Structural Response .....	60
4. CORRELATIONS BETWEEN GROUND MOTION INTENSITY MEASURES (IMs) and ENGINEERING DEMAND PARAMETERS (EDPs) .....	65
4.1. Introduction .....	65
4.2. Statistical Approaches Utilized.....	69
4.3. Regression on the Engineering Demand Parameters and Presentation of the Best Correlations .....	72
4.3.1. Maximum Floor Displacements – MFD .....	72
4.3.2. Maximum Inter-Story Drift Ratios – MIDR.....	73
4.3.3. Maximum Plastic Rotations – MPR.....	75
4.3.4. Maximum Floor Accelerations – MFA .....	76
4.3.5. Comparative Evaluation of Correlation Results and Prediction Functions for Engineering Demand Parameters.....	94
4.4. Probabilistic Evaluation of Engineering Demand Parameters .....	100
4.4.1. Comparison of Prediction Functions: Regression Predictions versus Probabilistic Predictions .....	101
4.4.2. Conditional Probabilistic Structural Response Surfaces .....	119
5. CONCLUSIONS .....	124
5.1. Summary of Findings.....	125
5.2. Future Research .....	126
REFERENCES.....	128
APPENDIX A: EXAMPLE OPENSEES SCRIPT FOR STRUCTURAL MODEL AND NONLINEAR DYNAMIC ANALYSIS .....	134



## LIST OF FIGURES

Figure 3.1.	5-, 10-, 15- and 20-story buildings .....	12
Figure 3.2.	5 per cent-damped elastic design spectrum constructed for ‘Seismic Zone 1’ and site class ‘Z3’ of Turkish Seismic Code-2007.....	14
Figure 3.3.	Concentrated plasticity at the end of beams by ‘ <i>beamWithHinges</i> ’ elements .....	15
Figure 3.4.	Modified Gauss-Radau integration adopted for concentrated plasticity .....	16
Figure 3.5.	Distributed plasticity for columns by ‘ <i>nonlinearBeamColumn</i> ’ elements .....	16
Figure 3.6.	Fiber discretization of a reinforced concrete section.....	17
Figure 3.7.	Hysteretic behavior of steel model w/o isotropic hardening (‘ <i>Steel02</i> ’ material, OpenSees v2.0 user command-language manual) .....	18
Figure 3.8.	Stress-strain model for the confined concrete (‘ <i>Concrete01</i> ’ material, OpenSees v2.0 user command-language manual).....	18
Figure 3.9.	Example moment-rotation hysteresis under PUL104 record of Northridge Earthquake for a 1 <sup>st</sup> story beam of 5-story buildings, R=2, R=4 and R=6 from top to bottom respectively.....	20
Figure 3.10.	Example moment-rotation hysteresis under PUL104 record of Northridge Earthquake for a 1 <sup>st</sup> story column of 10-story buildings, R=2, R=4 and R=6 from top to bottom respectively .....	21
Figure 3.11.	Variation of modal damping ratio with natural frequencies .....	23
Figure 3.12.	Variation of magnitudes, peak ground accelerations and peak ground velocities with Joyner-Boore distance from top to bottom, respectively ....	26

Figure 3.13.	Variation of peak ground displacements, Arias intensities and cumulative absolute velocities with Joyner-Boore distance from top to bottom, respectively.....	27
Figure 3.14.	Monitored joints (dark circles) and beams (solid lines) during the nonlinear dynamic analyses .....	33
Figure 3.15.	Peak floor displacements under Bin I records ( $M_w=5.5-5.99$ ).....	36
Figure 3.16.	Peak floor displacements under Bin II records ( $M_w=6.0-6.49$ ).....	37
Figure 3.17.	Peak floor displacements under Bin III records ( $M_w=6.5-6.99$ ) .....	38
Figure 3.18.	Peak floor displacements under Bin IV records ( $M_w=7.0-7.49$ ) .....	39
Figure 3.19.	Peak floor displacements under Bin V records ( $M_w > 7.5$ ).....	40
Figure 3.20.	Peak inter-story drift ratios under Bin I records ( $M_w=5.5-5.99$ ) .....	43
Figure 3.21.	Peak inter-story drift ratios under Bin II records ( $M_w=6.0-6.49$ ).....	44
Figure 3.22.	Peak inter-story drift ratios under Bin III records ( $M_w=6.5-6.99$ ) .....	45
Figure 3.23.	Peak inter-story drift ratios under Bin IV records ( $M_w=7.0-7.49$ ) .....	46
Figure 3.24.	Peak inter-story drift ratios under Bin V records ( $M_w > 7.5$ ).....	47
Figure 3.25.	Peak plastic rotations of mid-beams under Bin I records ( $M_w=5.5-5.99$ ) ...	49
Figure 3.26.	Peak plastic rotations of mid-beams under Bin II records ( $M_w=6.0-6.49$ ) .....	50
Figure 3.27.	Peak plastic rotations of mid-beams under Bin III records ( $M_w=6.5-6.99$ ) .....	51
Figure 3.28.	Peak plastic rotations of mid-beams under Bin IV records ( $M_w=7.0-7.49$ ) .....	52
Figure 3.29.	Peak plastic rotations of mid-beams under Bin V records ( $M_w > 7.5$ ) .....	53

Figure 3.30.	Peak floor accelerations under Bin I records ( $M_w=5.5-5.99$ ).....	55
Figure 3.31.	Peak floor accelerations under Bin II records ( $M_w=6.0-6.49$ ) .....	56
Figure 3.32.	Peak floor accelerations under Bin III records ( $M_w=6.5-6.99$ ) .....	57
Figure 3.33.	Peak floor accelerations under Bin IV records ( $M_w=7.0-7.49$ ).....	58
Figure 3.34.	Peak floor accelerations under Bin V records ( $M_w > 7.5$ ) .....	59
Figure 3.35.	Variation of MFD with distance.....	61
Figure 3.36.	Variation of MIDR with distance .....	62
Figure 3.37.	Variation of MPR with distance .....	63
Figure 3.38.	Variation of MFA with distance.....	64
Figure 4.1.	Combination of the lognormal probability distribution function of the maximum inter-story drift ratios with the ground motion hazard curve (After Cornell <i>et al.</i> , 2002).....	68
Figure 4.2.	Regression on structural response results for a given IM level (After Baker, 2007) .....	69
Figure 4.3.	A set of spectral acceleration and demand data pairs and the probabilistic model fit to these data points (After Jalayer and Cornell, 2003) .....	70
Figure 4.4.	Scatter plot of MFD vs. $S_a(T_1)$ resulting from each record bin, for the 5-story buildings ( $R=2$ , $R=4$ and $R=6$ from top to bottom respectively) and the best-fits obtained from the regression of the entire data sets.....	78
Figure 4.5.	Scatter plot of MIDR vs. $S_a(T_1)$ resulting from each record bin, for the 5-story buildings ( $R=2$ , $R=4$ and $R=6$ from top to bottom respectively) and the best-fits obtained from the regression of the entire data sets.....	79

- Figure 4.6. Scatter plot of MPR vs.  $S_a(T_1)$  resulting from each record bin, for the 5-story buildings ( $R=2$ ,  $R=4$  and  $R=6$  from top to bottom respectively) and the best-fits obtained from the regression of the entire data sets..... 80
- Figure 4.7. Scatter plot of MFA vs. PGA resulting from each record bin, for the 5-story buildings ( $R=2$ ,  $R=4$  and  $R=6$  from top to bottom respectively) and the best-fits obtained from the regression of the entire data sets..... 81
- Figure 4.8. Scatter plot of MFD vs.  $S_a(T_1)$  resulting from each record bin, for the 10-story buildings ( $R=2$ ,  $R=4$  and  $R=6$  from top to bottom respectively) and the best-fits obtained from the regression of the entire data sets..... 82
- Figure 4.9. Scatter plot of MIDR vs.  $S_a(T_1)$  resulting from each record bin, for the 10-story buildings ( $R=2$ ,  $R=4$  and  $R=6$  from top to bottom respectively) and the best-fits obtained from the regression of the entire data sets..... 83
- Figure 4.10. Scatter plot of MPR vs.  $S_a(T_1)$  resulting from each record bin, for the 10-story buildings ( $R=2$ ,  $R=4$  and  $R=6$  from top to bottom respectively) and the best-fits obtained from the regression of the entire data sets..... 84
- Figure 4.11. Scatter plot of MFA vs. AI resulting from each record bin, for the 10-story buildings ( $R=2$ ,  $R=4$  and  $R=6$  from top to bottom respectively) and the best-fits obtained from the regression of the entire data sets..... 85
- Figure 4.12. Scatter plot of MFD vs.  $S_a(T_1)$  resulting from each record bin, for the 15-story buildings ( $R=2$ ,  $R=4$  and  $R=6$  from top to bottom respectively) and the best-fits obtained from the regression of the entire data sets..... 86
- Figure 4.13. Scatter plot of MIDR vs. PGV resulting from each record bin, for the 15-story buildings ( $R=2$ ,  $R=4$  and  $R=6$  from top to bottom respectively) and the best-fits obtained from the regression of the entire data sets..... 87

Figure 4.14.	Scatter plot of MPR vs. PGV resulting from each record bin, for the 15-story buildings (R=2, R=4 and R=6 from top to bottom respectively) and the best-fits obtained from the regression of the entire data sets.....	88
Figure 4.15.	Scatter plot of MFA vs. AI resulting from each record bin, for the 15-story buildings (R=2, R=4 and R=6 from top to bottom respectively) and the best-fits obtained from the regression of the entire data sets.....	89
Figure 4.16.	Scatter plot of MFD vs. $S_a(T_1)$ resulting from each record bin, for the 20-story buildings (R=2, R=4 and R=6 from top to bottom respectively) and the best-fits obtained from the regression of the entire data sets.....	90
Figure 4.17.	Scatter plot of MIDR vs. PGV resulting from each record bin, for the 20-story buildings (R=2, R=4 and R=6 from top to bottom respectively) and the best-fits obtained from the regression of the entire data sets.....	91
Figure 4.18.	Scatter plot of MPR vs. PGV resulting from each record bin, for the 20-story buildings (R=2, R=4 and R=6 from top to bottom respectively) and the best-fits obtained from the regression of the entire data sets.....	92
Figure 4.19.	Scatter plot of MFA vs. AI resulting from each record bin, for the 20-story buildings (R=2, R=4 and R=6 from top to bottom respectively) and the best-fits obtained from the regression of the entire data sets.....	93
Figure 4.20.	Prediction curves of maximum floor displacements for 5-, 10-, 15- and 20-story buildings (from top to bottom respectively).....	96
Figure 4.21.	Prediction curves of maximum inter-story drifts for 5-, 10-, 15- and 20-story buildings (from top to bottom respectively).....	97
Figure 4.22.	Prediction curves of maximum plastic beam rotations for 5-, 10-, 15- and 20-story buildings (from top to bottom respectively) .....	98

Figure 4.23.	Prediction curves of maximum floor accelerations for 5-, 10-, 15- and 20-story buildings (from top to bottom respectively).....	99
Figure 4.24.	Example cumulative lognormal distribution function of EDP conditioned on IM .....	101
Figure 4.25.	Comparison of regression predictions with the log-normally distributed median, 16 <sup>th</sup> – and 84 <sup>th</sup> –percentile predictions of maximum floor displacements, MFD, for 5-story buildings .....	103
Figure 4.26.	Comparison of regression predictions with the log-normally distributed median, 16 <sup>th</sup> – and 84 <sup>th</sup> –percentile predictions of maximum inter-story drift ratios, MIDR, for 5-story buildings .....	104
Figure 4.27.	Comparison of regression predictions with the log-normally distributed median, 16 <sup>th</sup> – and 84 <sup>th</sup> –percentile predictions of maximum beam plastic rotations, MPR, for 5-story buildings .....	105
Figure 4.28.	Comparison of regression predictions with the log-normally distributed median, 16 <sup>th</sup> – and 84 <sup>th</sup> –percentile predictions of maximum floor accelerations, MFA, for 5-story buildings .....	106
Figure 4.29.	Comparison of regression predictions with the log-normally distributed median, 16 <sup>th</sup> – and 84 <sup>th</sup> –percentile predictions of maximum floor displacements, MFD, for 10-story buildings.....	107
Figure 4.30.	Comparison of regression predictions with the log-normally distributed median, 16 <sup>th</sup> – and 84 <sup>th</sup> –percentile predictions of maximum inter-story drift ratios, MIDR, for 10-story buildings.....	108
Figure 4.31.	Comparison of regression predictions with the log-normally distributed median, 16 <sup>th</sup> – and 84 <sup>th</sup> –percentile predictions of maximum beam plastic rotations, MPR, for 10-story buildings .....	109
Figure 4.32.	Comparison of regression predictions with the log-normally distributed median, 16 <sup>th</sup> – and 84 <sup>th</sup> –percentile predictions of maximum floor accelerations, MFA, for 10-story buildings .....	110

Figure 4.33.	Comparison of regression predictions with the log-normally distributed median, 16 <sup>th</sup> – and 84 <sup>th</sup> –percentile predictions of maximum floor displacements, MFD, for 15-story buildings.....	111
Figure 4.34.	Comparison of regression predictions with the log-normally distributed median, 16 <sup>th</sup> – and 84 <sup>th</sup> –percentile predictions of maximum inter-story drift ratios, MIDR, for 15-story buildings.....	112
Figure 4.35.	Comparison of regression predictions with the log-normally distributed median, 16 <sup>th</sup> – and 84 <sup>th</sup> –percentile predictions of maximum beam plastic rotations, MPR, for 15-story buildings .....	113
Figure 4.36.	Comparison of regression predictions with the log-normally distributed median, 16 <sup>th</sup> – and 84 <sup>th</sup> –percentile predictions of maximum floor accelerations, MFA, for 15-story buildings .....	114
Figure 4.37.	Comparison of regression predictions with the log-normally distributed median, 16 <sup>th</sup> – and 84 <sup>th</sup> –percentile predictions of maximum floor displacements, MFD, for 20-story buildings.....	115
Figure 4.38.	Comparison of regression predictions with the log-normally distributed median, 16 <sup>th</sup> – and 84 <sup>th</sup> –percentile predictions of maximum inter-story drift ratios, MIDR, for 20-story buildings.....	116
Figure 4.39.	Comparison of regression predictions with the log-normally distributed median, 16 <sup>th</sup> – and 84 <sup>th</sup> –percentile predictions of maximum beam plastic rotations, MPR, for 20-story buildings .....	117
Figure 4.40.	Comparison of regression predictions with the log-normally distributed median, 16 <sup>th</sup> – and 84 <sup>th</sup> –percentile predictions of maximum floor accelerations, MFA, for 20-story buildings .....	118
Figure 4.41.	Example cumulative probability function of a specified level of demand .....	119
Figure 4.42.	Example cumulative probability functions for MFD.....	120

Figure 4.43.	Example cumulative probability functions for MIDR.....	121
Figure 4.44.	Example cumulative probability functions for MPR.....	122
Figure 4.45.	Example cumulative probability functions for MFA.....	123



## LIST OF TABLES

Table 3.1.	Free vibration fundamental periods of the buildings for the first three modes .....	12
Table 3.2.	Section and material characteristics of the buildings .....	14
Table 3.3.	Parameters for Mander's confined concrete model.....	19
Table 3.4.	Number of the records in Bin I based on the event, faulting mechanism and site class grouping .....	28
Table 3.5.	Number of the records in Bin I based on site class and distance grouping .....	28
Table 3.6.	Number of the records in Bin II based on the event, faulting mechanism and site class grouping .....	29
Table 3.7.	Number of the records in Bin II based on site class and distance grouping .....	29
Table 3.8.	Number of the records in Bin III based on the event, faulting mechanism and site class grouping .....	30
Table 3.9.	Number of the records in Bin III based on site class and distance grouping .....	30
Table 3.10.	Number of the records in Bin IV based on the event, faulting mechanism and site class grouping .....	31
Table 3.11.	Number of the records in Bin IV based on site class and distance grouping .....	31
Table 3.12.	Number of the records in Bin V based on the event, faulting mechanism and site class grouping .....	32

Table 3.13.	Number of the records in Bin V based on site class and distance grouping .....	32
Table 4.1.	Summary of regression results: the highest three correlations between ground motion intensity measures (IM) and engineering demand parameters (EDP) for each building .....	94

## LIST OF SYMBOLS/ABBREVIATIONS

$c$	Damping matrix
$F$	Cumulative distribution function
$f'_c$	Nominal concrete compressive strength
$f_{pc}$	Confined concrete strength
$f_u$	Ultimate strength of steel
$f_y$	Characteristic yield strength of steel
$\epsilon_{sc0}$	Concrete strain at peak stress
$\epsilon_{su}$	Concrete ultimate strain
$G$	Dead load
$h_B$	Beam height
$K$	Stiffness matrix
$L$	Likelihood function
$L_p$	Plastic hinge length
$M$	Mass matrix
$M_w$	Moment magnitude
$Q$	Live load
$R$	Strength reduction factor
$R_{JB}$	Joyner-Boore distance
$R^2$	Coefficient of determination in regression
$S_a(T_1)$	Spectral acceleration at the first mode period of the building
$S_d(T_1)$	Spectral displacement at the first mode period of the building
$S_v(T_1)$	Spectral velocity at the first mode period of the building
$V_{s,30}$	Shear-wave propagation velocity for the upper 30 m-layer
$\zeta$	Modal damping ratio
$\omega_1$	1 <sup>st</sup> mode natural frequency of the building
$\omega_3$	3 <sup>rd</sup> mode natural frequency of the building
$\omega_n$	n <sup>th</sup> mode natural frequency of the building
$AI$	Arias intensity

BPPR	Peak plastic rotation of mid beam
CAV	Cumulative absolute velocity
EDP	Engineering demand parameter
IM	Intensity measure
MDOF	Multi-degree of freedom
MFA	Maximum floor acceleration
MFD	Maximum floor displacement
MIDR	Maximum inter-story drift ratio
MPR	Maximum plastic rotation of beam
NEHRP	National Earthquake Hazard Reduction Program
PEER	Pacific Earthquake Engineering Research Center
PFA	Peak floor acceleration
PFD	Peak floor displacement
PGA	Peak ground acceleration
PGD	Peak ground displacement
PGV	Peak ground velocity
PIDR	Peak inter-story drift ratio
RC	Reinforced concrete
SDOF	Single-degree of freedom

## 1. INTRODUCTION

Since a severe earthquake ground excitation is expected to deform a structure into the inelastic range, design and assessment guidelines are increasingly requiring nonlinear dynamic analysis in the design process as well as for the seismic performance evaluation of existing structures and the nonlinear dynamic analyses under the actions resulting from acceleration time histories are becoming more frequently used procedures. The assessment of the structural response via nonlinear dynamic analyses requires some characterization of the correlations between ground motion intensity measures and structural response parameters. It gains more significance to understand which properties of a recorded ground motion are most strongly related to the response caused in the structure.

Performance-based earthquake engineering allows the designer to specify and predict, with a reasonable accuracy, the performance (degree of damage) of the structure for a specified level of ground motion intensity. This requires using input ground motion records that adequately represent the damage potential for given seismic hazard levels and structural characteristics. Records to use in nonlinear time-domain analyses should be selected considering magnitude, distance, site condition and other parameters that control the ground motion characteristics. Nonetheless the input ground motions are compatible with the results of seismic hazard disaggregation and represent well the hazard level at the site the same structure might respond very differently under the actions of selected input ground motions and a great scatter in the analyses results might be observed.

If the relationships between ground motion intensity measures, such as peak ground acceleration, spectral displacement or Arias intensity, and structural response parameters, such as floor displacement, inter-story drift, member plastic rotation, are identified and the best correlated pairs are provided the selection and scaling/modification of ground motion recordings as input for the nonlinear dynamic analyses can more easily and effectively be done by considering and utilizing those correlations. The well established correlations might also help in developing better intensity measures that sufficiently and efficiently incorporate the seismic hazard at the site and that also reduce the scatter in the nonlinear structural response when using a limited number of records. In this way, furthermore,

estimation of the average structural response and/or assessment of full probabilistic distribution of the response parameter conditioned on a given ground motion intensity measure can be achieved more accurately.

### 1.1. Objectives and Outline of the Thesis

The primary objective of this study is to investigate the correlations between ground motion intensity measures and structural response parameters through nonlinear dynamic analyses of multi-degree-of-freedom (MDOF) structures under real earthquake recordings. Although most of them had dealt with the single-degree-of-freedom (SDOF) models there are numerous studies available in the literature which investigated the relations between ground motion parameters and the structural response demands. Relatively fewer numbers of works which evaluate the correlations of inelastic demands in MDOF systems with the ground motion intensity measures can be found. However, those works are limited to specific buildings (Shome *et al.*, 1998, Cornell *et al.*, 2002, Hancock, 2006, Haselton *et al.*, 2008, Buratti, 2009). To capture relatively wider range of nonlinear structural responses, buildings with varying natural vibration periods and strength characteristics are included in the study. For this purpose, a parametric investigation on reinforced concrete buildings is carried out. The building groups are five-, ten-, fifteen- and twenty-story reinforced concrete, code-conforming, regular moment-resisting frames. They are designed for different strength reduction factors,  $R=2, 4$  and  $6$ . Hence there are 12 buildings under consideration in total. Finite element analysis of the buildings is achieved by using line elements in *OpenSees* v2.0 (UC Berkeley, 2008) environment. The line elements are composed of fiber sections and utilize the distributed plasticity approach for columns and concentrated plasticity approach for beams.

The input ground motion dataset consists of 734 horizontal components of earthquake accelerograms. They are compiled from *PEER* database based on the magnitude-distance selection criterion. The magnitudes ( $M_w$ ) and source-to-site distances ( $R_{JB}$ ) are ranging between 5.5-7.62 and 0-100 km respectively. The recordings are coming from different soil conditions which follow the *NEHRP* site classes (B, C, D and E) based on the  $V_{s,30}$  values and faulting mechanisms (strike-slip, normal, reverse, reverse oblique and normal oblique). For the buildings under consideration, 8,808 nonlinear time history

analyses are performed under unscaled ground motions. The relative joint (one joint at each floor) accelerations and displacements as well as the plastic end rotations of beams at each floor are monitored. The scatter diagrams of ground motion intensity measures, namely magnitude ( $M_w$ ), distance ( $R_{JB}$ ), peak ground acceleration ( $PGA$ ), peak ground velocity ( $PGV$ ), peak ground displacement ( $PGD$ ), spectral acceleration ( $S_d(T_1)$ ), spectral velocity ( $S_v(T_1)$ ), spectral displacement ( $S_d(T_1)$ ), Arias intensity ( $AI$ ) and cumulative absolute velocity ( $CAV$ ) versus structural response parameters, namely maximum inter-story drift ratio ( $MIDR$ ), maximum floor displacement ( $MFD$ ), maximum floor acceleration ( $MFA$ ) and maximum plastic end rotation of beams ( $MPR$ ) are plotted.

The best correlations between ground motion and structural response parameters are provided and the mean functions to predict the structural response via ground motion intensity measure are computed. This is done by non-parametric statistical approach, i.e. regression analysis. Then a parametric statistical evaluation procedure based on a log-normal distribution assumption is applied to the best correlations and median prediction functions are obtained. In order to make a cross-check, the mean prediction functions resulting from non-parametric evaluation are compared to the median prediction functions obtained from the parametric method. In addition, examples of three-dimensional structural response surfaces are provided in order to utilize for damage assessment of the buildings with similar characteristics.

This thesis study encompasses five chapters. Following the introduction, Chapter 2 provides a summary of literature survey on the engineering characterization of strong ground motion and structural response. Chapter 3 deals with the structural systems used in the study, nonlinear modeling and analysis and, the analyses results. Chapter 4 introduces the statistical approaches utilized in the study and presents the correlations and comparisons of the results. Chapter 5 concludes the thesis with the summary of findings and future research ideas.

## **2. ENGINEERING CHARACTERIZATION OF STRONG GROUND MOTION AND STRUCTURAL RESPONSE: INTENSITY MEASURES (IMs) and ENGINEERING DEMAND PARAMETERS (EDPs)**

### **2.1. Introduction**

“The basic data of earthquake engineering are recordings of ground accelerations during earthquakes. A knowledge of the ground motion is essential to an understanding of the earthquake behavior of structures” (Housner, 1970). Ground motion time series contain valuable characteristics and information that are used directly, or indirectly, in seismic analysis and design. Parameters such as peak ground motion values (acceleration, velocity and displacement), measures of the frequency content of the ground motion

In the present section, following the brief information about the types of strong ground motion records, a short description of the seismic ground motion parameters that are used within the context of this thesis study is given.

### **2.2. Strong Ground Motion Records**

Strong ground motion records can be classified into three groups: Real records, artificial records and simulated (synthetic) records.

#### **2.2.1. Real Records**

Real records are the ones recorded during the event of an earthquake ground excitation. The advantage of using real records is that they are genuine records of shaking produced by earthquakes. Therefore they carry all ground motion characteristics e.g. amplitude, frequency and energy content, duration and phase characteristics, and reflect all the factors that influence accelerograms (characteristics of the source, path and site).



### 2.2.2. Artificial Records

Artificial records are generated to match a target response spectrum. Disadvantage of artificial accelerograms is that they do not have appearance of real earthquake accelerograms, with unrealistically high cycle numbers of motion. This is because of the target spectrum is generally a uniform hazard spectrum (UHS), which is an envelope of the spectra corresponding to earthquakes in different seismic sources and the conservative scenario of earthquakes occurring in different seismic sources simultaneously is implicitly taken into account. The artificial records are problematic because they have to match the smooth code spectrum at all periods. Additionally in order to get other characteristics of artificial spectrum-compatible record, such as duration, it is necessary to obtain supplementary information about the expected earthquake motion apart from the response spectrum.

### 2.2.3. Simulated (Synthetic) Records

The number of real accelerograms has increased significantly in the last years, but a couple of decades ago there was a lack of records obtained at short distances from the causative fault ruptures of severe earthquakes. The use of simulated records was necessary in order to overcome this lack of real records. Even today, with the large number of accelerograms recorded during the past three decades, it may still be difficult to find accelerograms that fulfill the requirements of certain magnitude and distance bins, especially for large magnitude and close distances.

The simulation of the accelerograms is mainly made by either deterministic or stochastic ground motion modeling methods. Long-period motions generally behave in a deterministic manner, while short-period motions behave stochastically. The period of transition from deterministic to stochastic behavior is uncertain, but is often taken as about  $T \sim 1$  s (Stewart *et al.*, 2001). The simulation methods to generate earthquake accelerograms are able to approximate the effects of physical process on observed ground motions (earthquake source process, wave propagation and shallow soil response).

The earthquake source process denotes the generation of seismic waves as part of the strain energy released from the rupture of an active geologic fault. In simulation procedure, a kinematic source model is typically used to describe the fault slip process. The fault slip can be modeled as a point or finite source. When a site is close to the source of a large-magnitude earthquake, a finite source is necessary for the simulation of near-fault effects. At distances far from the fault, a finite source can be simplified as a point source model, which reduces considerably the amount of computational work and the number of input parameters required.

After the fault rupture, seismic waves propagate through the Earth's crust. This is called the path effect. Typical path effects can be simulated by utilizing the Green's functions, which include attenuation of wave amplitude, reflection and refraction at the interface of different rock types and wave scattering from small-scale heterogeneities in the crust. At the moment when seismic waves approach the surface of the Earth, they experience further modifications while propagating through shallow soils.

### 2.3. Time Domain Parameters of Strong Ground Motions

Both time and frequency domain characteristics of the strong ground motion are used in engineering applications. Parameterization of these characteristics is a useful tool for their incorporation in further studies such as assessment of earthquake hazard or structural response to a particular seismic excitement. In the present section a short description of the seismic ground motion parameters that are used within the context of this thesis study will be given. Comprehensive descriptions can be found in Kramer, (1996) and Stewart *et al.*, (2001).

Peak ground acceleration (PGA), velocity (PGV), and displacement (PGD) are the most common and easily recognizable time domain parameters of strong ground motion time histories. Peak values give the largest absolute amplitudes of the respective (mostly non-filtered but base-line corrected) time series:

$$PGA \equiv \max(|a|) = \max(|\ddot{u}_g|) \quad (2.1)$$

$$PGV \equiv \max(|v|) = \max(|\dot{u}_g|) \quad (2.2)$$

$$PGD \equiv \max(|u_g|) \quad (2.3)$$

where  $u_g=d(t)$  is the ground displacement time history at a particular station. Peak values can be obtained for all three components of ground shaking, i.e. for the two orthogonal horizontal and the vertical components. The two horizontal components are in general given as components in NS and EW directions in recorded time histories, whereas in fault normal and fault parallel directions in simulated ones. Peak horizontal values can refer to the maximum peak value of the two horizontal components, their average (mean) value or to the peak value of the resultant time series after taking the vector sum of both. In this work peak horizontal values refer to the peak value of an individual component recorded during an earthquake.

In earthquake engineering, damage has traditionally been associated with PGA, that is practically taken equal to the effective peak acceleration which, when multiplied with the mass of the structure gives the lateral earthquake load. However recent studies and observations on the dynamic response of structures have demonstrated the importance of PGV, PGD and differential displacements in the damage observed in different types of structures such as high-rise buildings, pipelines, tunnels and bridges.

## 2.4. Spectral Parameters of Strong Ground Motions

Fourier amplitude spectra and particularly response spectra are the two commonly used tools in earthquake engineering for the quantification and analysis of the ground motion in the frequency domain.

- Fourier Amplitude Spectra (FAS):

Using a Fourier series, a periodic function,  $x(t)$ , can be expressed as:

$$x(t) = c_0 + \sum_{n=1}^{\infty} c_n \cos(\omega_n t + \phi_n) \quad (2.4)$$

In this form,  $c_n$  and  $\phi_n$  are the amplitude and the phase angle, respectively of the  $n^{th}$  harmonic of the Fourier series. The Fourier series provides a complete description of the ground motion in the frequency domain since the time history can be recaptured by the Inverse Fourier Transform. The Fourier Amplitude Spectrum (FAS) is a plot of the amplitude,  $c_n$ , versus frequency and is used to see how the amplitude of the motion is distributed with respect to frequency. FAS of acceleration records plotted in logarithmic scale exhibit a plateau over an intermediate frequency range. The lower bound of this plateau is the cut off frequency which is inversely proportional to the cube root of seismic moment (Brune, 1970). This indicates that large earthquakes produce greater low-frequency motions than the smaller ones. The predominant period,  $T_p$ , of an earthquake ground motion recording is the period of vibration corresponding to the maximum value of its smoothed FAS, and provides a useful but rough representation of the frequency content.

- Response Spectra:

Response spectrum which is extensively used in earthquake engineering, describes the maximum linear (visco-elastic) response of a single degree of freedom system (SDOF) to a particular input motion as a function of its natural period of vibration and damping ratio. The response may be expressed in terms of acceleration, velocity or displacement. These spectral amplitudes can be used to define the earthquake load on a particular structure if a more specific time history analysis is not required. The maximum value of the structural response to a particular input motion depends only on the natural frequency and the damping ratio of the SDOF system. The maximum values of acceleration, velocity and displacement are referred to as spectral acceleration ( $S_a$ ), spectral velocity ( $S_v$ ) and spectral displacement ( $S_d$ ) respectively. For linear, elastic SDOF systems, the spectral displacement, velocity and acceleration are approximately related to each other by the following expressions:

$$S_d = \max|u| \quad (2.5)$$

$$S_v = \max|\dot{u}| \approx \omega_0 S_d = PSV \quad (2.6)$$

$$S_a = \max|\ddot{u}| \approx \omega_0^2 S_d = \omega_0 PSV = PSA \quad (2.7)$$

where  $u$  and  $\omega_0$  are the displacement and natural frequency of the SDOF system. PSV and PSA are the pseudo spectral velocity and the pseudo spectral acceleration respectively. Although they are not the true maxima of the acceleration and velocity response they are very close and can approximately be assumed to be equal to  $S_v$  and  $S_a$ .

## 2.5. Energy-Related Parameters of Strong Ground Motions

Arias intensity (AI) and cumulative absolute velocity (CAV) can be considered as two of the energy related parameters of strong ground motions.

Arias intensity has been used to evaluate damage potential of the ground motions. It is defined as:

$$I_A = \frac{\pi}{2g} \int_0^{t_d} [a_g(t)]^2 dt \quad (2.8)$$

where  $a_g(t)$  is the acceleration time history of total duration  $t_d$ .

Cumulative absolute velocity is a more recently introduced parameter that might be used for the quantification of the energy content of ground motion record. It is defined as:

$$CAV = \int_0^{t_d} |a(t)| dt \quad (2.9)$$

where  $a(t)$  is the acceleration time history of total duration  $t_d$ .

## 2.6. Structural Response: Engineering Demand Parameters (EDP)

Following the terminology conventions of the Pacific Earthquake Engineering Research (PEER) Center, the Intensity Measure (IM) is defined as the quantification of effect of an earthquake ground motion on a structure. As the ground motion IM, one of the above defined time domain, spectral or energy related parameters of the ground motions is considered in this study. The structural response parameter that might be used as a measure

of the dynamic structural response or as the quantification of damage induced by the strong ground motion is termed as an Engineering Demand Parameter (EDP). In this study, the following parameters are considered as the EDPs:

- Maximum Inter-story Drift Ratio (MIDR)
- Maximum Floor Displacement (MFD)
- Maximum Floor Acceleration (MFA)
- Maximum Plastic Rotations of Beams (MPR)

### **3. STRUCTURAL SYSTEMS, ANALYTICAL MODELING AND NONLINEAR DYNAMIC ANALYSES**

#### **3.1. Introduction**

Increasingly, design and assessment guidelines are requiring nonlinear analysis in the design process as well as for the seismic performance evaluation since a severe earthquake ground excitation is expected to deform a structure into the inelastic range (Filippou and Fenves, 2004).

This chapter introduces the buildings used in this study and gives information on the seismic design and finite element modeling of the buildings, nonlinear dynamic analysis methodology and the selected input ground motions for the dynamic analyses. Following the presentation of the analyses results, the findings about the relations between structural responses and magnitude, distance, site class and faulting mechanism are presented at the end of the chapter.

#### **3.2. Generic Buildings Used in the Study**

Regular five-bay planar reinforced concrete (RC) frame type buildings with four different heights, five, ten, fifteen and twenty stories as depicted in Figure 3.1, were selected. Typical story height of 3 m. and span length of 5 m. were assumed for all the buildings. Three different ductility levels, i.e., low, medium and high, were adopted in the design of the frames. Therefore, totally 12 different frame systems were considered. The buildings were chosen to vary across a range of natural vibration periods and strength levels as well (Table 3.1).

Table 3.1. Free vibration fundamental periods of the buildings for the first three modes

Period (s)	5-story			10-story			15-story			20-story		
	R=2	R=4	R=6	R=2	R=4	R=6	R=2	R=4	R=6	R=2	R=4	R=6
$T_1$	0.55	0.63	0.65	1.04	1.16	1.24	1.43	1.6	1.71	1.8	2.0	2.15
$T_2$	0.19	0.21	0.22	0.38	0.42	0.44	0.53	0.59	0.62	0.67	0.75	0.80
$T_3$	0.11	0.12	0.12	0.23	0.25	0.26	0.32	0.35	0.37	0.40	0.45	0.47

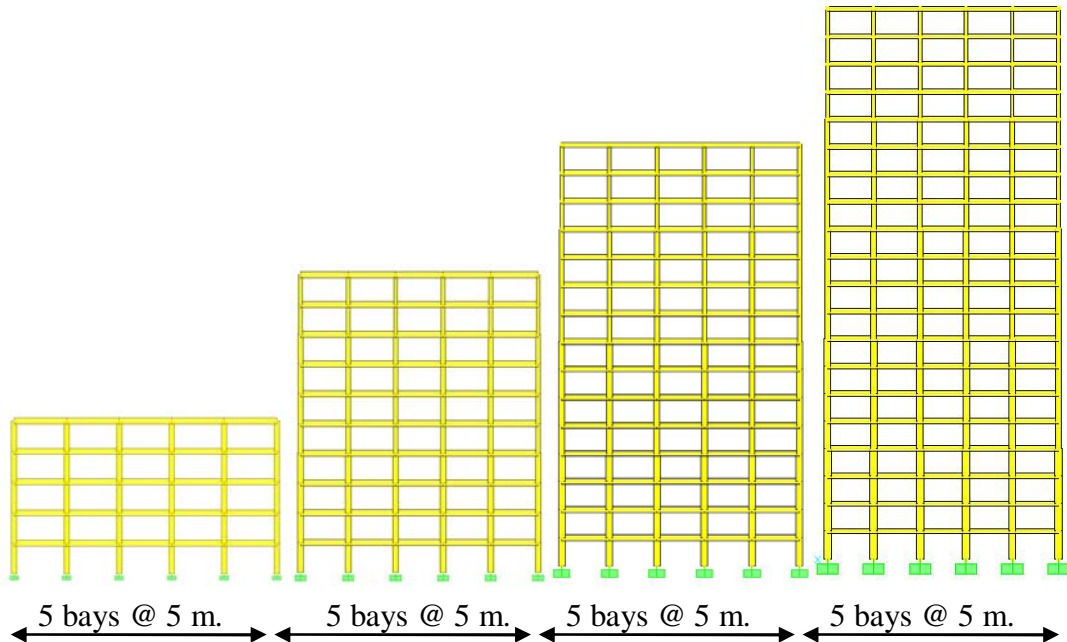


Figure 3.1. 5-, 10-, 15- and 20-story buildings

Each frame system has been designed in accordance with Turkish Seismic Code (2007) provisions. Three ductility levels (low, medium and high) have been adopted in the design of the frames, for which strength reduction factors,  $R$ , are specified as two, four and six, respectively. However, the initial stiffness of the frames remains unchanged, regardless of the strength levels assigned. A code-based five per cent -damped elastic response spectrum that corresponds to Seismic Zone 1 and site class Z3 of Turkish Seismic Code (2007) as shown in Figure 3.2 is used as design basis earthquake.



The buildings were designed based on strong column-weak beam principle. The linear response spectrum analysis is performed for determining the elastic design forces for each building. The peak modal responses are calculated for those modes contributing significantly to the response and which are sufficient to capture at least 90 per cent of the participating mass of the building. The five per cent-damped elastic design spectrum is reduced by the strength reduction factors of two, four and six. Earthquake forces from the reduced response spectrum are combined with the gravity loads ( $G + 0.3Q$ ). Distributed dead load value of  $5.25 \text{ kN/m}^2$  and live load value of  $2.0 \text{ kN/m}^2$  are considered. Under the action of design forces which are composed of lateral loads and gravity loads, required reinforcement ratios for each structural element are computed. In order to obtain strength distribution consistent with design forces throughout the structure, required reinforcement ratios of the sections are selected so that its flexural capacity is approximately equal to the design forces obtained from the analysis. As a result of the design procedure summarized above, geometrical properties of the sections and the characteristic material strengths used in the design are presented in Table 3.2.

Minimum reinforcement requirements control the design of the beams at the upper story levels and therefore their flexural strength are larger than the required strength corresponding to the sectional forces obtained from the analysis for  $R=4$  and  $6$ . However, it has been observed that sectional design forces obtained from the analysis for low ductility level ( $R=2$ ) are dominant in the design of the structural elements throughout the structures.

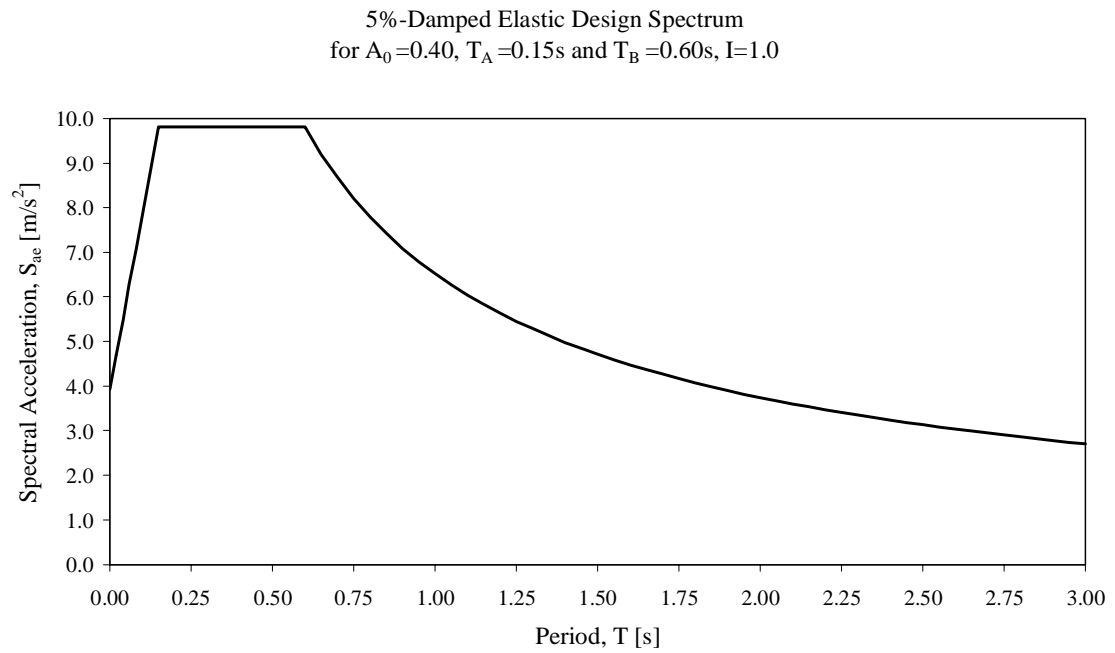


Figure 3.2. 5 per cent-damped elastic design spectrum constructed for ‘Seismic Zone 1’ and site class ‘Z3’ of Turkish Seismic Code-2007

Table 3.2. Section and material characteristics of the buildings

Building	Floor Levels	Columns (cm)	Beams (cm)	Concrete $f_c'$ (MPa)	Steel $f_y$ (MPa)
5-story	1 - 5	50 x 50	30 x 60	25	420
10-story	1 - 4	60 x 60	30 x 60	25	420
	5 - 8	50 x 50			
	9 - 10	40 x 40			
15-story	1 - 4	70 x 70	30 x 60	30	420
	5 - 8	60 x 60			
	9 - 12	50 x 50			
	13 - 15	40 x 40			
20-story	1 - 4	80 x 80	30 x 60	35	420
	5 - 8	70 x 70			
	9 - 12	60 x 60			
	13 - 16	50 x 50			
	17 - 20	40 x 40			

### 3.3. Analytical Modeling

The finite element models of the buildings were realized by using OpenSees v2.0 (Open System for Earthquake Engineering Simulation, McKenna *et al.*, 2002). The analytical models of the frame systems consist of two-node line elements connected at the nodes representing the joints. The joints and the floor diaphragms at each story level are assumed to be infinitely rigid. The base of the columns at the foundation level is fixed for all the degrees of freedoms. The mass of the buildings are assigned to the nodes of the models by utilizing lumped mass assumption. Story masses are calculated in accordance with the combination of dead load and live load ( $G + 0.3Q$ ).

'*beamWithHinges*' elements and '*nonlinearBeamColumn*' elements of the OpenSees software package were used for modeling the beams and columns respectively. '*beamWithHinges*' element is based on the iterative flexibility formulation, and considers plasticity to be concentrated over the specified hinge lengths at the element ends. The hinge properties have been defined by assigning to each a previously-defined fiber section. The hinge length,  $L_p$ , at both ends of a beam has been assumed to be equal to the half of the beam height ( $h_B / 2$ ). The frame element is assumed to be divided into three parts: two hinges at the ends, and a linear-elastic region in the middle (Figure 3.3). '*beamWithHinges*' element localizes the hinges at the element ends only by the integration points in the hinge regions to be able represent the curvature distribution accurately. OpenSees adopts the Modified Gauss-Radau Integration, developed by Scott and Fenves, (2006) that applies the Gauss-Radau hinge integration over  $4L_p$  instead of  $L_p$  as given in Figure 3.4. Elastic properties are then applied to the interior integration points, where a closed-form solution is used.

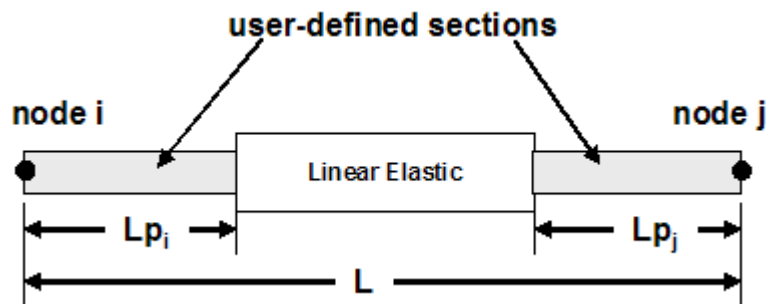


Figure 3.3. Concentrated plasticity at the end of beams by '*beamWithHinges*' elements

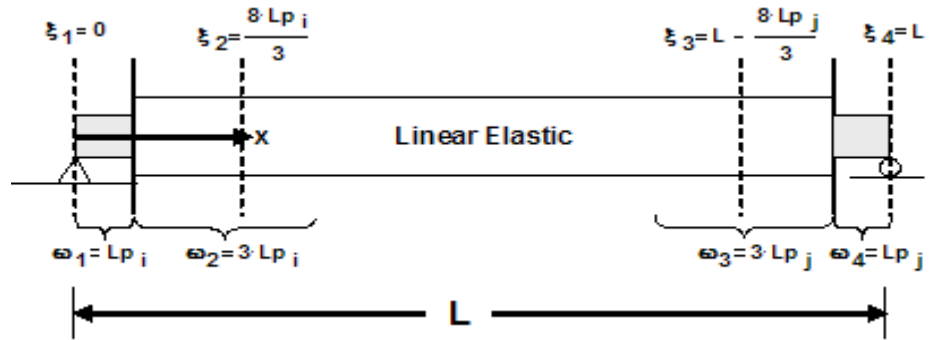


Figure 3.4. Modified Gauss-Radau integration adopted for concentrated plasticity

The limitation of concentrated plasticity elements is that the inelastic deformations take place at predetermined locations at the ends of the element. While this may be a reasonable assumption in lower floors of moment-resisting frames it does not account for the possibility of inelastic deformation taking place within the element in the upper floors of the building. This is especially correct for columns where the combination of gravity and earthquake forces may lead to the formation of a plastic hinge away from the member ends particularly in higher floors (Filippou and Fenves, 2004). ‘*nonlinearBeamColumn*’ elements used for modeling the columns is based on the iterative force formulation and considers the spread of plasticity along the element. The end moment-rotation relation is obtained by the integration of the section response along the element with the help of integration control points. OpenSees utilizes the Gauss-Radau (Jamei *et al.*, 2005) rule to obtain the element deformations by integrating the section internal forces. Five integration points along the columns in all buildings under consideration have been assigned (Figure 3.5).

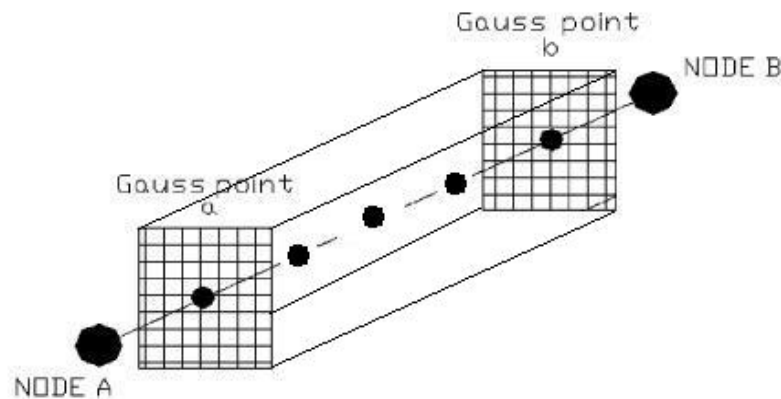


Figure 3.5. Distributed plasticity for columns by ‘*nonlinearBeamColumn*’ elements

The line elements, which are used to model beams and columns, consist of fiber sections. By the use of fiber sections, the hysteretic response is defined by the material properties and moment-curvature relations of the sections automatically included in the analysis. The influence of varying axial force on strength and stiffness is directly modeled (Priestly *et al.*, 2007)

In a reinforced concrete section it is important to represent the area and distribution of reinforcement relatively well since the hysteretic response is governed by the behavior of reinforcing steel. Fiber section representation of a reinforced concrete member has layers for the reinforcement steels and core and cover concretes as illustrated in Figure 3.6. Reinforcing bars are represented by straight layers and associated with the bar areas and material behavior model. The cross-sectional concrete area is divided into subsections, so-called fibers, and associated with the confined and unconfined concrete models for the core and cover concretes respectively. 2 cm. by 2 cm. fiber sections have been used for the concrete areas.

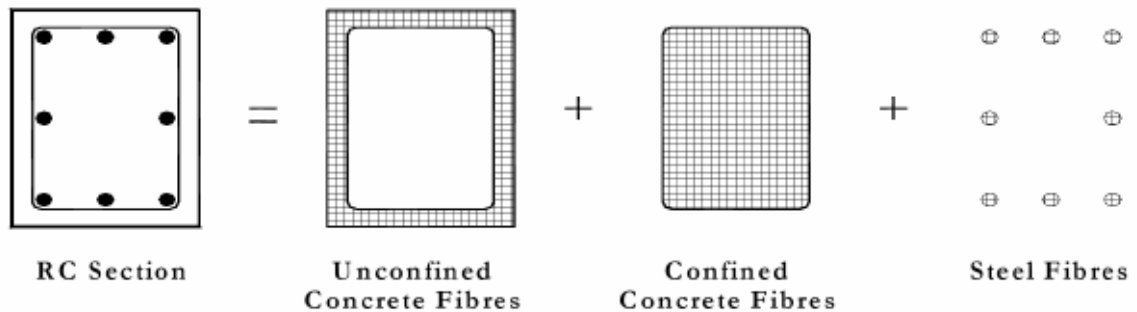


Figure 3.6. Fiber discretization of a reinforced concrete section

It is needed to define a constitutive model for the material to establish the section response. The stress-strain relation of Menegotto and Pinto, (1973) has been adopted for the steel behavior. Figure 3.7 represents the hysteretic behavior with strain-hardening for the ‘Steel02’ material of OpenSees. The characteristic yield strength of  $f_y=420$  MPa and ultimate strength of  $f_u=550$  MPa with a  $6.64 \times 10^{-3}$  of strain hardening ratio are used.

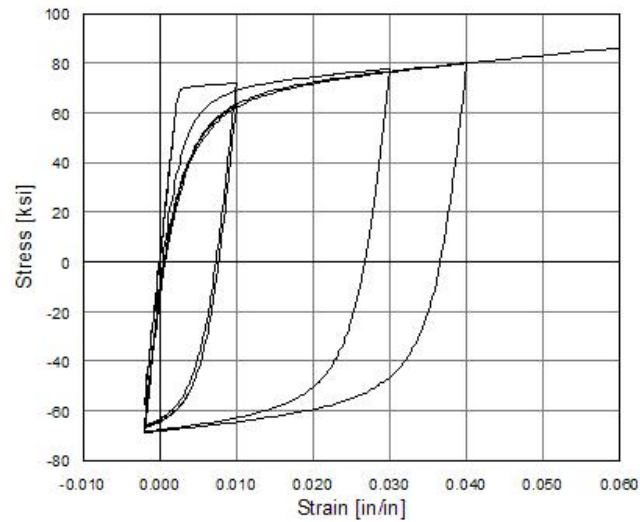


Figure 3.7. Hysteretic behavior of steel model w/o isotropic hardening ('*Steel02*' material, OpenSees v2.0 user command-language manual)

Confined and unconfined concrete models have been adopted for the core and cover concretes respectively. Confined concrete model proposed by Mander *et al.*, (1989) is used and strength and strain values are given in Table 3.3. Figure 3.8 shows the stress-strain model used for '*Concrete01*' material of OpenSees which does not account for the tensile strength of concrete. For the unconfined concrete, the ultimate stress is assumed to be zero and the strains at peak stress and at ultimate stress are 0.002 and 0.005 respectively.

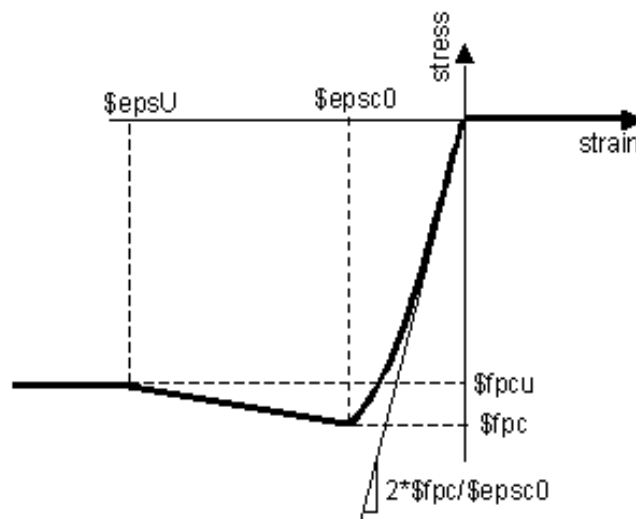


Figure 3.8. Stress-strain model for the confined concrete ('*Concrete01*' material, OpenSees v2.0 user command-language manual)

Table 3.3. Parameters for Mander's confined concrete model

<b>Nominal Concrete Compressive Strength (<math>f'_c</math>)</b>	25 MPa	30 MPa	35 MPa
<b>Confined Concrete Strength (<math>f_{pc}</math>)</b>	32.9 MPa	39.6 MPa	44.8 MPa
<b>Strain at Peak Stress (<math>\epsilon_{sc0}</math>)</b>	0.00517	0.00519	0.0048
<b>Ultimate Strain (<math>\epsilon_{su}</math>)</b>	0.02	0.02	0.0195

Based on the definitions and assumptions as described above for the analytical modeling of the buildings, an example OpenSees script is provided in Appendix A and example moment-rotation hysteresis for the columns and beams are shown in Figure 3.9 and Figure 3.10.

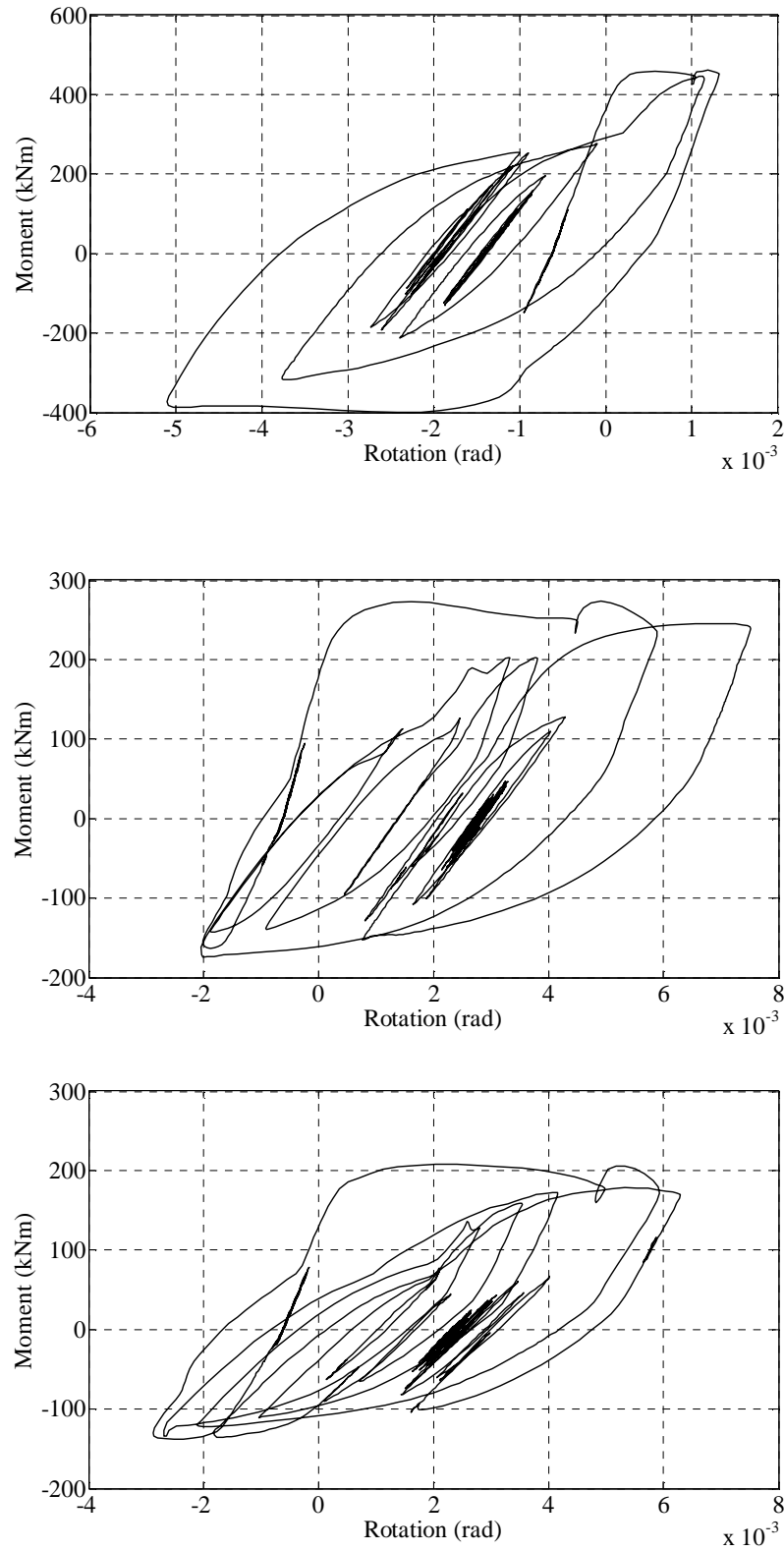


Figure 3.9. Example moment-rotation hysteresis under PUL104 record of Northridge Earthquake for a 1<sup>st</sup> story beam of 5-story buildings,  $R=2$ ,  $R=4$  and  $R=6$  from top to bottom respectively



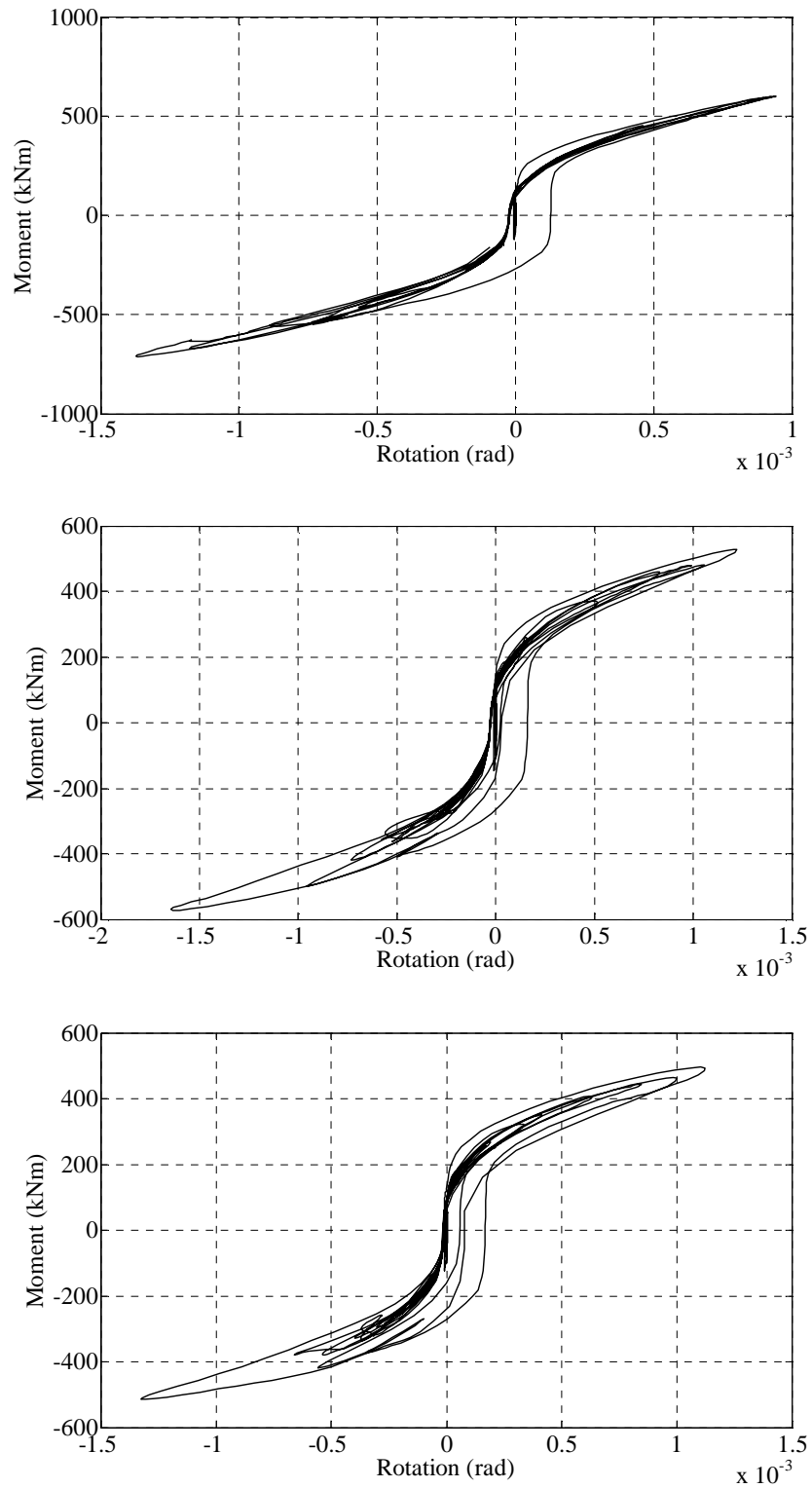


Figure 3.10. Example moment-rotation hysteresis under PUL104 record of Northridge Earthquake for a 1<sup>st</sup> story column of 10-story buildings, R=2, R=4 and R=6 from top to bottom respectively

### 3.4. Nonlinear Dynamic Analyses

Nonlinear time-domain analyses were performed under real earthquake recordings. Twelve buildings which have been described in previous sections were analyzed under the action of a suite of 734 horizontal components of unscaled ground motion acceleration recordings. Hence a total number of 8,808 analyses have been conducted. Using six desktop and one laptop computers the analyses runtimes took more than 2,500 hours.

First gravity load analysis as a combination of dead loads and live loads ( $G+0.3Q$ ) is performed. Eigen values are computed through free vibration analysis. Then the buildings are analyzed under the actions of uniform ground motion excitation. P-delta effects are not included in the analyses.

#### 3.4.1. Damping Modeling and Solution Algorithm

For dynamic analysis, Rayleigh damping was assumed based on a modal damping ratio of  $\zeta = 0.05$  for the 1<sup>st</sup> and the 3<sup>rd</sup> natural vibration modes. Damping matrix is specified as combination of the stiffness and mass matrices:

$$c = a_0 * M + a_1 * K \quad (3.1)$$

where  $M$  and  $K$  are the mass and stiffness matrices, respectively. The constants of  $a_0$  and  $a_1$  have units of  $\text{sec}^{-1}$  and  $\text{sec}$ , respectively, and given as (Chopra, 2001):

$$a_0 = \zeta \frac{2\omega_1\omega_3}{\omega_1 + \omega_3}, \quad a_1 = \zeta \frac{2}{\omega_1 + \omega_3} \quad (3.2)$$

Variation of modal damping ratio with natural frequencies is given in Figure 3.11. The damping ratio for the  $n$ th mode is calculated as:

$$\zeta_n = \frac{a_0}{2\omega_n} + \frac{a_1}{2}\omega_n \quad (3.3)$$

Rayleigh damping may be modeled proportional to the tangent stiffness matrix or the initial stiffness matrix. The last committed stiffness has been considered in the analyses. OpenSees calculates the trial stiffness and the committed stiffness. The trial stiffness is calculated at each iteration whereas the committed stiffness is the final trial stiffness that occurs at convergence. So the last committed stiffness is the value that is converged upon at the end of the last time step.

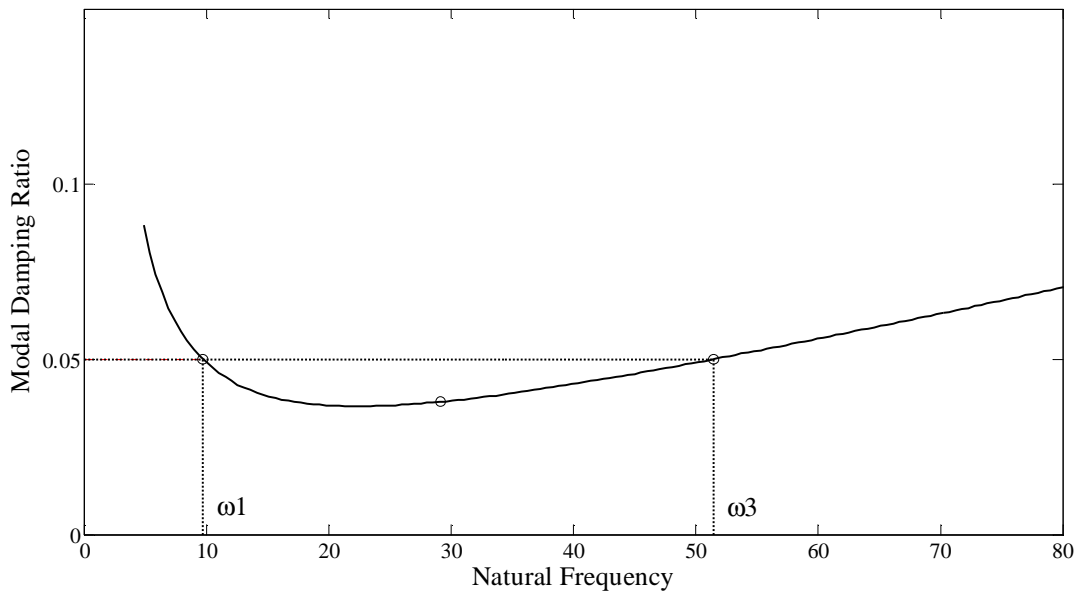


Figure 3.11. Variation of modal damping ratio with natural frequencies

Newmark's time integration method with the integration coefficients of  $\beta=0.25$  and  $\gamma=0.5$  was used for the numerical integration of the equations of motion. The equilibrium equations at each time step of  $dt = 0.005$  s are solved using modified Newton-Raphson algorithm. Modified Newton-Raphson method calculates the tangent stiffness matrix at time  $i$ , the beginning of the time step, and it is used through all iterations within that time step.

### 3.4.2. Input Ground Motions

A large number of time-domain analyses is required to derive correlations / empirical relationships between ground motion intensity measures and the structural response parameters. It is also important to represent record-to-record and event-to-event variability

in the input ground motion bin in order to obtain a conditional probabilistic distribution of the structural response which might be able to reflect the expected inelastic structural responses under the actions imposed by possible future earthquakes.

Records with similar magnitude and distance can exhibit significant variability in phase and frequency content. This variability in the records leads to substantial variability in the calculated nonlinear response of structures. To cover a wide range of ground motion excitation and structural response in the elastic and inelastic range, the ground motions in the bin need to be frequency scaled. This implicitly means that the accelerograms should come from earthquakes with different magnitudes and distances. The input ground motion database compiled from PEER website (<http://peer.berkeley.edu/smcat/>) consists of 734 horizontal components of recordings from 34 earthquakes. The selection is based on the moment magnitude and the Joyner–Boore distance ( $R_{JB}$ ) of the records. Moment magnitude,  $M_w$ , is a measure of the size of the earthquake and is computed using the seismic moment. Joyner-Boore distance is defined as the shortest horizontal distance from the recording site to the vertical projection of the fault rupture. For the input ground motion dataset, the magnitudes ( $M_w$ ) and source-to-site distances ( $R_{JB}$ ) range between 5.5-7.62 and 0-100 km respectively. The selected recordings came from different soil conditions designated with the *NEHRP* site classes (B, C, D and E) based on the  $V_{s,30}$  values and faulting mechanisms identified by the rake angle and source mechanism (strike-slip, normal, reverse, reverse oblique and normal oblique). Accelerograms were only chosen if their moment magnitude, Joyner-Boore distance, site classification and faulting mechanism were known and this reduced the size of the input ground motion dataset.

In order to observe the effect of the magnitude on the structural response, the input ground motion database is divided into five sub-groups based on the moment magnitude ranges as follow and the nonlinear dynamic analyses are conducted separately for each bin of records.

- **Bin I** :  $M_w=5.5\sim5.99$
- **Bin II** :  $M_w= 6.0\sim6.49$
- **Bin III** :  $M_w= 6.5\sim6.99$
- **Bin IV** :  $M_w= 7.0\sim7.49$
- **Bin V** :  $M_w > 7.5$

The variation of peak ground acceleration, peak ground velocity, peak ground displacement, Arias intensity and cumulative absolute velocity values of the selected records with the corresponding source-to-site distances are given in Figure 3.12 and Figure 3.13. The number of records in each bin with respect to event, faulting mechanism, site class and distance grouping are given in Table 3.4 - Table 3.13. The ranges of the peak ground accelerations, velocities and displacements, Arias intensities and cumulative absolute velocities are provided as follow:

PGAs : 0.012-1.59 g

PGVs : 1-127.4 cm/s

PGDs : 0.12 – 92.57 cm

AIs : 0.15-997 cm/s

CAVs : 28.2-3365 cm/s

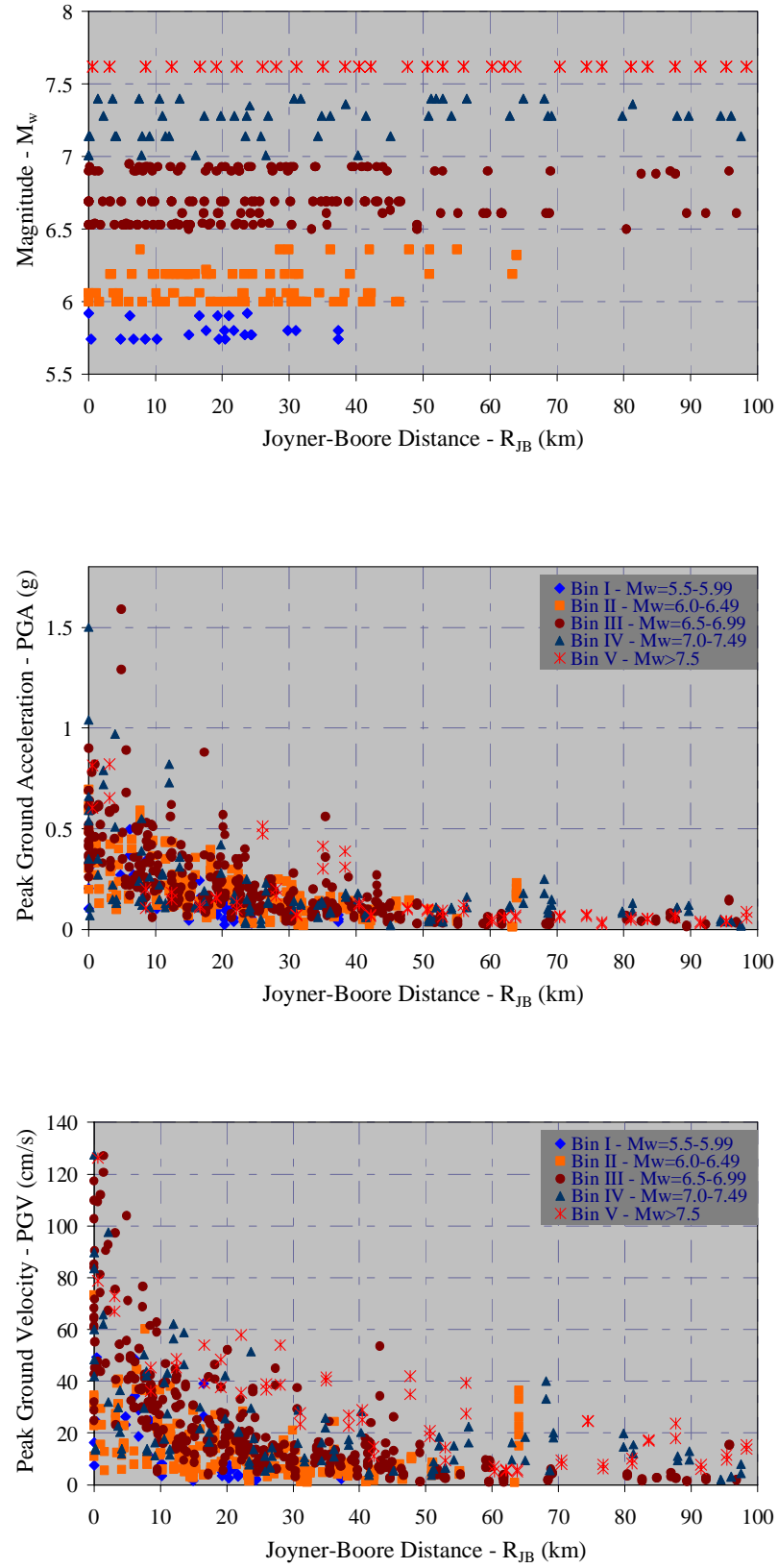


Figure 3.12. Variation of magnitudes, peak ground accelerations and peak ground velocities with Joyner-Boore distance from top to bottom, respectively

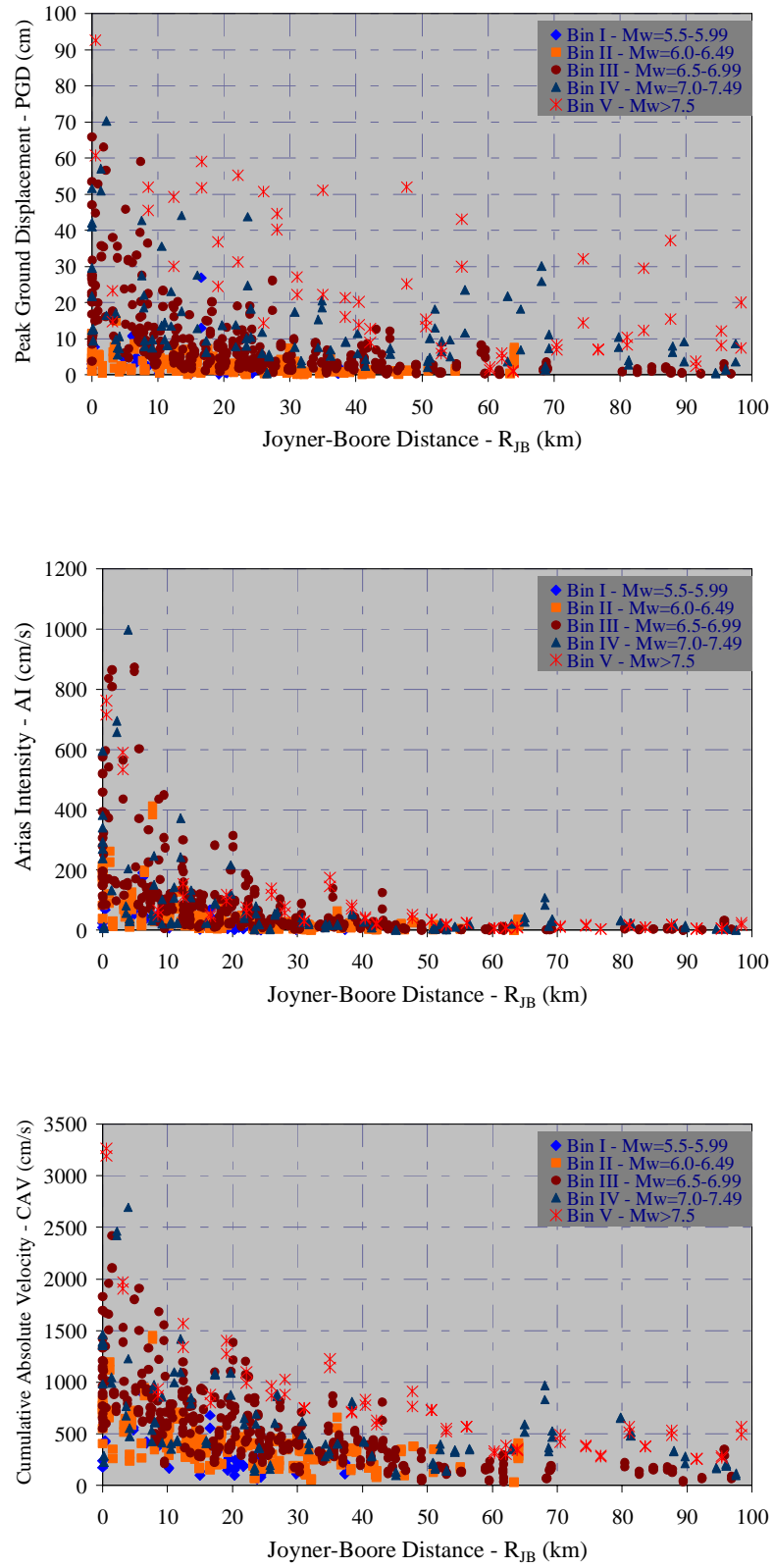


Figure 3.13. Variation of peak ground displacements, Arias intensities and cumulative absolute velocities with Joyner-Boore distance from top to bottom, respectively

Table 3.4. Number of the records in Bin I based on the event, faulting mechanism and site class grouping

$M_w = 5.5 - 5.99$				Site Class (NEHRP)			
Event Name		Faulting Mechanism		B	C	D	E
Coyote Lake 1979/08/06 17:05	16	42	Strike Slip	2	6	8	-
Livermore 1980/01/24 19:00	12			4	8	-	-
Chalfant Valley 1986/07/20 14:29	8			-	-	8	-
Westmorland 1981/04/26 12:09	6			-	2	4	-
Taiwan SMART1(5) 1981/01/29	2	2	Reverse Normal	-	-	2	-
Santa Barbara 1978/08/13	4	4	Reverse Oblique	-	4	-	-
<b>TOTAL</b>	<b>48</b>			6	20	22	0

Table 3.5. Number of the records in Bin I based on site class and distance grouping

$M_w = 5.5 - 5.99$	Joyner-Boore Distance (km)				
Site Class (NEHRP)	$R_{JB} \leq 10$	$10 < R_{JB} \leq 20$	$20 < R_{JB} \leq 40$	$40 < R_{JB} \leq 80$	$80 < R_{JB} \leq 100$
<b>B</b>	2	-	-	-	-
<b>C</b>	4	4	8	-	-
<b>D</b>	8	6	16	-	-
<b>E</b>	-	-	-	-	-
<b>TOTAL</b>	14	10	24	0	0



Table 3.6. Number of the records in Bin II based on the event, faulting mechanism and site class grouping

$M_w = 6.0 - 6.49$				Site Class (NEHRP)			
Event Name		Faulting Mechanism		B	C	D	E
Morgan Hill 1984/04/24 21:15	30	56	Strike Slip	2	12	16	-
Parkfield 1966/06/28 04:26	10			-	6	4	-
Chalfant Valley 1986/07/21 14:42	14			-	-	14	-
Superstition Hills(A) 1987/11/24 05:14	2			-	-	2	-
Coalinga 1983/05/02 23:42	16	22	Reverse Normal	-	10	6	-
Taiwan SMART1(40) 1986/05/20	6			-	-	6	-
N. Palm Springs 1986/07/08 09:20	32	104	Reverse Oblique	-	10	22	-
Whittier Narrows 1987/10/01 14:42	72			4	24	44	-
Mammoth Lakes 1980/05/25 16:34	6	6	Normal Oblique	-	2	4	-
<b>TOTAL</b>	<b>188</b>			6	64	118	0

Table 3.7. Number of the records in Bin II based on site class and distance grouping

$M_w = 6.0 - 6.49$	Joyner-Boore Distance (km)				
Site Class (NEHRP)	$R_{JB} \leq 10$	$10 < R_{JB} \leq 20$	$20 < R_{JB} \leq 40$	$40 < R_{JB} \leq 80$	$80 < R_{JB} \leq 100$
<b>B</b>	-	4	2	-	-
<b>C</b>	16	10	26	12	-
<b>D</b>	20	40	40	18	-
<b>E</b>	-	-	-	-	-
<b>TOTAL</b>	36	54	68	30	0

Table 3.8. Number of the records in Bin III based on the event, faulting mechanism and site class grouping

$M_w = 6.50 - 6.99$				Site Class (NEHRP)			
Event Name		Faulting Mechanism		B	C	D	E
Kobe 1995/01/16 20:46	20	104	Strike slip	-	8	10	2
Erzincan, Turkey 1992/03/13	2			-	-	2	-
Superstitt Hills(B) 1987/11/24 13:16	16			-	2	14	-
Imperial Valley 1940/05/19 04:37	2			-	-	2	-
Imperial Valley 1979/10/15 23:16	62			-	6	54	2
Borrego Mtn 1968/04/09 02:30	2			-	-	2	-
Borah Peak 1983/10/28 14:06	6	30	Normal	-	6	-	-
Irpinia, Italy 1980/11/23 19:34	24			10	10	4	-
Northridge 1994/01/17 12:31	84	136	Reverse normal	14	32	38	-
San Fernando 1971/02/09 14:00	44			4	24	16	-
Friuli, Italy 1976/05/06 20:00	8			-	4	4	-
Loma Prieta 1989/10/18 00:05	58	58	Reverse oblique	2	32	22	2
<b>TOTAL</b>		<b>328</b>		30	124	168	6

Table 3.9. Number of the records in Bin III based on site class and distance grouping

$M_w = 6.50 - 6.99$	Joyner-Boore Distance (km)				
Site Class (NEHRP)	$R_{JB} \leq 10$	$10 < R_{JB} \leq 20$	$20 < R_{JB} \leq 40$	$40 < R_{JB} \leq 80$	$80 < R_{JB} \leq 100$
<b>B</b>	10	6	4	8	2
<b>C</b>	18	24	40	32	10
<b>D</b>	56	32	52	22	6
<b>E</b>	-	2	2	2	-
<b>TOTAL</b>	84	64	98	64	18

Table 3.10. Number of the records in Bin IV based on the event, faulting mechanism and site class grouping

M <sub>w</sub> = 7.0 - 7.49				Site Class (NEHRP)			
Event Name		Faulting Mechanism		B	C	D	E
Duzce, Turkey 1999/11/12	26	92	Strike slip	2	16	8	-
Kocaeli, Turkey 1999/08/17	26			4	8	12	2
Landers 1992/06/28 11:58	40			-	14	26	-
Cape Mendocino 1992/04/25 18:06	12	18	Reverse normal	-	8	4	-
Kern County 1952/07/21 11:53	4			-	4	-	-
Tabas, Iran 1978/09/16	2			-	-	2	-
TOTAL	110			6	50	52	2

Table 3.11. Number of the records in Bin IV based on site class and distance grouping

$M_w = 7.0 - 7.49$	Joyner-Boore Distance (km)				
Site Class (NEHRP)	$R_{JB} \leq 10$	$10 < R_{JB} \leq 20$	$20 < R_{JB} \leq 40$	$40 < R_{JB} \leq 80$	$80 < R_{JB} \leq 100$
<b>B</b>	4	-	2	-	-
<b>C</b>	14	8	12	10	6
<b>D</b>	8	8	12	18	6
<b>E</b>	-	-	-	-	2
<b>TOTAL</b>	26	16	26	28	14

Table 3.12. Number of the records in Bin V based on the event, faulting mechanism and site class grouping

$M_w > 7.5$		Site Class (NEHRP)			
Event Name	Faulting Mechanism	B	C	D	E
Chi-Chi, Taiwan 1999/09/20	Reverse oblique	2	28	26	4
<b>TOTAL</b>	<b>60</b>	2	28	26	4

Table 3.13. Number of the records in Bin V based on site class and distance grouping

$M_w > 7.5$	Joyner-Boore Distance (km)				
Site Class (NEHRP)	$R_{JB} \leq 10$	$10 < R_{JB} \leq 20$	$20 < R_{JB} \leq 40$	$40 < R_{JB} \leq 80$	$80 < R_{JB} \leq 100$
<b>B</b>	-	-	-	2	-
<b>C</b>	2	2	8	12	4
<b>D</b>	4	4	4	6	8
<b>E</b>	-	-	-	4	-
<b>TOTAL</b>	6	6	12	24	12

### 3.4.3. Analyses Results

Through the OpenSees simulations for 8,808 nonlinear dynamic analyses, acceleration and displacement time histories of a selected joint at each floor of the buildings were monitored. The selected joint was the left-outer beam-column node at the floor levels and the same through the elevation of the building. The recorded acceleration and displacement values at that joint were the relative values with respect to supports of the building (Figure 3.14). Also, plastic end rotation time histories of the mid-span beams at each floor were tracked. The outputs were post-processed using an ensemble of MATLAB scripts and the peak responses over the time were obtained.

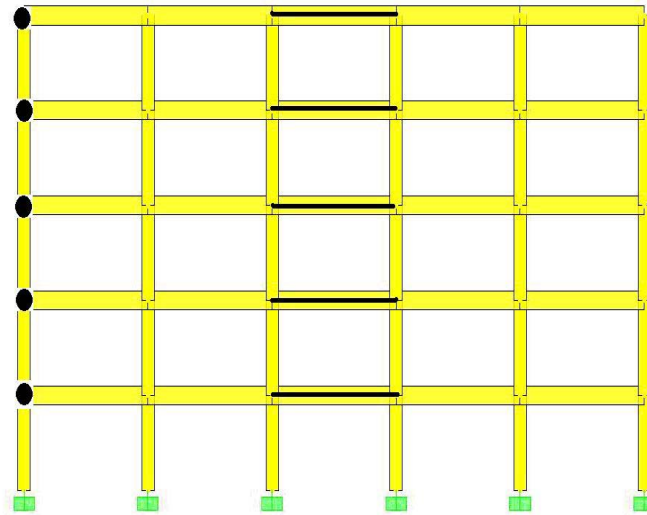


Figure 3.14. Monitored joints (dark circles) and beams (solid lines) during the nonlinear dynamic analyses

The results of the nonlinear dynamic analyses are presented in terms of the following structural response parameters:

- Peak floor displacements
- Peak inter-storey drift ratios
- Peak plastic end rotations of beams
- Peak floor accelerations

The peak responses through the elevations of the buildings are presented in Figure 3.15 - Figure 3.34. Since the input ground motion dataset is subdivided into five bins based on magnitude ranges the results are separately plotted for each bin. The variation in the response of the buildings reflects both the record-to-record variability within a bin and between different bins. In this way, dependency of the structural responses on the magnitude of the earthquake can be observed.

**Peak Floor Displacements (PFD).** Peak floor displacement is the maximum value of the absolute displacement of each floor over the entire time history. In Figure 3.15 - Figure 3.19, peak floor displacements resulting from the nonlinear dynamic analyses under each of five record bins are plotted.

Hancock (2006) gives a summary of literature survey that the maximum floor displacements are related to the duration of individual acceleration pulses, rather than total duration of strong shaking (Bertero *et al.*, 1978, Naeim, 1995, Bonelli, 1998a, 1998b, Araya and Saragoni, 1980). Acceleration pulses with long duration can be caused by a range of different phenomena including fling, forward directivity and constructive interference of reflected waves. Fling is only observed at sites close to the fault rupture and is caused by a displacement pulse created by the permanent deformation along the fault. Forward-directivity is also a near-field effect and is the result of the propagation of the fault rupture towards the site, which causes constructive interference of the seismic radiation leading to concentrated pulse or pulses of motion. The dominant period, or duration, of these pulses increases with earthquake magnitude (Trifunac and Novikova, 1995, Somerville *et al.*, 1997, Somerville, 2000, Bommer *et al.*, 2001). Pulses can also be caused at greater distances by the constructive interference of surface waves reflected from horizontal sediment layers, although these typically have lower energy content than the near-field pulses (e.g. Yamada *et al.*, 1988).

In general, record-to-record variability of displacement demands follow similar patterns for all buildings and there is not too much difference between the demands in buildings with  $R=2$ ,  $R=4$  and  $R=6$ , under Bin I records which have moment magnitudes between 5.5-5.99. The demand variation tends to increase for higher ranges of magnitudes.

The greatest peak floor displacements for all buildings result from the Bin III records which have moment magnitudes between 6.5-6.99.

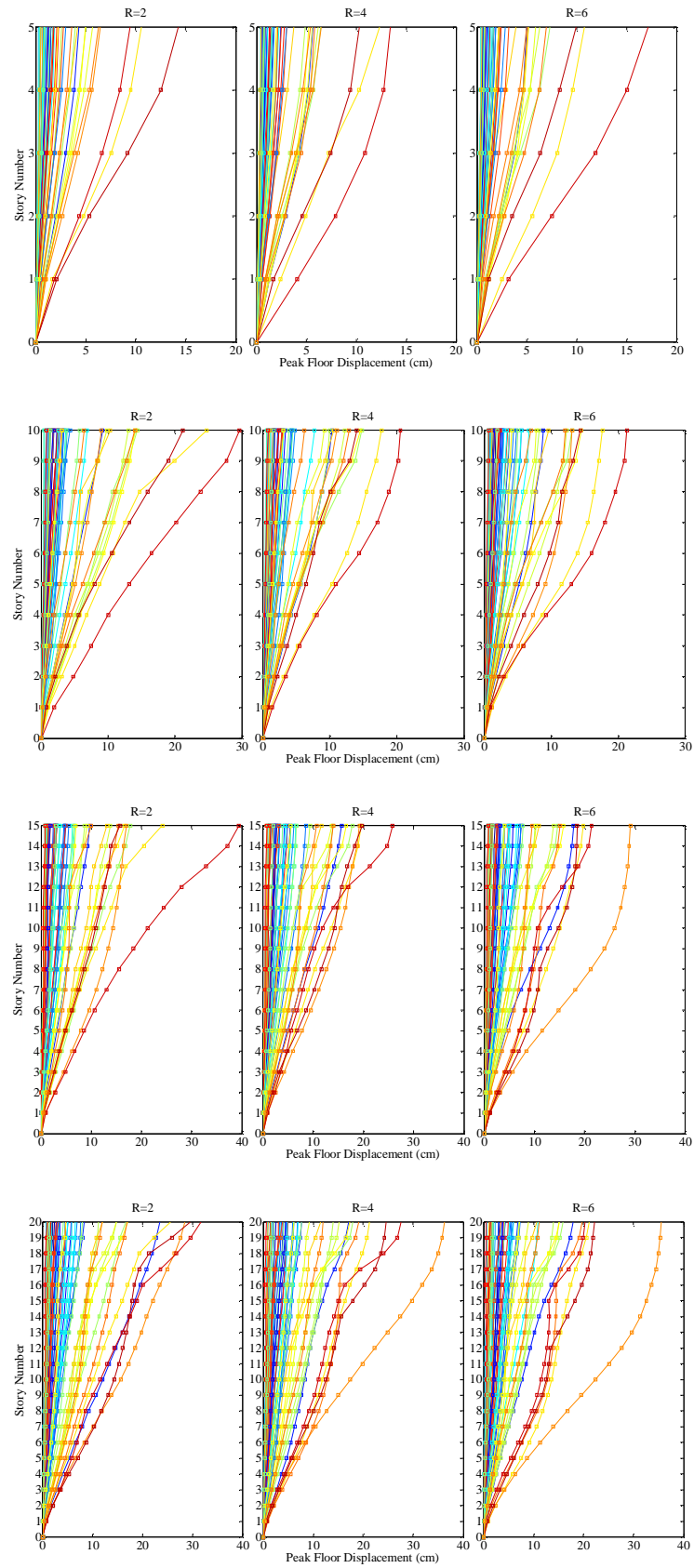


Figure 3.15. Peak floor displacements under Bin I records ( $M_w=5.5-5.99$ )



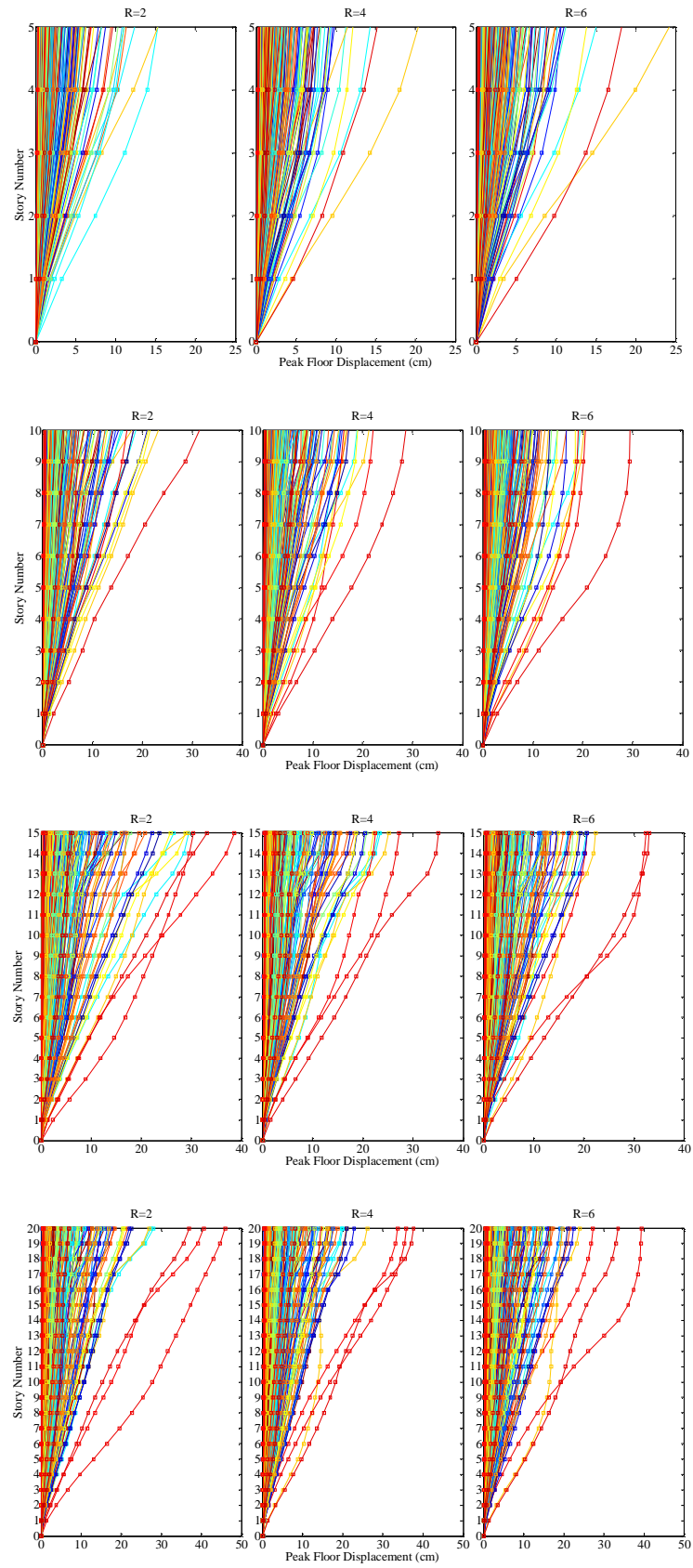


Figure 3.16. Peak floor displacements under Bin II records ( $M_w=6.0-6.49$ )

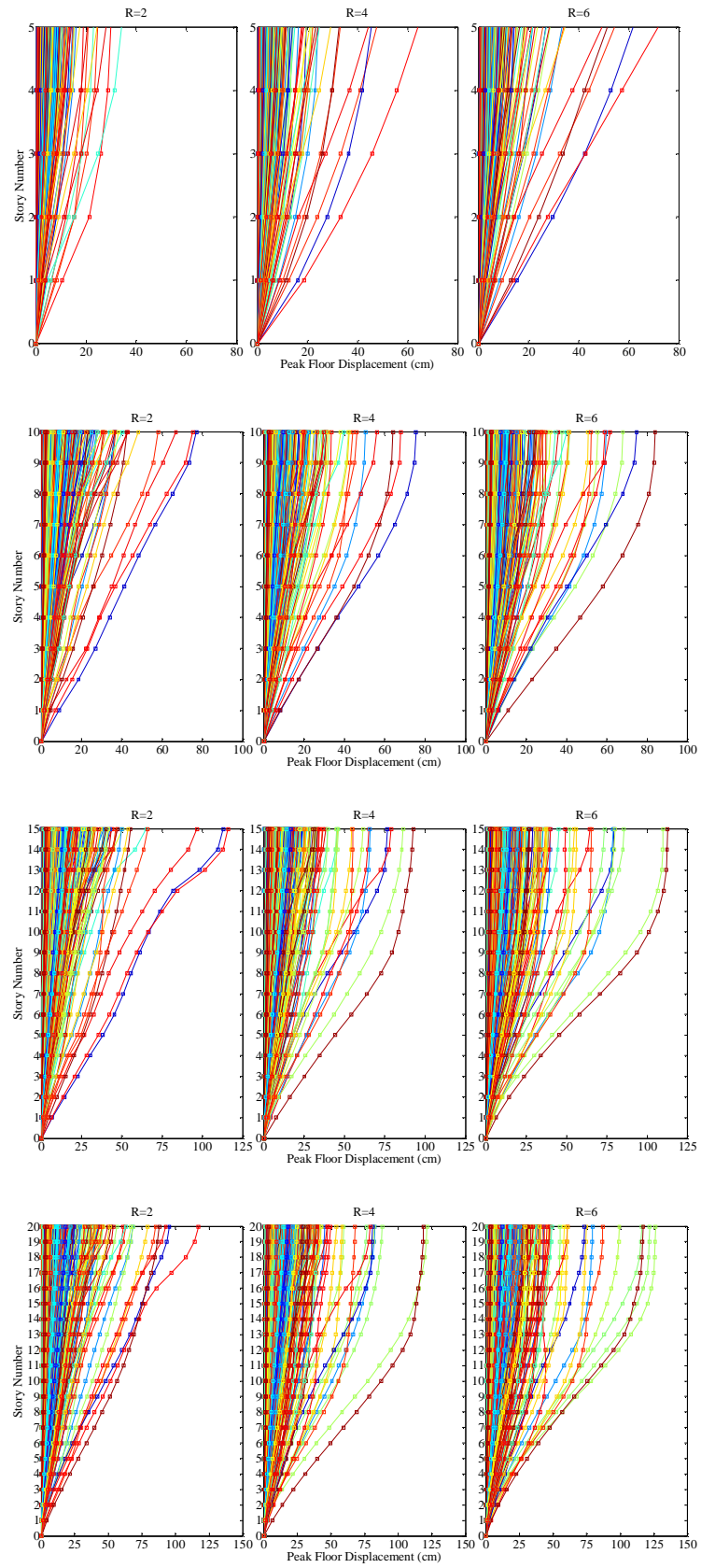


Figure 3.17. Peak floor displacements under Bin III records ( $M_w=6.5-6.99$ )

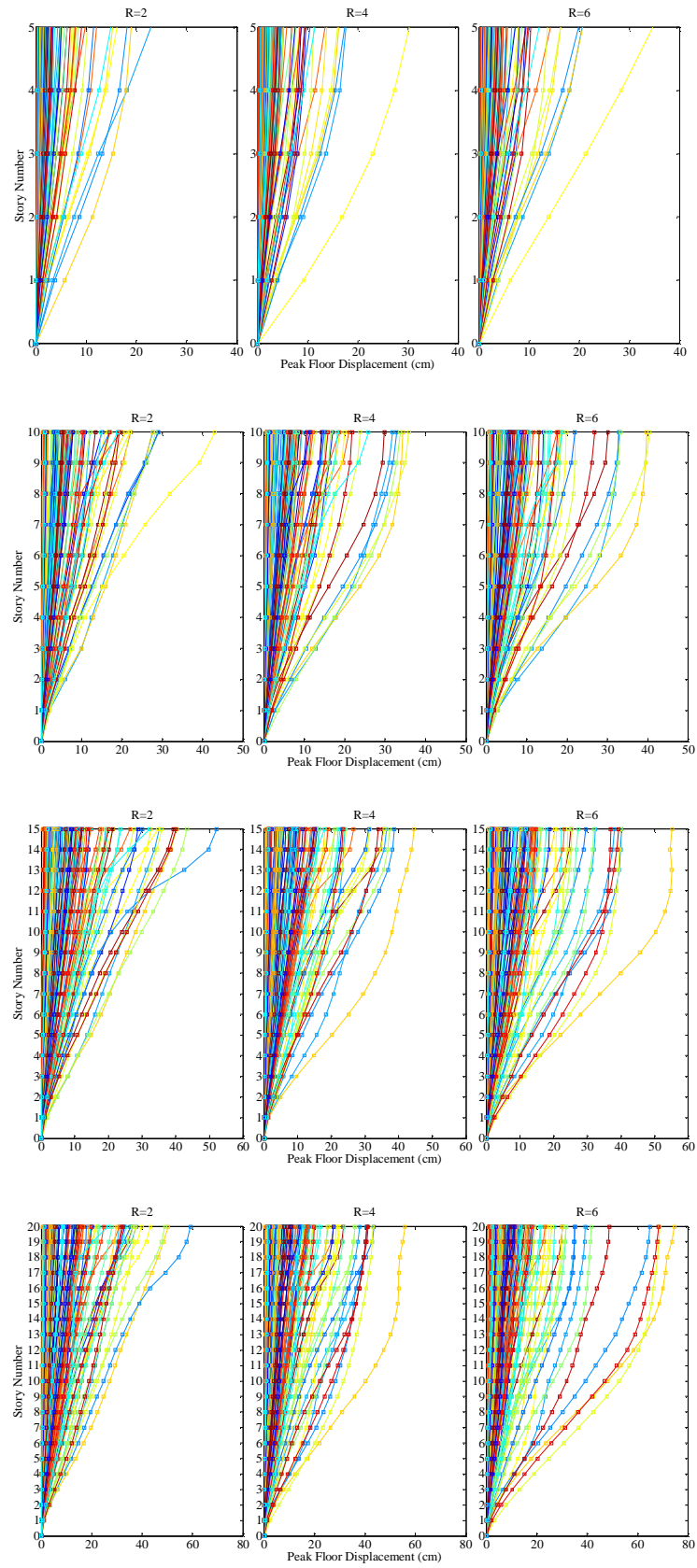


Figure 3.18. Peak floor displacements under Bin IV records ( $M_w=7.0-7.49$ )

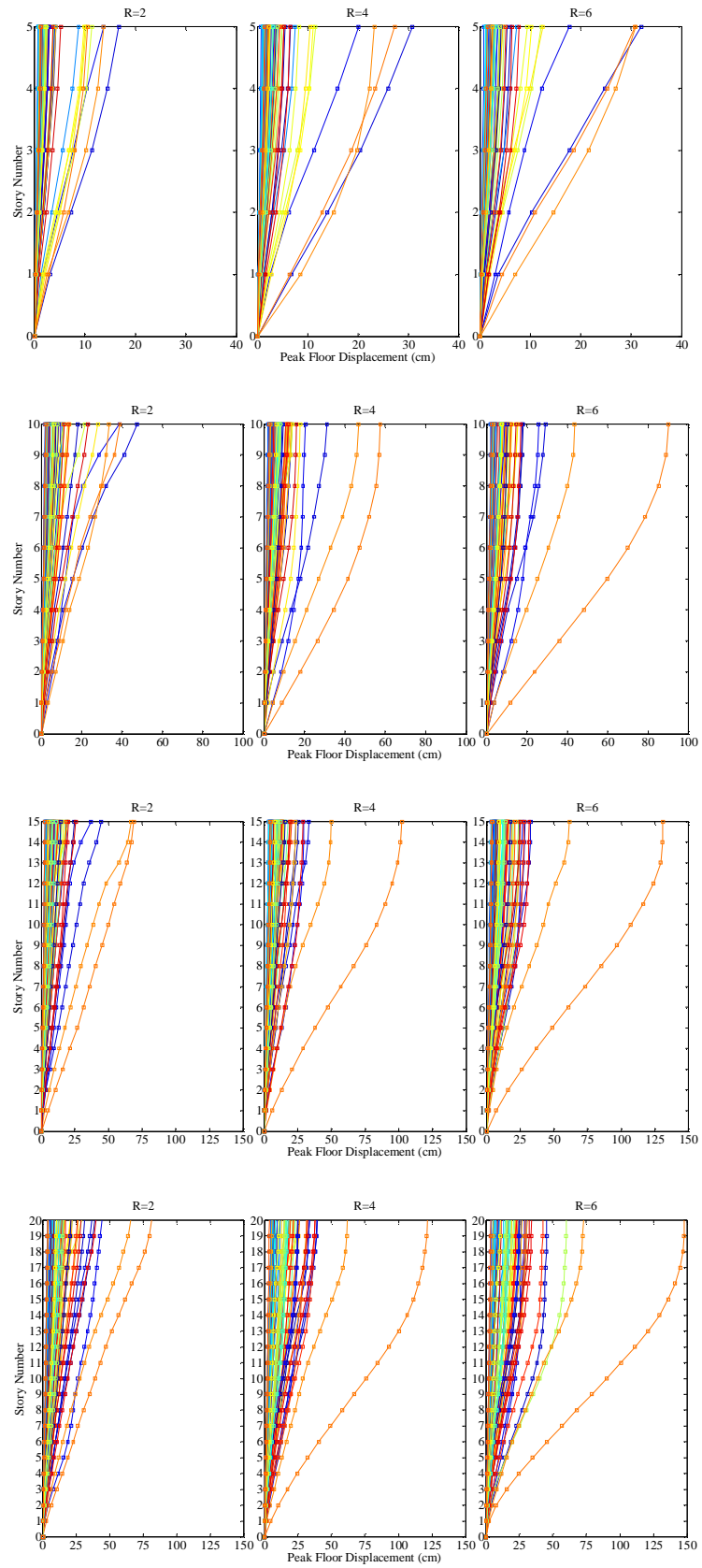


Figure 3.19. Peak floor displacements under Bin V records ( $M_w > 7.5$ )

**Peak Inter-Story Drift Ratios (PIDR).** Inter-story drift ratio is computed as the difference between horizontal displacements of the adjacent stories divided by the story height. Peak inter-story ratio is the maximum value of the absolute inter-story drift ratios at each story level over the entire time history. In Figure 3.20- Figure 3.24, peak inter-story drift ratios resulting from the nonlinear dynamic analyses under each of five record bins are plotted.

In general, record-to-record variability in drift demands gets apparent as the R value increases for all buildings. There is not too much difference between demands in buildings with R=4 and R=6, however, the difference becomes relatively bigger as the building gets taller. The demand variation tends to increase for higher ranges of magnitudes. The greatest peak inter-story drift ratios for all buildings result from the Bin III records which have moment magnitudes between 6.5-6.99.

In five-story buildings, the greater peak inter-story drift ratios are encountered at the second story levels for the lower magnitude values, i.e. under Bin I records, whereas the greatest demands occur at the first story level and relatively uniform demand distributions for middle stories are observed under the actions of the other bins' records.

For the other building groups, which are taller and might be considered as high-rise buildings, the drift profiles for the middle stories have a uniform distribution especially for the buildings with R=2. As the R value increases the variation in peak inter-story drift ratios especially at upper stories becomes greater. While the buildings get taller the contribution of the higher modes to the response of the structure gain more significance. Drifts at higher levels of the building are influenced by higher mode effects. The greatest peak inter-story drift ratios are encountered at the upper levels of ten-, fifteen- and twenty-story buildings. However, the records from Bin III cause considerably high drift demands at the first story levels.

Priestley *et al.*, (2007) and Onem (2008) conducted an investigative study on four-, eight-, twelve-, sixteen- and twenty-story regular reinforced concrete frames and they found similar results. They reported that for the shorter frames, the maximum drift was not greatly affected by higher mode effects and the peak drifts occurred at the first story. For

the sixteen- and twenty-story frames higher mode amplification was substantial and maximum drifts occurred at about of 80 per cent of the frame heights.

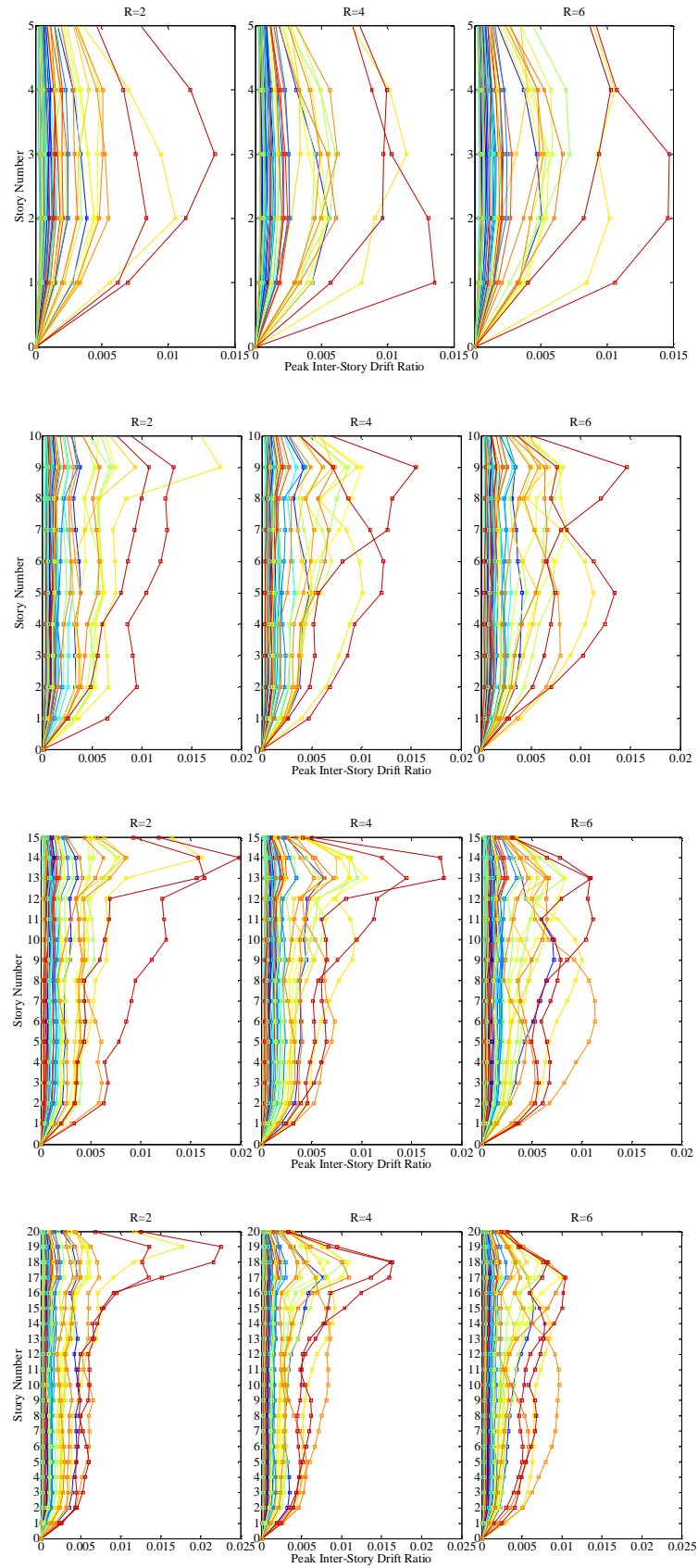


Figure 3.20. Peak inter-story drift ratios under Bin I records ( $M_w=5.5-5.99$ )



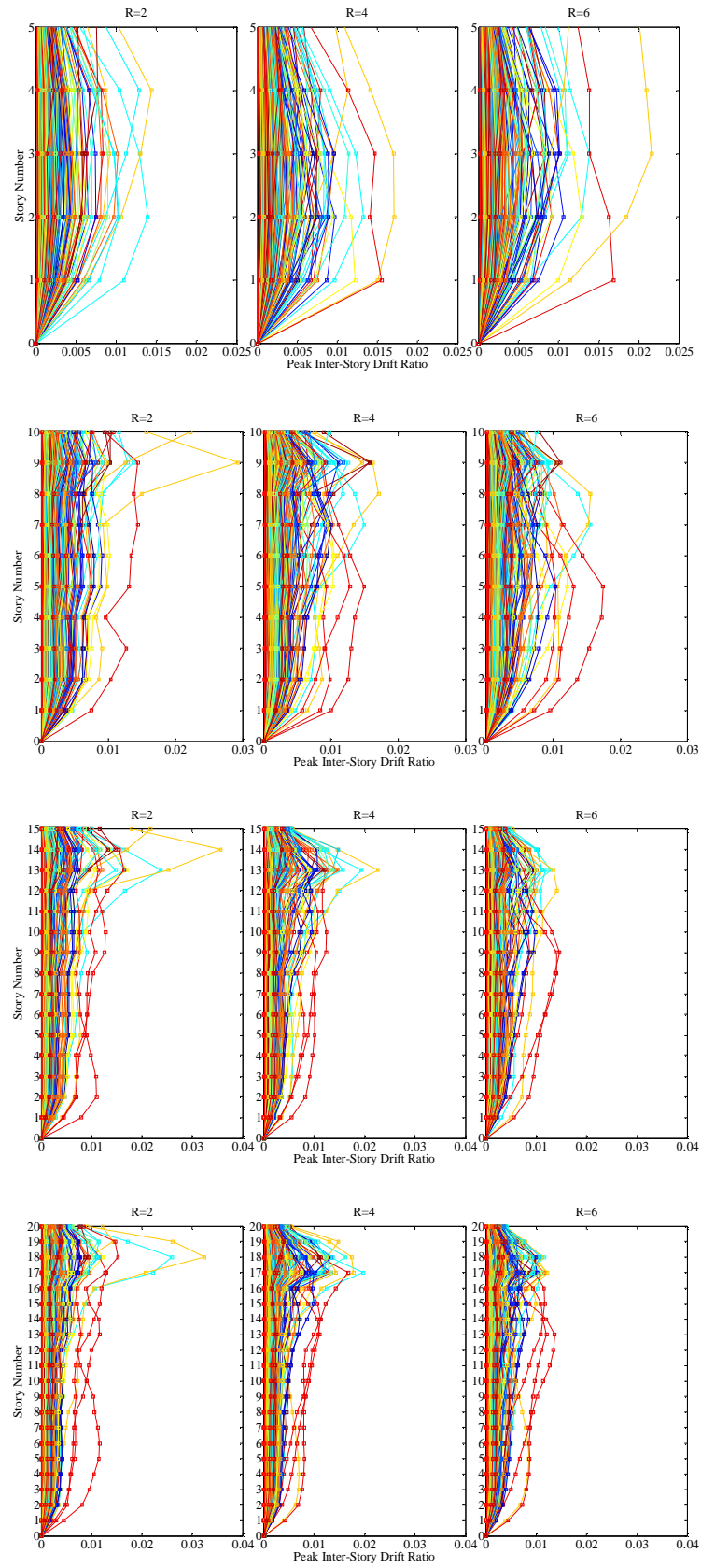


Figure 3.21. Peak inter-story drift ratios under Bin II records ( $M_w=6.0-6.49$ )



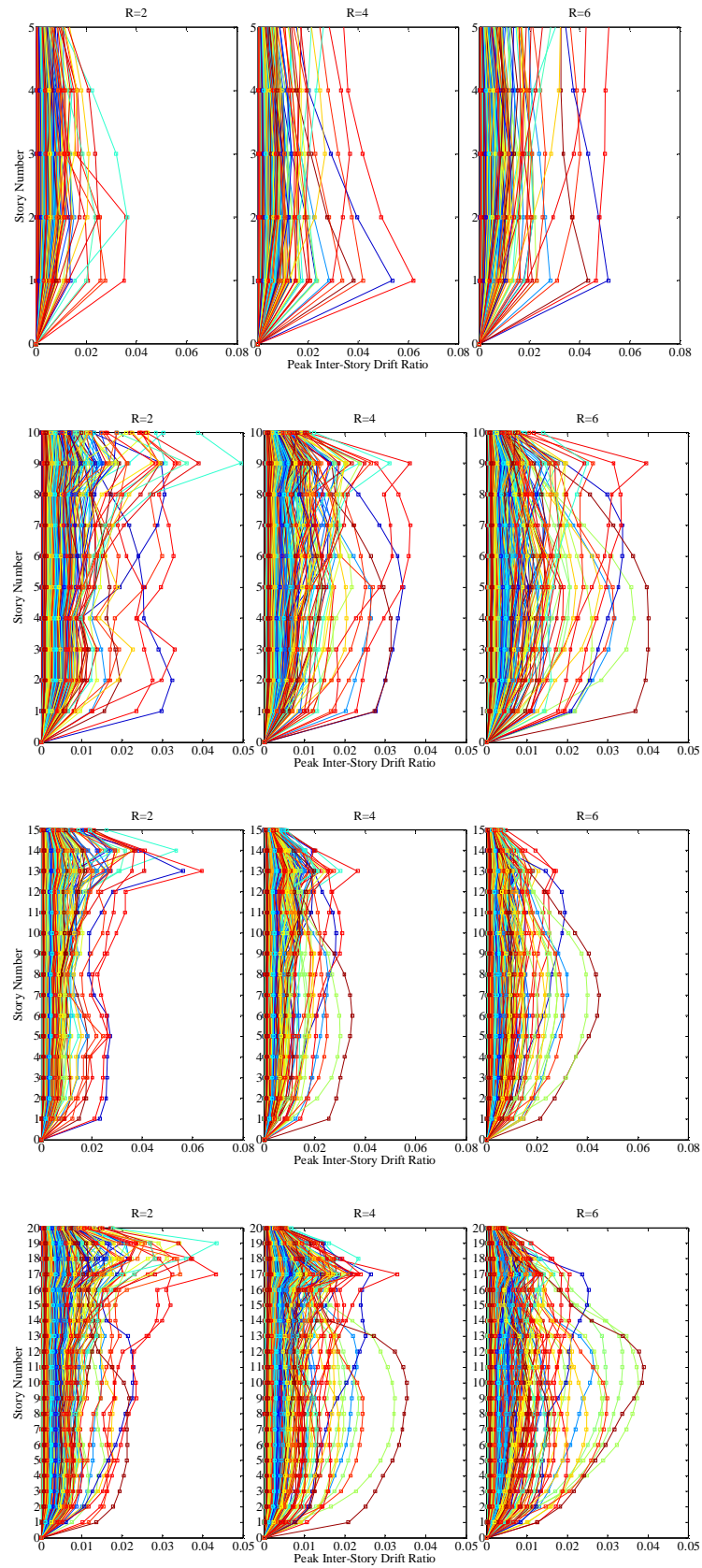


Figure 3.22. Peak inter-story drift ratios under Bin III records ( $M_w=6.5-6.99$ )

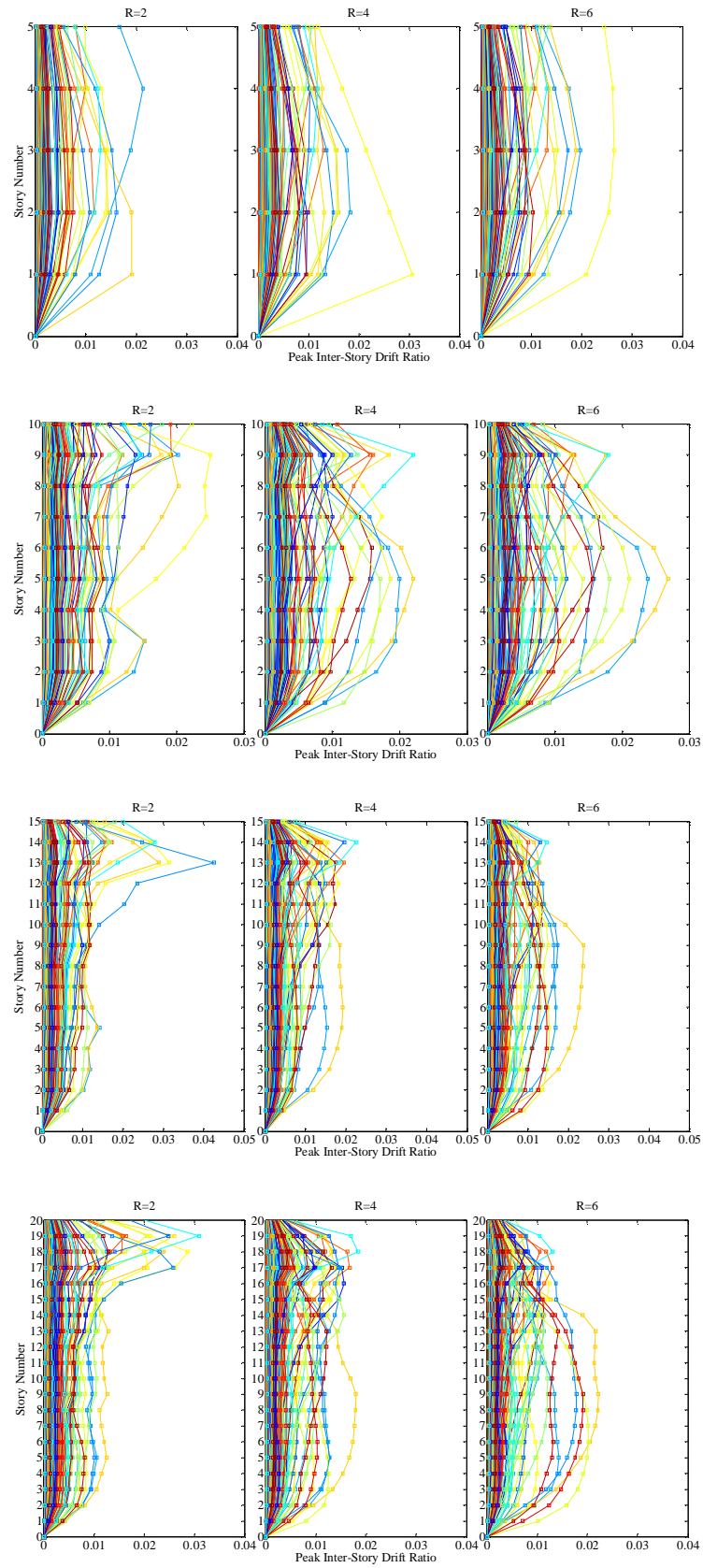


Figure 3.23. Peak inter-story drift ratios under Bin IV records ( $M_w=7.0-7.49$ )

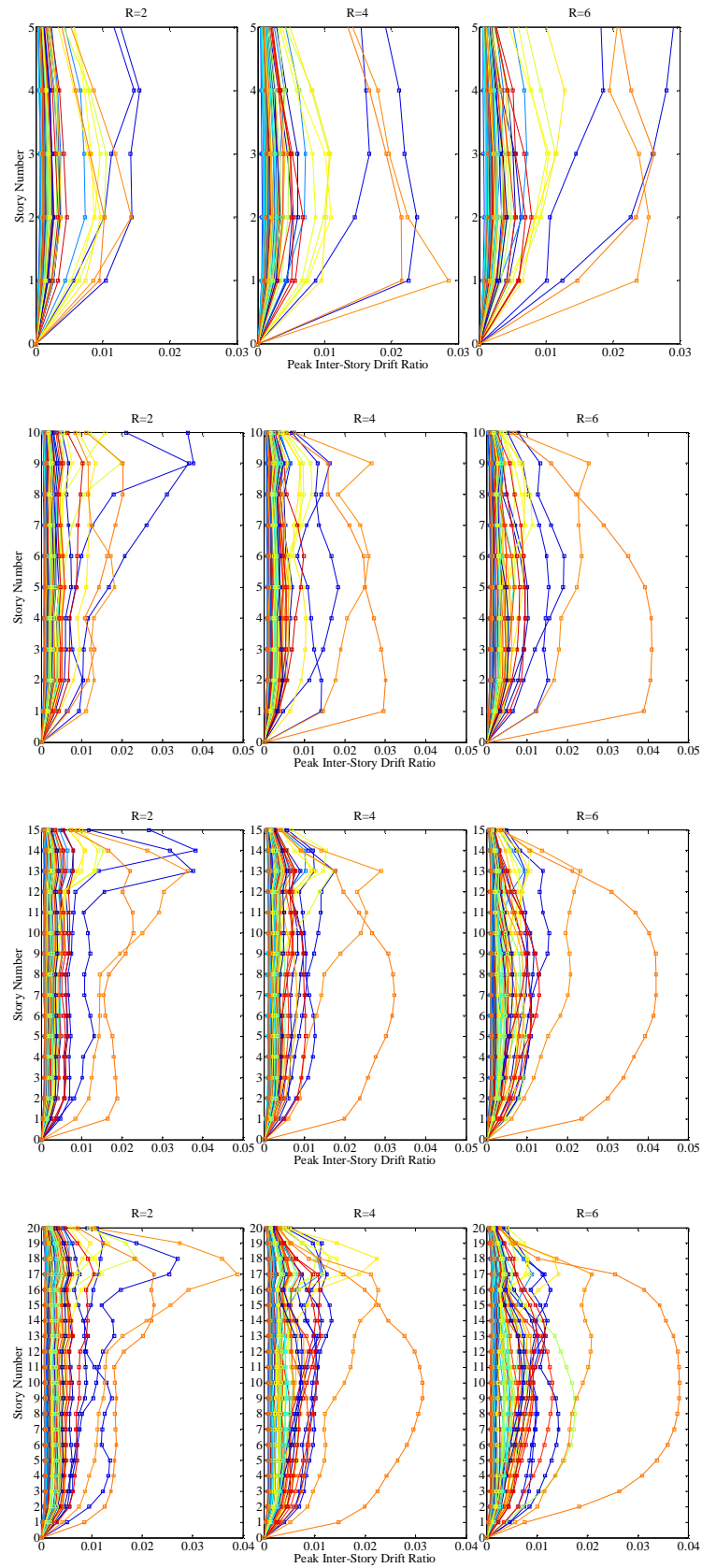


Figure 3.24. Peak inter-story drift ratios under Bin V records ( $M_w > 7.5$ )

**Peak Plastic Rotations of Mid-Beams (BPPR).** Member end rotation is defined as the rotational displacement over the end of the member ( $\theta_{\max}$ ) induced by the earthquake ground motion. Member end rotation is measured in local element co-ordinates so is the rotational displacement over the end of the member relative to the rotation of the joint at the end of the member. Peak end rotation is the maximum value of the plastic rotations computed at both ends of the beams at each floor over the entire time history. In Figure 3.25 -Figure 3.29, peak end rotations resulting from the nonlinear dynamic analyses under each of five record bins are plotted.

Since the buildings designs were based on the strong column - weak beam principle, the distribution of plastic end rotations of beams is consistent with the distribution of the inter-story drift ratios.

In general, record-to-record variability in plastic rotations gets apparent as the R value increases for all buildings. There is not too much difference between demands in buildings with R=4 and R=6, however, the difference becomes relatively bigger as the building gets taller. The demand variation tends to increase for higher ranges of magnitudes as the structure start responding in nonlinear range. The greatest peak plastic rotations for all buildings result from the Bin III records which have moment magnitudes between 6.5-6.99.

In 5-story buildings, the greatest plastic rotations are encountered at the first story levels and the variation over the elevation of the building tends to have a uniform distribution. For ten-, fifteen- and twenty-story buildings the rotation profiles for the middle stories have a uniform distribution especially for the buildings with R=2 under lower magnitude ranges. As the R value increases the variation in the rotation demands especially at upper stories becomes greater. While the buildings get taller the contribution of the higher modes to the response of the structure gain more significance.

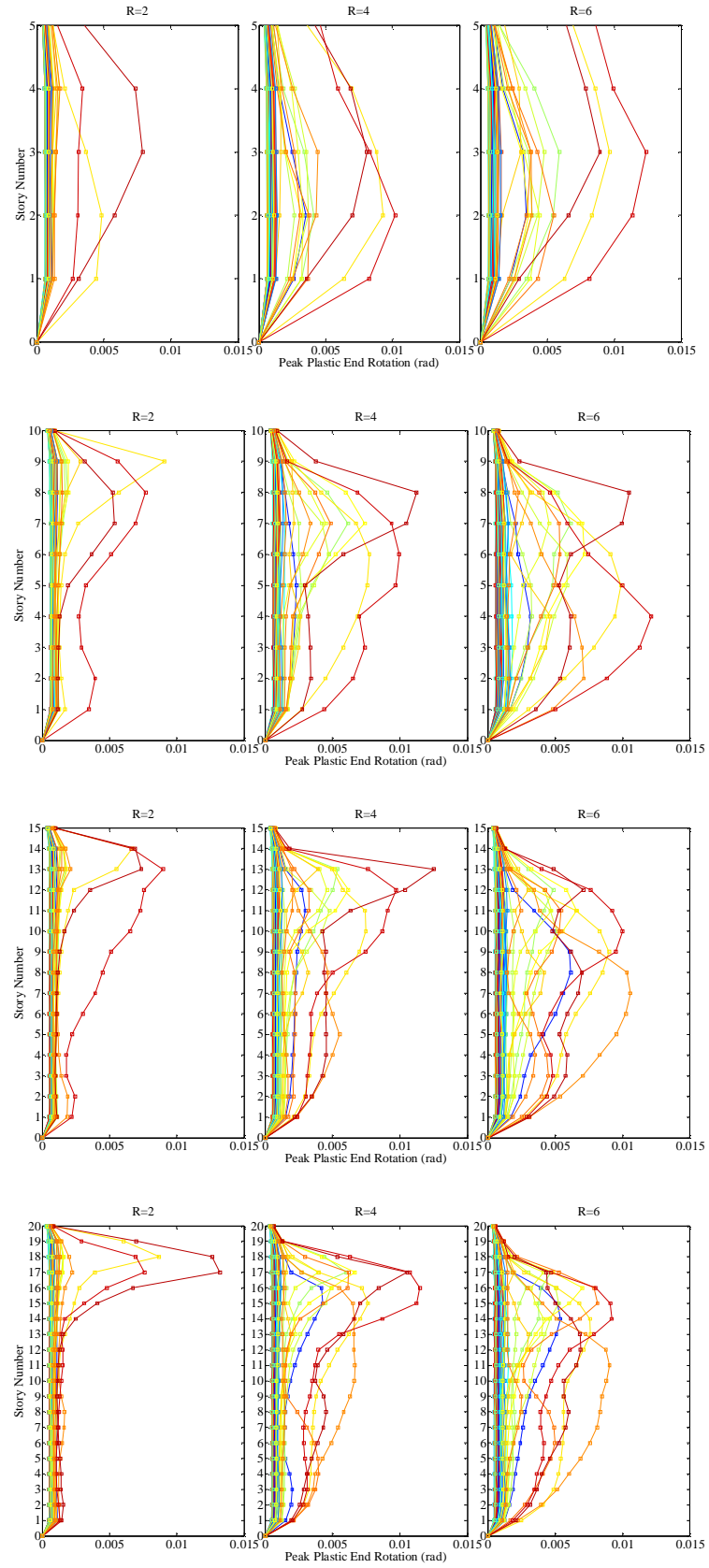


Figure 3.25. Peak plastic rotations of mid-beams under Bin I records ( $M_w=5.5-5.99$ )

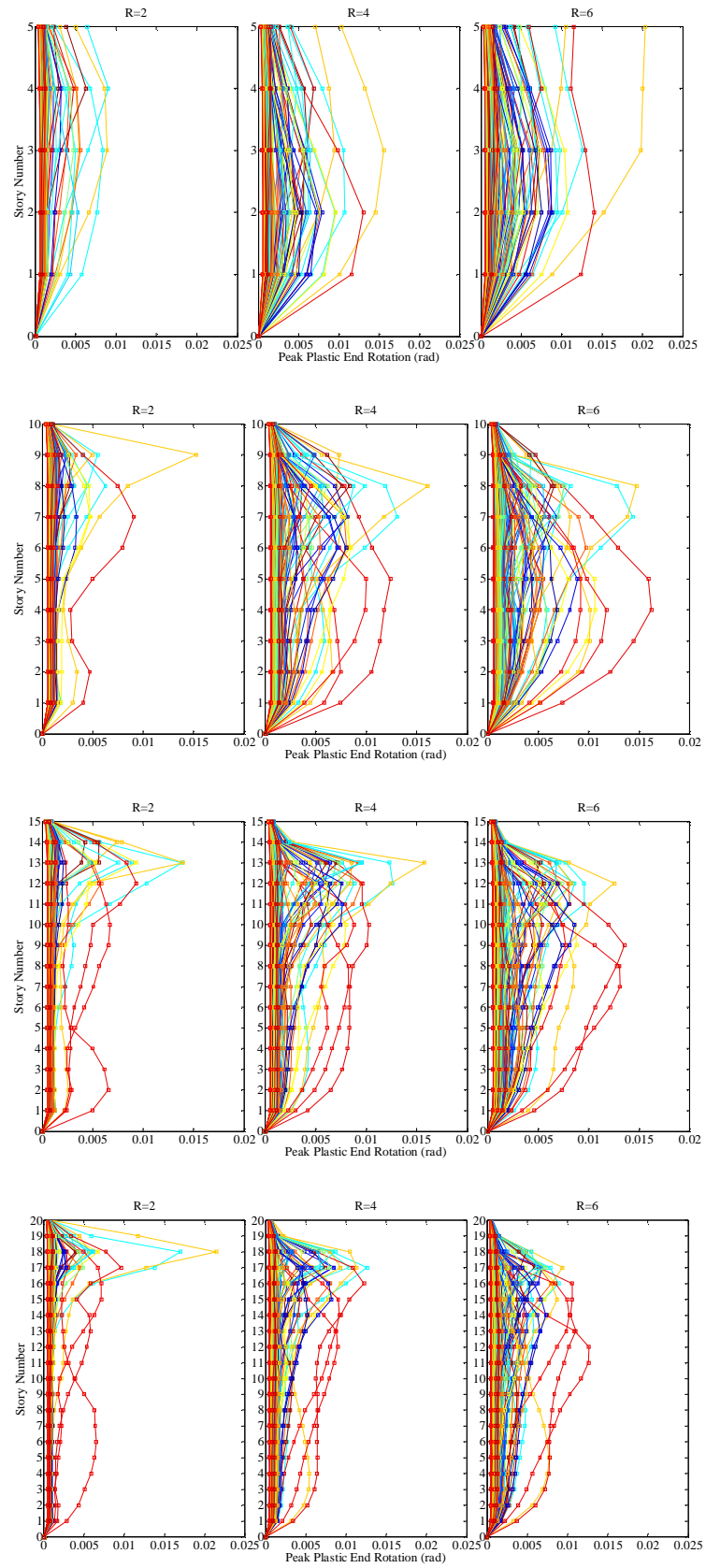


Figure 3.26. Peak plastic rotations of mid-beams under Bin II records ( $M_w=6.0-6.49$ )



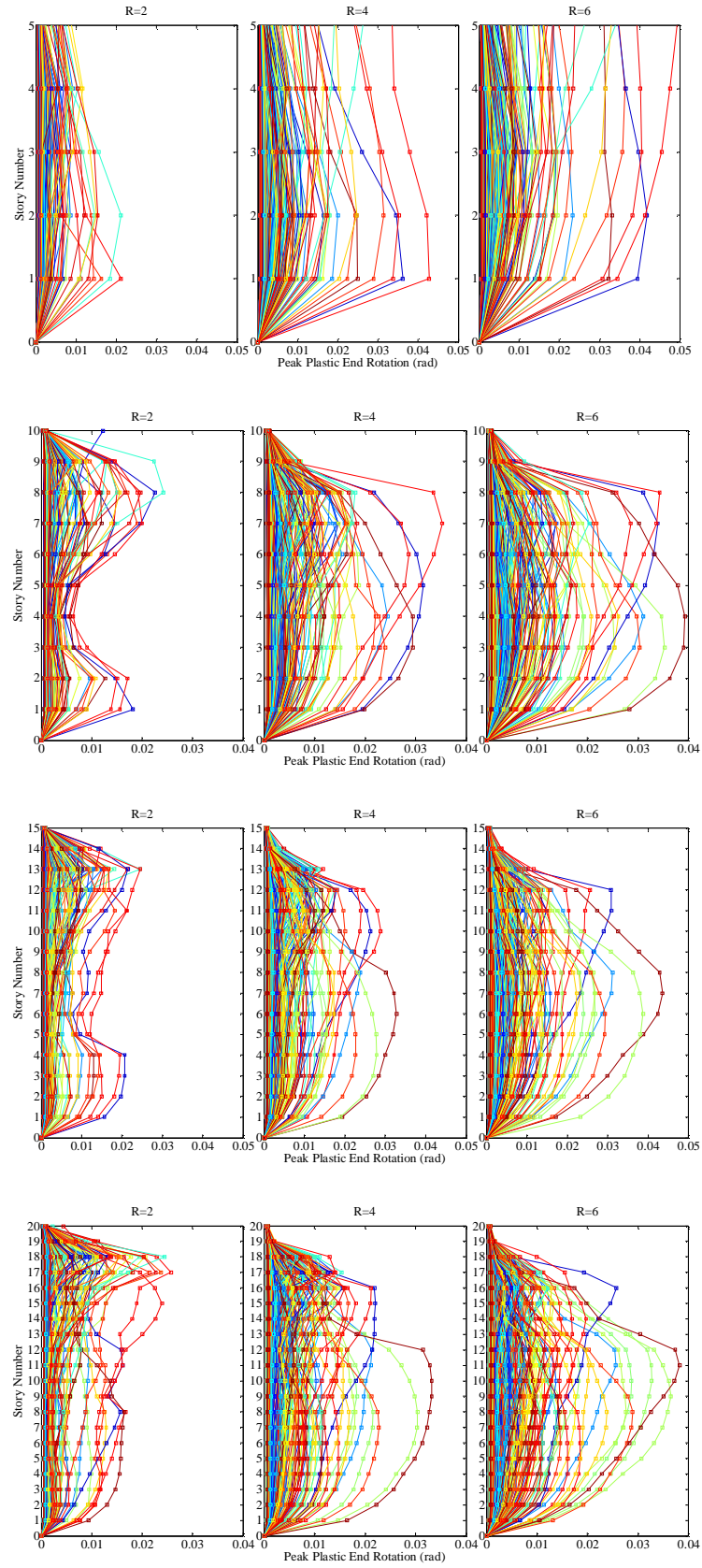


Figure 3.27. Peak plastic rotations of mid-beams under Bin III records ( $M_w=6.5-6.99$ )

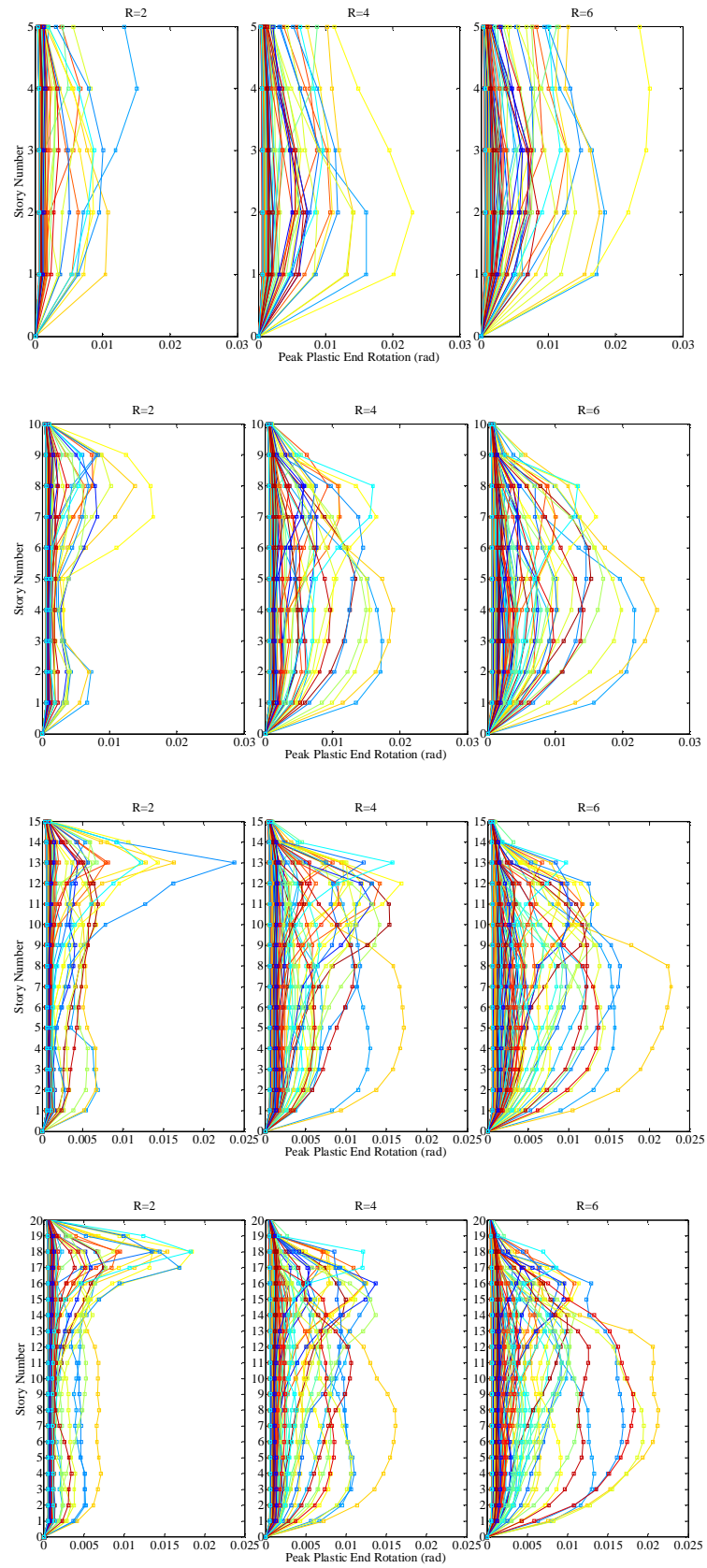


Figure 3.28. Peak plastic rotations of mid-beams under Bin IV records ( $M_w=7.0-7.49$ )



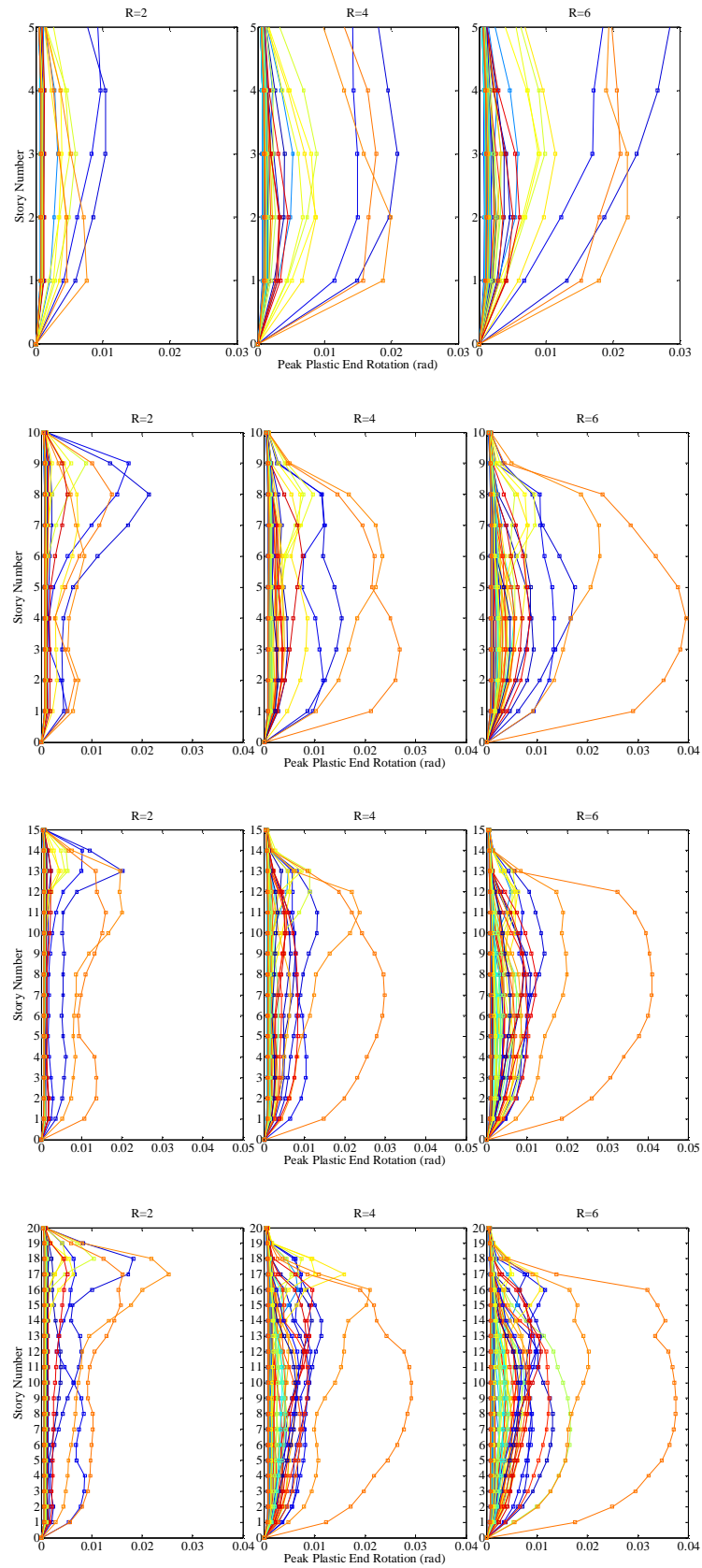


Figure 3.29. Peak plastic rotations of mid-beams under Bin V records ( $M_w > 7.5$ )

**Peak Floor Accelerations (PFA).** Peak floor acceleration is the maximum value of the absolute acceleration of each floor over the entire time history. In Figure 3.30 - Figure 3.34, peak floor accelerations resulting from the nonlinear dynamic analyses under each of five record bins are plotted.

The larger acceleration demands occur in buildings with  $R=2$  as compared to  $R=4$  and  $R=6$  under Bin I records which have moment magnitudes between 5.5-5.99. As the magnitudes of the records increase the acceleration demands get similar for the buildings with different  $R$  values. Record-to-record variability in acceleration demands becomes to be more prominent for higher ranges of magnitudes.

In five- and ten-story buildings, the greatest acceleration demands occur at upper floors under Bin I and Bin II records whereas the similar situation is observed at lower floors of fifteen- and twenty-story buildings. For higher levels ground motion intensity in terms of magnitude, all the buildings have the largest acceleration demands at lower floors. It is also observed that for high levels of ground motion where the building response is strongly nonlinear the reduction in the acceleration values is larger at lower floors of the buildings where the nonlinear behavior of the structure has less effect on filtering the ground motions.

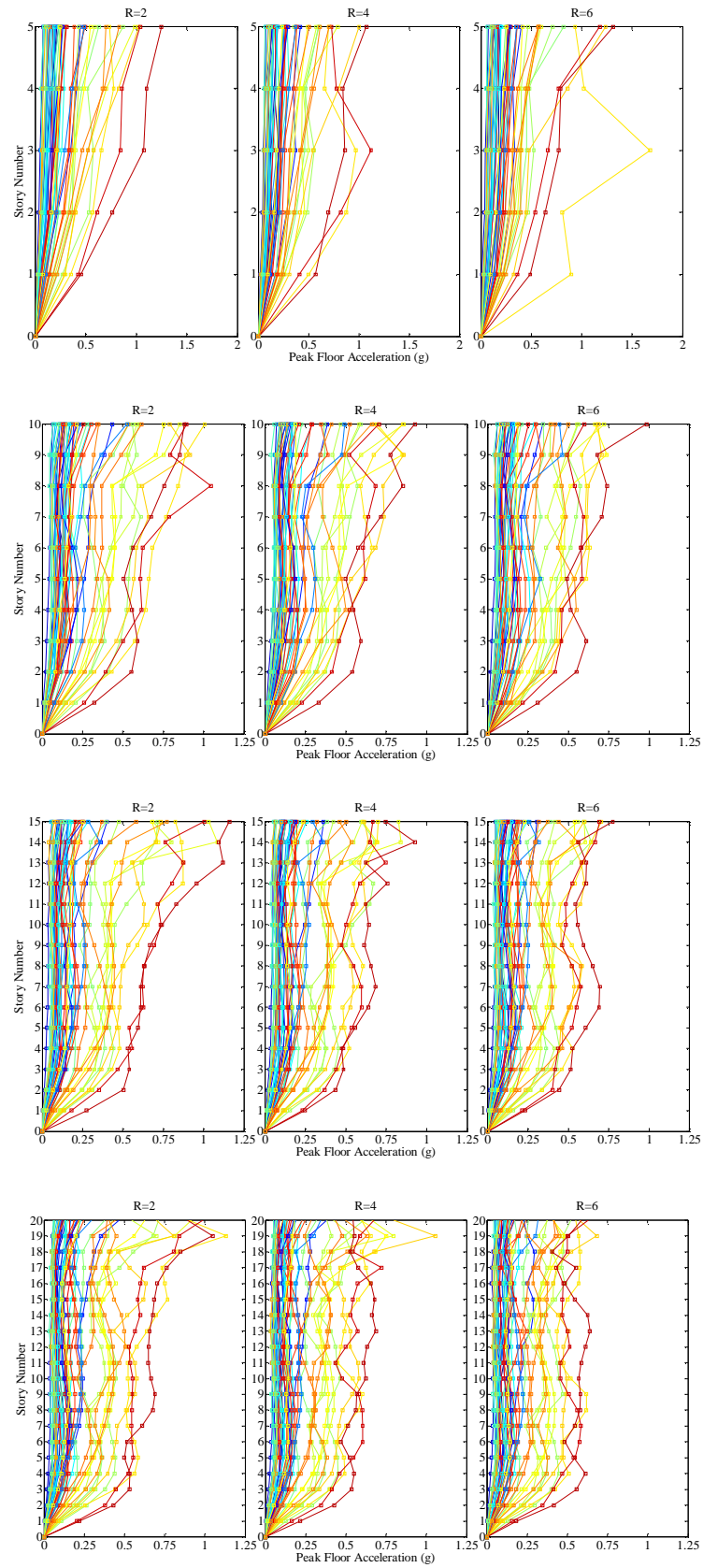


Figure 3.30. Peak floor accelerations under Bin I records ( $M_w=5.5-5.99$ )

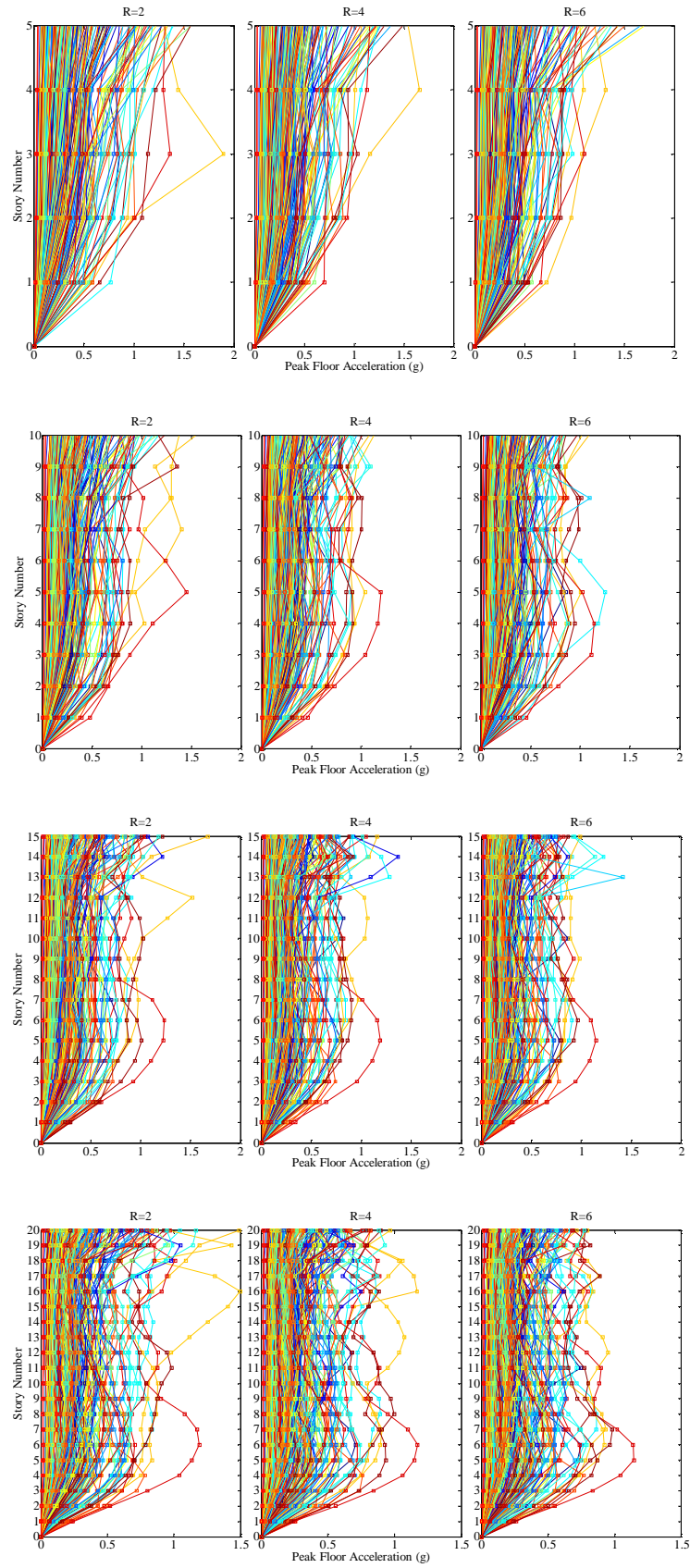


Figure 3.31. Peak floor accelerations under Bin II records ( $M_w=6.0-6.49$ )

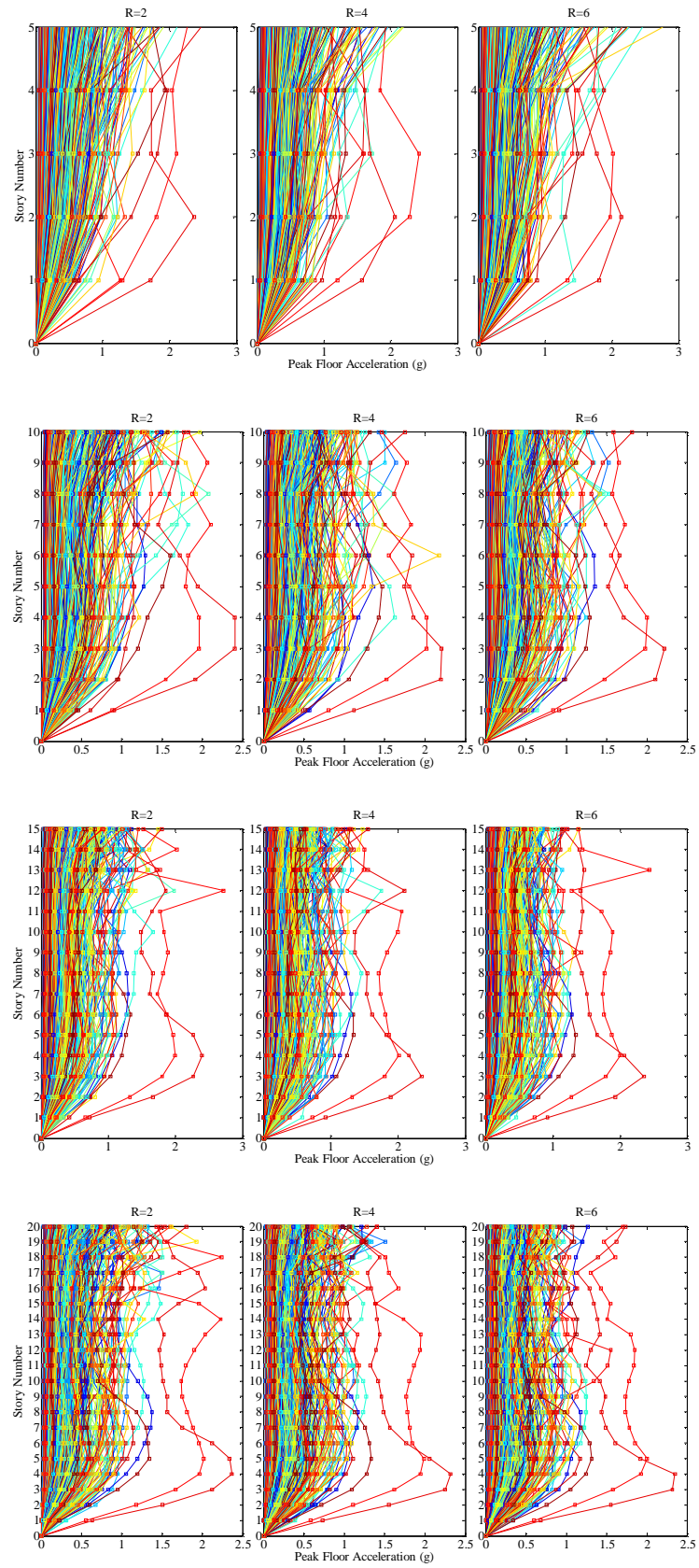


Figure 3.32. Peak floor accelerations under Bin III records ( $M_w=6.5-6.99$ )



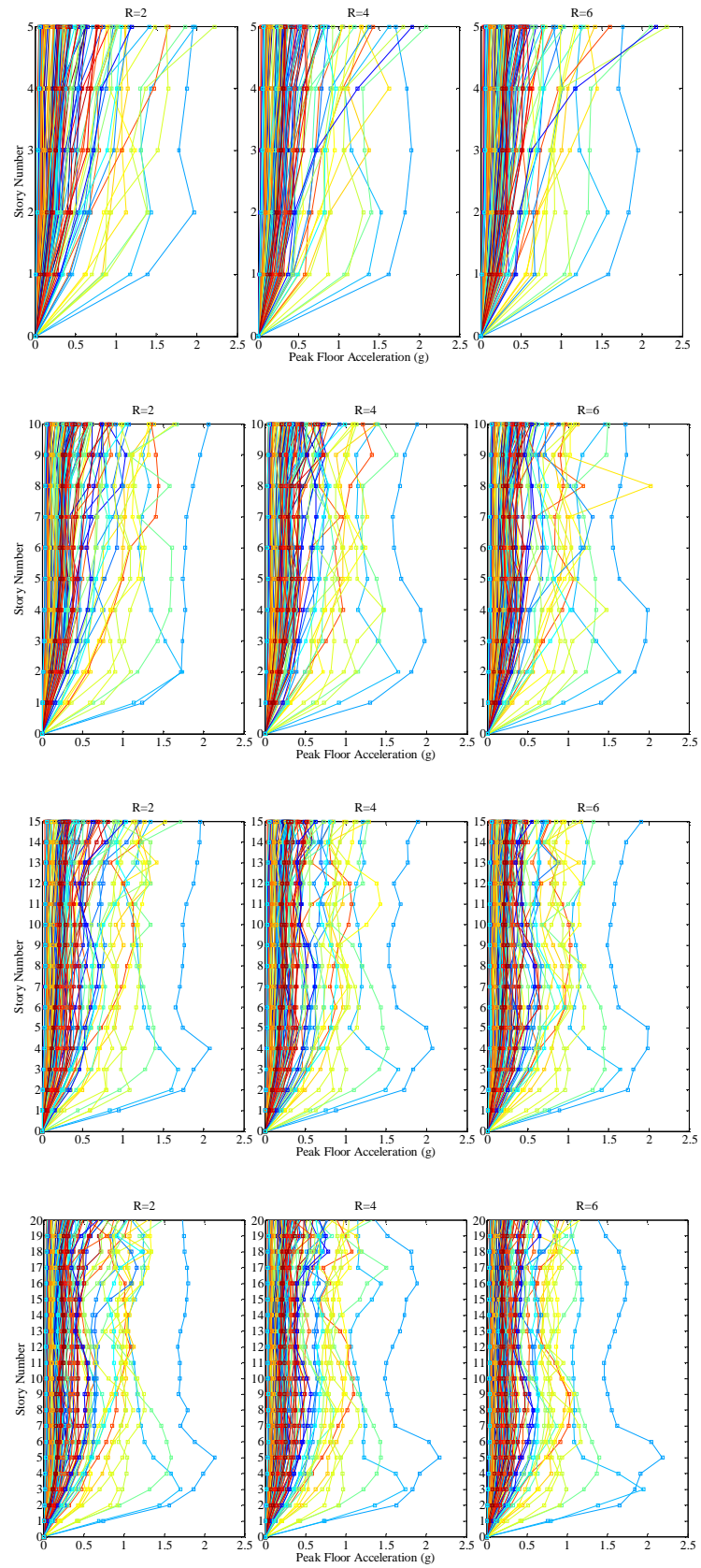


Figure 3.33. Peak floor accelerations under Bin IV records ( $M_w=7.0-7.49$ )

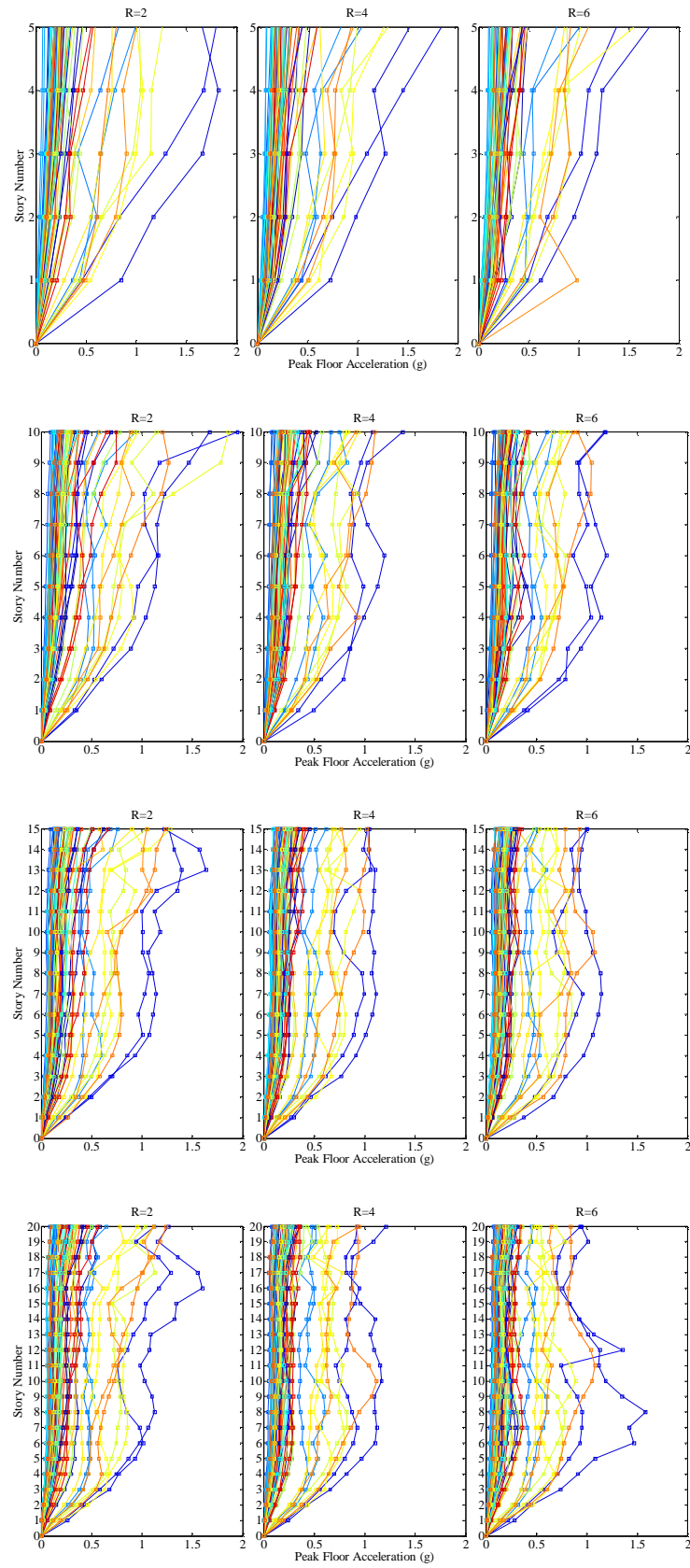


Figure 3.34. Peak floor accelerations under Bin V records ( $M_w > 7.5$ )

### **3.5. Effects of Magnitude, Source-to-Site Distance, Site Class and Faulting Mechanism on the Structural Response**

Magnitude affects the amplitude and frequency content of the ground motion. Source-to-site distance has an effect on the frequency content and near-fault characteristics. Site conditions at the recording station have an impact on the frequency content of the recorded motion. Faulting mechanism affects the amplitude of the ground motion also controls the near-fault characteristics.

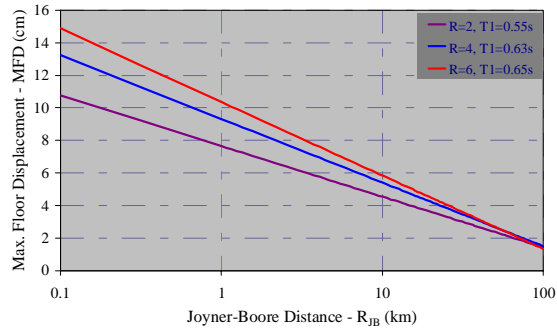
Magnitude, source-to-site distance, soil conditions and faulting mechanism are directly related to the spectral parameters of ground motion via the ground motion prediction equations; thus, additional dependence of the structural response on magnitude and distance is small and can be ignored. The correlations of spectral acceleration values have previously been found to be independent of parameters such as earthquake magnitude or distance (Baker and Cornell, 2005).

The peak ground acceleration reveals a good correlation at very short periods and for structures behaving elastically or almost responding in the elastic range. As the level of inelastic deformation increases and the period shifts towards larger values, PGA correlates poorly with the SDOF deformation demand. The increase in PGV values is associated with an increase in earthquake magnitude and effective duration of records. The frequency composition of ground motions systematically becomes richer in the long period range for increasing PGV (Akkar and Ozen, 2005).

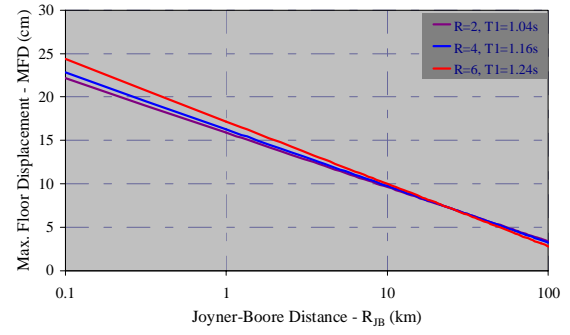
It has been observed from the analyses results that it is difficult to propose a direct correlation between the structural responses and ground motion characteristics in terms of earthquake magnitude, faulting mechanism and soil conditions. However the analyses results allowed for developing the functions for the variation of the structural responses with source-to-site distance as shown in Figure 3.35 - Figure 3.38.



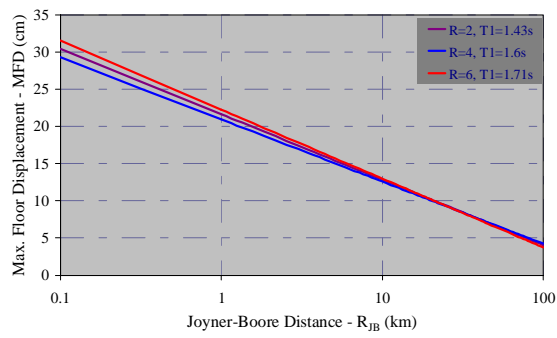
5-story buildings



10-story buildings



15-story buildings



20-story buildings

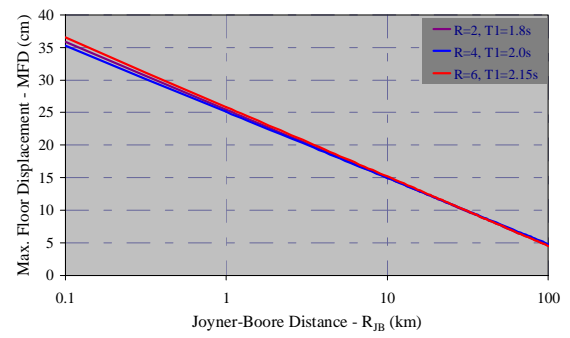
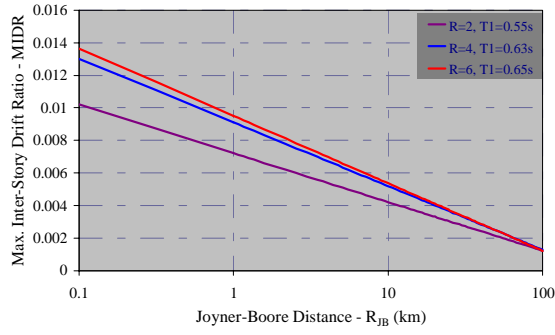
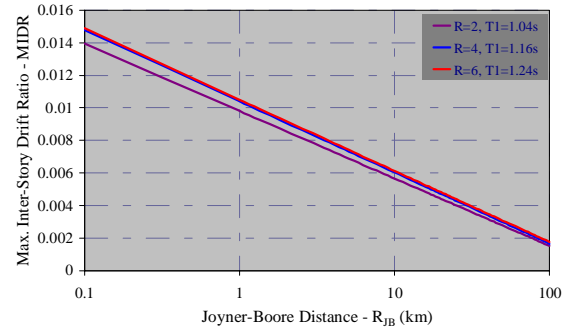


Figure 3.35. Variation of MFD with distance

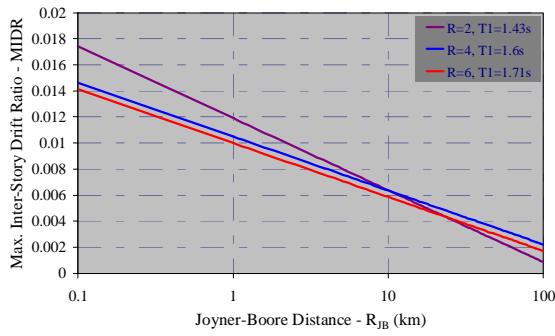
5-story buildings



10-story buildings



15-story buildings



20-story buildings

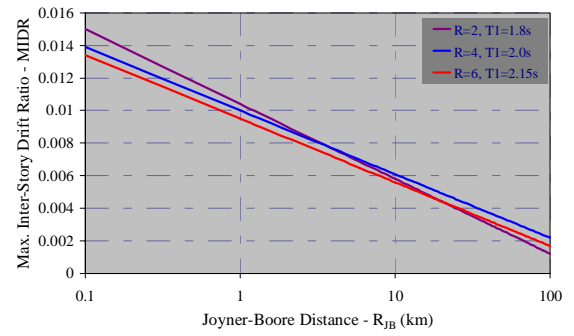
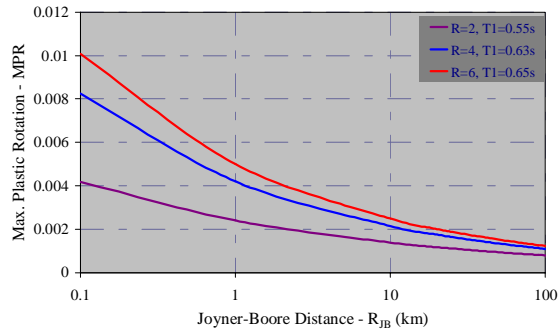
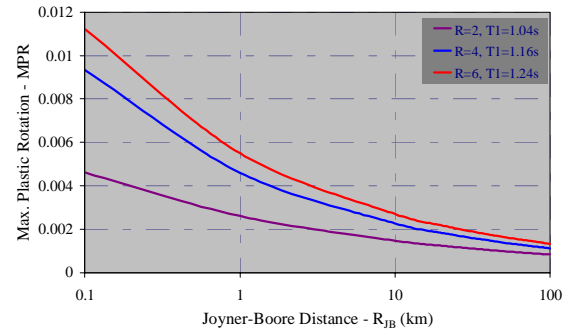


Figure 3.36. Variation of MIDR with distance

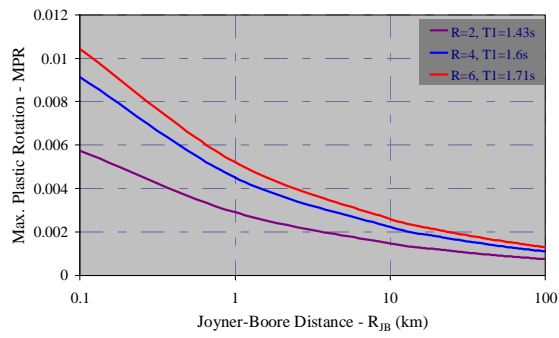
5-story buildings



10-story buildings



15-story buildings



20-story buildings

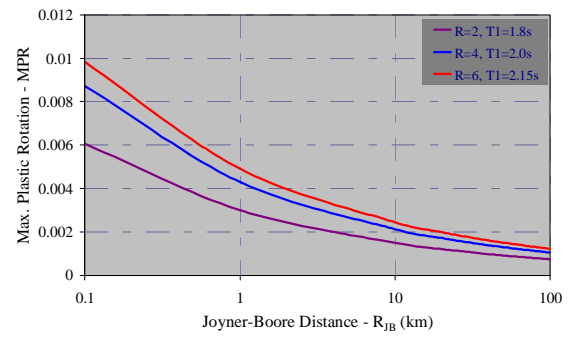
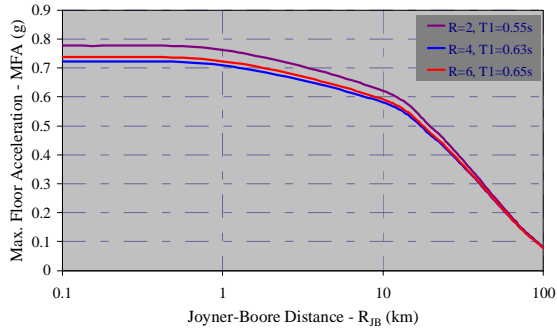
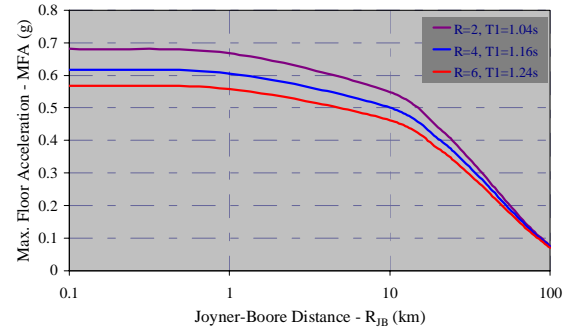


Figure 3.37. Variation of MPR with distance

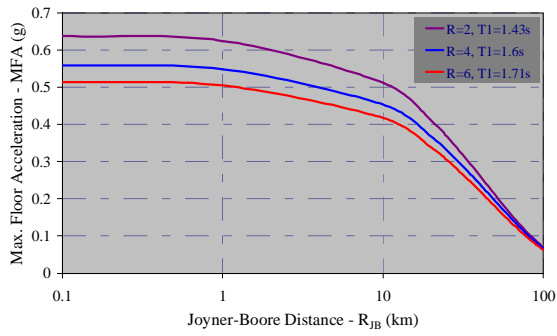
5-story buildings



10-story buildings



15-story buildings



20-story buildings

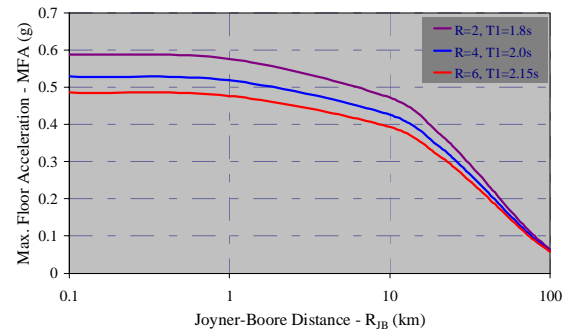


Figure 3.38. Variation of MFA with distance

## **4. CORRELATIONS BETWEEN GROUND MOTION INTENSITY MEASURES (IMs) and ENGINEERING DEMAND PARAMETERS (EDPs)**

### **4.1. Introduction**

For earthquake resistant design and for seismic assessment of existing structures the nonlinear dynamic analysis under the actions resulting from acceleration time histories is becoming more frequently used procedure. As they are utilized more commonly for evaluating the demand on a structure due to earthquake excitation, it increasingly gains more significance to understand which properties of a recorded ground motion are most strongly related to the response caused in the structure. Performance-based earthquake engineering allows the designer to specify and predict, with a reasonable accuracy, the performance (degree of damage) of the structure for a specified level of ground motion intensity. This requires using input ground motion records that adequately represent the damage potential for given seismic hazard levels and structural characteristics. Records to use in nonlinear time-domain analyses should be selected considering magnitude, distance, site condition and other parameters that control the ground motion characteristics. Nonetheless even for the input ground motions that are compatible with the results of seismic hazard disaggregation and represent well the hazard level at the site, the same structure might respond differently under the actions of the input ground motions and a great scatter in the analyses results might be observed.

If the relationships between ground motion intensity and structural response are identified and well-correlated pairs of ground motion and structural response parameters are provided, the selection of the earthquake records as input for the nonlinear dynamic analyses can be done prudently. Furthermore, the estimation of the average structural response and/or the assessment of full probabilistic distribution of the response parameters conditioned on a given ground motion intensity measure can be obtained more accurately.

Given the occurrence of an earthquake, the ground excitation is a continuous random process in time that depends on source characteristics, distance and site condition. The structural response is also a random process that depends on the ground excitation and structural characteristics and excitation parameters. Although such random process models have been developed on the basis of the random process theory, the nonstationarity in the excitation and quite often nonlinear and inelastic dynamic responses of the system render the theoretical treatment difficult for real structural systems (Wen, 2004). To simplify this problem, extensive research has been made on finding some key ground motion intensity measures that correlate well with the structural demand parameter, e.g. Shome *et al.*, (1998), Malhotra, (1999), Kurama and Farrow, (2003). The peak ground acceleration, velocity and displacement have been traditionally used for this purpose.

More recently, spectral response values, e.g. spectral acceleration or spectral displacement at the first mode period of vibration, have been used as intensity measures. One advantage of using spectral parameter as ground motion intensity measure is that these quantities can be directly related to magnitude, source-to-site distance, soil conditions and faulting mechanism via the ground motion prediction equations, thus, additional dependence of the structural response on magnitude and distance becomes small and can be ignored.

Luco, (2002) and Luco and Cornell, (2007) studied on the response of steel structures with different designs and configurations under the actions of recorded ground motions. They examined a number of intensity measures that reflect the structural characteristics such as fundamental period and damping ratio. Based on the regression of the responses, the results showed that the five per cent-damped spectral acceleration or displacement at the fundamental period of the structure generally accurately predicts the structural response. They also examined intensity measures consisting of the combined first and second mode spectral accelerations or displacements and first mode elastic and inelastic spectral accelerations to incorporate the effects of higher modes and inelastic response. The combined measures of the ground motion intensity gave better results as indicated by reducing the dispersion in the regression relationship compared to using only spectral values at the first mode period. However it was achieved at the expense of a more complicated form of the intensity measure.

Baker and Cornell, (2005) proposed a vector-valued ground motion intensity measure consisting of spectral acceleration and epsilon, where epsilon is a measure of the difference between the spectral acceleration of a record and the mean spectral acceleration resulting from a ground motion prediction equation at a specific period. They showed that the epsilon is an indicator of the spectral shape and thereby an effective intensity measure when coupled with first-period-spectral acceleration. Their study proposes that if ground motion records, as input for the nonlinear dynamic analyses are selected and scaled considering the epsilon value together with the spectral parameters the scatter in the structural responses will decrease and, further, the required number of analyses to estimate an accurate and reliable average structural response will be reduced.

To derive empirical relationships between ground motion intensity measures and structural demand parameters, one can perform a regression analysis of nonlinear time-history responses under recorded ground motions. In this way, the correlations between the intensity measure and the structural response can be obtained. Furthermore, relationships between ground motion intensity and structural response can be evaluated within a probabilistic framework and be combined with ground motion hazard models to compute the seismic reliability of structures (Bazzurro and Cornell, 1994, Cornell and Krawinkler, 2000, Deierlein, 2004). For example, on the basis of extensive regression analyses of response of steel structures, Cornell *et al.*, (2002) proposed that the maximum inter-story drift can be estimated as a simple power function of the spectral acceleration:

$$D = a(S_a)^b \quad (4.1)$$

Such a relationship estimates the mean demand conditional on a given value of the ground motion intensity measure. The regression prediction implicitly includes the effects of the other ground excitation parameters on the structural response. The efficiency and sufficiency of the demand prediction by regression analysis also depend on the sample size, i.e. the number of nonlinear analyses performed, and the level of nonlinearity in the structure. Those randomness and uncertainties which inherently arise from the ground motion characteristics and nonlinear behavior of the structures and also which result from the structural modeling and analyses conducted to estimate the response can be evaluated within a probabilistic framework. For this purpose, given the ground motion intensity the

structural response demand can be described by a random variable of a given distribution, generally the lognormal distribution. Having the conditional probability distribution of the engineering demand parameter (EDP) for a given intensity measure (IM), it can then be combined with a ground motion hazard curve to compute the mean annual rate of exceeding a pre-defined demand level (Figure 4.1).

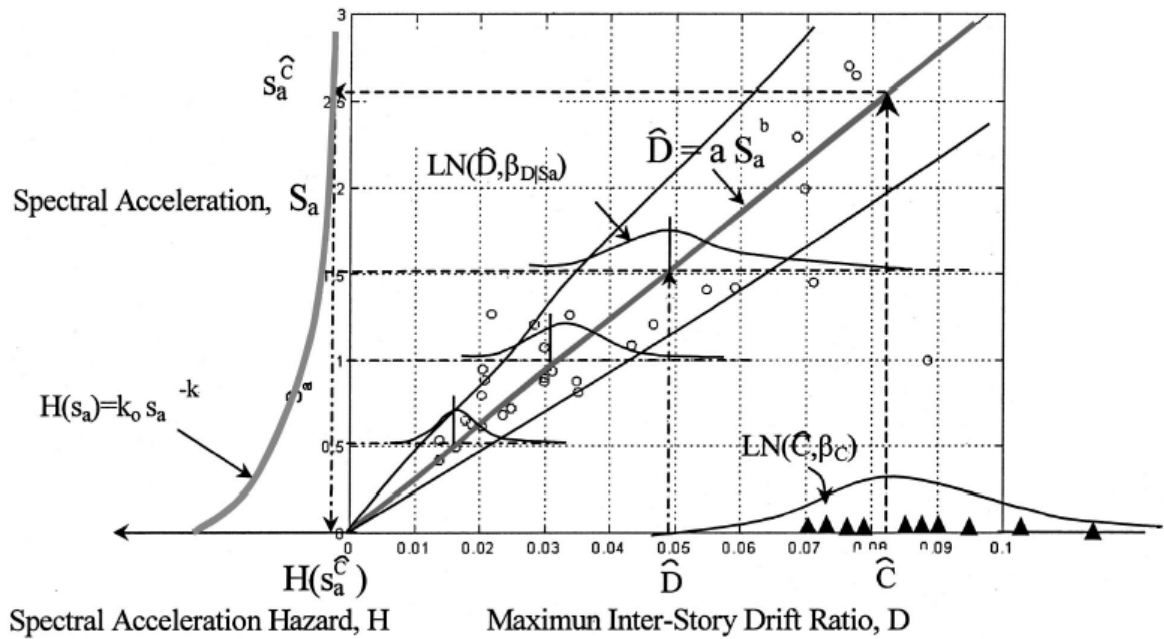


Figure 4.1. Combination of the lognormal probability distribution function of the maximum inter-story drift ratios with the ground motion hazard curve (After Cornell *et al.*, 2002)

This chapter, first, introduces the statistical approaches utilized. Then regression on the engineering demand parameters and the best correlations are presented. Following the regression analyses, probabilistic evaluation of the nonlinear dynamic analyses results is performed and both statistical approaches are compared. Finally, complementary structural response surfaces are provided.



## 4.2. Statistical Approaches Utilized

The properties of a random variable from a finite sample of data can be estimated by statistical inference. Two classes of statistical inference approaches are considered in this study: non-parametric model and parametric approach.

With non-parametric model (Lehman and D'Abrera, 1998), the nonlinear dynamic analyses of a structure are performed under a large set of ground motion records. Regression is used on the records' IM values and associated EDP values obtained from nonlinear dynamic analyses to compute the conditional mean and standard deviation of EDP given IM (Figure 4.2). A linear relationship between the logarithms of the two variables often provides a reasonable estimate of the mean value of EDP over the range of ground motion intensity levels covered by the records in the input motion ensemble (Baker, 2007).

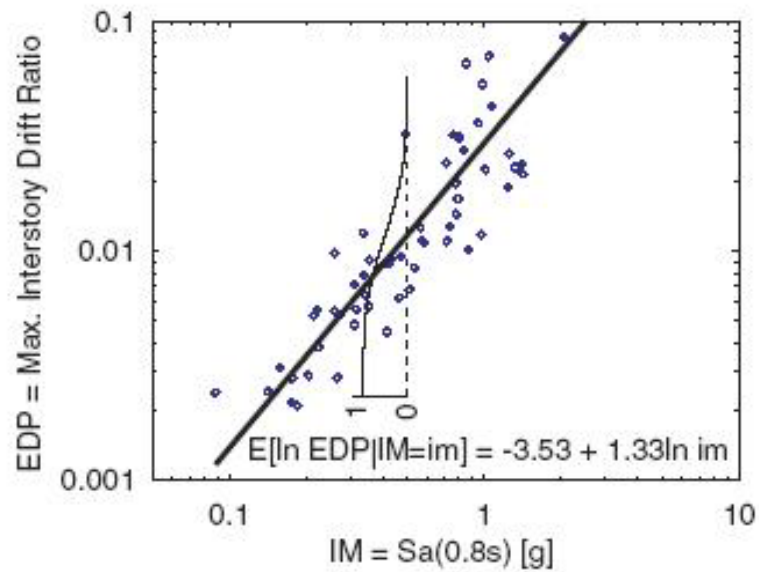


Figure 4.2. Regression on structural response results for a given IM level (After Baker, 2007)

In parametric approaches, the random variable EDP is assumed to have some probability distribution, e.g. lognormal distribution, which is defined by a few parameters, i.e. lognormal median and standard deviation. Once calculated the lognormal median and

standard deviation a conditional probability function is fitted to the distribution (Figure 4.3). This can be repeated any given level of EDP and the exceeding probability conditioned on any IM level of that EDP level is computed (Krawinkler and Miranda, 2004).

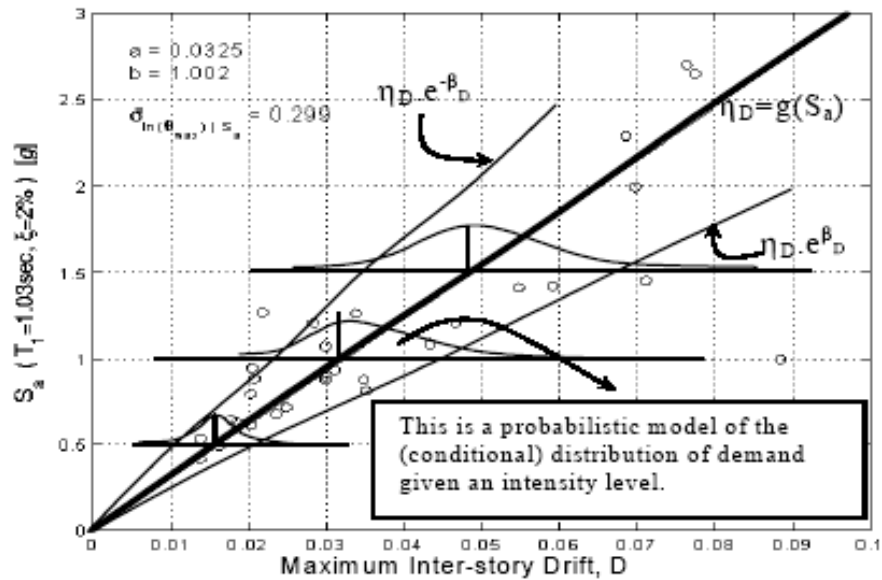


Figure 4.3. A set of spectral acceleration and demand data pairs and the probabilistic model fit to these data points (After Jalayer and Cornell, 2003)

In this study, the following ground motion parameters are considered as the ground motion intensity measures (IMs):

- Peak time-domain values,
  - Peak ground acceleration, *PGA*
  - Peak ground velocity, *PGV*
  - Peak ground displacement, *PGD*
- Energy-duration related parameters,
  - Arias Intensity, *AI*
  - Cumulative absolute velocity, *CAV*
- Spectral parameters,
  - Spectral acceleration at the 1<sup>st</sup> natural vibration period of the building,  $S_a(T_1)$
  - Spectral velocity at the 1<sup>st</sup> natural vibration period of the building,  $S_v(T_1)$
  - Spectral displacement at the 1<sup>st</sup> natural vibration period of the building,  $S_d(T_1)$

As for the engineering demand parameters (EDPs), the following structural response parameters are considered:

- Maximum floor displacement, *MFD* : the maximum of the peak floor displacements among all stories.
- Maximum inter-story drift ratio, *MIDR* : the maximum of the peak inter-storey drift ratios among all stories.
- Maximum plastic rotation, *MPR* : the maximum of the peak plastic end rotations of beams among all stories.
- Maximum floor acceleration, *MFA* : the maximum of the peak floor accelerations among all stories.

First, the scatter diagrams of ground motion intensity measures versus associated engineering demand parameters, resulting from the nonlinear dynamic analyses conducted under the actions of 734 horizontal accelerograms and presented in detail in section 3.4, are plotted each-by-each, e.g. *MIDR* vs. *PGA*, *MIDR* vs. *PGV*, *MPR* vs.  $S_a(T_1)$ , *MPR* vs. *PGD*, *MFA* vs.  $S_v(T_1)$ , *MFA* vs. *AI*, and so on. Then regression analyses on the sample datasets consisting of EDP-IM pairs are performed. The best correlated pairs of ground motion and structural response parameters resulting from the regression analyses are provided. For all the studied buildings, twelve RC frames, the regression predictions of each EDPs are compared to each other in order to observe the variation in EDP predictions conditioned on a specific ground motion intensity measure by accounting for the structural characteristics as well, i.e. first-mode natural periods and the design strengths of buildings.

Following the parametric statistical evaluation approach summarized above, log-normally distributed structural median responses for the entire ground motion intensity range covered by the input motion dataset are obtained. The cumulative probability density functions of EDPs are computed and plotted as three-dimensional structural response surfaces. In order to make a cross-check, for each building, the regression predictions of EDPs are compared with the log-normal median predictions. In this way, agreement between the results of two statistical approaches is observed. Furthermore, it can be checked whether the structural demand parameter follows the widely-used lognormal distribution assumption for any level of ground motion intensity.

### 4.3. Regression on the Engineering Demand Parameters and Presentation of the Best Correlations

Regression is a statistical technique that finds a mathematical expression that best describes a set of data. A linear trend line is fitted through the scatter diagram wherein structural responses, i.e. maximum floor accelerations, are plotted versus a ground motion intensity measure, i.e. peak ground acceleration, using least squares regression and the coefficient of determination ( $R^2$ ) of the trend is calculated to provide an indication of the dispersion of the data. The coefficient of determination ( $R^2$ ) has a value between zero and one. If the structural response perfectly correlates with the ground motion parameter, the trend line will have a gradient and correlation coefficient of unity.

For all the buildings under consideration, 12 buildings, the scatter diagrams of each EDP (4 in total) with each IM (8 in total) have been plotted and the regression analyses on  $12 \times 4 \times 8 = 384$  sample datasets have been performed. The best correlated pairs of EDP-IM have been decided based on the correlation coefficients, i.e. greater the  $R^2$  better the correlation.  $R^2 = 0.70$  was assumed as the threshold for correlation coefficient in identifying the best correlations.

#### 4.3.1. Maximum Floor Displacements – MFD

**5-story buildings.** MFD is best correlated with the spectral values at the first-mode period of the buildings, e.g.  $S_a(T_1)$ , and the correlation coefficient for MFD- $S_a(T_1)$  pair vary between 0.95-0.97 for the buildings with  $R=2, 4$  and  $6$ . The regression analyses result in a power function of  $S_a(T_1)$  to predict MFD. There are also high correlations between MFD and AI and PGV. The correlation coefficients for MFD-AI pair ranges between 0.80-0.83. However for the building with  $R=2$  there is a higher correlation between MFD and AI, whereas, for the buildings with  $R=4$  and  $6$  the MFD-PGV correlation is greater. MFD- $S_a(T_1)$  scatter diagrams and the regression predictions for 5-story buildings are presented in Figure 4.4.

**10-story buildings.** MFD is best correlated with the spectral values at the first-mode period of the buildings, e.g.  $S_a(T_1)$ , and the correlation coefficient for MFD- $S_a(T_1)$  pair vary between 0.96-0.98 for the buildings with  $R=2, 4$  and  $6$ . The regression analyses result

in a power function of  $S_a(T_1)$  to predict MFD. There are also high correlations between MFD and PGV. The correlation coefficients for MFD-PGV pair ranges between 0.86-0.88. Furthermore, it should be noted that the correlations of MFDs with AI yield correlation coefficients greater 0.71 for all buildings. MFD- $S_a(T_1)$  scatter diagrams and the regression predictions for 10-story buildings are presented in Figure 4.8.

**15-story buildings.** MFD is best correlated with the spectral values at the first-mode period of the buildings, e.g.  $S_a(T_1)$ , and the correlation coefficient for MFD- $S_a(T_1)$  pair vary between 0.96-0.98 for the buildings with  $R=2, 4$  and  $6$ . The regression analyses result in a power function of  $S_a(T_1)$  to predict MFD. There are also high correlations between MFD and PGV. The correlation coefficients for MFD-PGV pair ranges between 0.86-0.88. Furthermore, it should be noted that MFDs start correlating with PGD with the correlation coefficients as high as 0.73 especially for the buildings with  $R=4$  and  $6$ . MFD- $S_a(T_1)$  scatter diagrams and the regression predictions for 15-story buildings are presented in Figure 4.12.

**20-story buildings.** MFD is best correlated with the spectral values at the first-mode period of the buildings, e.g.  $S_a(T_1)$ , and the correlation coefficient for MFD- $S_a(T_1)$  pair vary between 0.96-0.98 for the buildings with  $R=2, 4$  and  $6$ . The regression analyses result in a power function of  $S_a(T_1)$  to predict MFD. There are also high correlations between MFD and PGV. The correlation coefficients for MFD-PGV pair ranges between 0.84-0.86. Furthermore, it should be noted that MFDs start correlating with PGD with the correlation coefficients between 0.71-0.77. MFD- $S_a(T_1)$  scatter diagrams and the regression predictions for 20-story buildings are presented in Figure 4.16.

#### **4.3.2. Maximum Inter-Story Drift Ratios – MIDR**

**5-story buildings.** MIDR is best correlated with the spectral values at the first-mode period of the buildings, e.g.  $S_a(T_1)$ , and the correlation coefficient for MIDR- $S_a(T_1)$  pair vary between 0.95-0.96 for the buildings with  $R=2, 4$  and  $6$ . The regression analyses result in a power function of  $S_a(T_1)$  to predict MIDR. There are also high correlations between MIDR and AI, PGV and PGA. The correlation coefficients for MIDR-AI pair ranges between 0.84-0.86. However for the building with  $R=2$  there is a higher correlation

between MIDR and AI, whereas, for the buildings with  $R=4$  and  $6$  the MIDR-PGV correlation is greater. On the other hand, vice versa is observed for PGA case, while the MIDRs of the buildings  $R=4$  and  $6$  are less correlated with PGA the MIDR-PGA correlation gets greater for the building with  $R=2$ . MIDR- $S_a(T_1)$  scatter diagrams and the regression predictions for 5-story buildings are presented in Figure 4.5.

**10-story buildings.** MIDR is best correlated with the spectral values at the first-mode period of the buildings, e.g.  $S_a(T_1)$ , and the correlation coefficient for MIDR- $S_a(T_1)$  pair vary between 0.89-0.90 for the buildings with  $R=2, 4$  and  $6$ . The regression analyses result in a power function of  $S_a(T_1)$  to predict MIDR. There are also high correlations between MIDR and PGV and AI. The correlation coefficients for MIDR-PGV pair ranges between 0.85-0.90. However for the building with  $R=2$  there is a lower correlation between MIDR and PGV, whereas, for the buildings with  $R=4$  and  $6$  the MIDR-PGV correlation is greater. On the other hand, vice versa is observed for AI case, while the MIDRs of the buildings  $R=4$  and  $6$  are less correlated with AI the MIDR-AI correlation gets greater for the building with  $R=2$ . MIDR- $S_a(T_1)$  scatter diagrams and the regression predictions for 10-story buildings are presented in Figure 4.9.

**15-story buildings.** MIDR is best correlated with peak ground velocity, PGV, and the correlation coefficient for MIDR-PGV pair vary between 0.87-0.91 for the buildings with  $R=2, 4$  and  $6$ . The regression analyses result in a power function of PGV to predict MIDR. There are also high correlations between MIDR and the spectral values at the first-mode period of the buildings and AI. The correlation coefficients for MIDR-  $S_a(T_1)$  and MIDR-AI pairs range between 0.82-0.84 and 0.80-0.85, respectively. MIDR-PGV scatter diagrams and the regression predictions for 15-story buildings are presented in Figure 4.13.

**20-story buildings.** MIDR is best correlated with peak ground velocity, PGV, and the correlation coefficient for MIDR-PGV pair vary between 0.89-0.91 for the buildings with  $R=2, 4$  and  $6$ . The regression analyses result in a power function of PGV to predict MIDR. There are also high correlations between MIDR and the spectral values at the first-mode period of the buildings as well as Arias intensity, AI, and cumulative absolute velocity, CAV. The correlation coefficients for MIDR-  $S_a(T_1)$  MIDR- AI and MIDR-CAV pairs

range between 0.77-0.81, 0.77-0.83 and 0.75-0.78, respectively. MIDR-PGV scatter diagrams and the regression predictions for 20-story buildings are presented in Figure 4.17.

#### 4.3.3. Maximum Plastic Rotations – MPR

**5-story buildings.** MPR is best correlated with the spectral values at the first-mode period of the buildings, e.g.  $S_a(T_1)$ , and the correlation coefficient for MPR- $S_a(T_1)$  pair vary between 0.71-0.87 for the buildings with  $R=2, 4$  and  $6$ . The MPRs in buildings with  $R=4$  and  $6$  correlate better with  $S_a(T_1)$  through the entire range of  $S_a(T_1)$  and the regression analyses result in power functions of  $S_a(T_1)$  in order to predict MPR. On the other hand, the correlation of MPR with  $S_a(T_1)$  for the building with  $R=2$  yields relatively a lower correlation coefficient of 0.71 if a power functional form is adopted. The MPR predictions for this building follow an exponential functional for lower  $S_a(T_1)$  levels and then correspond to a power functional form for higher intensity levels. For the sake of simplicity, it is assumed that all buildings have power functions to predict MPR via  $S_a(T_1)$  as shown in Figure 4.6. As secondary correlations, there is high correlation between MPR and AI. Similarly the correlation for buildings with  $R=4$  and  $6$  is greater and can be expressed only as a power function of AI.

**10-story buildings.** MPR is best correlated with the spectral values at the first-mode period of the buildings, e.g.  $S_a(T_1)$ , and the correlation coefficient for MPR- $S_a(T_1)$  pair vary between 0.67-0.87 for the buildings with  $R=2, 4$  and  $6$ . The MPRs in buildings with  $R=4$  and  $6$  correlate better with  $S_a(T_1)$  through the entire range of  $S_a(T_1)$  and the regression analyses result in power functions of  $S_a(T_1)$  in order to predict MPR. On the other hand, the correlation of MPR with  $S_a(T_1)$  for the building with  $R=2$  yields relatively a lower correlation coefficient of 0.67 if a power functional form is adopted. The MPR predictions for this building follow an exponential function for lower  $S_a(T_1)$  levels and then correspond to a power functional form for higher intensity levels. For the sake of simplicity, it is assumed that all buildings have power functions to predict MPR via  $S_a(T_1)$  as shown in Figure 4.10. As secondary correlations, there is high correlation between MPR and PGV. Similarly the correlation for buildings with  $R=4$  and  $6$  is greater and can be expressed only as a power function of PGV.

**15-story buildings.** MPR is best correlated with peak ground velocity, PGV, and the correlation coefficient for MPR-PGV pair vary between 0.66-0.85 for the buildings with  $R=2, 4$  and 6. The MPRs in buildings with  $R=4$  and 6 correlate better with PGV through the entire range of PGV and the regression analyses result in power functions of PGV in order to predict MPR. On the other hand, the correlation of MPR with PGV for the building with  $R=2$  yields relatively a lower correlation coefficient of 0.66 if a power functional form is adopted. The MPR predictions for this building follow an exponential function for lower PGV levels and then correspond to a power functional form for higher intensity levels. For the sake of simplicity, it is assumed that all buildings have power functions to predict MPR via PGV as shown in Figure 4.14. There are also high correlations between MPR and the spectral values at the first-mode period of the buildings and AI. The correlation coefficients for MPR-  $S_a(T_1)$  and MPR- AI pairs range between 0.64-0.84 and 0.64-0.70, respectively.

**20-story buildings.** MPR is best correlated with peak ground velocity, PGV, and the correlation coefficient for MPR-PGV pair vary between 0.67-0.86 for the buildings with  $R=2, 4$  and 6. The MPRs in buildings with  $R=4$  and 6 correlate better with PGV through the entire range of PGV and the regression analyses result in power functions of PGV in order to predict MPR. On the other hand, the correlation of MPR with PGV for the building with  $R=2$  yields relatively a lower correlation coefficient of 0.67 if a power functional form is adopted. The MPR predictions for this building follow an exponential function for lower PGV levels and then correspond to a power functional form for higher intensity levels. For the sake of simplicity, it is assumed that all buildings have power functions to predict MPR via PGV as shown in Figure 4.18. There are also high correlations between MPR and the spectral values at the first-mode period of the buildings and AI. The correlation coefficients for MPR-  $S_a(T_1)$  and MPR- AI pairs range between 0.59-0.82 and 0.64-0.69, respectively.

#### **4.3.4. Maximum Floor Accelerations – MFA**

**5-story buildings.** MFA is best correlated with peak ground acceleration, PGA, and the correlation coefficient for MFA-PGA pair vary between 0.90-0.91 for the buildings with  $R=2, 4$  and 6. The regression analyses result in a power function of PGA to predict MFA.



There are also high correlations between MFA and AI and  $S_a(T_1)$ . The correlation of MFA with AI reveals at high correlation coefficients ranging between 0.87-0.88 which are very close to those of PGA case. It is also noted that the correlation of MFA with  $S_a(T_1)$  decreases as the period of the building increases. MFA-PGA scatter diagrams and the regression predictions for 5-story buildings are presented in Figure 4.7.

**10-story buildings.** MFA is best correlated with peak ground acceleration, PGA, and Arias intensity, AI, at the same time. The correlation coefficients are very close for MFA-PGA and MFA-AI pairs and vary between 0.90-0.92 for the buildings with  $R=2, 4$  and  $6$ . The regression analyses result in a power function of PGA or AI to predict MFA. Only MFA-AI scatter diagrams and the regression predictions for 10-story buildings are presented in Figure 4.11.

**15-story buildings.** MFA is best correlated with peak ground acceleration, PGA, and Arias intensity, AI, at the same time. The correlation coefficients are very close for MFA-PGA and MFA-AI pairs and vary between 0.91-0.93 for the buildings with  $R=2, 4$  and  $6$ . The regression analyses result in a power function of PGA or AI to predict MFA. Only MFA-AI scatter diagrams and the regression predictions for 15-story buildings are presented in Figure 4.15.

**20-story buildings.** MFA is best correlated with peak ground acceleration, PGA, and Arias intensity, AI, at the same time. The correlation coefficients are very close for MFA-PGA and MFA-AI pairs and vary between 0.91-0.93 for the buildings with  $R=2, 4$  and  $6$ . The regression analyses result in a power function of PGA or AI to predict MFA. Only MFA-AI scatter diagrams and the regression predictions for 20-story buildings are presented in Figure 4.19.

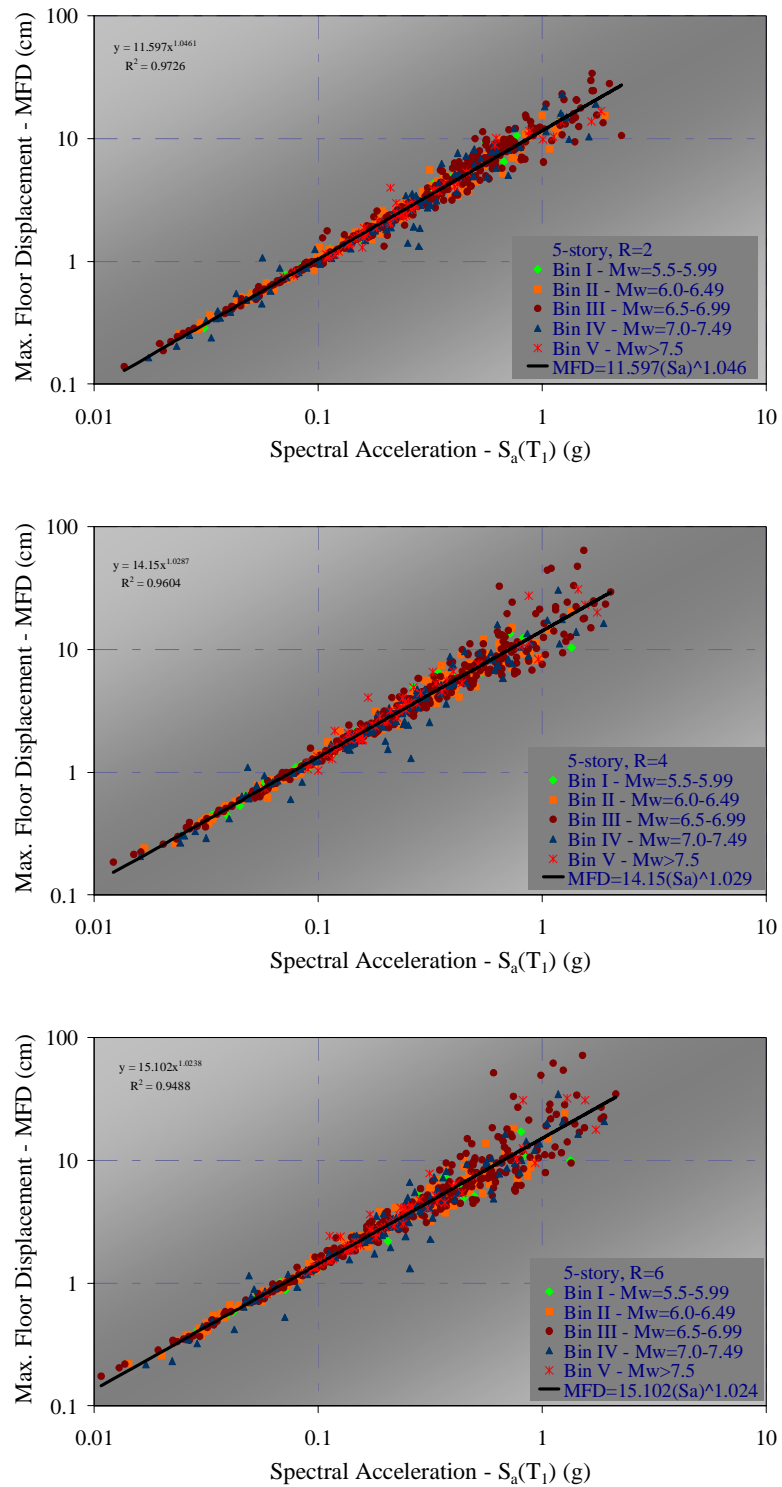


Figure 4.4. Scatter plot of MFD vs.  $S_a(T_1)$  resulting from each record bin, for the 5-story buildings (R=2, R=4 and R=6 from top to bottom respectively) and the best-fits obtained from the regression of the entire data sets

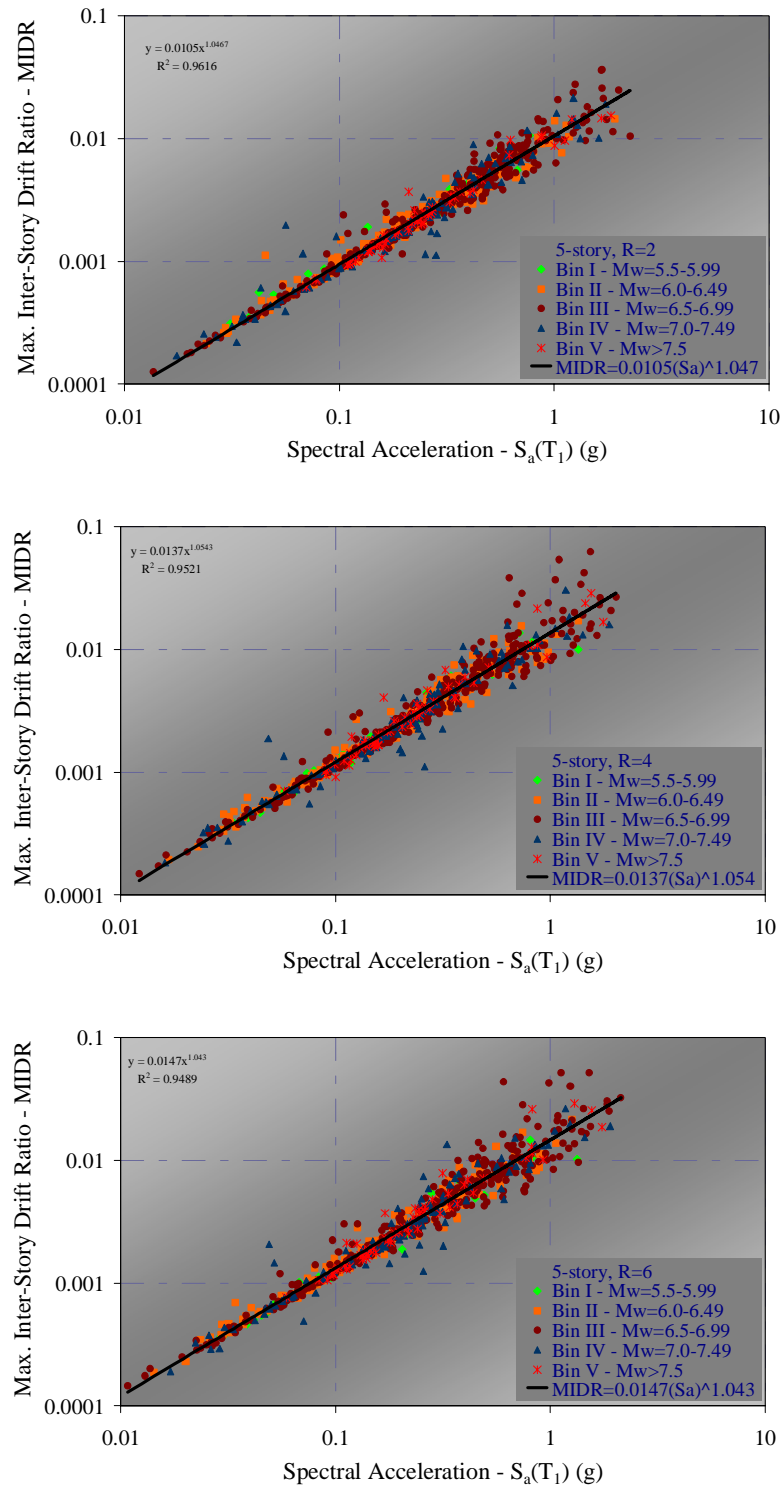


Figure 4.5. Scatter plot of MIDR vs.  $S_a(T_1)$  resulting from each record bin, for the 5-story buildings (R=2, R=4 and R=6 from top to bottom respectively) and the best-fits obtained from the regression of the entire data sets

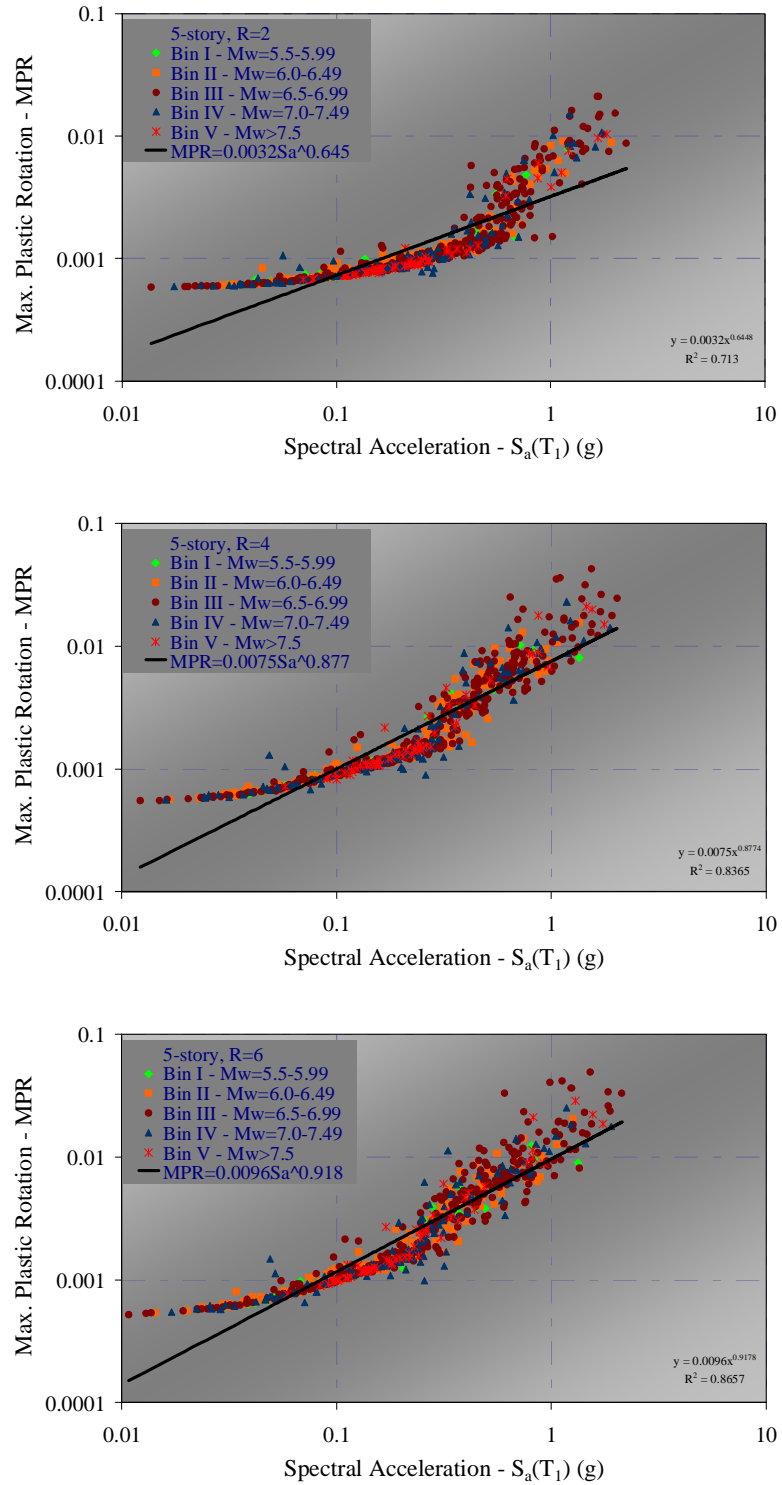


Figure 4.6. Scatter plot of MPR vs.  $S_a(T_1)$  resulting from each record bin, for the 5-story buildings (R=2, R=4 and R=6 from top to bottom respectively) and the best-fits obtained from the regression of the entire data sets

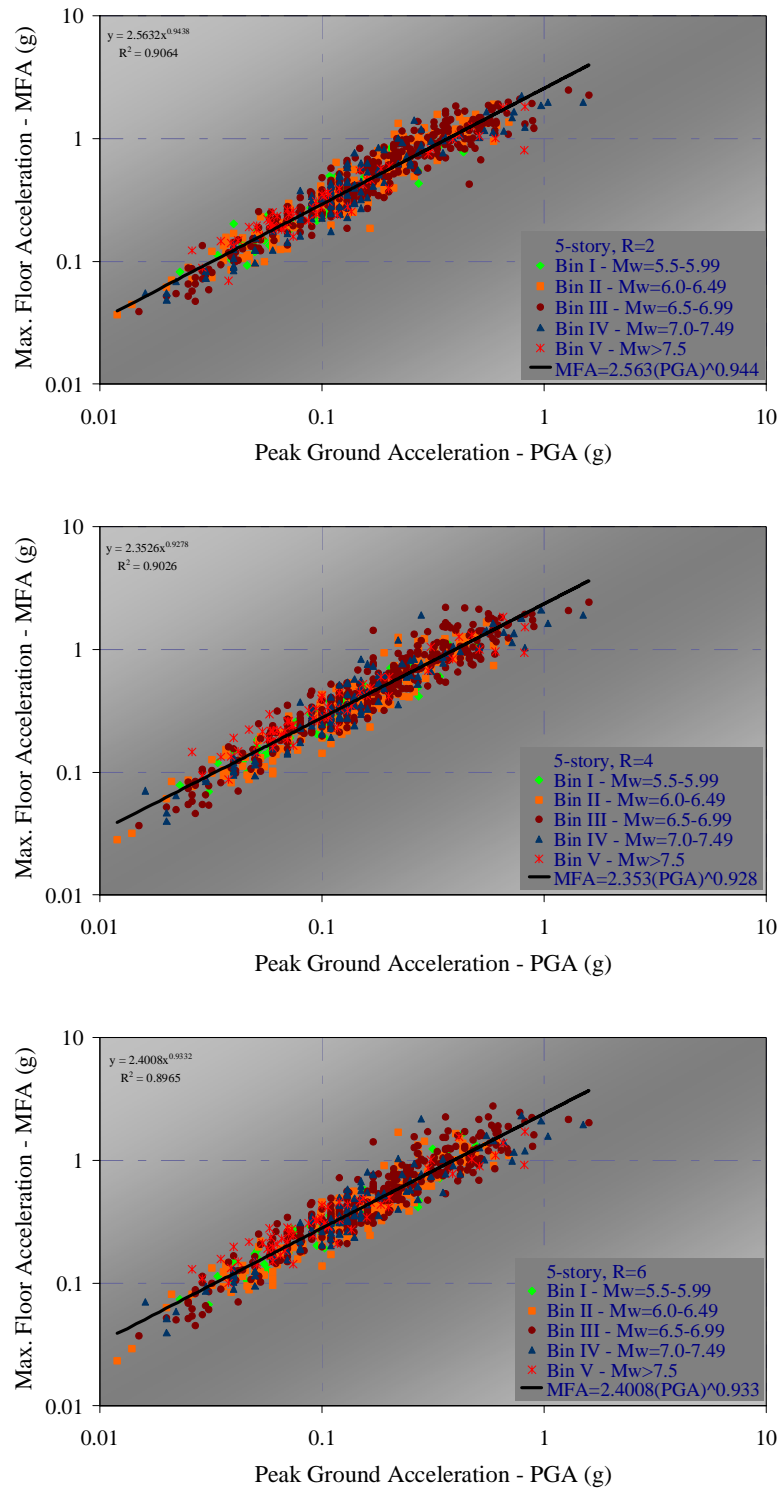


Figure 4.7. Scatter plot of MFA vs. PGA resulting from each record bin, for the 5-story buildings (R=2, R=4 and R=6 from top to bottom respectively) and the best-fits obtained from the regression of the entire data sets

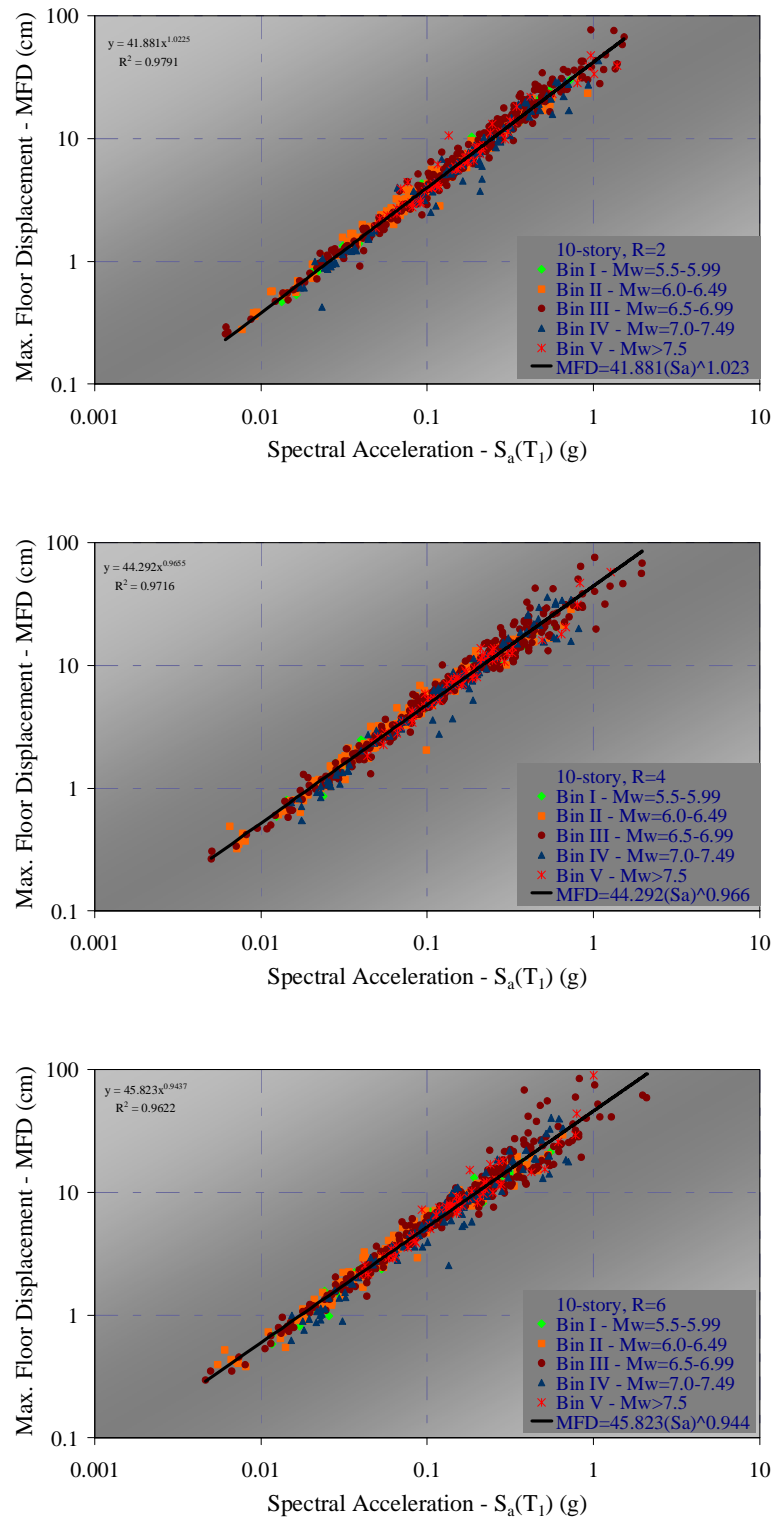


Figure 4.8. Scatter plot of MFD vs.  $S_a(T_1)$  resulting from each record bin, for the 10-story buildings (R=2, R=4 and R=6 from top to bottom respectively) and the best-fits obtained from the regression of the entire data sets

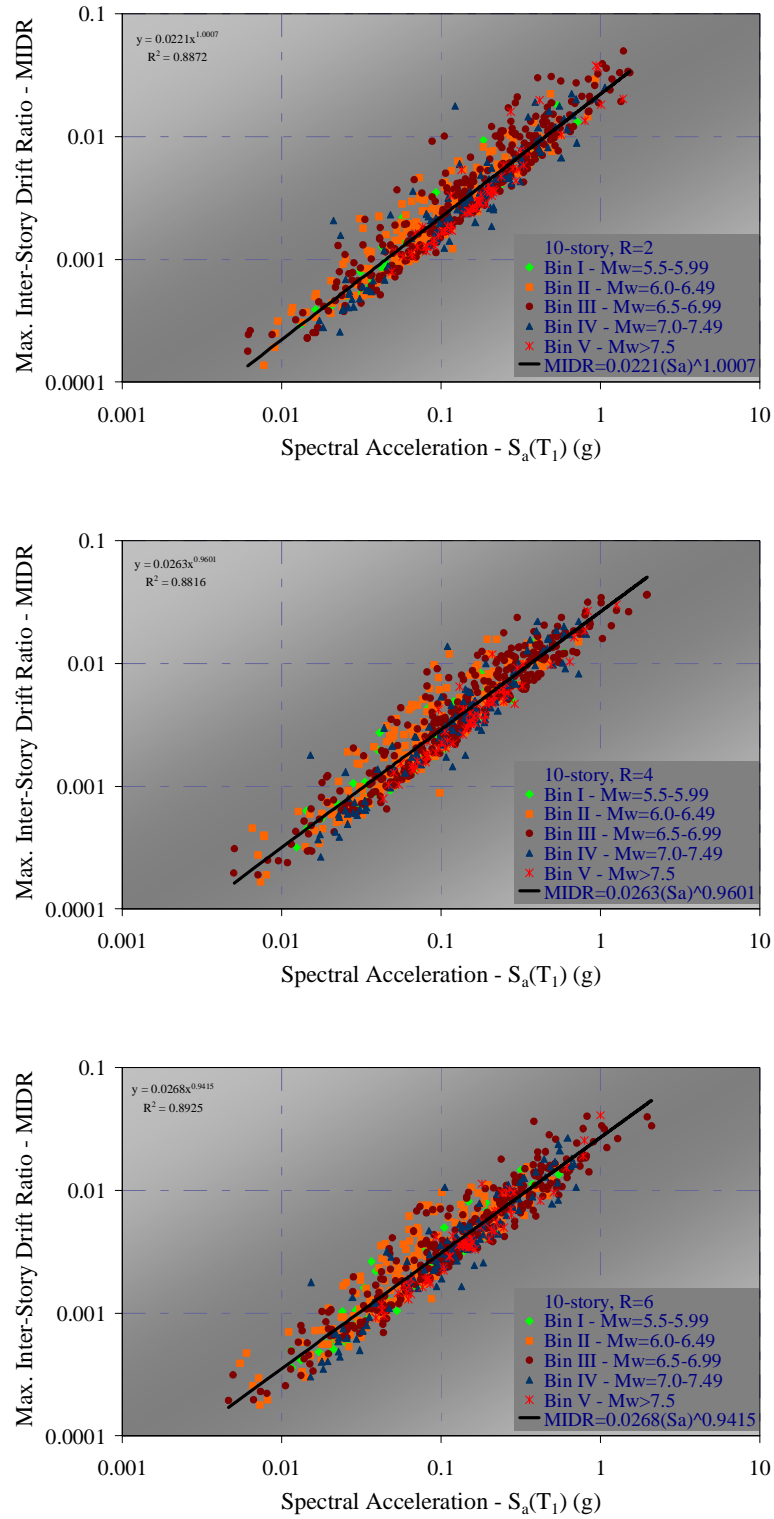


Figure 4.9. Scatter plot of MIDR vs.  $S_a(T_1)$  resulting from each record bin, for the 10-story buildings (R=2, R=4 and R=6 from top to bottom respectively) and the best-fits obtained from the regression of the entire data sets

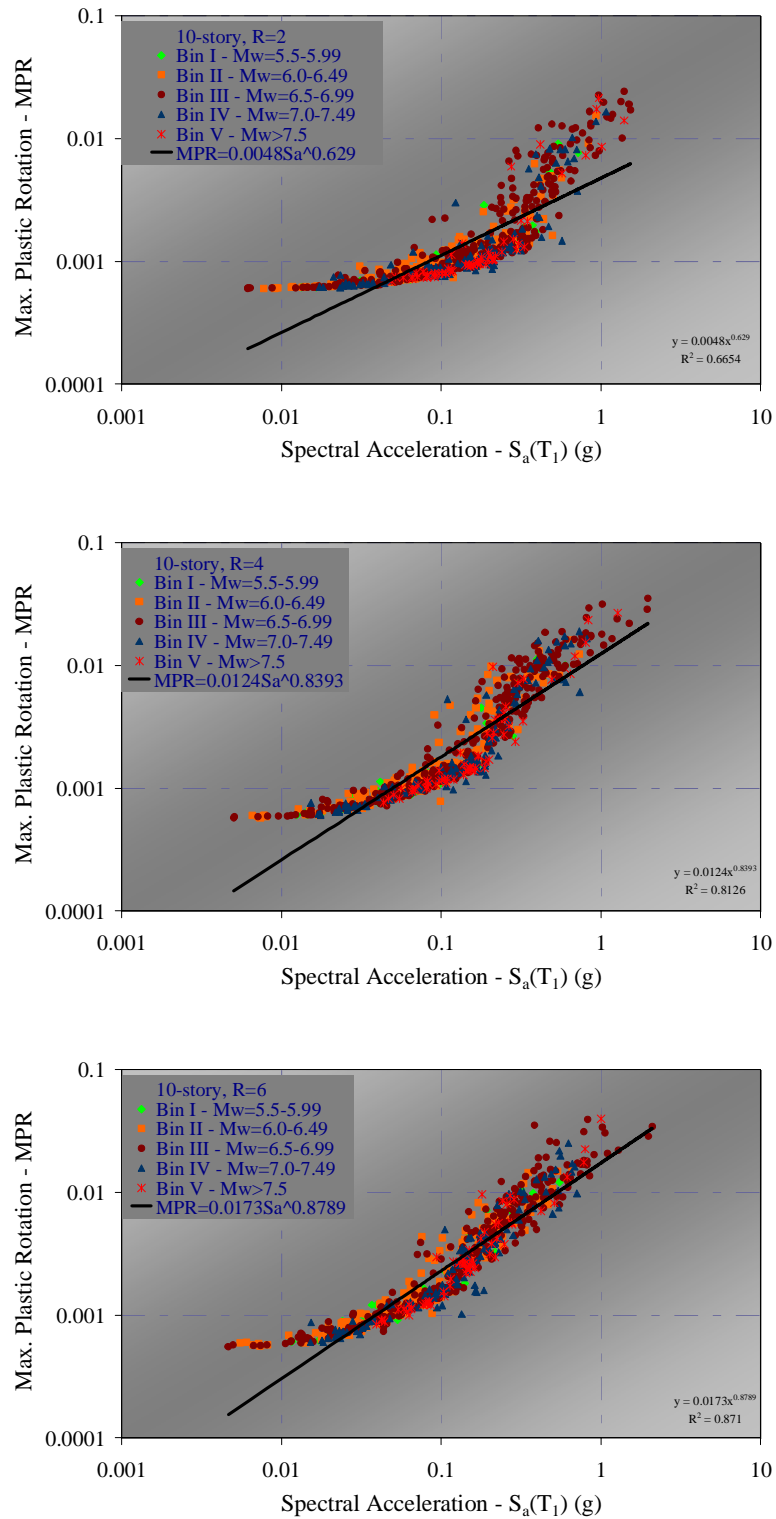


Figure 4.10. Scatter plot of MPR vs.  $S_a(T_1)$  resulting from each record bin, for the 10-story buildings (R=2, R=4 and R=6 from top to bottom respectively) and the best-fits obtained from the regression of the entire data sets



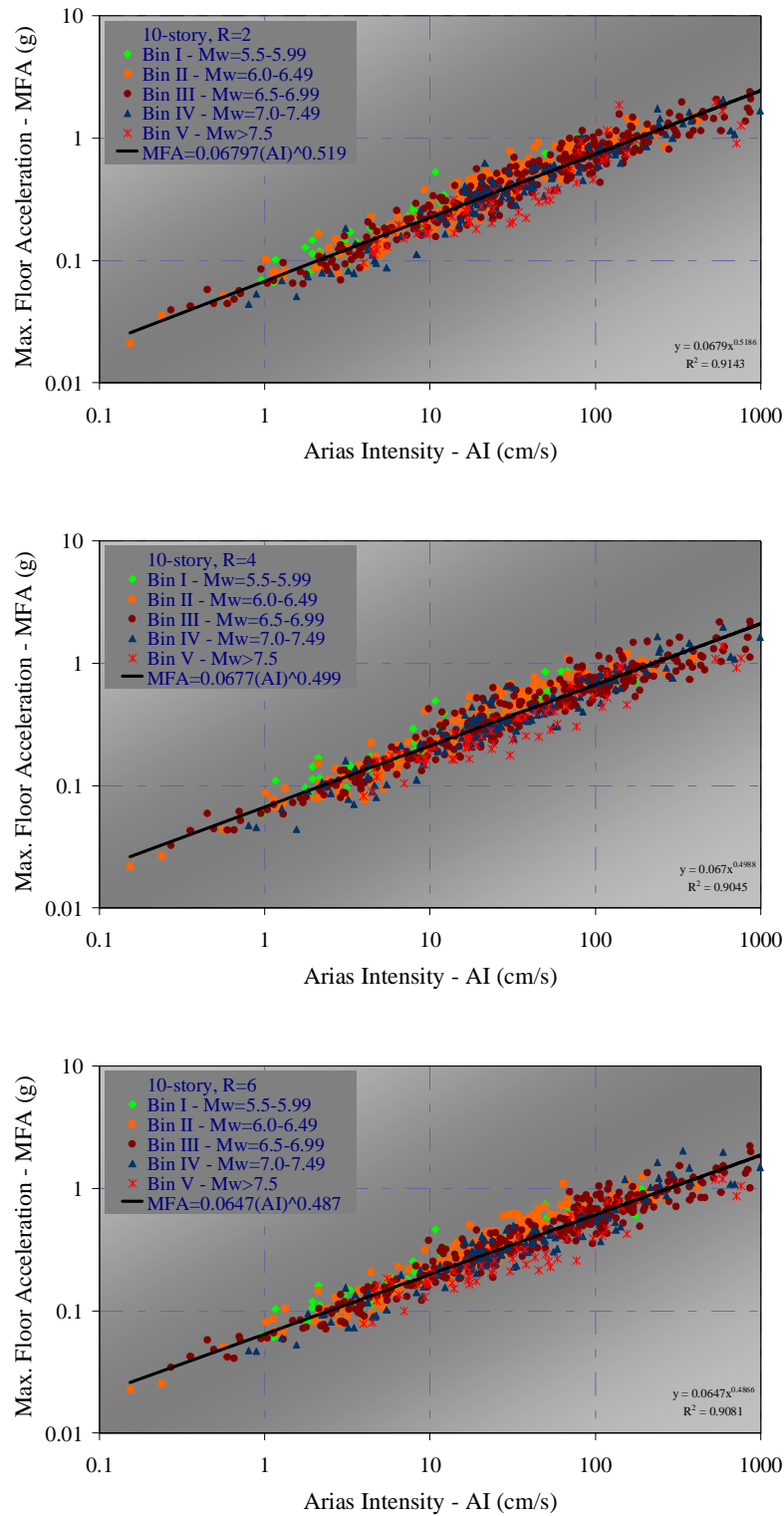


Figure 4.11. Scatter plot of MFA vs. AI resulting from each record bin, for the 10-story buildings (R=2, R=4 and R=6 from top to bottom respectively) and the best-fits obtained from the regression of the entire data sets

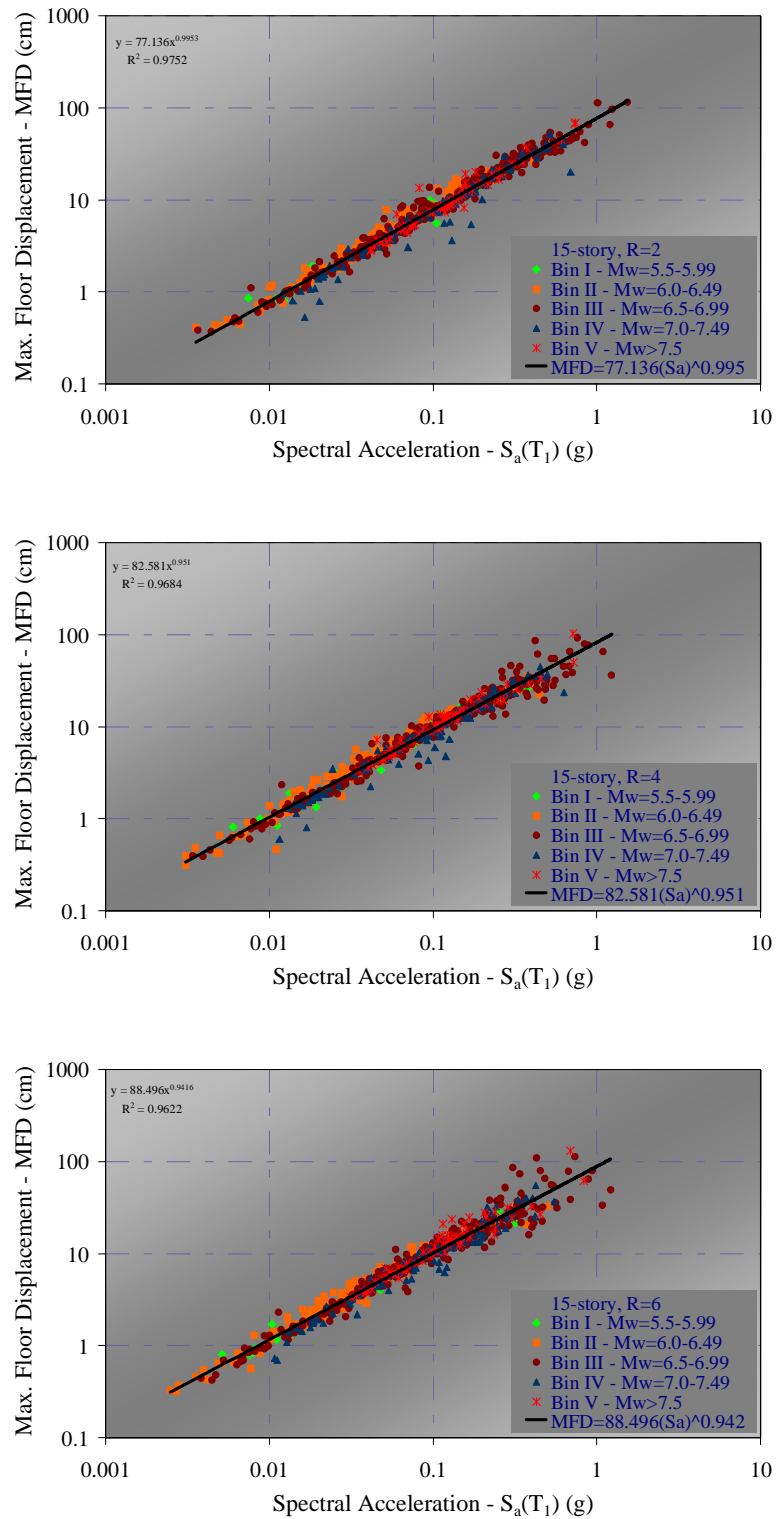


Figure 4.12. Scatter plot of MFD vs.  $S_a(T_1)$  resulting from each record bin, for the 15-story buildings (R=2, R=4 and R=6 from top to bottom respectively) and the best-fits obtained from the regression of the entire data sets

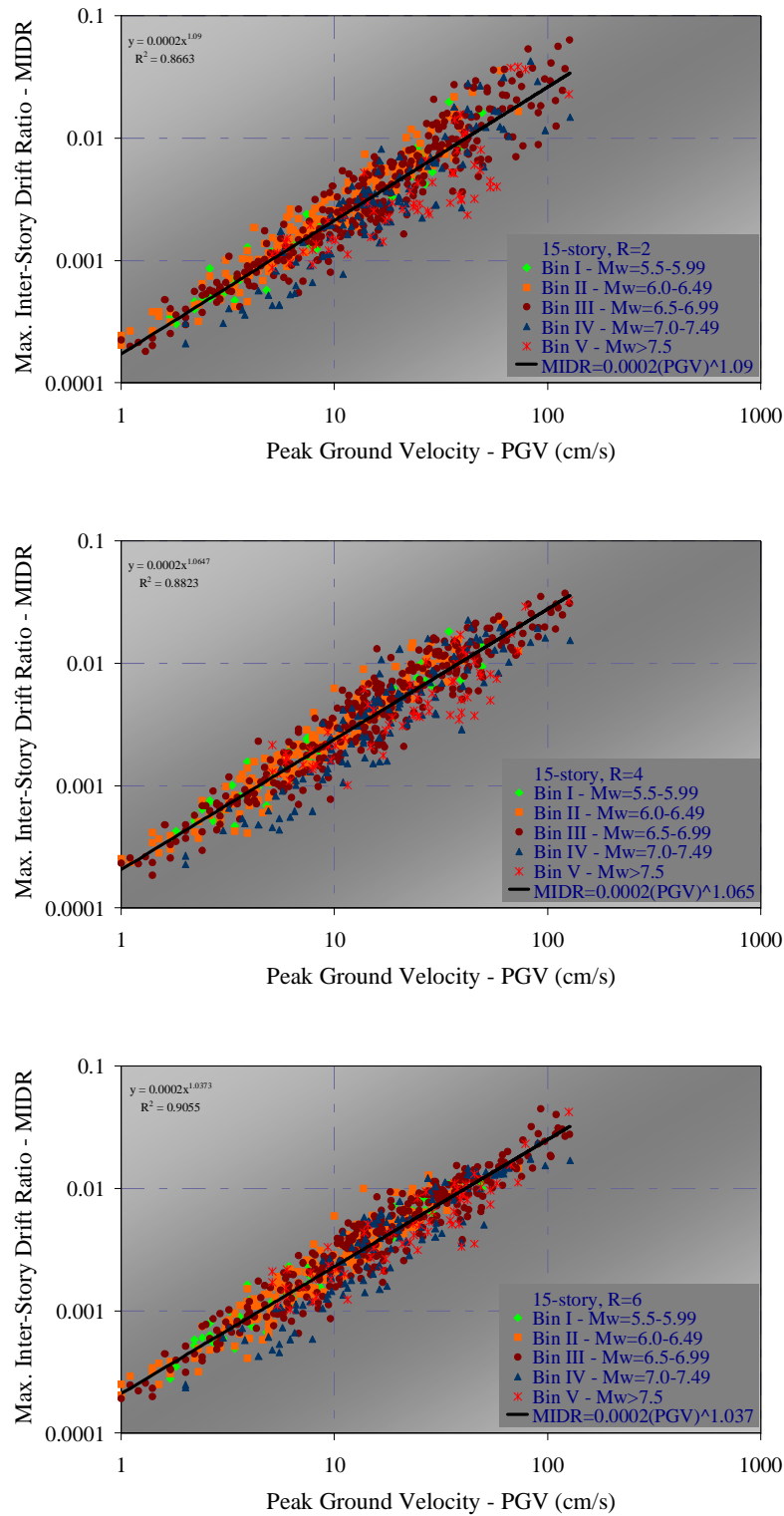


Figure 4.13. Scatter plot of MIDR vs. PGV resulting from each record bin, for the 15-story buildings (R=2, R=4 and R=6 from top to bottom respectively) and the best-fits obtained from the regression of the entire data sets

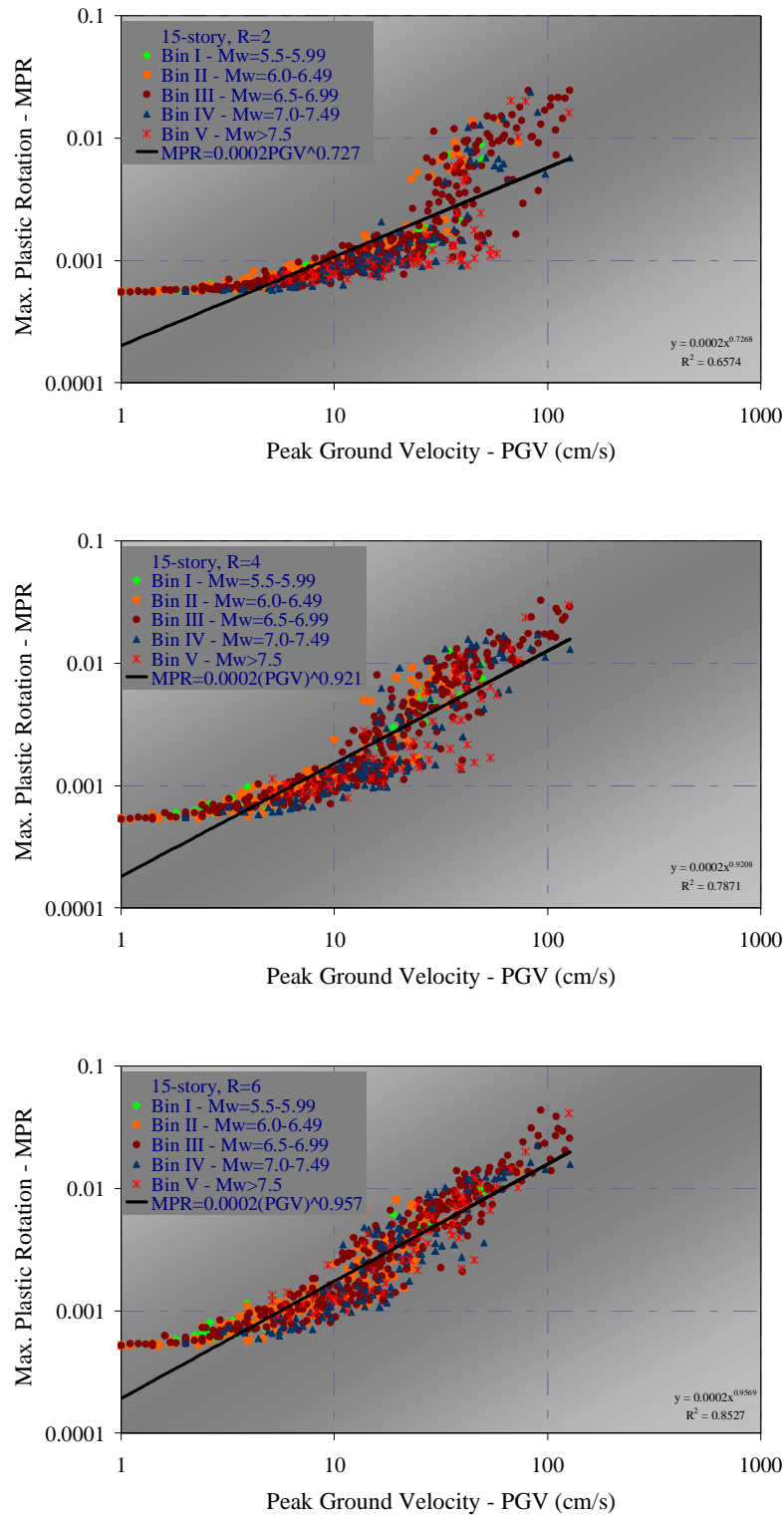


Figure 4.14. Scatter plot of MPR vs. PGV resulting from each record bin, for the 15-story buildings (R=2, R=4 and R=6 from top to bottom respectively) and the best-fits obtained from the regression of the entire data sets

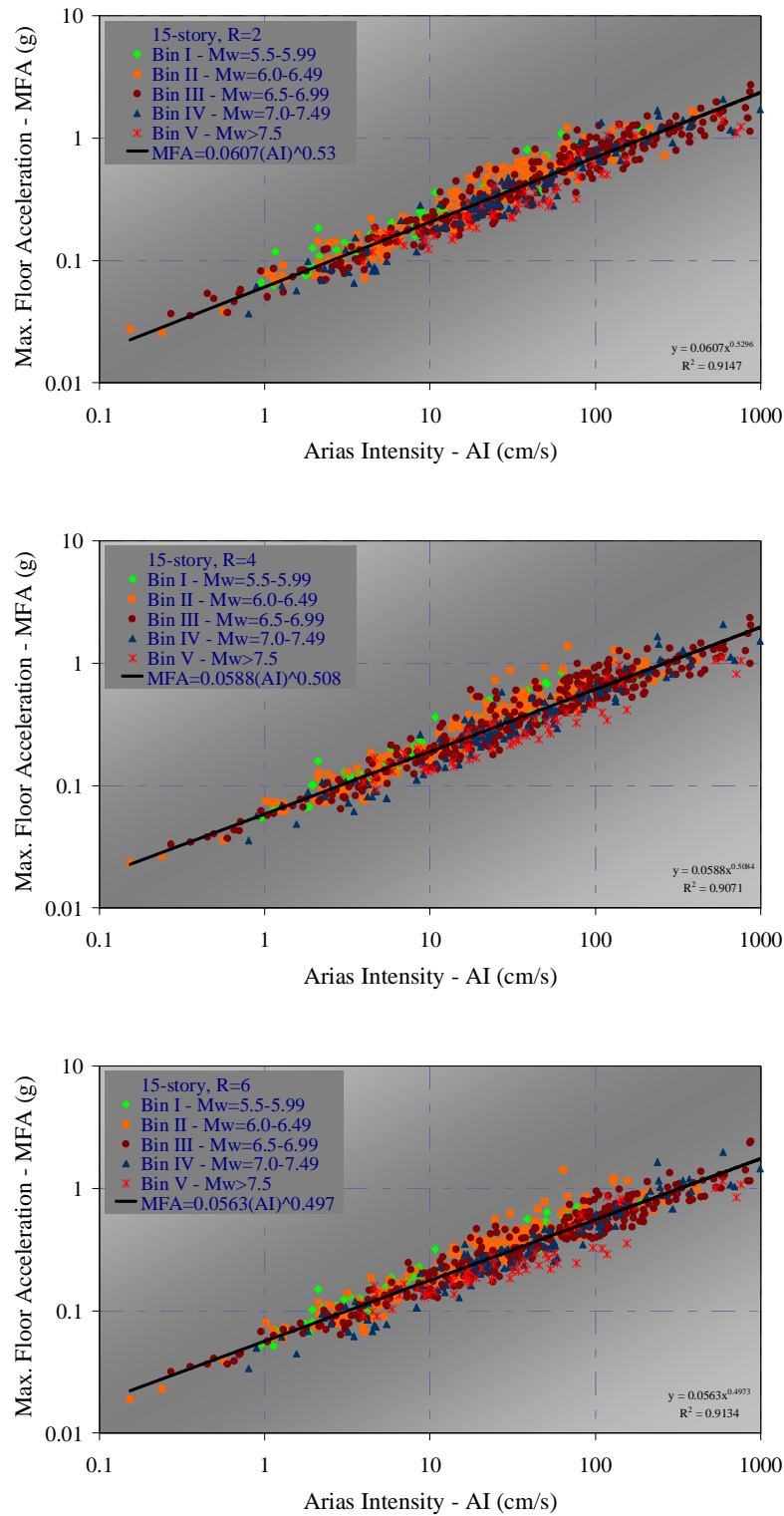


Figure 4.15. Scatter plot of MFA vs. AI resulting from each record bin, for the 15-story buildings (R=2, R=4 and R=6 from top to bottom respectively) and the best-fits obtained from the regression of the entire data sets

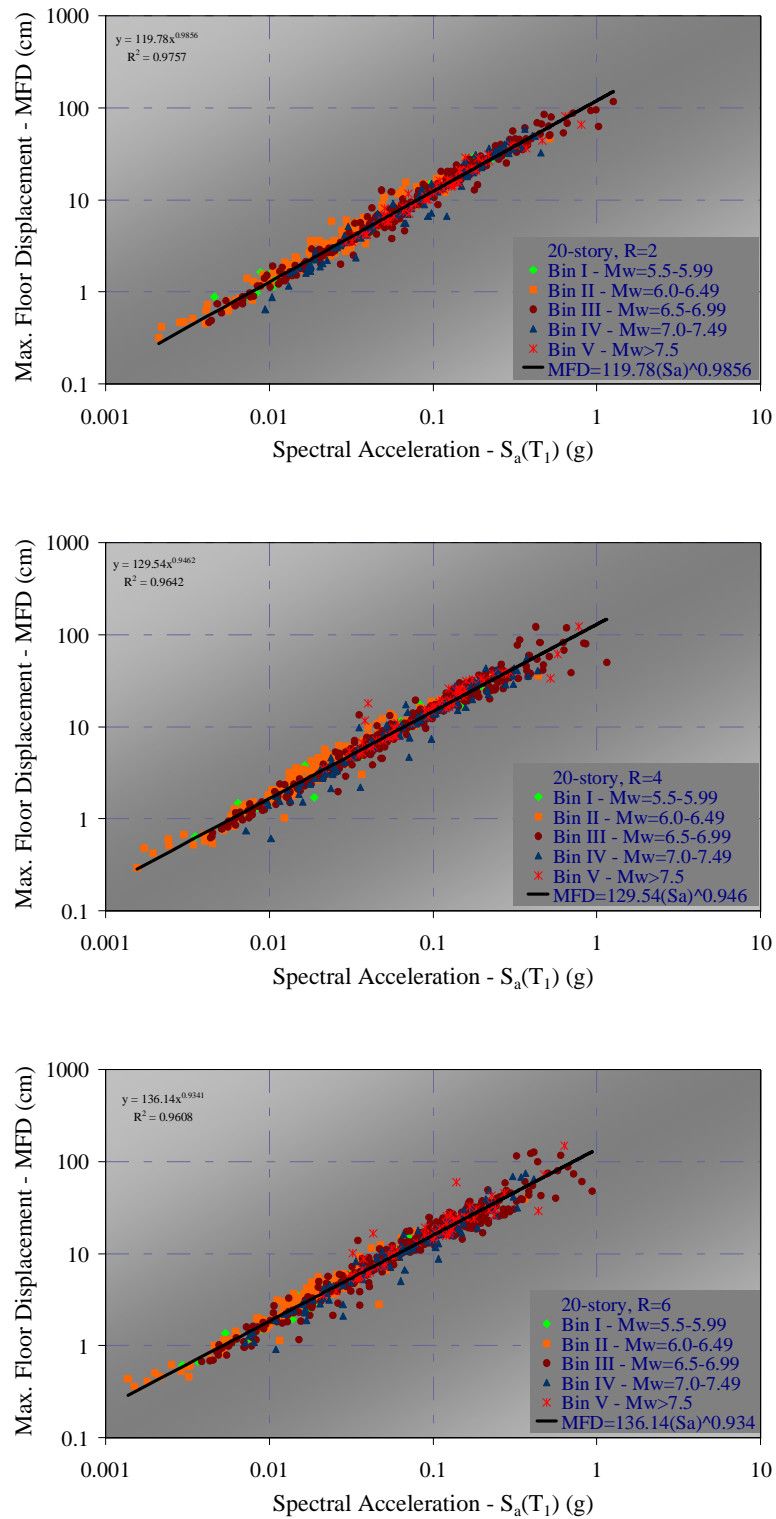


Figure 4.16. Scatter plot of MFD vs.  $S_a(T_1)$  resulting from each record bin, for the 20-story buildings (R=2, R=4 and R=6 from top to bottom respectively) and the best-fits obtained from the regression of the entire data sets

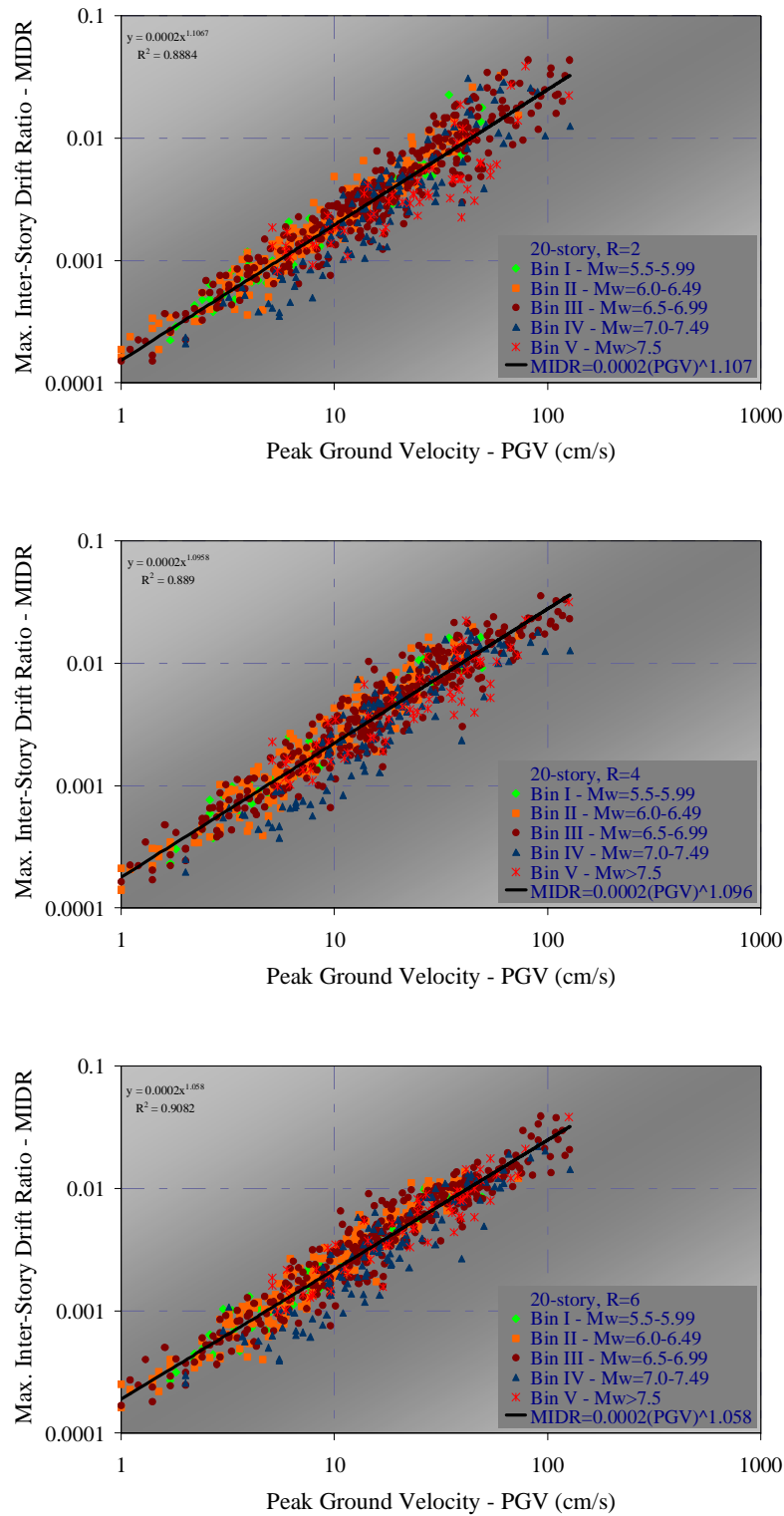


Figure 4.17. Scatter plot of MIDR vs. PGV resulting from each record bin, for the 20-story buildings (R=2, R=4 and R=6 from top to bottom respectively) and the best-fits obtained from the regression of the entire data sets

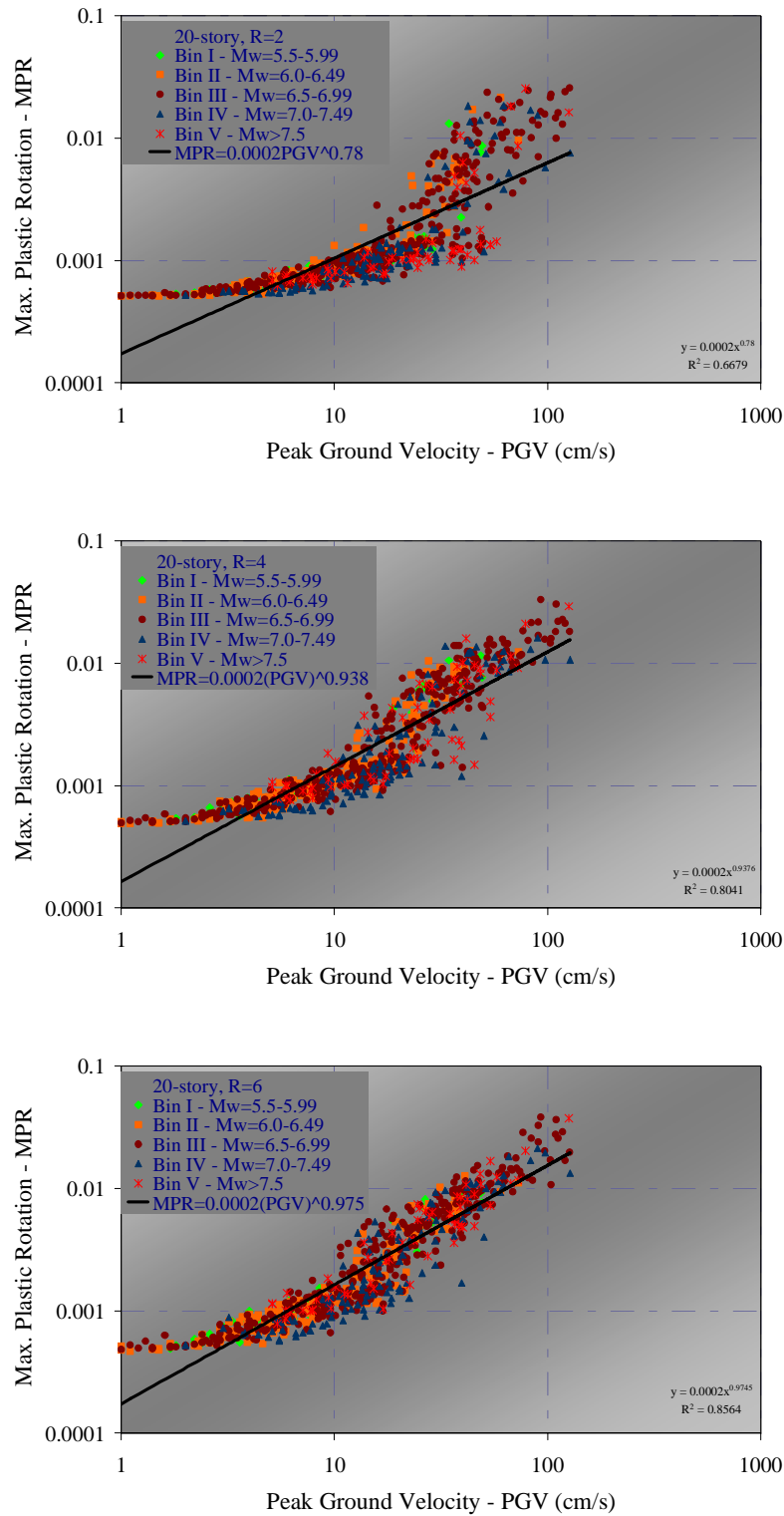


Figure 4.18. Scatter plot of MPR vs. PGV resulting from each record bin, for the 20-story buildings ( $R=2$ ,  $R=4$  and  $R=6$  from top to bottom respectively) and the best-fits obtained from the regression of the entire data sets



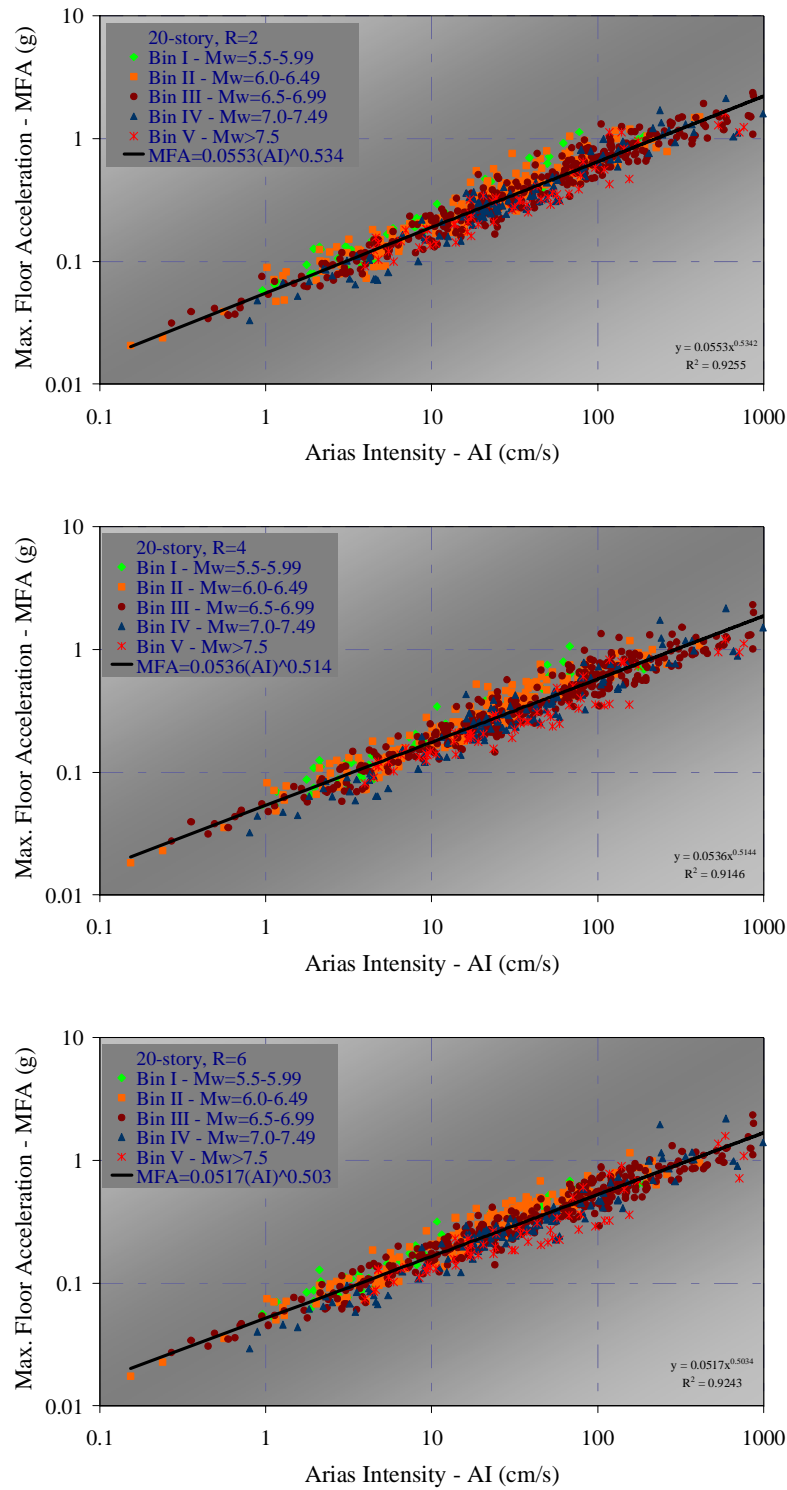


Figure 4.19. Scatter plot of MFA vs. AI resulting from each record bin, for the 20-story buildings (R=2, R=4 and R=6 from top to bottom respectively) and the best-fits obtained from the regression of the entire data sets

#### 4.3.5. Comparative Evaluation of Correlation Results and Prediction Functions for Engineering Demand Parameters

The highest correlations resulting from the regression analyses between ground motion intensity measures and engineering demand parameters are summarized in Table 4.1. The cells of Table 4.1 represent the first three intensity measures which correlate well with the structural response parameter based on a descending ranking. For example, in the cell for maximum inter-story drift ratio (MIDR) of the ten-story building designed for strength reduction factor of  $R=4$  the greatest correlation is with the spectral acceleration ( $S_a(T_1)$ ), then secondly with peak ground velocity (PGV) and thirdly with Arias intensity (AI).

Table 4.1. Summary of regression results: the highest three correlations between ground motion intensity measures (IM) and engineering demand parameters (EDP) for each building

Building		MFD (max. floor disp.)	MIDR (max. inter-story drift ratio)	MPR (max. plastic rot.)	MFA (max. floor acc.)
5-story	R=2	$S_a(T_1)$ , AI, PGV	$S_a(T_1)$ , AI, PGA	$S_a(T_1)$ , AI, PGA	PGA, AI, $S_a(T_1)$
	R=4	$S_a(T_1)$ , PGV, AI	$S_a(T_1)$ , AI, PGV	$S_a(T_1)$ , AI, PGV	PGA, AI, $S_a(T_1)$
	R=6	$S_a(T_1)$ , PGV, AI	$S_a(T_1)$ , AI, PGV	$S_a(T_1)$ , AI, PGV	PGA, AI, $S_a(T_1)$
10-story	R=2	$S_a(T_1)$ , PGV, AI	$S_a(T_1)$ , AI, PGV	$S_a(T_1)$ , AI, PGV	AI-PGA, CAV, PGV
	R=4	$S_a(T_1)$ , PGV, AI	$S_a(T_1)$ , PGV, AI	$S_a(T_1)$ , PGV, AI	AI-PGA, CAV, PGV
	R=6	$S_a(T_1)$ , PGV, AI	$S_a(T_1)$ -PGV, AI	$S_a(T_1)$ , PGV, AI	PGA-AI, CAV, PGV
15-story	R=2	$S_a(T_1)$ , PGV, AI	PGV, AI, $S_a(T_1)$	PGV, AI, $S_a(T_1)$	AI-PGA, CAV, PGV
	R=4	$S_a(T_1)$ , PGV, PGD	PGV, $S_a(T_1)$ , AI	PGV, $S_a(T_1)$ , AI	AI-PGA, CAV, PGV
	R=6	$S_a(T_1)$ , PGV, PGD	PGV, $S_a(T_1)$ , AI	PGV, $S_a(T_1)$ , AI	PGA-AI, CAV, PGV
20-story	R=2	$S_a(T_1)$ , PGV, PGD	PGV, AI, $S_a(T_1)$	PGV, AI, $S_a(T_1)$	AI-PGA, CAV, PGV
	R=4	$S_a(T_1)$ , PGV, PGD	PGV, AI, $S_a(T_1)$	PGV, $S_a(T_1)$ , AI	AI-PGA, CAV, PGV
	R=6	$S_a(T_1)$ , PGV, PGD	PGV, $S_a(T_1)$ , AI	PGV, $S_a(T_1)$ , AI	PGA-AI, CAV, PGV

It is observed that maximum floor displacements at all buildings have a strong correlation with the first period spectral acceleration. In high-period buildings, the effect of peak ground displacement on maximum floor displacements become more apparent. For relatively low- to medium-period buildings, five- and ten-story, maximum inter-story drift ratios and maximum plastic rotations of beams best correlate with the first period spectral

acceleration. As the building gets taller and its period becomes longer, the effect of the first period spectral acceleration start diminishing. The greatest correlations of maximum inter-story drift ratios and maximum plastic rotations of beams in fifteen- and twenty-story buildings reveals at peak ground velocity. In short-period buildings, maximum floor accelerations are directly influenced by peak ground acceleration. In taller buildings, both peak ground acceleration and Arias intensity have the strongest impact on the maximum floor accelerations. Furthermore, cumulative absolute velocity starts affecting the maximum floor accelerations as the building gets taller.

In Figure 4.20 - Figure 4.23, the prediction curves for engineering parameters are presented and compared. In general, it is observed that the prediction curves estimate very close structural responses at relatively lower values of ground motion intensities for each building classes. It means that the strength reduction factors which the buildings have been designed for do not have much effect on the structural response under low ground shaking intensities. As the ground motion intensity measures get greater the predicted engineering demand parameters start comparatively differing within each building group.

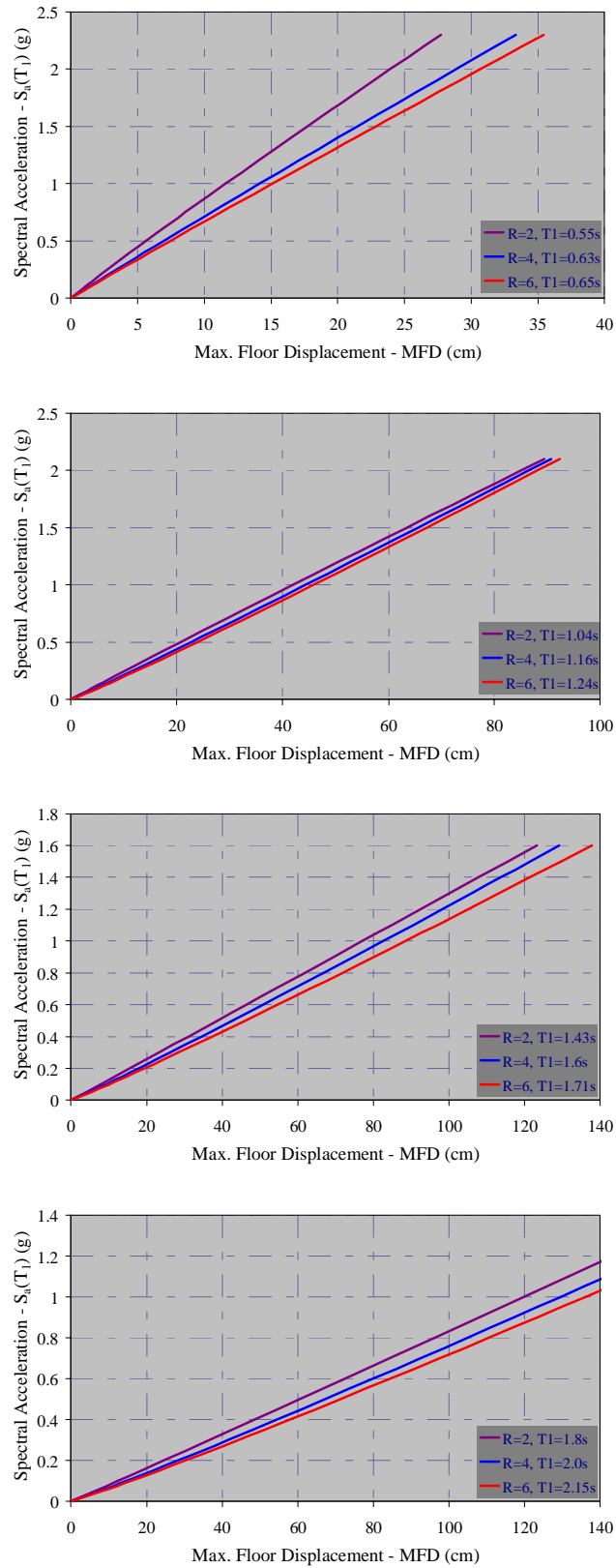


Figure 4.20. Prediction curves of maximum floor displacements for 5-, 10-, 15- and 20-story buildings (from top to bottom respectively)

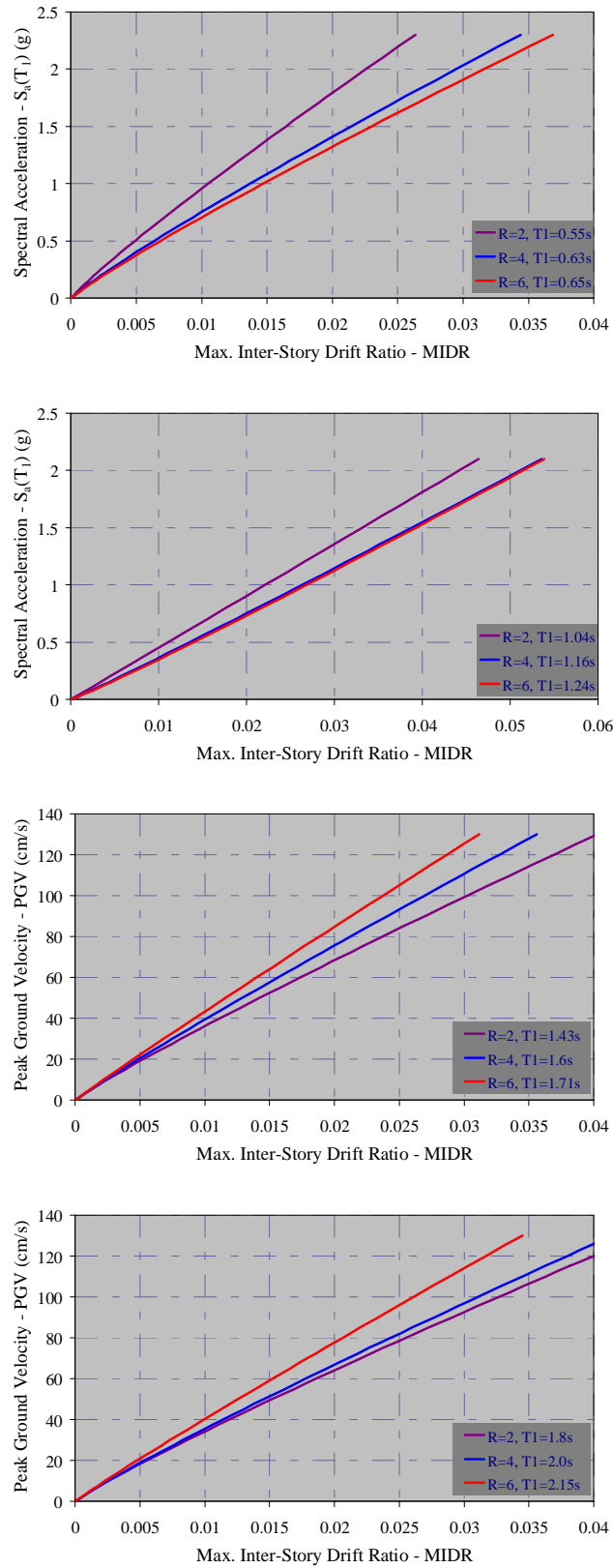


Figure 4.21. Prediction curves of maximum inter-story drifts for 5-, 10-, 15- and 20-story buildings (from top to bottom respectively)

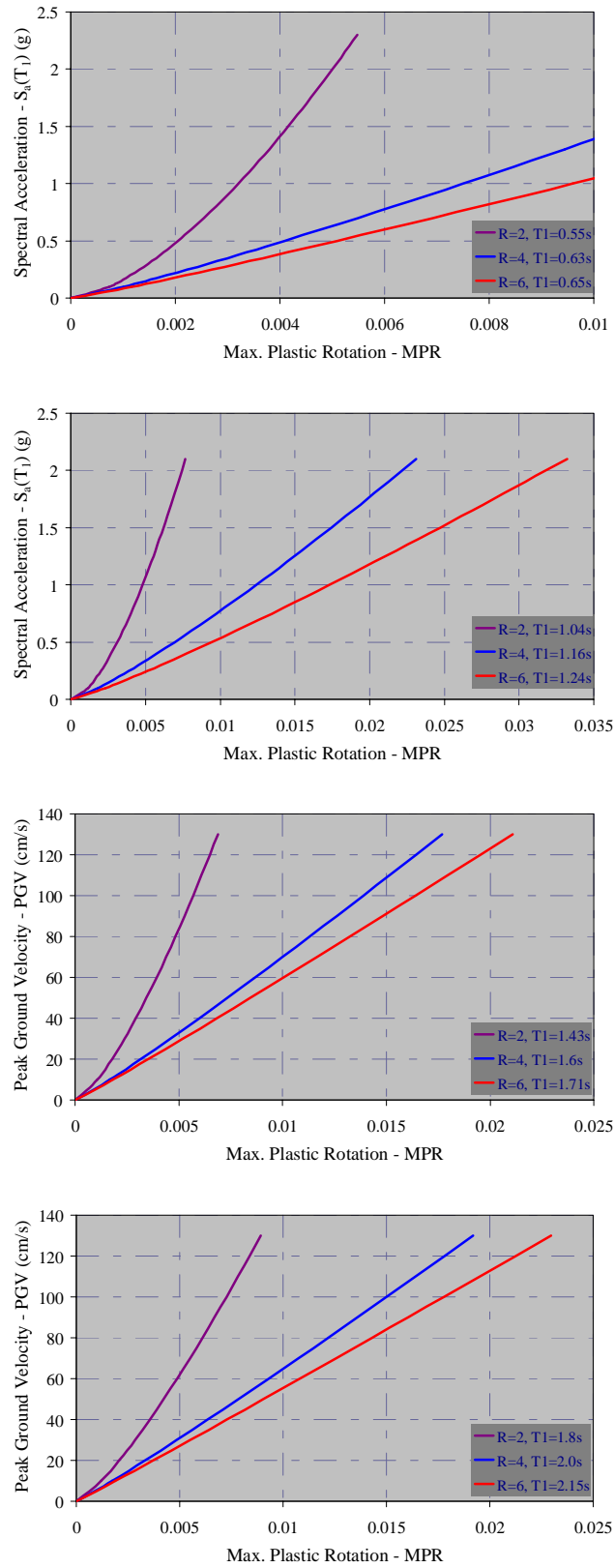


Figure 4.22. Prediction curves of maximum plastic beam rotations for 5-, 10-, 15- and 20-story buildings (from top to bottom respectively)

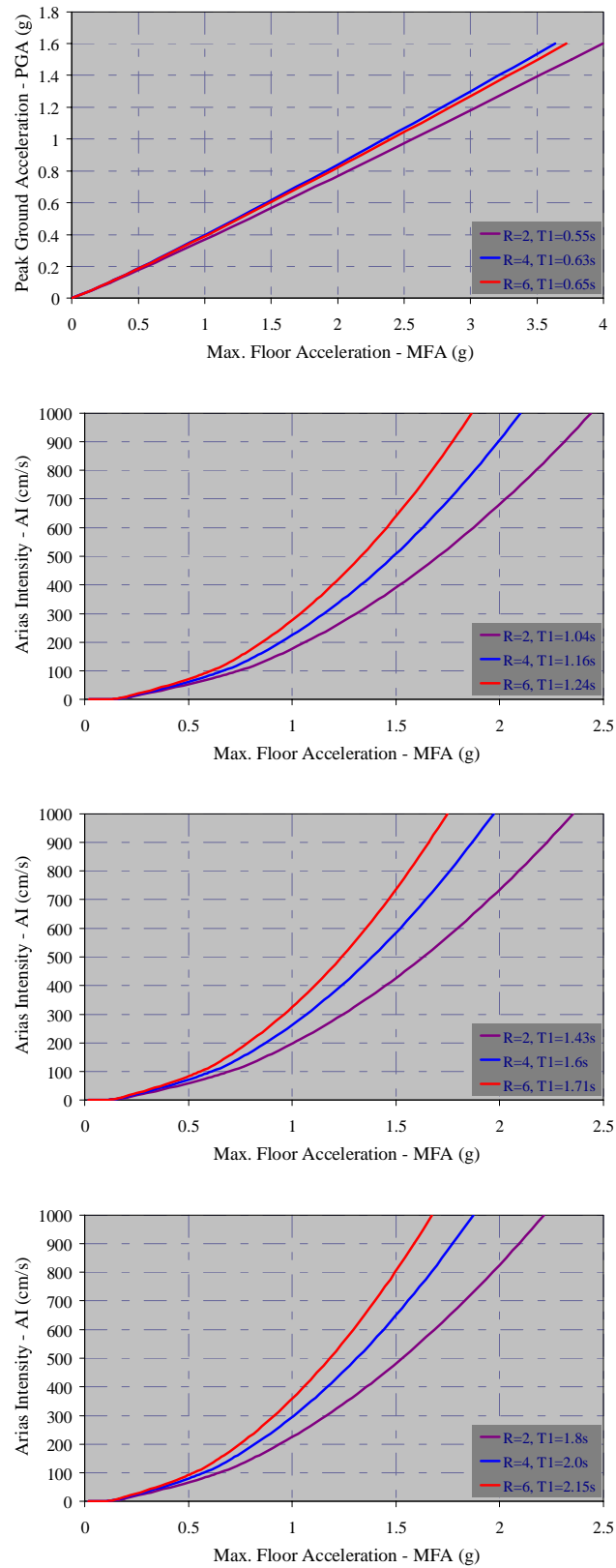


Figure 4.23. Prediction curves of maximum floor accelerations for 5-, 10-, 15- and 20-story buildings (from top to bottom respectively)

#### 4.4. Probabilistic Evaluation of Engineering Demand Parameters

Parametric approach is followed for probabilistic evaluation of engineering demand parameters. Two-parameter lognormal distribution function is assumed for the parametric evaluation. The parameters of the lognormal distribution, i.e. median and standard deviation are estimated by maximum likelihood procedure given in Shinozuka *et al.*, (2001). This is done by estimating, by the maximum likelihood method, the two parameters of each lognormal distribution function for a given value of engineering demand parameter. The likelihood function is expressed as:

$$L = [F(a)]^x [1 - F(a)]^{1-x} \quad (4.2)$$

where  $F$  represents the cumulative distribution function for a given engineering demand value,  $a$  is the value of ground motion intensity measure to which the building is subjected,  $x$  represents realizations of the Bernoulli random variable and takes the value of 0 or 1 depending on whether or not the building experiences with the demand under given ground motion intensity level.

Under the current lognormal assumption, to estimate the cumulative distribution function of the engineering demand parameter (EDP) for a given level of ground motion intensity measure (IM),  $F(\cdot)$  takes the following analytical form:

$$F_{\langle EDP|IM \rangle}(\langle y|im \rangle) = \Phi\left(\frac{\ln y - \mu}{\sigma}\right) \quad (4.3)$$

where  $\Phi$  is the standardized normal distribution function and  $\mu$  and  $\sigma$  are median and standard deviation of the EDP values resulting from the nonlinear dynamic analyses. The two parameters  $\mu$  and  $\sigma$ , i.e. median and standard deviation, are computed as  $\mu_0$  and  $\sigma_0$  satisfying the following equations to maximize  $\ln L$  and hence  $L$ :

$$\frac{d \ln L}{d\mu} = \frac{d \ln L}{d\sigma} = 0 \quad (4.4)$$



This computation is performed by implementing a straightforward optimization algorithm and is repeated for specified engineering demands to obtain the conditional cumulative distribution functions. An example of the maximum likelihood optimization and the fitted lognormal distribution curve is shown in Figure 4.24.

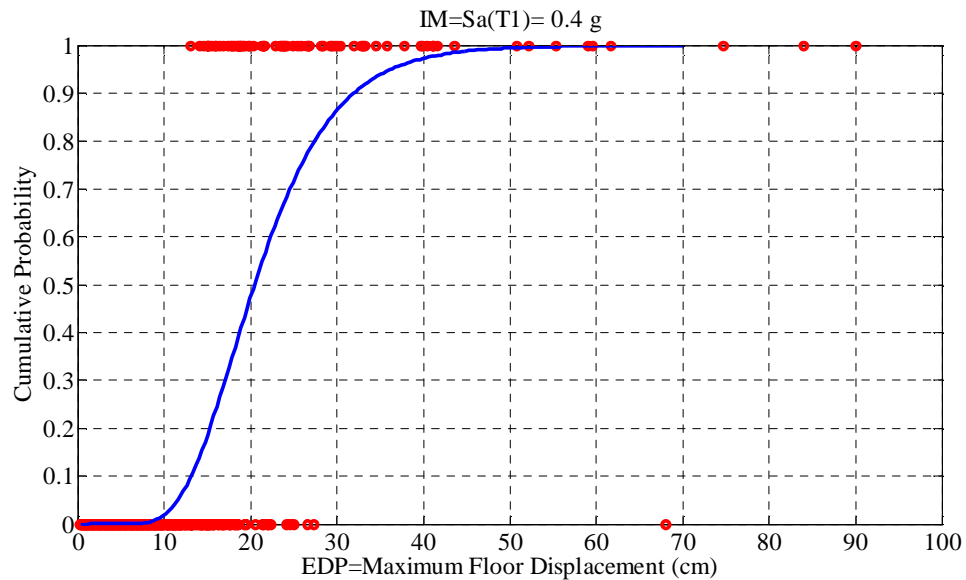


Figure 4.24. Example cumulative lognormal distribution function of EDP conditioned on IM

#### 4.4.1. Comparison of Prediction Functions: Regression Predictions versus Probabilistic Predictions

The best correlated pairs of ground motion intensity measures and engineering demand parameters are evaluated by utilizing a parametric methodology described in previous section. The log-normal median values of engineering demand parameters are computed for the entire ground motion intensity range represented by the records used in the nonlinear dynamic analyses. Hence the median prediction functions for engineering demand parameters as well as the 16<sup>th</sup> – and 84<sup>th</sup> – percentile predictions as for confidence intervals are obtained. The prediction functions resulting from the non-parametric evaluation, i.e. regression analysis, are compared to the parametric prediction functions in Figure 4.25 and Figure 4.40.

In order to make a cross-check, for each building, the regression predictions of EDPs are compared with the log-normal median predictions. In this way, agreement between the results of two statistical approaches is observed. Furthermore, it can be checked whether the structural demand parameter follows the widely-used lognormal distribution assumption for any level of ground motion intensity.

In general, it is observed that two statistical approaches, non-parametric and parametric models, produce highly comparable results especially for lower ground motion intensity levels. The resemblance between two predictions is very high for stiffer buildings. As the buildings get taller and have longer periods, the consistency of regression models with the log-normal distributions becomes relatively lesser. It can be concluded that, on the other hand, the plastic rotations of beams in buildings with  $R=2$  do not follow a log-normal distribution. If one concerns about the plastic rotations he should be careful in following log-normal distribution assumption. A similar situation is also observed for the maximum floor accelerations especially for high levels of response.

For all buildings and all cases, the regression predictions fall between 16<sup>th</sup> – and 84<sup>th</sup> – percentile confidence intervals of probabilistic predictions. This can be interpreted as the best correlations have been accurately investigated by the regression analyses with some plausible uncertainty.

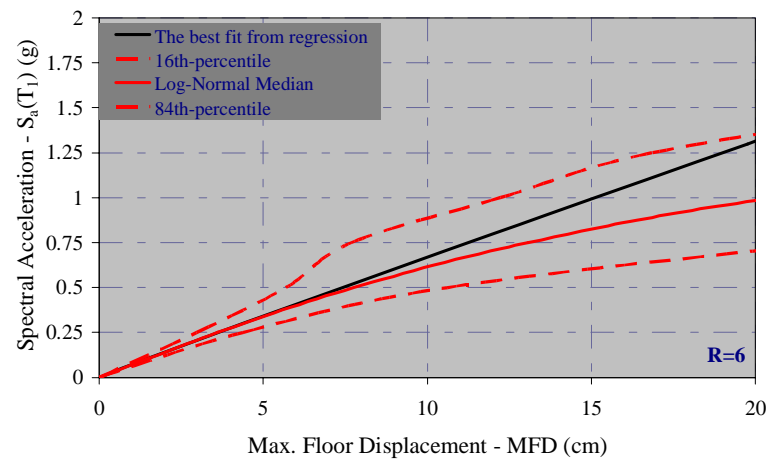
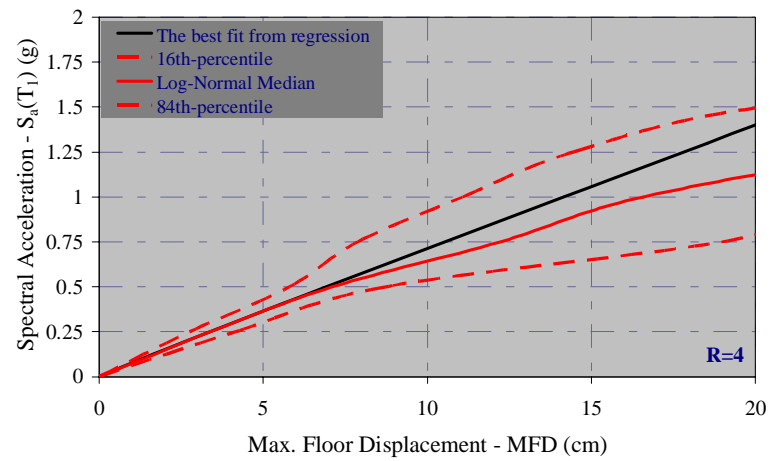
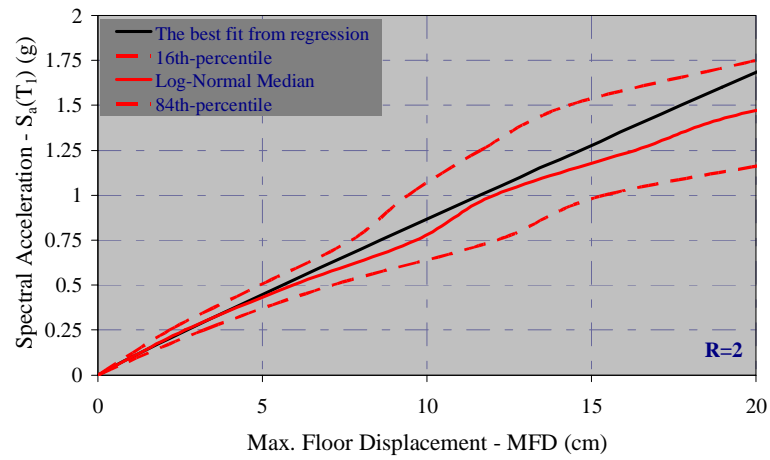


Figure 4.25. Comparison of regression predictions with the log-normally distributed median, 16<sup>th</sup> – and 84<sup>th</sup> –percentile predictions of maximum floor displacements, MFD, for 5-story buildings

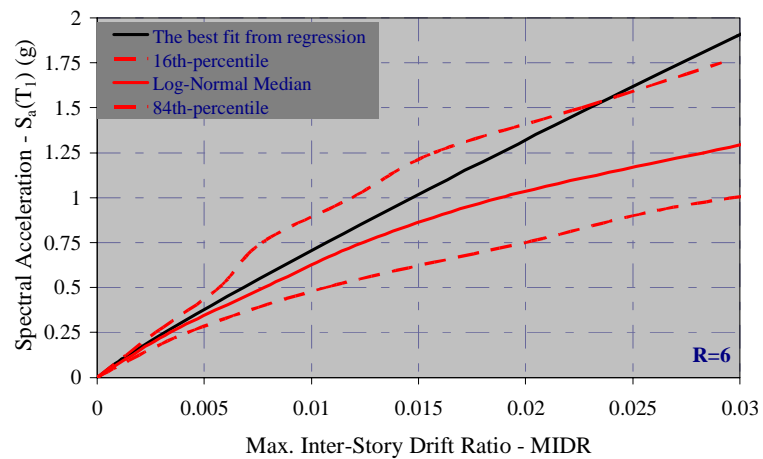
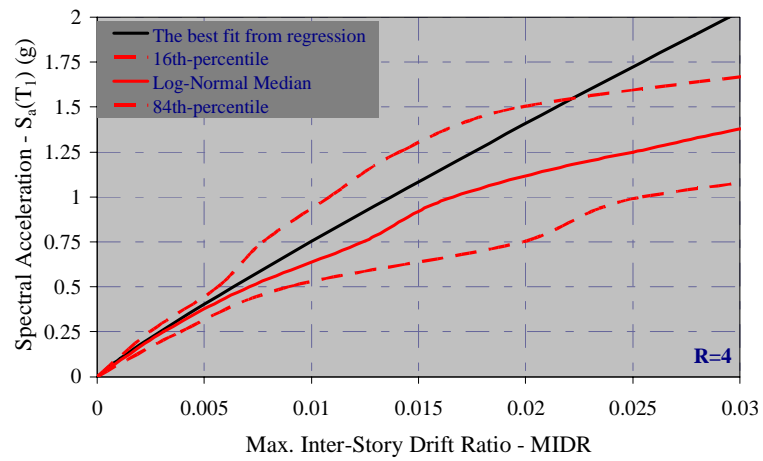
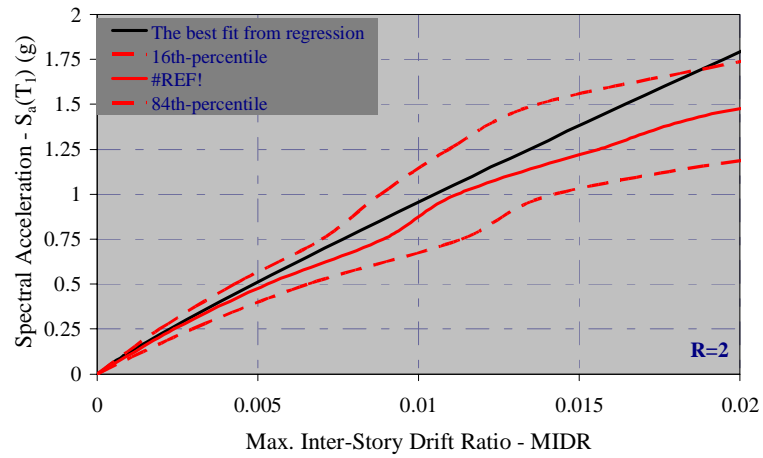


Figure 4.26. Comparison of regression predictions with the log-normally distributed median, 16<sup>th</sup> – and 84<sup>th</sup> –percentile predictions of maximum inter-story drift ratios, MIDR, for 5-story buildings

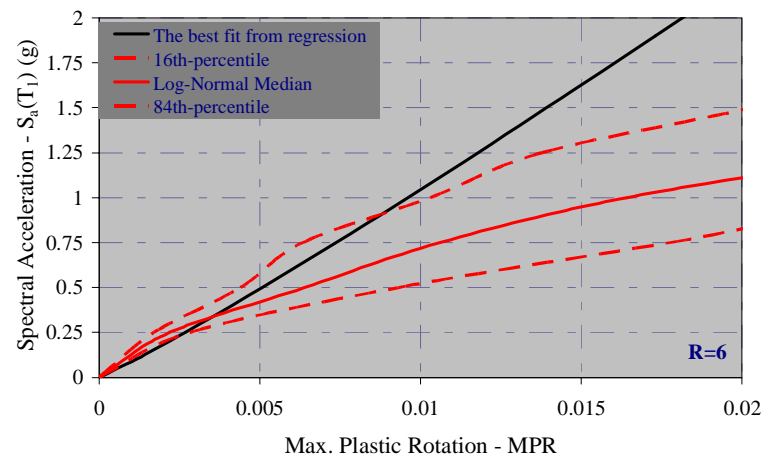
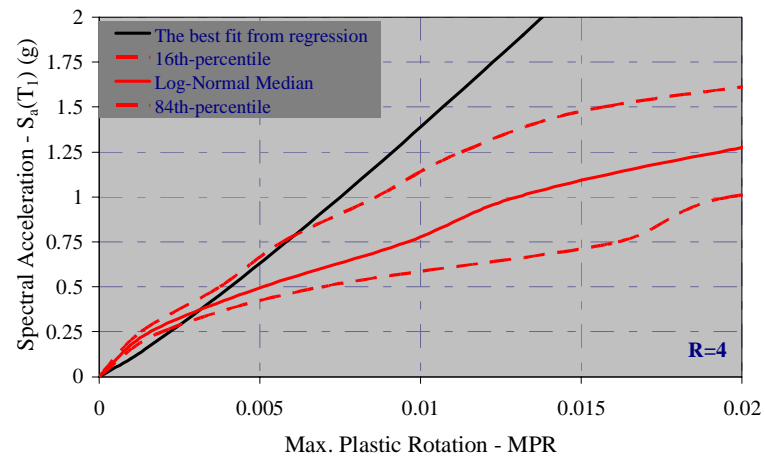
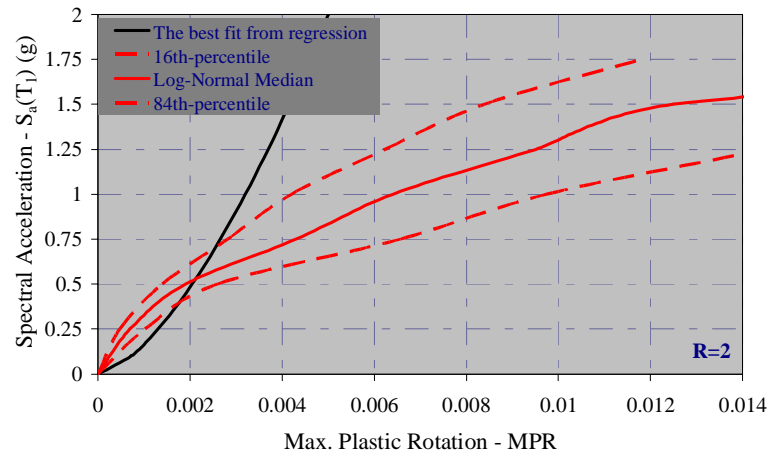


Figure 4.27. Comparison of regression predictions with the log-normally distributed median, 16<sup>th</sup> – and 84<sup>th</sup> –percentile predictions of maximum beam plastic rotations, MPR, for 5-story buildings

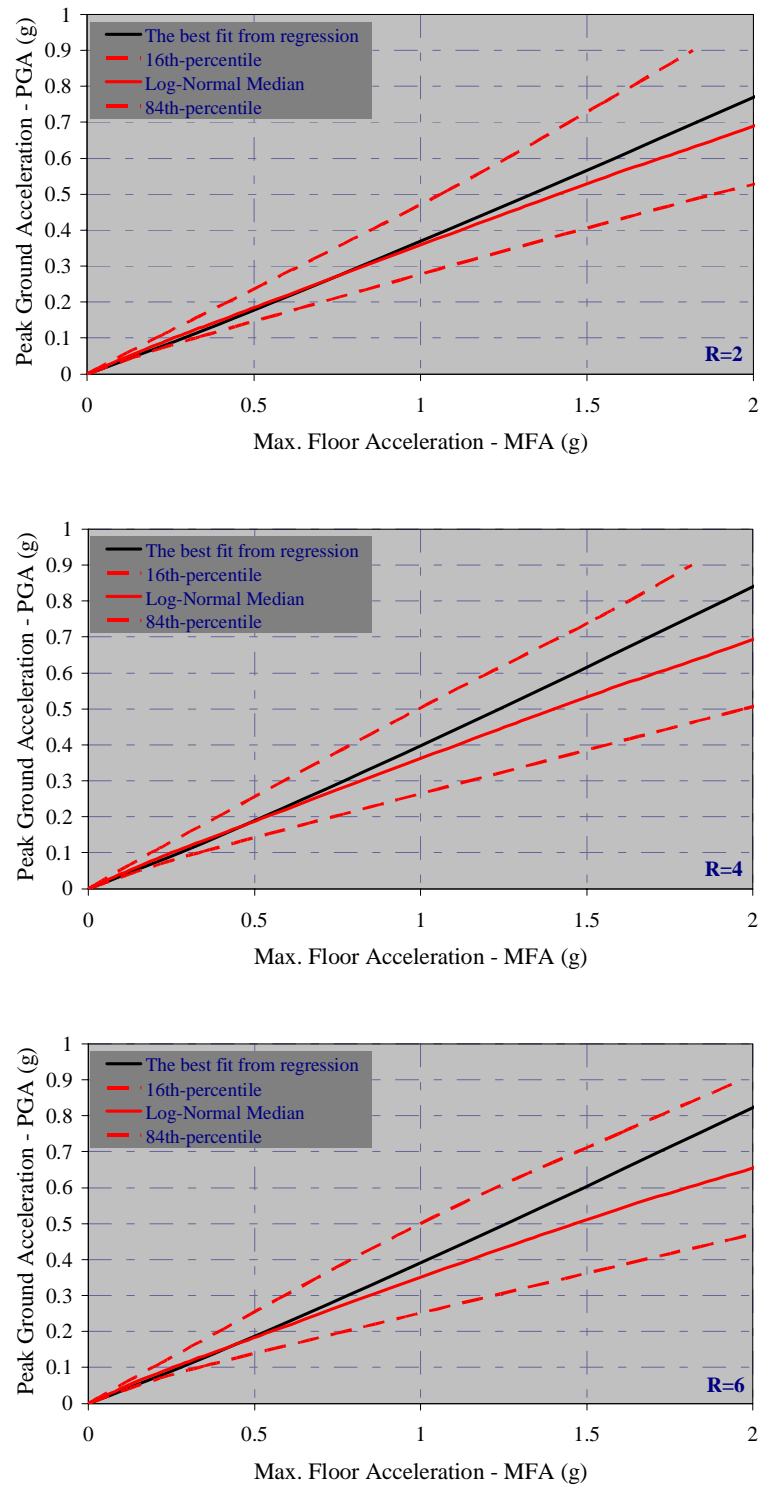


Figure 4.28. Comparison of regression predictions with the log-normally distributed median, 16<sup>th</sup> – and 84<sup>th</sup> –percentile predictions of maximum floor accelerations, MFA, for 5-story buildings

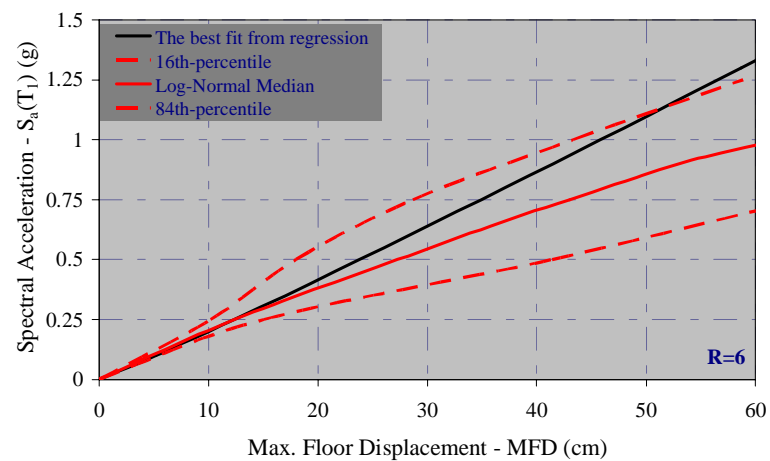
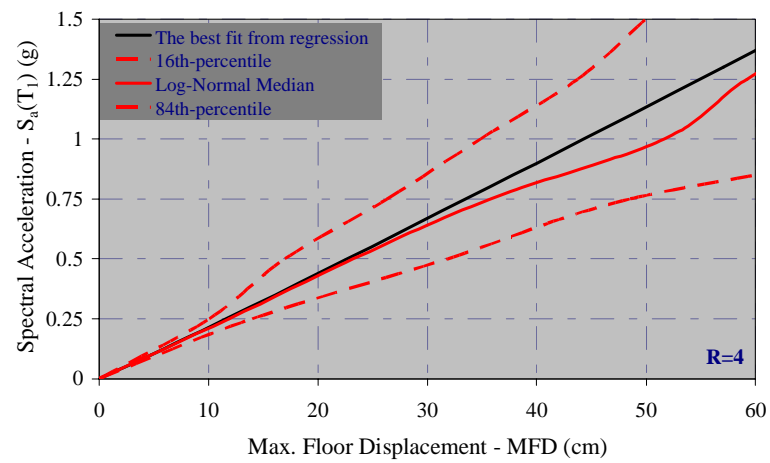
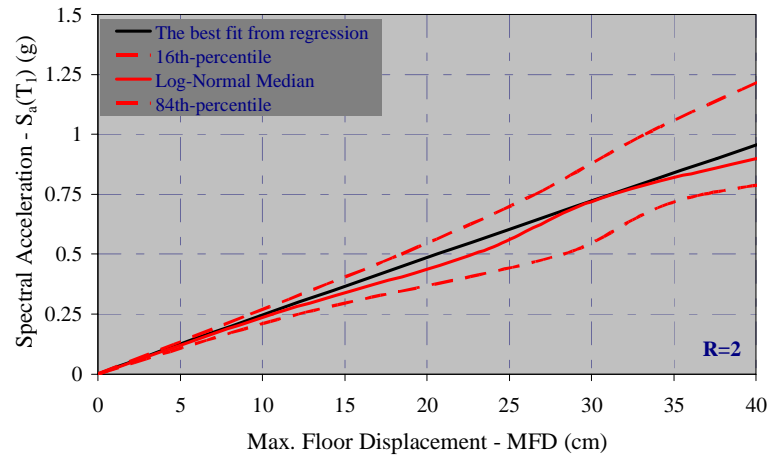


Figure 4.29. Comparison of regression predictions with the log-normally distributed median, 16<sup>th</sup> – and 84<sup>th</sup> –percentile predictions of maximum floor displacements, MFD, for 10-story buildings

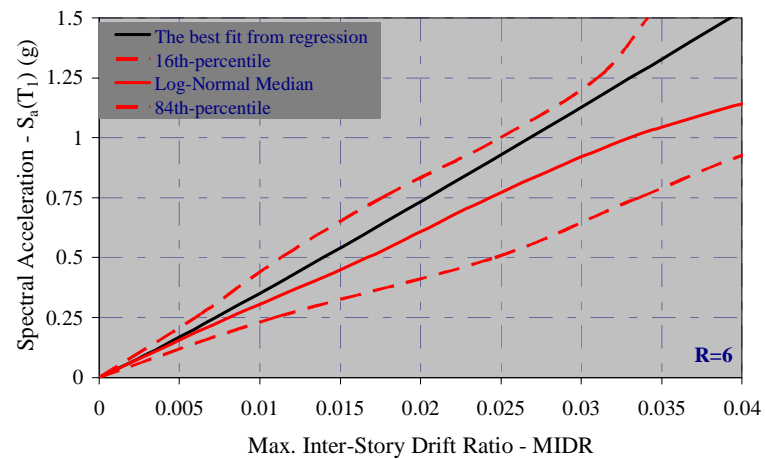
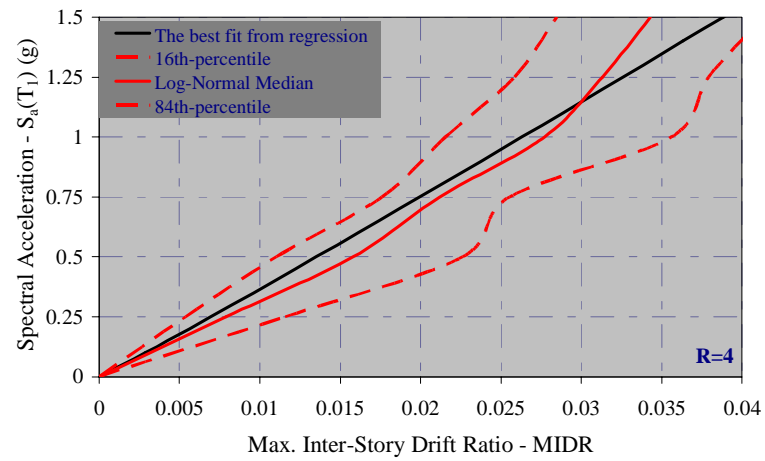
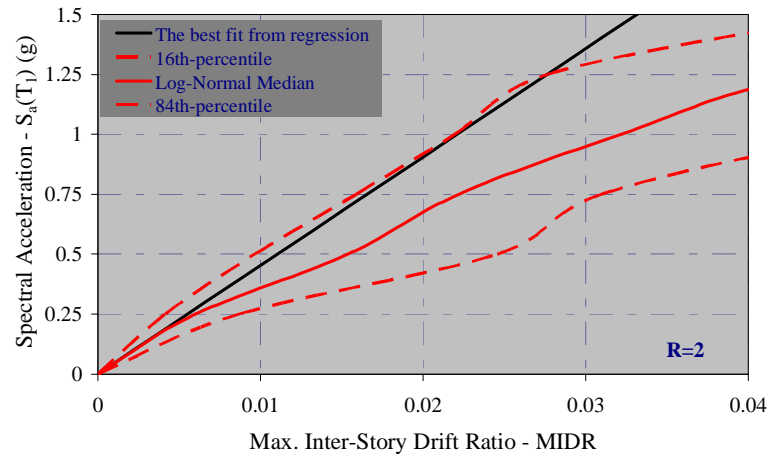


Figure 4.30. Comparison of regression predictions with the log-normally distributed median, 16<sup>th</sup> – and 84<sup>th</sup> –percentile predictions of maximum inter-story drift ratios, MIDR, for 10-story buildings



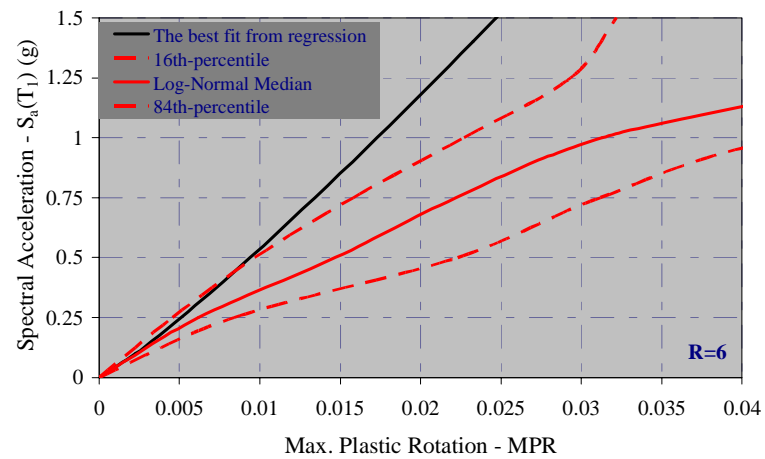
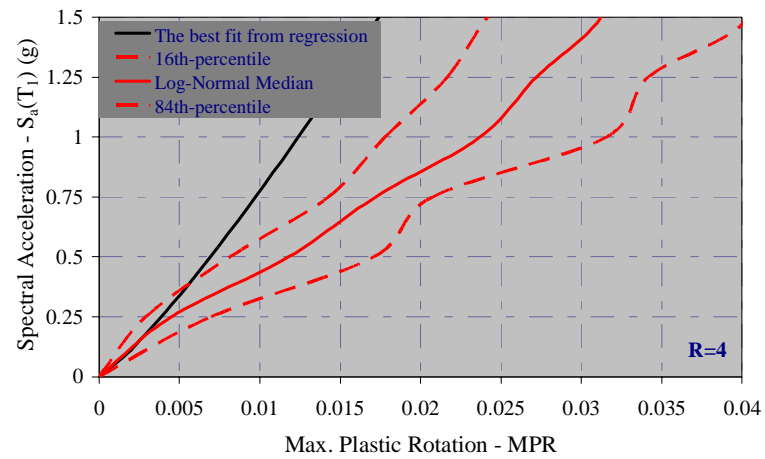
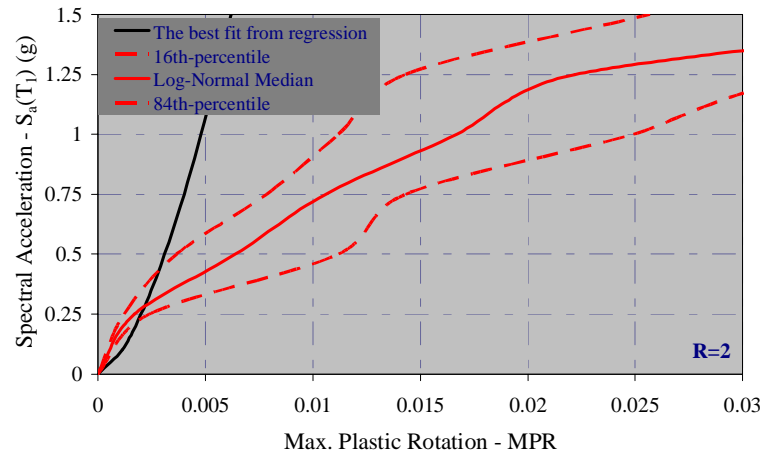


Figure 4.31. Comparison of regression predictions with the log-normally distributed median, 16<sup>th</sup> – and 84<sup>th</sup> –percentile predictions of maximum beam plastic rotations, MPR, for 10-story buildings

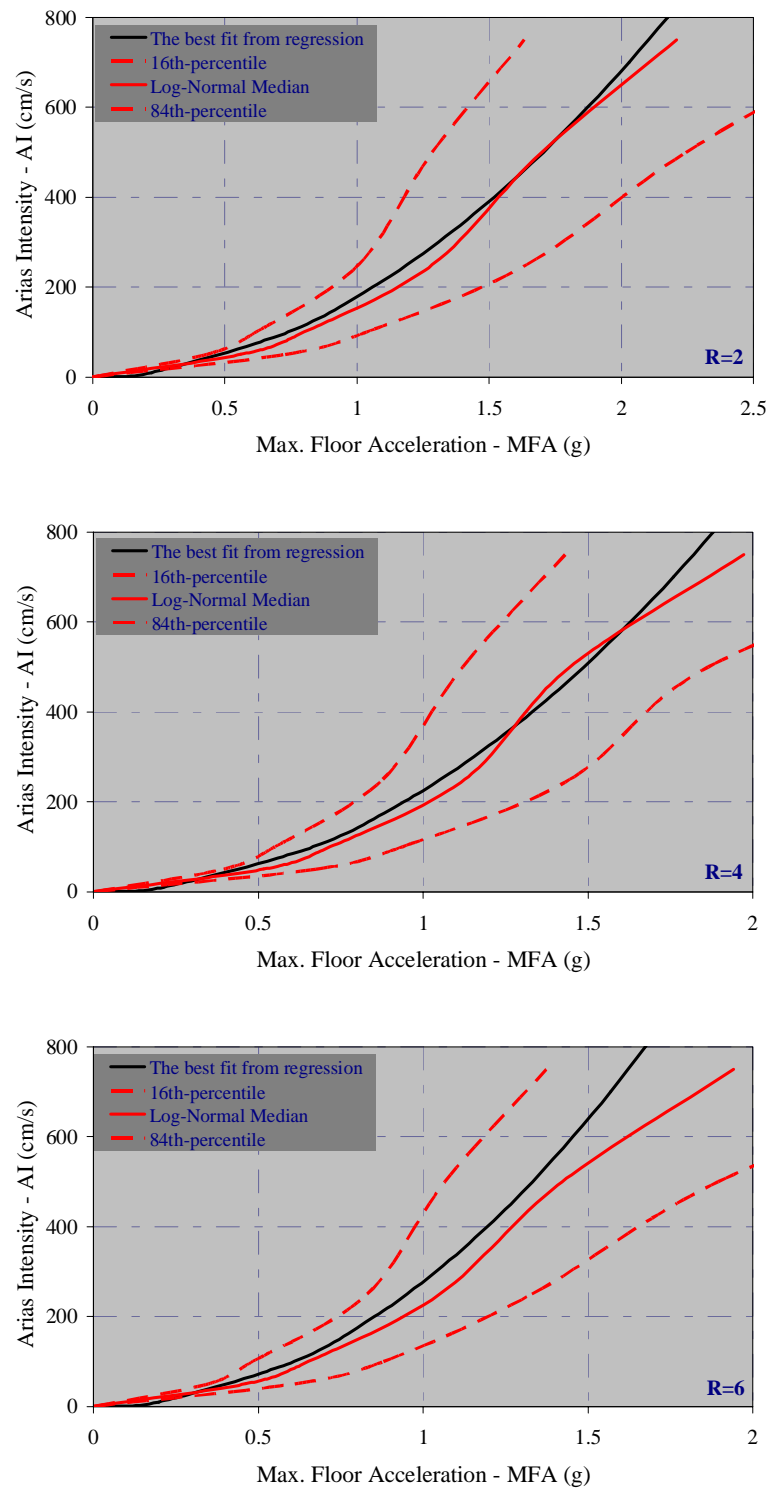


Figure 4.32. Comparison of regression predictions with the log-normally distributed median, 16<sup>th</sup> – and 84<sup>th</sup> –percentile predictions of maximum floor accelerations, MFA, for 10-story buildings

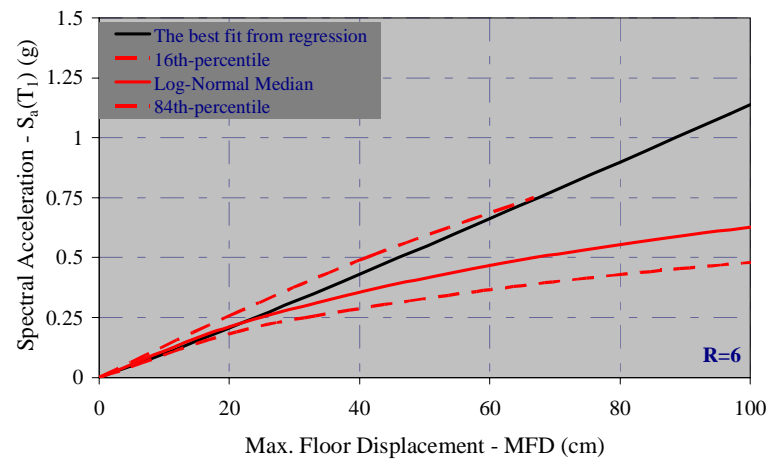
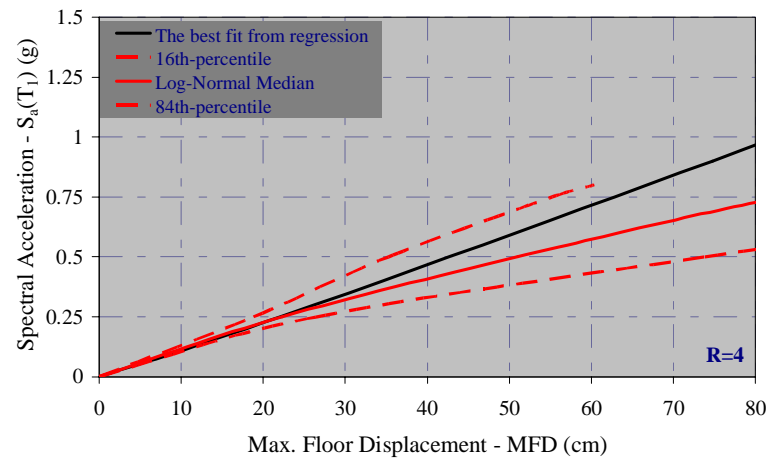
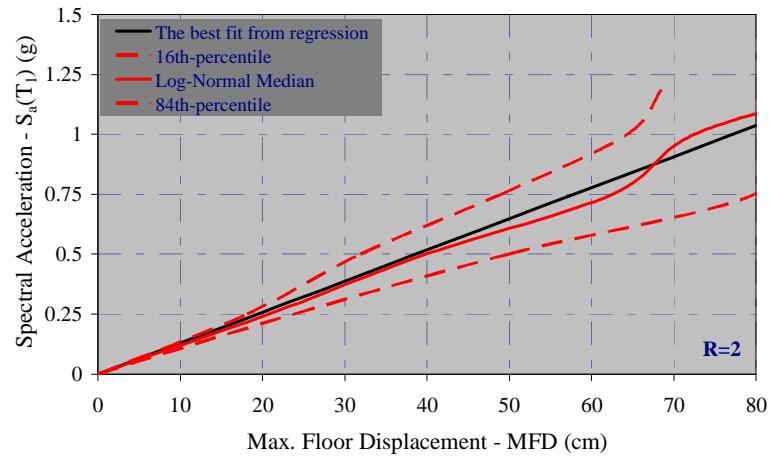


Figure 4.33. Comparison of regression predictions with the log-normally distributed median, 16<sup>th</sup> – and 84<sup>th</sup> –percentile predictions of maximum floor displacements, MFD, for 15-story buildings

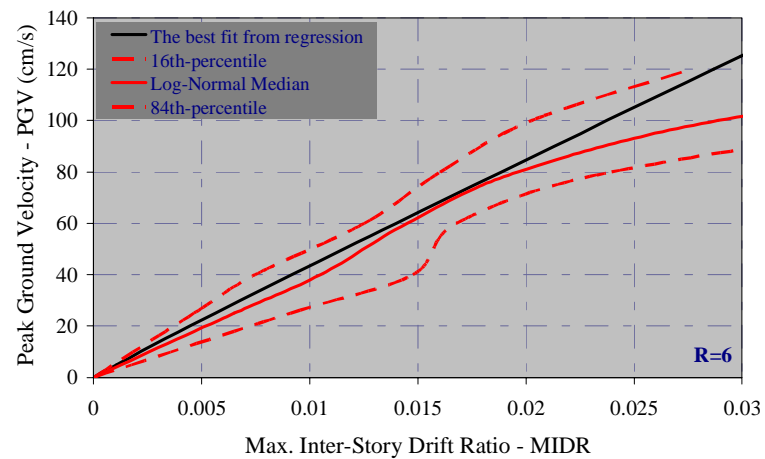
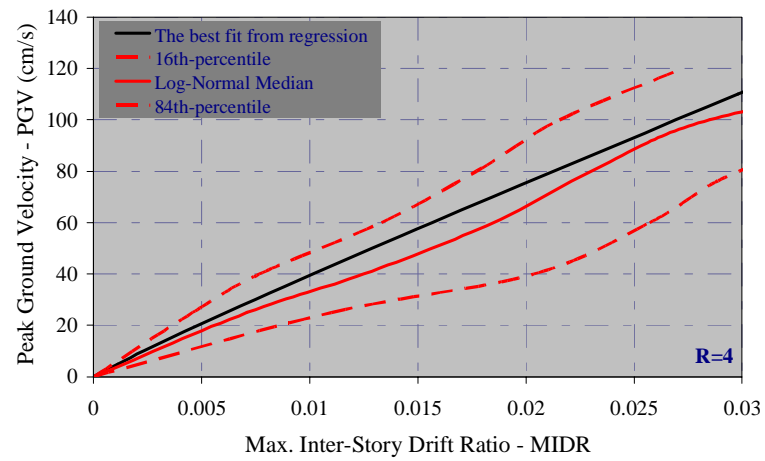
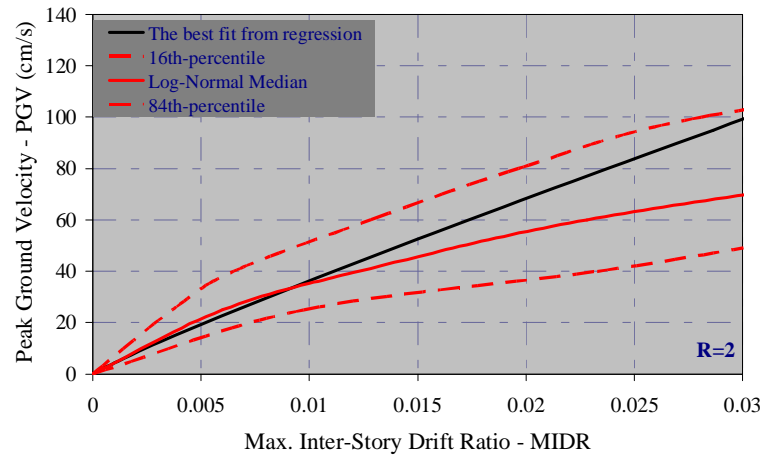


Figure 4.34. Comparison of regression predictions with the log-normally distributed median, 16<sup>th</sup> – and 84<sup>th</sup> –percentile predictions of maximum inter-story drift ratios, MIDR, for 15-story buildings

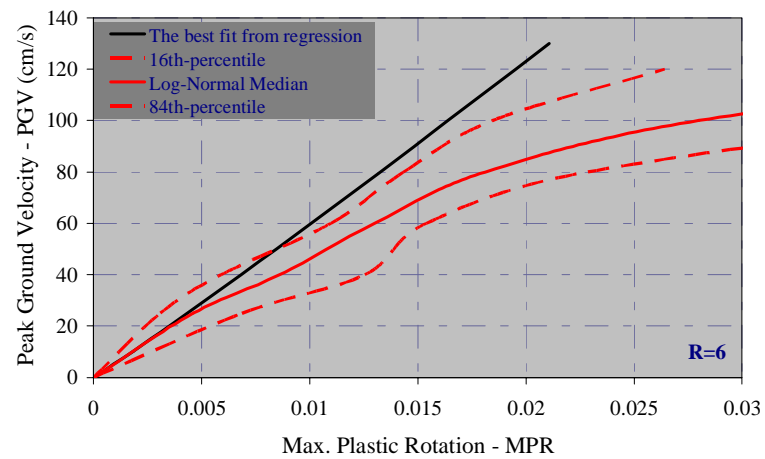
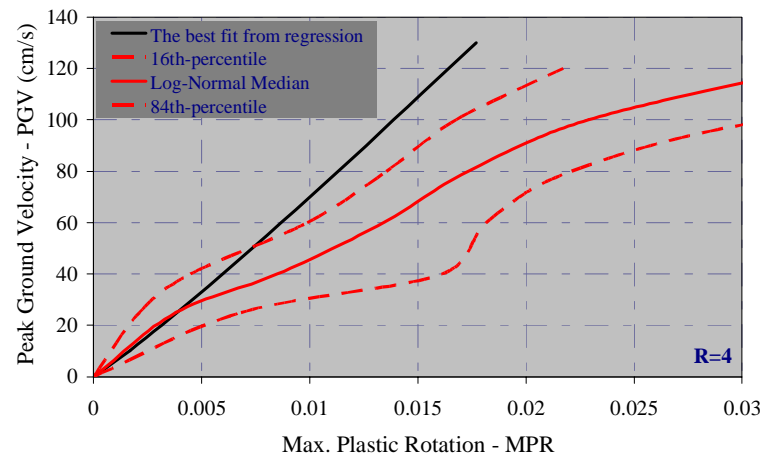
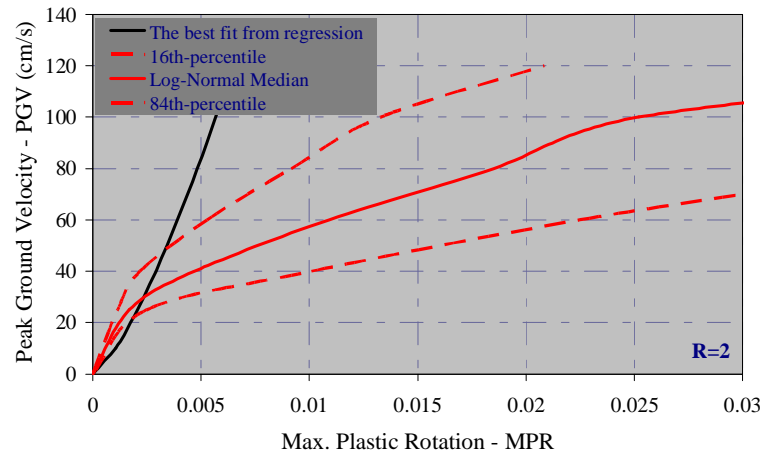


Figure 4.35. Comparison of regression predictions with the log-normally distributed median, 16<sup>th</sup> – and 84<sup>th</sup> –percentile predictions of maximum beam plastic rotations, MPR, for 15-story buildings

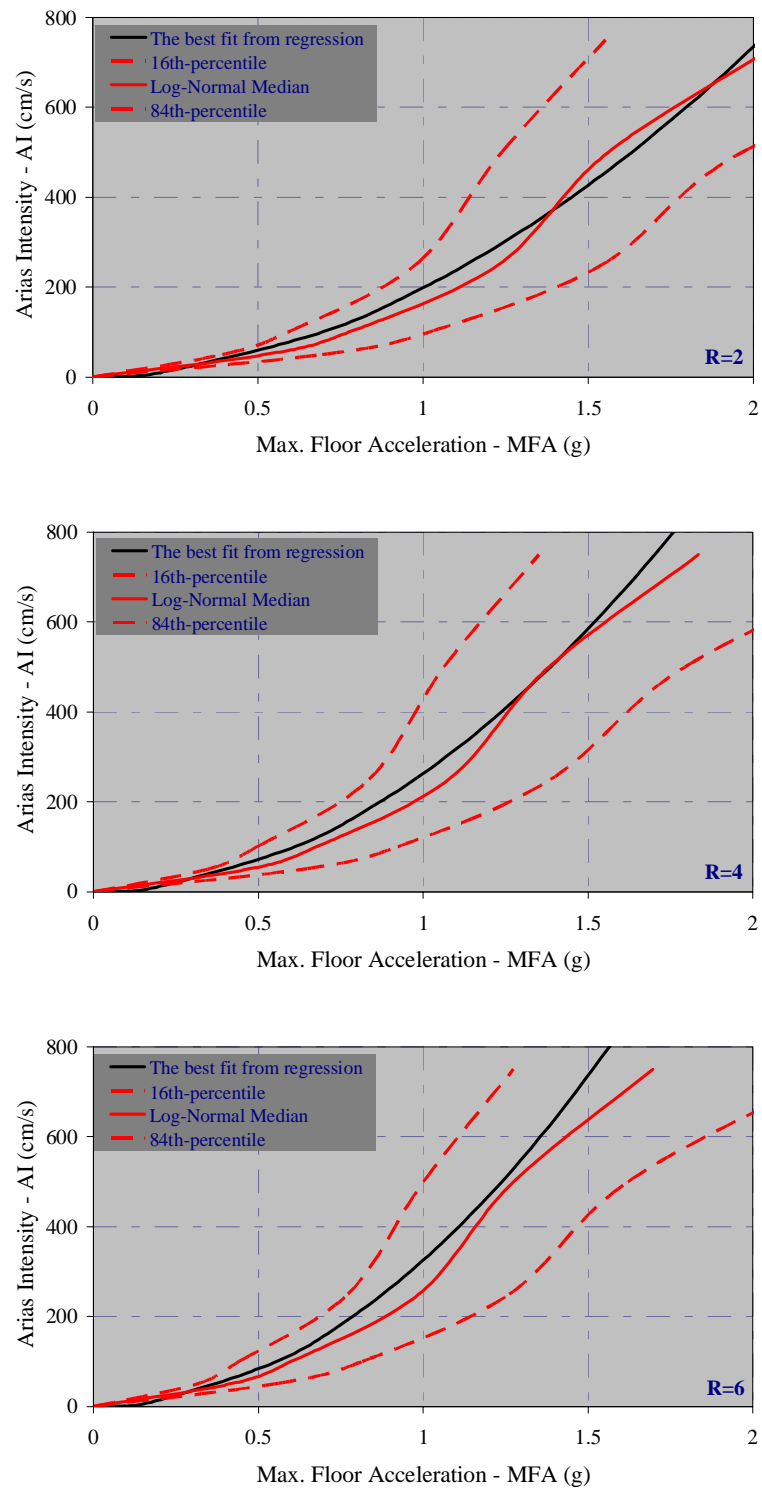


Figure 4.36. Comparison of regression predictions with the log-normally distributed median, 16<sup>th</sup> – and 84<sup>th</sup> –percentile predictions of maximum floor accelerations, MFA, for 15-story buildings

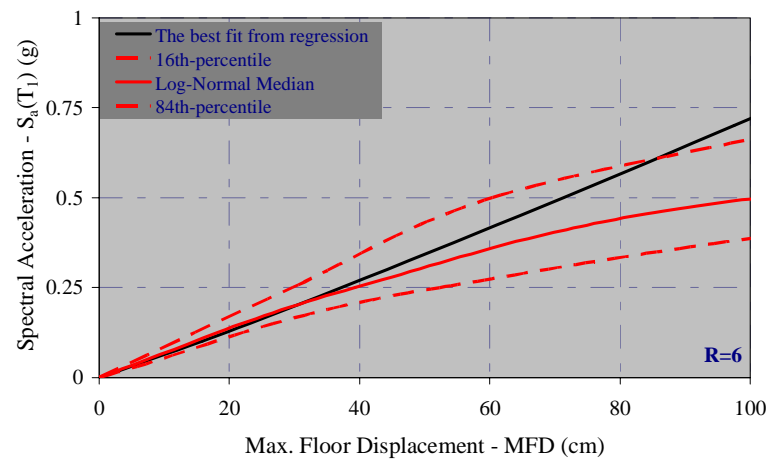
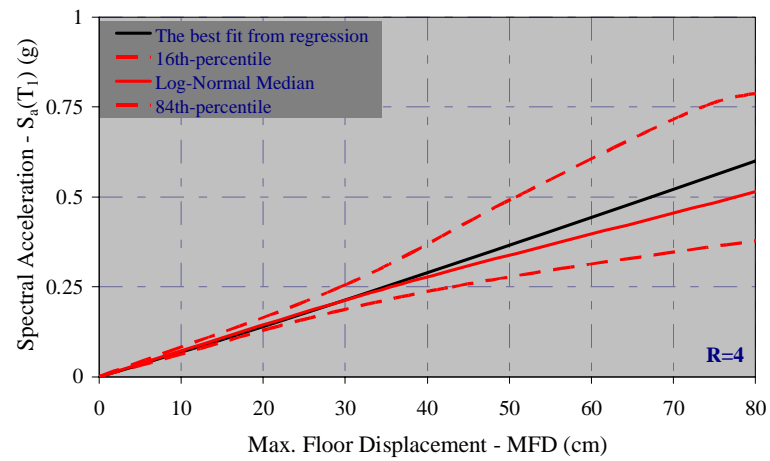
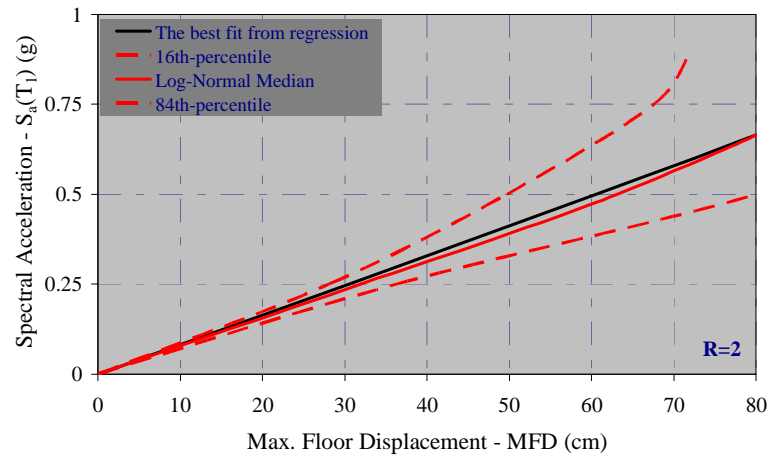


Figure 4.37. Comparison of regression predictions with the log-normally distributed median, 16<sup>th</sup> – and 84<sup>th</sup> –percentile predictions of maximum floor displacements, MFD, for 20-story buildings

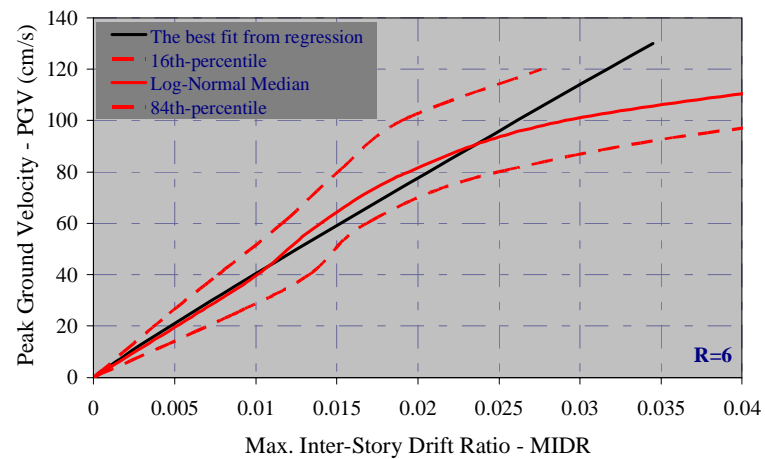
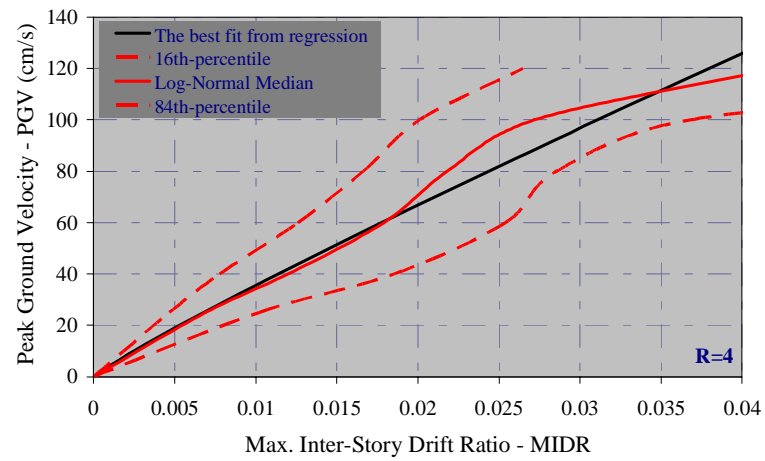
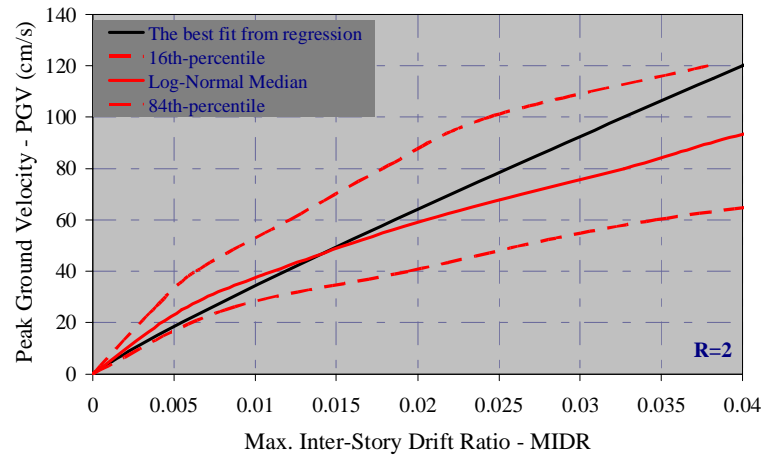


Figure 4.38. Comparison of regression predictions with the log-normally distributed median, 16<sup>th</sup> – and 84<sup>th</sup> –percentile predictions of maximum inter-story drift ratios, MIDR, for 20-story buildings



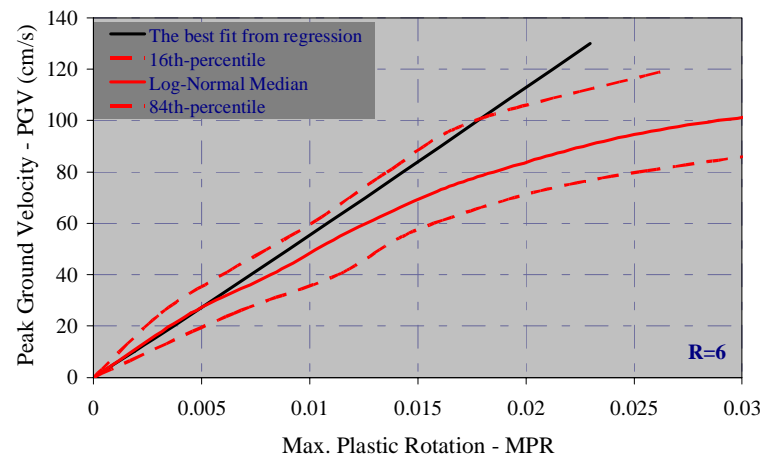
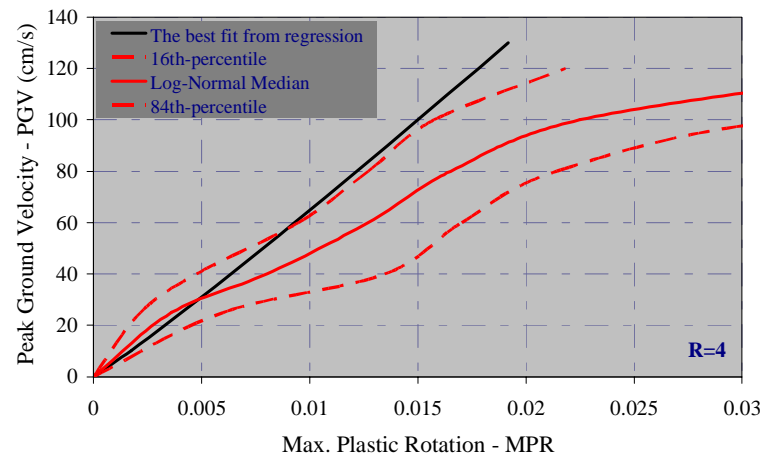
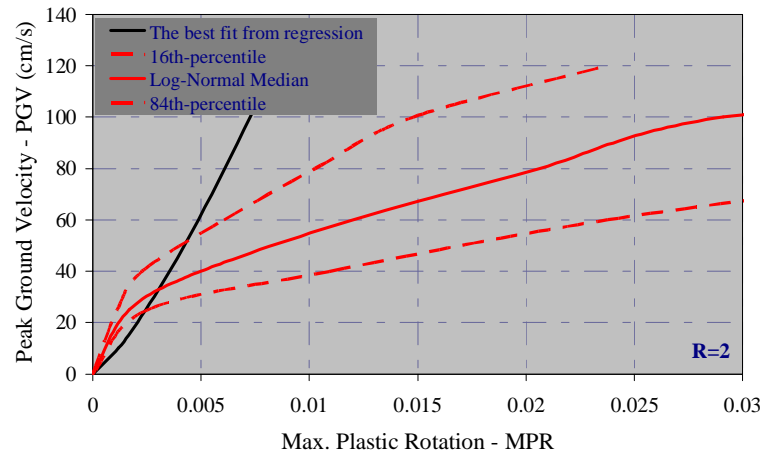


Figure 4.39. Comparison of regression predictions with the log-normally distributed median, 16<sup>th</sup> – and 84<sup>th</sup> –percentile predictions of maximum beam plastic rotations, MPR, for 20-story buildings

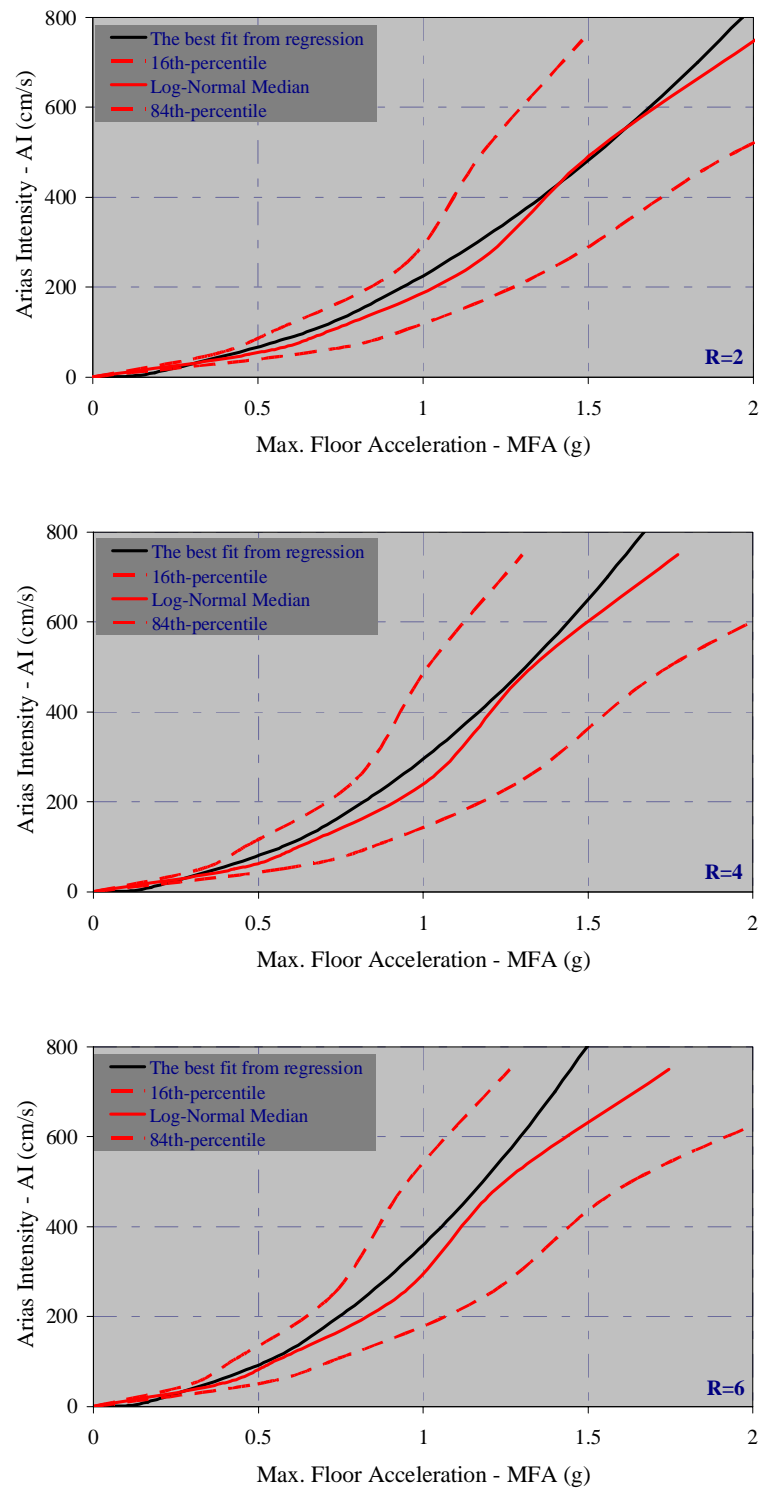


Figure 4.40. Comparison of regression predictions with the log-normally distributed median, 16<sup>th</sup> – and 84<sup>th</sup> –percentile predictions of maximum floor accelerations, MFA, for 20-story buildings

#### 4.4.2. Conditional Probabilistic Structural Response Surfaces

The procedure given in the previous section can easily be adopted to account for the records that cause the building to have a specified demand level and thus, to obtain exceeding probability of a given level of engineering demand parameter as a function of the ground motion intensity measure (Figure 4.41). Once having calculated the lognormal distribution function of an engineering demand parameter conditioned on ground motion intensity measure, those functions can be visualized in three dimensions as the structural response surfaces (Figure 4.42- Figure 4.45). The structural response surfaces serve as the fragility functions and can be utilized in structural and non-structural damage assessments of buildings with similar characteristics to those under consideration.

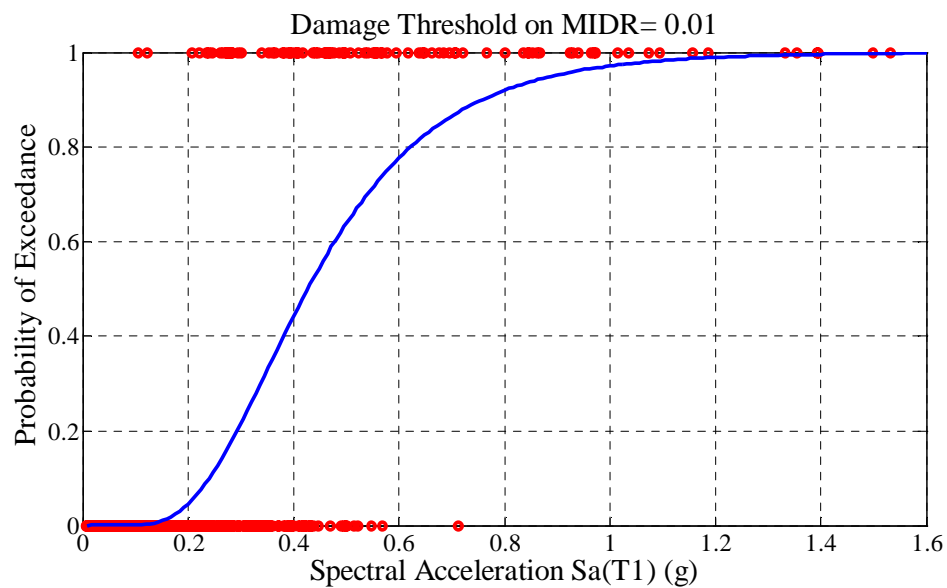


Figure 4.41. Example cumulative probability function of a specified level of demand

If one concerns about a damage threshold on engineering demand parameter, e.g. 0.01 of MIDR is the threshold for moderate damage, the cumulative exceeding probability of having moderate damage under a given level of ground motion intensity can easily be obtained by the proposed conditional structural response surfaces.

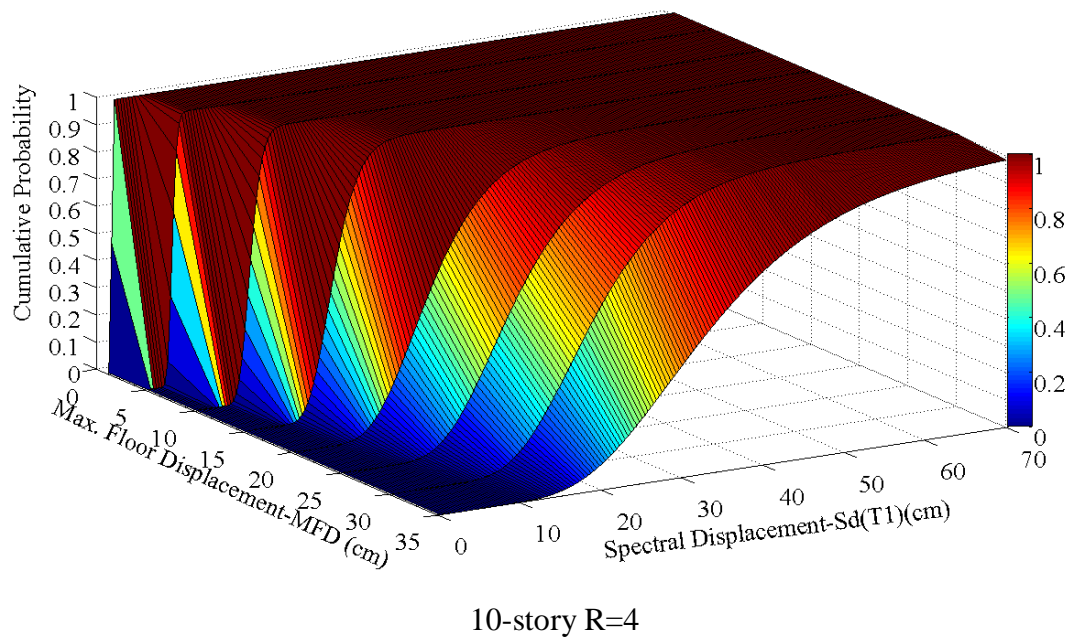
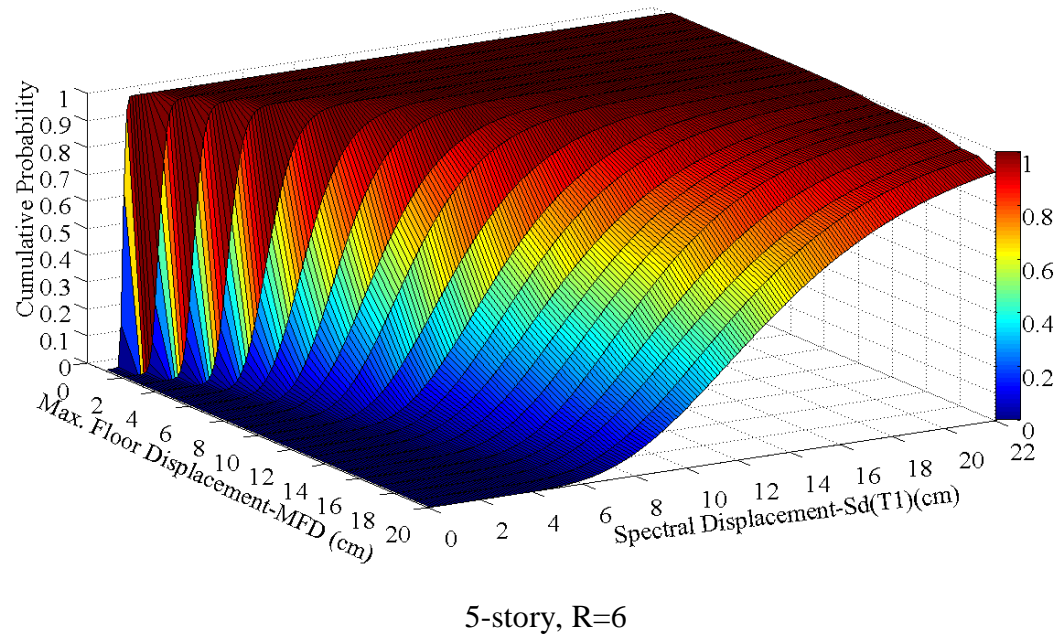


Figure 4.42. Example cumulative probability functions for MFD

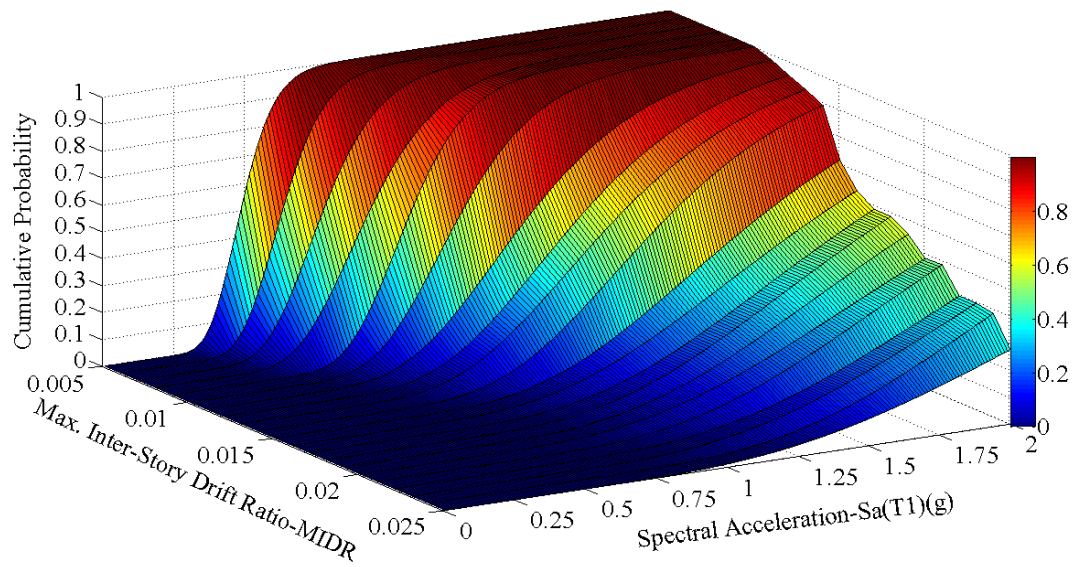
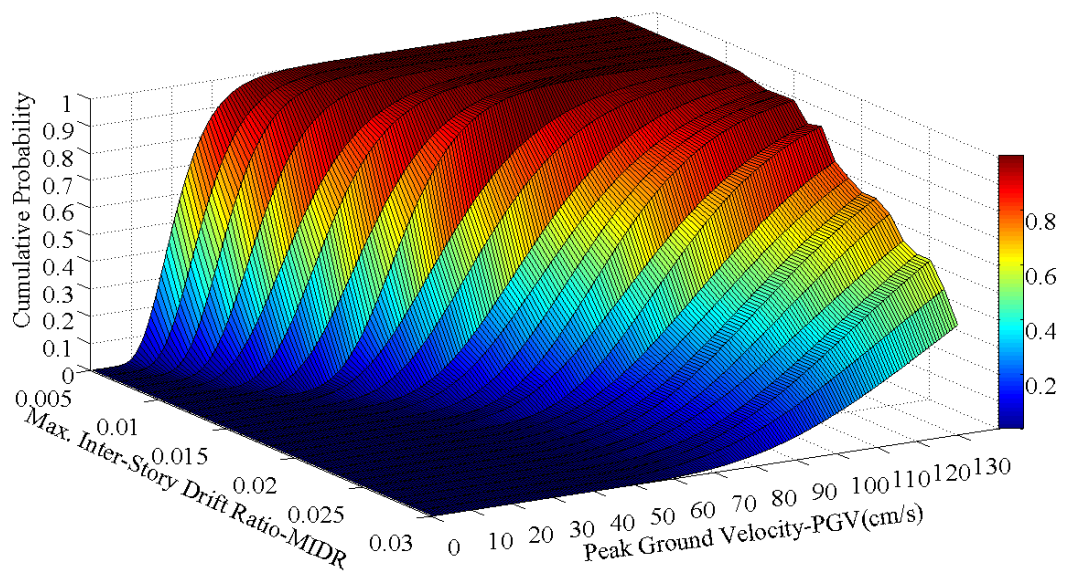
5-story,  $R=2$ 20-story  $R=6$ 

Figure 4.43. Example cumulative probability functions for MIDR

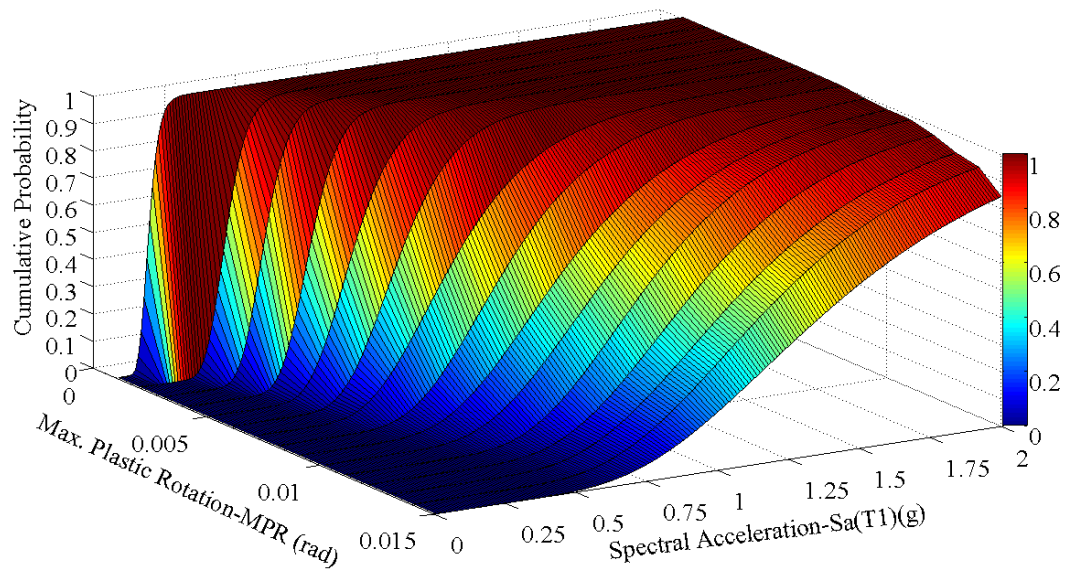
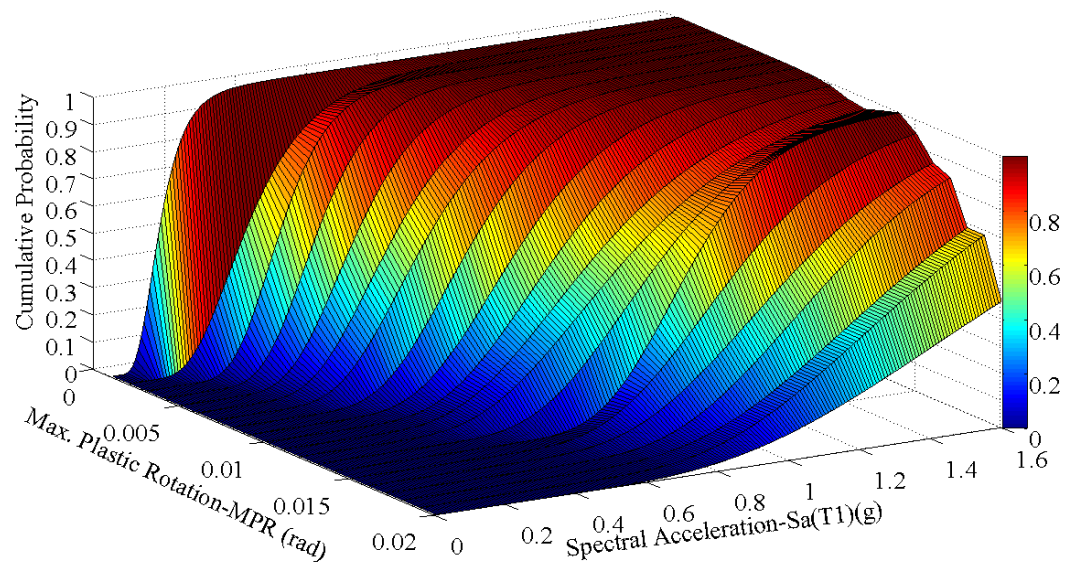
5-story,  $R=4$ 10-story,  $R=2$ 

Figure 4.44. Example cumulative probability functions for MPR



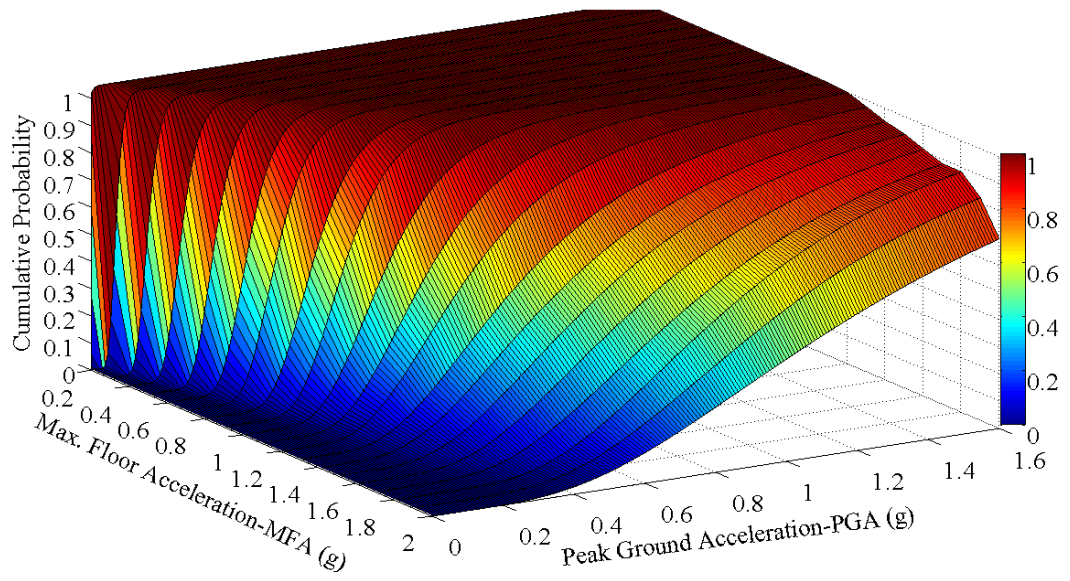
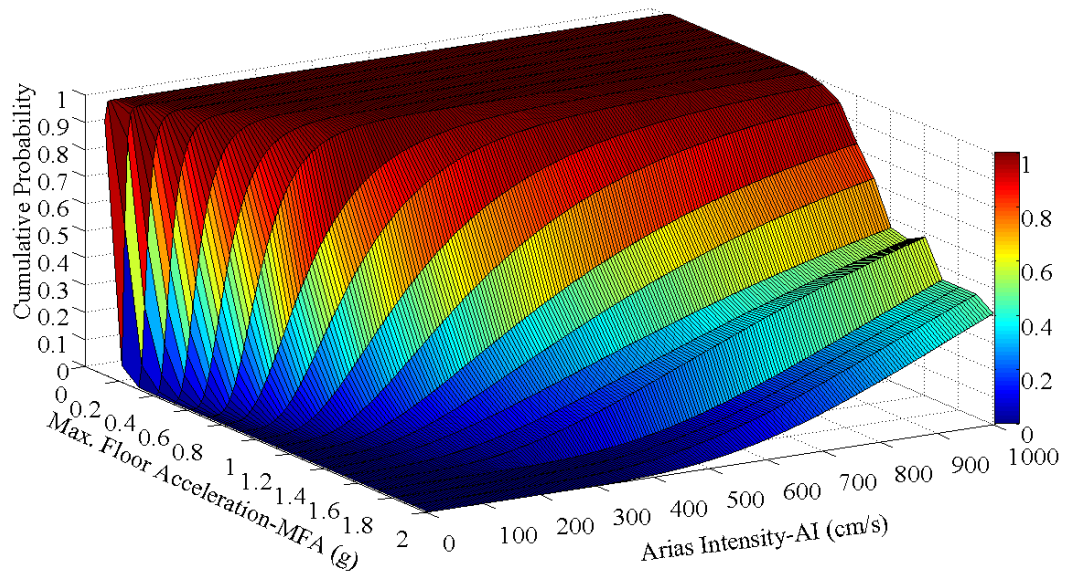
5-story,  $R=6$ 10-story  $R=4$ 

Figure 4.45. Example cumulative probability functions for MFA

## 5. CONCLUSIONS

In this study, a parametric investigation on reinforced concrete buildings is carried out in order to provide correlations between ground motion intensity measures and structural response parameters through nonlinear dynamic analyses of multi-degree-of-freedom (MDOF) structures under real earthquake recordings. The building groups are five-, ten-, fifteen- and twenty-story reinforced concrete, code-conforming, regular moment-resisting frames. They are designed for different strength reduction factors,  $R=2, 4$  and  $6$ . For the buildings under consideration, 8,808 nonlinear time history analyses are performed under 734 horizontal components of unscaled earthquake accelerograms whose magnitudes ( $M_w$ ) and source-to-site distances ( $R_{JB}$ ) vary between 5.5-7.62 and 0-100 km respectively. As ground motion intensity measures (IM), peak ground acceleration ( $PGA$ ), peak ground velocity ( $PGV$ ), peak ground displacement ( $PGD$ ), spectral acceleration ( $S_a(T_I)$ ), spectral velocity ( $S_v(T_I)$ ) spectral displacement ( $S_d(T_I)$ ), Arias intensity ( $AI$ ) and cumulative absolute velocity ( $CAV$ ) are considered. As engineering demand parameters (EDP), maximum floor displacements ( $MFD$ ), maximum inter-story drift ratios ( $MIDR$ ), maximum plastic end rotations of beams ( $MPR$ ) and maximum floor accelerations ( $MFA$ ) are considered. The best correlations between ground motion intensity measures and engineering demand parameters are provided and the functions to predict the structural response via ground motion intensity measure are computed. This is done by non-parametric statistical approach, i.e. regression analysis. Then a parametric statistical evaluation procedure based on a log-normal distribution assumption is applied to the best correlations and median prediction functions are obtained. In order to make a cross-check, the prediction functions resulting from non-parametric evaluation are compared to the median prediction functions obtained from the parametric method. In addition, examples of three-dimensional structural response surfaces are provided in order to utilize in damage assessment of the buildings with similar characteristics.

The findings resulting from the study are summarized below.



### 5.1. Summary of Findings

It is observed that maximum floor displacements at all buildings have a strong correlation with the first period spectral acceleration. In high-period buildings, the effect of peak ground displacement on maximum floor displacements become more apparent. For relatively low- to medium-period buildings, five- and ten-story, maximum inter-story drift ratios and maximum plastic rotations of beams best correlate with the first period spectral acceleration. As the building gets taller and its period becomes longer, the effect of the first period spectral acceleration start diminishing. The greatest correlations of maximum inter-story drift ratios and maximum plastic rotations of beams in fifteen- and twenty-story buildings reveals at peak ground velocity. In short-period buildings, maximum floor accelerations are directly influenced by peak ground acceleration. In taller buildings, both peak ground acceleration and Arias intensity have the strongest impact on the maximum floor accelerations. Additionally, cumulative absolute velocity starts affecting the maximum floor accelerations as the building gets taller.

In general, it is observed that both approaches used for the statistical evaluations, non-parametric and parametric models, produce highly comparable prediction functions of engineering demand parameters especially for lower ground motion intensity levels. For all buildings and all cases, the regression predictions fall between 16<sup>th</sup> – and 84<sup>th</sup> – percentile confidence intervals of probabilistic predictions. This can be interpreted as the best correlations have been accurately investigated by the regression analyses with some plausible uncertainty.

The resemblance between two predictions is very high for stiffer buildings. As the buildings get taller and have longer periods, the consistency of regression models with the log-normal distributions becomes relatively lesser. It can be concluded that, on the other hand, the plastic rotations of beams in buildings with  $R=2$  do not follow a log-normal distribution. This should be taken into consideration that the beam plastic rotations do not obey log-normal distribution assumption in buildings designed for low strength reduction factors, i.e.  $R=2$ , if one concerns about the plastic rotations in a performance assessment study or probabilistic seismic demand analysis. A similar situation is also observed for the maximum floor accelerations especially for high levels of response.

The findings and observations should prudently be utilized in selection and scaling/modification of ground motion recordings as input for the nonlinear dynamic analyses. The provided correlations might also help in developing better intensity measures that sufficiently and efficiently incorporate the seismic hazard at the site and that also reduce the scatter in the nonlinear structural response when using a smaller number of records. The proposed structural response surfaces serve as the fragility functions and can be utilized in structural and non-structural damage assessments of buildings with similar characteristics to those under consideration.

## **5.2. Future Research**

Although nonlinear dynamic analysis specific to the structural system and seismic environment is the best way to identify nonlinear dynamic response characteristics of the structure, when the analysis is performed the true response of the structure cannot be reliably determined by the use of only one ground motion acceleration time history. Performance-based earthquake engineering allows the designer to specify and predict, with a reasonable accuracy, the performance (degree of damage) of the structure for a specified level of ground motion intensity. This requires using several input ground motion records that adequately represent the damage potential for given seismic hazard levels and structural characteristics. Records to use in nonlinear time-domain analyses should be selected considering magnitude, distance, site condition and other parameters that control the ground motion characteristics. Guidelines on procedures for the selection of appropriate suites of acceleration time-series as input to dynamic analysis are lacking, and seismic design codes are particularly poor in this respect because dominant magnitude-distance scenarios are not identified. Currently, the minimum number of records required to be used in inelastic dynamic analysis by design codes varies but is frequently based on the guidance of the Uniform Building Code (UBC, 1994). Similarly to the UBC-1994, some other codes and regulatory documents such as Standard for Minimum Design Loads for Buildings and Other Structures-ASCE 7-05, Standard for Seismic Rehabilitation of Existing Buildings -ASCE 41-06, International Building Code-IBC 2006 and Eurocode 8-EC8 require using at least three ground motion records. In this case, the maximum response from those three analyses should be used. The nonlinear time history analysis results can be averaged if seven or more records are used. Magnitude, fault distance, and

source mechanism characteristics that control the seismic hazard should be considered in the selection of suit of acceleration time histories. EC8 also requires inclusion of the site class of the building location as the selection criteria. Furthermore, the code-based prescriptions for records as input to dynamic analysis often necessitate compatibility with a smooth design acceleration response spectrum. The EC8 prescriptions ask for matching of the average spectral ordinates of the chosen record set to the target code-based spectral shape, with a 10% tolerance, in a broad range of periods depending on the dynamic characteristics of the structure under consideration.

In the light of the findings of this study, criteria for selecting and scaling/modifying accelerograms which might be incorporated in the next generations of Eurocode 8 might be proposed. This can be accomplished through comparative evaluation of various options for scaling and matching accelerograms for obtaining the expected inelastic response of a structure as assessed by some damage measure. For this purpose, the methods for ground motion selection and modification as well as for the statistical evaluation of the dynamic analysis results which are already available in the literature can be applied to the nonlinear dynamic analyses results of the building group considered in this thesis study.

## REFERENCES

- Akkar, S. and O. Ozen, 2005, “Effect of Peak Ground Velocity on Deformation Demands for SDOF Systems”, *Earthquake Engineering and Structural Dynamics*, Vol.34, No. 13, pp. 1551-1571.
- Araya, R., and G.R. Saragoni, 1980, “Capacity of the Strong Ground-Motion to Cause Structural Damage”, *Proceedings of the Seventh World Conference on Earthquake Engineering*, pp. 483-490, Istanbul.
- Arias, A., 1970, “A Measure of Earthquake Intensity”, *Seismic Design for Nuclear Power Plants*, pp. 438-483, R.J. Hansen (editor), MIT Press, Cambridge.
- Baker, J. W. and C. A. Cornell, 2005, “A Vector-Valued Ground Motion Intensity Measure Consisting of Spectral Acceleration and Epsilon”, *Earthquake Engineering and Structural Dynamics*, Vol. 34, pp. 1193-1217.
- Baker, J. W., 2007, “Probabilistic Structural Response Assessment Using Vector-valued Intensity Measures”, *Earthquake Engineering and Structural Dynamics*, Vol. 36, pp. 1861-1883.
- Bazzurro, P. and C. A. Cornell, 1994, “Seismic Hazard Analysis of Nonlinear Structures I: Methodology”, *Journal of Structural Engineering*, Vol. 120, pp. 3320–3344.
- Bertero, V.V., S. A. Mahin, and R. A. Herrera, 1978, “Aseismic Design Implications of Near-Fault San Fernando Earthquake Records”, *Earthquake Engineering and Structural Dynamics*, Vol. 6, pp. 31-42.
- Bommer, J.J., G. Georgallides and I. J. Tromans, 2001, “Is There a Near-Field for Small-to-Moderate Magnitude Earthquakes?”, *Journal of Earthquake Engineering*, Vol. 5, No. 3, pp. 395-423.

- Bonelli, P., 1998a, "Long Seismic Velocity Pulse Effect and Damage", *Structural Engineering World Wide*, T227-3.
- Bonelli, P., 1998b, "An Evaluation of the Effects of Long Acceleration Pulses on the Seismic Response of Structures", *Proceedings of the 11th European Conference on Earthquake Engineering*, Acapulco, Mexico.
- Bozorgnia, Y. and K. Campbell, 2004, "Engineering Characterization of Ground Motion", *Earthquake Engineering from Engineering Seismology to Performance-Based Engineering*, ed. by Bozorgnia, Y. and V.V. Bertero, CRS Press LLC.
- Brune, J. N., 1970, "Tectonic Stress and the Spectra of Seismic Shear Waves from Earthquakes", *Journal of Geophysical Research*, Vol. 75, No. 26, pp. 4997-5009.
- Chopra, A. K., 2001, *Dynamics of Structures*, Prentice Hall, Upper Saddle River, NJ, USA.
- Cornell, C. A. and H. Krawinkler, 2000, "Progress and Challenges in Seismic Performance Assessment", *PEER Center News*, Vol. 3, <http://peer.berkeley.edu/news/200spring/performance.html>.
- Cornell, C. A., F. Jalayer, R. O. Hamburger and D. A. Foutch, 2002, "Probabilistic Basis for 2000 SAC Federal Emergency Management Agency Steel Moment Frame Guidelines", *Journal of Structural Engineering*, Vol. 128, No. 4, 526, ASCE.
- Deierlein, G. G., 2004, "Overview of A Comprehensive Framework For Earthquake Performance Assessment", *Proceedings of International Workshop on Performance-Based Seismic Design Concepts and Implementation*, Bled, Slovenia.
- Filippou, F. C. and G. L. Fenves, 2004, "Methods of Analysis for Earthquake-Resistant Structures", *Earthquake Engineering from Engineering Seismology to Performance-Based Engineering*, ed. by Bozorgnia, Y. and V.V. Bertero, CRS Press LLC.

- Hancock, J., 2006, *The Influence of Duration and the Selection and Scaling of Accelerograms in Engineering Design and Assessment*, Ph.D. Dissertation, Imperial College.
- Haselton, C. B., C. A. Goulet, J. M. Reiser, J. L. Beck, G. G. Deierlein, K. A. Porter, J. P. Stewart, E. Taciroglu, 2008, “An Assessment to Benchmark the Seismic Performance of a Code-Conforming Reinforced Concrete Moment-Frame Building”, *PEER Report 2007/12*, Pacific Earthquake Engineering Research Center of University of California, Berkeley, USA.
- Housner, G. W., 1970, “Strong Ground Motion”, *Earthquake Engineering*, ed. by Wiegel, R. L., Prentice-Hall, Upper Saddle River, New Jersey.
- Jalayer, F. and C. A. Cornell, 2003, “A Technical Framework for Probability-Based Demand and Capacity Factor Design (DCFD) Seismic Formats”, *PEER Report 2003/08*, Pacific Earthquake Engineering Research Center of University of California, Berkeley, USA.
- Jamei, M.M., M. R. Eslahchi, M. Dehghan, 2005, “On Numerical Improvement of Gauss–Radau Quadrature Rules”, *Applied Mathematics and Computation*, Vol. 168, No. 1, pp. 51-64.
- Kramer, S., 1996, *Geotechnical Earthquake Engineering*, International series in Civil Engineering and Engineering Mechanics, Prentice-Hall, New Jersey.
- Krawinkler, H. and E. Miranda, 2004, “Performance-Based Earthquake Engineering”, *Earthquake Engineering from Engineering Seismology to Performance-Based Engineering*, ed. by Bozorgnia, Y. and V.V. Bertero, CRS Press LLC.
- Kurama, Y. C. and K. T. Farrow, 2003, “Ground Motion Scaling Methods for Different Site Conditions and Structure Characteristics”, *Earthquake Engineering and Structural Dynamics*, Vol. 32, pp. 2425-2450.

- Lehmann, E. L. and H. J. M. D'Abrera, 1998, *Nonparametrics: Statistical Methods Based on Ranks*, Prentice-Hall, Upper Saddle River, NJ, USA.
- Luco, N., 2002, *Probabilistic Seismic Demand Analysis, SMFR Connection Fractures and Near-Source Effect*, Ph.D. Dissertation, Stanford University.
- Luco, N., and C. A. Cornell, 2007, "Structure-Specific Scalar Intensity Measures for Near-Source and Ordinary Earthquake Ground Motions", *Earthquake Spectra*, Vol. 23, pp.357.
- Malhotra, P. K., 1999, "Response of Buildings to Near-Field Pulse-Like Ground Motions", *Earthquake Engineering and Structural Dynamics*, Vol. 28, No. 11, pp. 1309-1326.
- Mander, J.B., M. J. N. Priestley, and Park, 1989, "Theoretical Stress-Strain Model for Confined Concrete", *Journal of Structural Engineering*, Vol. 114, No. 8, pp. 1804-1826.
- Mazzoni, S., F. McKenna, M. H. Scott, and G. L. Fenves, 2009, "OpenSees v2.0 user command-language manual", Pacific Earthquake Engineering Research Center of University of California, Berkeley, USA.
- McKenna, F., *et al.*, 2008, "OpenSees v2.0 - Open System for Earthquake Engineering Simulation", Pacific Earthquake Engineering Research Center of University of California, Berkeley, USA.
- Menegotto, M. and P.E. Pinto, 1973, "Method of Analysis for Cyclically Loaded R.C. Plane Frames Including Changes in Geometry and Non-Elastic Behavior of Elements Under Combined Normal Force and Bending", *Proceedings of Symposium on The Resistance and Ultimate Deformability of Structures Acted on By Well Defined Repeated Loads*, pp. 15-22, International Association for Bridge and Structural Engineering, Zurich, Switzerland

- Naeim, F., 1995, "On Seismic Design Implications of the 1994 Northridge Earthquake Records", *Earthquake Spectra*, Vol. 11, No. 1, pp. 91-109.
- Onem, G., 2008, *Evaluation of Practice-Oriented Nonlinear Analysis Methods For Seismic Performance Assessment*, Ph.D. Dissertation, Bogazici University.
- Priestley, M. J. N., G. M. Calvi and M. J. Kowalsky, 2007, *Displacement-Based Seismic Design of Structures*, IUSS Press, Pavia, Italy.
- Scott, M. H. and G. L. Fenves, 2006, "Plastic Hinge Integration Methods for Force-Based Beam-Column Elements", *Journal of Structural Engineering*, Vol. 132, No. 2, pp. 244-252, ASCE.
- Shinozuka, M., M. Q. Feng, H. Kim, T. Uzawa, and T. Ueda, 2001, "Statistical Analysis of Fragility Curves", *MCEER Technical Report*, Department of Civil and Environmental Engineering, University of Southern California, LA, USA.
- Shome, N., C. A. Cornell, P. Bazzurro and J. E. Carballo, J. E., 1998, "Earthquakes, records and nonlinear responses, *Earthquake Spectra*, Vol. 14, No. 3, pp. 469–500.
- Somerville, P.G., N.F. Smith, R. W. Graves and N. A. Abrahamson, 1997, "Modification of Empirical Strong Ground Motion Attenuation Relations to Include the Amplitude and Duration Effects of Rupture Directivity", *Seismological Research Letters*, Vol. 68, No. 1, pp. 199-222.
- Somerville, P., 2000 "New Developments in Seismic Hazard Estimation", *Proceedings of the Sixth International Conference on Seismic Zonation*, Palm Springs, California.
- Stewart, J., S. Chiou, J. Bray, R. Graves, P. Somerville, and N. Abrahamson, 2001, "Ground Motion Evaluation Procedures for Performance-Based Design", *PEER Report 2001/09*, *Pacific Earthquake Engineering Research Center*, College of Engineering, University of California, Berkeley.



The MathWorks Inc., 2008, MATLAB v7.7.0, The Language of Technical Computing, USA.

Trifunac, M.D. and E. I. Novikova, 1995, “Duration of Earthquake Fault Motion in California”, *Earthquake Engineering and Structural Dynamics*, Vol. 24, pp. 781-799.

Turkish Seismic Design Code, 2007, *Specification for Buildings to be Built in Seismic Areas*, (in Turkish), Ministry of Public Works and Settlement, Ankara, Turkey.

Wen, Y. K., 2004, “Probabilistic Aspects of Earthquake Engineering”, *Earthquake Engineering from Engineering Seismology to Performance-Based Engineering*, ed. by Bozorgnia, Y. and V.V. Bertero, CRS Press LLC.

Yamada, M., Kasahara and K., Kotoda, 1988, “Seismic Pulses Repeated in Coda Part of Strong Seismic Waves”, *Proceedings of the 9th World Conference on Earthquake Engineering*, pp. 313-318, Tokyo Japan.

## APPENDIX A: EXAMPLE OPENSEES SCRIPT FOR STRUCTURAL MODEL AND NONLINEAR DYNAMIC ANALYSIS

```

*****
# 5-story RC Building, for Ry=2
# Ufuk HANCILAR, Jan. 2008
#*****
# Modeling Assumptions:
# Concrete C25,  $E_c=5000*\sqrt{25}=25000$  MPa
# Steel S420
# Uncracked sections
# No rigid zones @ element ends
# Uniformly distributed loads on beams
# Distributed plasticity for columns, by nonlinearBeamColumn elements
# Concentrated plasticity for beams, by beamWithHinges elements
# No P-Delta effects
# Units are kN, m, kPa
# -----
# NOTE: in order to run this script, you need Materials.tcl,
Recorders.tcl and DynamicAnalysis.tcl
# in the same folder!
# -----
wipe;          # clear memory of all past model definitions
model BasicBuilder -ndm 2 -ndf 3;# Define the model builder,
ndm=#dimension, ndf=#dofs
#
set PI [expr 2*asin(1.0)]
set Gravity 9.81
# Define GEOMETRY -----
# Define structure-geometry parameters
set H 3.0;# story height
set LBeam 5.0;    # span width (beam length)
set NStory 5;# number of stories above ground level
set NBay 5;# number of bays
#
# calculated MODEL PARAMETERS

```

```

puts "Number of Stories: $NStory Number of bays: $NBay"
# Define NODAL COORDINATES
for {set level 1} {$level <=[expr $NStory+1]} {incr level 1} {
  set Y [expr ($level-1)*$H];
  for {set pier 1} {$pier <= [expr $NBay+1]} {incr pier 1} {
    set X [expr ($pier-1)*$LBeam];
    set nodeID [expr $level*10+$pier]
    node $nodeID $X $Y;}
}
# BOUNDARY CONDITIONS
fixY 0.0 1 1 1;# fix all Y=0.0 nodes
# assign NODAL MASSes-----
-----
mass 219.929.929.92000
mass 2215.6615.6615.66000
mass 2315.6615.6615.66000
mass 2415.6615.6615.66000
mass 2515.6615.6615.66000
mass 269.929.929.92000
mass 319.929.929.92000
mass 3215.6615.6615.66000
mass 3315.6615.6615.66000
mass 3415.6615.6615.66000
mass 3515.6615.6615.66000
mass 369.929.929.92000
mass 419.929.929.92000
mass 4215.6615.6615.66000
mass 4315.6615.6615.66000
mass 4415.6615.6615.66000
mass 4515.6615.6615.66000
mass 469.929.929.92000
mass 519.929.929.92000
mass 5215.6615.6615.66000
mass 5315.6615.6615.66000
mass 5415.6615.6615.66000
mass 5515.6615.6615.66000
mass 569.929.929.92000
mass 617.047.047.04000

```

```

mass 6211.8111.8111.81000
mass 6311.8111.8111.81000
mass 6411.8111.8111.81000
mass 6511.8111.8111.81000
mass 667.047.047.04000
set NormalFloorMass 82.48;
set TopFloorMass 61.32;
set TotalMass [expr ($NStory-1)*$NormalFloorMass+$TopFloorMass];#
total mass of the building
puts "Total Mass of the Building: $TotalMass"
set TotalWeight [expr $TotalMass*$Gravity];# total weight of the
building
puts "Total Weight of the Building: $TotalWeight"
# -----
source Materials.tcl
# -----
# Materials.tcl
# MATERIAL parameters
# confined and unconfined CONCRETE
# nominal concrete compressive strength
set fc0 -25E+3;# Nominal Concrete Compressive Strength, kPa
(+Tension, -Compression)
set Ec [expr (5000*sqrt($fc0/-1000))*1000];# Concrete Elastic
Modulus, kPa
# Mander Confined Concrete Model
set fcc -32.93E+3;# Confined concrete strength (from Xtract)
set Epscc [expr -0.002*(1+5*(($fcc/$fc0)-1))];# strain at maximum
stress
set Epscu -20E-3;# strain at ultimate stress (from Xtract)
set Esec [expr $fcc/$Epscc];# secant modulus
set x [expr $Epscu/$Epscc];
set r [expr $Ec/($Ec-$Esec)];
set fcu [expr ($fcc*$x*$r)/($r-1.+pow($x,$r))];# ultimate stress
# unconfined concrete
set Epsc0 -0.002;# strain at maximum strength of unconfined concrete
set fcU 0;# ultimate stress
set EpscU -0.005;# strain at crushing strength
#

```

```

uniaxialMaterial Concrete01 1 $fcc $Epscc $fcu $EpscU;# Core concrete
(confined)
uniaxialMaterial Concrete01 2 $fc0 $Epsc0 0 $EpscU;# Cover concrete
(unconfined)
#
# REINFORCING STEEL parameters
set Fy 420E+3;# STEEL yield stress, kPa
set Es 2E+8;# modulus of steel, kPa
set Bs 6.64E-3;# strain-hardening ratio
set R0 18;# control the transition from elastic to plastic branches
set cR1 0.925;# control the transition from elastic to plastic
branches
set cR2 0.15;# control the transition from elastic to plastic
branches
#
uniaxialMaterial Steel02 3 $Fy $Es $Bs $R0 $cR1 $cR2

# Define SECTIONS
# Section Properties:
# Columns
set HCol 0.50; # square-Column width, parallel to y-axis
set BCol $HCol
# FIBER SECTION properties
# Column section geometry: 50x50, with fibers of 2cm
    set coverCol 0.04; # rectangular-RC-Column cover
    set nfCoreColY 25; #[expr $HCol/0.02];# number of fibers in the
core patch in the y direction
set nfCoreColZ 25; #[expr $BCol/0.02];# number of fibers in the core
patch in the z direction
set nfCoverColY 25; #[expr $HCol/0.02];# number of fibers in the
cover patches with long sides in the y direction
set nfCoverColZ 25; #[expr $BCol/0.02];# number of fibers in the
cover patches with long sides in the z direction

    set coverColY [expr $HCol/2.0];# The distance from the section
z-axis to the edge of the cover concrete -- outer edge of cover
concrete

```

```

set coverColZ [expr $BCol/2.0];# The distance from the section y-axis
to the edge of the cover concrete -- outer edge of cover concrete
set coreColY [expr $coverColY-$coverCol];# The distance from the
section z-axis to the edge of the core concrete -- edge of the core
concrete/inner edge of cover concrete
set coreColZ [expr $coverColZ-$coverCol];# The distance from the
section y-axis to the edge of the core concrete -- edge of the core
concrete/inner edge of cover concrete
# -----
# for columns 111 and 116
set numBarsTotal111 12;          # number of longitudinal-reinforcement
bars in the column
    set numBarsTopCol111 4;# number of longitudinal-reinforcement
bars on top layer
set numBarsBotCol111 4;# number of longitudinal-reinforcement bars on
bottom layer
set numBarsIntCol111 2;# number of reinforcing bars on the
intermediate layers
set barAreaTotal111 59.44E-4; # total longitudinal-reinforcement bar
area
set barArea111 [expr $barAreaTotal111/$numBarsTotal111];#
longitudinal-reinforcement bar area
# Define the fiber section, rectangular section with one layer of
steel evenly distributed around the perimeter and a confined core.
section fiberSec 111 {
# Define the core patch
# PatchQuad:  matTag  NSIJ      NSJK      Iy      Iz      Jy      Jz
Ky      Kz      Ly      Lz
    patch quadr 1 $nfCoreColZ $nfCoreColY -$coreColY
$coreColZ -$coreColY -$coreColZ $coreColY -$coreColZ $coreColY
$coreColZ

# Define the four cover patches
    # PatchQuad:  matTag NSIJ  NSJK      Iy      Iz      Jy      Jz
Ky      Kz      Ly      Lz
    patch quadr 2 2 $nfCoverColY -$coverColY $coverColZ -$coreColY
$coreColZ $coreColY $coreColZ $coverColY $coverColZ

```

```

patch quadr 2 2 $nfCoverColY -$scoreColY -$scoreColZ -$coverColY -
$coverColZ $coverColY -$coverColZ $scoreColY -$scoreColZ
patch quadr 2 $nfCoverColZ 2 -$coverColY $coverColZ -$coverColY -
$coverColZ -$scoreColY -$scoreColZ -$scoreColY $scoreColZ
patch quadr 2 $nfCoverColZ 2 $scoreColY $scoreColZ $scoreColY -$scoreColZ
$coverColY -$coverColZ $coverColY $coverColZ

# define reinforcing layers
      # LayerStraight :      matTag      numBar      areaBar      yStart
zStart      yEnd      zEnd
layer straight 3 $numBarsIntCol111 $barArea111 -$scoreColY $scoreColZ
$scoreColY $scoreColZ;      # intermediate skin reinf. +z
layer straight 3 $numBarsIntCol111 $barArea111 -$scoreColY -$scoreColZ
$scoreColY -$scoreColZ;# intermediate skin reinf. -z
layer straight 3 $numBarsTopCol111 $barArea111 $scoreColY $scoreColZ
$scoreColY -$scoreColZ;# top layer reinforcement
layer straight 3 $numBarsBotCol111 $barArea111 -$scoreColY $scoreColZ
-$scoreColY -$scoreColZ;# bottom layer reinforcement

};# end of fibersection definition
# -----
# for columns 112 and 115
set numBarsTotal112 12;      # number of longitudinal-reinforcement
bars in the column
      set numBarsTopCol112 4;# number of longitudinal-reinforcement
bars on top layer
set numBarsBotCol112 4;# number of longitudinal-reinforcement bars on
bottom layer
set numBarsIntCol112 2;# number of reinforcing bars on the
intermediate layers
set barAreaTotal112 50.26E-4; # total longitudinal-reinforcement bar
area
set barArea112 [expr $barAreaTotal112/$numBarsTotal112];#
longitudinal-reinforcement bar area
# Define the fiber section, rectangular section with one layer of
steel evenly distributed around the perimeter and a confined core.
section fiberSec 112 {
# Define the core patch

```

```

# PatchQuad:  matTag  NSIJ      NSJK      Iy      Iz      Jy      Jz
Ky      Kz      Ly      Lz
      patch quadr 1 $nfCoreColZ $nfCoreColY -$scoreColY
$scoreColZ -$scoreColY -$scoreColZ $scoreColY -$scoreColZ $scoreColY
$scoreColZ

# Define the four cover patches
      # PatchQuad:  matTag NSIJ  NSJK      Iy      Iz      Jy      Jz
Ky      Kz      Ly      Lz
patch quadr 2 2 $nfCoverColY -$coverColY $coverColZ -$scoreColY
$scoreColZ $scoreColY $scoreColZ $coverColY $coverColZ
patch quadr 2 2 $nfCoverColY -$scoreColY -$scoreColZ -$coverColY -
$coverColZ $coverColY -$coverColZ $scoreColY -$scoreColZ
patch quadr 2 $nfCoverColZ 2 -$coverColY $coverColZ -$coverColY -
$coverColZ -$scoreColY -$scoreColZ -$scoreColY $scoreColZ
patch quadr 2 $nfCoverColZ 2 $scoreColY $scoreColZ $scoreColY -$scoreColZ
$coverColY -$coverColZ $coverColY $coverColZ

# define reinforcing layers
      # LayerStraight :  matTag      numBar      areaBar      yStart
zStart      yEnd      zEnd
layer straight 3 $numBarsIntCol112 $barArea112 -$scoreColY $scoreColZ
$scoreColY $scoreColZ;      # intermediate skin reinf. +z
layer straight 3 $numBarsIntCol112 $barArea112 -$scoreColY -$scoreColZ
$scoreColY -$scoreColZ;# intermediate skin reinf. -z
layer straight 3 $numBarsTopCol112 $barArea112 $scoreColY $scoreColZ
$scoreColY -$scoreColZ;# top layer reinforcement
layer straight 3 $numBarsBotCol112 $barArea112 -$scoreColY $scoreColZ
-$scoreColY -$scoreColZ;# bottom layer reinforcement

};# end of fibersection definition
# -----
# for columns 113 and 114
set numBarsTotal113 12;      # number of longitudinal-reinforcement
bars in the column
      set numBarsTopCol113 4;# number of longitudinal-reinforcement
bars on top layer

```



```

set numBarsBotCol113 4;# number of longitudinal-reinforcement bars on
bottom layer
set numBarsIntCol113 2;# number of reinforcing bars on the
intermediate layers
set barAreaTotal113 48.39E-4; # total longitudinal-reinforcement bar
area
set barArea113 [expr $barAreaTotal113/$numBarsTotal113];#
longitudinal-reinforcement bar area
# Define the fiber section, rectangular section with one layer of
steel evenly distributed around the perimeter and a confined core.
section fiberSec 113 {
# Define the core patch
# PatchQuad:  matTag  NSIJ      NSJK      Iy      Iz      Jy      Jz
Ky      Kz      Ly      Lz
      patch quadr 1 $nfCoreColZ $nfCoreColY -$scoreColY
$scoreColZ -$scoreColY -$scoreColZ $scoreColY -$scoreColZ $scoreColY
$scoreColZ

# Define the four cover patches
      # PatchQuad:  matTag NSIJ  NSJK      Iy      Iz      Jy      Jz
Ky      Kz      Ly      Lz
patch quadr 2 2 $nfCoverColY -$coverColY $coverColZ -$scoreColY
$scoreColZ $scoreColY $scoreColZ $coverColY $coverColZ
patch quadr 2 2 $nfCoverColY -$scoreColY -$scoreColZ -$coverColY -
$coverColZ $coverColY -$coverColZ $scoreColY -$scoreColZ
patch quadr 2 $nfCoverColZ 2 -$coverColY $coverColZ -$coverColY -
$coverColZ -$scoreColY -$scoreColZ -$scoreColY $scoreColZ
patch quadr 2 $nfCoverColZ 2 $scoreColY $scoreColZ $scoreColY -$scoreColZ
$coverColY -$coverColZ $coverColY $coverColZ

# define reinforcing layers
      # LayerStraight :   matTag   numBar   areaBar   yStart
zStart   yEnd   zEnd
layer straight 3 $numBarsIntCol113 $barArea113 -$scoreColY $scoreColZ
$scoreColY $scoreColZ;      # intermediate skin reinf. +z
layer straight 3 $numBarsIntCol113 $barArea113 -$scoreColY -$scoreColZ
$scoreColY -$scoreColZ;# intermediate skin reinf. -z

```

```

layer straight 3 $numBarsTopCol113 $barArea113 $scoreColY $scoreColZ
$scoreColY -$scoreColZ;# top layer reinforcement
layer straight 3 $numBarsBotCol113 $barArea113 -$scoreColY $scoreColZ
-$scoreColY -$scoreColZ;# bottom layer reinforcement

};# end of fibersection definition
# -----
# for columns 121 and 126
set numBarsTotal121 12; # number of longitudinal-reinforcement
bars in the column
    set numBarsTopCol121 4;# number of longitudinal-reinforcement
bars on top layer
set numBarsBotCol121 4;# number of longitudinal-reinforcement bars on
bottom layer
set numBarsIntCol121 2;# number of reinforcing bars on the
intermediate layers
set barAreaTotal121 34.96E-4; # total longitudinal-reinforcement bar
area
set barArea121 [expr $barAreaTotal121/$numBarsTotal121];#
longitudinal-reinforcement bar area
# Define the fiber section, rectangular section with one layer of
steel evenly distributed around the perimeter and a confined core.
section fiberSec 121 {
# Define the core patch
# PatchQuad: matTag NSIJ NSJK Iy Iz Jy Jz
Ky Kz Ly Lz
    patch quadr 1 $nfCoreColZ $nfCoreColY -$scoreColY
$scoreColZ -$scoreColY -$scoreColZ $scoreColY -$scoreColZ $scoreColY
$scoreColZ

# Define the four cover patches
    # PatchQuad: matTag NSIJ NSJK Iy Iz Jy Jz
Ky Kz Ly Lz
patch quadr 2 2 $nfCoverColY -$coverColY $coverColZ -$scoreColY
$scoreColZ $scoreColY $scoreColZ $coverColY $coverColZ
patch quadr 2 2 $nfCoverColY -$scoreColY -$scoreColZ -$coverColY -
$coverColZ $coverColY -$coverColZ $scoreColY -$scoreColZ

```

```

patch quadr 2 $nfCoverColZ 2 -$coverColY $coverColZ -$coverColY -
$coverColZ -$scoreColY -$scoreColZ -$scoreColY $scoreColZ
patch quadr 2 $nfCoverColZ 2 $scoreColY $scoreColZ $scoreColY -$scoreColZ
$coverColY -$coverColZ $coverColY $coverColZ

# define reinforcing layers
      # LayerStraight :      matTag      numBar      areaBar      yStart
zStart      yEnd      zEnd
layer straight 3 $numBarsIntCol121 $barArea121 -$scoreColY $scoreColZ
$scoreColY $scoreColZ;      # intermediate skin reinf. +z
layer straight 3 $numBarsIntCol121 $barArea121 -$scoreColY -$scoreColZ
$scoreColY -$scoreColZ;# intermediate skin reinf. -z
layer straight 3 $numBarsTopCol121 $barArea121 $scoreColY $scoreColZ
$scoreColY -$scoreColZ;# top layer reinforcement
layer straight 3 $numBarsBotCol121 $barArea121 -$scoreColY $scoreColZ
-$scoreColY -$scoreColZ;# bottom layer reinforcement

};# end of fibersection definition
# -----
# for columns 122 and 125
set numBarsTotal122 12;      # number of longitudinal-reinforcement
bars in the column
      set numBarsTopCol122 4;# number of longitudinal-reinforcement
bars on top layer
set numBarsBotCol122 4;# number of longitudinal-reinforcement bars on
bottom layer
set numBarsIntCol122 2;# number of reinforcing bars on the
intermediate layers
set barAreaTotal122 42.06E-4; # total longitudinal-reinforcement bar
area
set barArea122 [expr $barAreaTotal122/$numBarsTotal122];#
longitudinal-reinforcement bar area
# Define the fiber section, rectangular section with one layer of
steel evenly distributed around the perimeter and a confined core.
section fiberSec 122 {
# Define the core patch
# PatchQuad:  matTag  NSIJ      NSJK      Iy      Iz      Jy      Jz
Ky      Kz      Ly      Lz

```

```

        patch quadr 1 $nfCoreColZ $nfCoreColY -$scoreColY
$scoreColZ -$scoreColY -$scoreColZ $scoreColY -$scoreColZ $scoreColY
$scoreColZ

# Define the four cover patches
        # PatchQuad:  matTag NSIJ  NSJK      Iy      Iz      Jy      Jz
Ky      Kz      Ly      Lz
patch quadr 2 2 $nfCoverColY -$coverColY $coverColZ -$scoreColY
$scoreColZ $scoreColY $scoreColZ $coverColY $coverColZ
patch quadr 2 2 $nfCoverColY -$scoreColY -$scoreColZ -$coverColY -
$coverColZ $coverColY -$coverColZ $scoreColY -$scoreColZ
patch quadr 2 $nfCoverColZ 2 -$coverColY $coverColZ -$coverColY -
$coverColZ -$scoreColY -$scoreColZ -$scoreColY $scoreColZ
patch quadr 2 $nfCoverColZ 2 $scoreColY $scoreColZ $scoreColY -$scoreColZ
$coverColY -$coverColZ $coverColY $coverColZ

# define reinforcing layers
        # LayerStraight :  matTag      numBar      areaBar      yStart
zStart      yEnd      zEnd
layer straight 3 $numBarsIntCol122 $barArea122 -$scoreColY $scoreColZ
$scoreColY $scoreColZ;      # intermediate skin reinf. +z
layer straight 3 $numBarsIntCol122 $barArea122 -$scoreColY -$scoreColZ
$scoreColY -$scoreColZ;# intermediate skin reinf. -z
layer straight 3 $numBarsTopCol122 $barArea122 $scoreColY $scoreColZ
$scoreColY -$scoreColZ;# top layer reinforcement
layer straight 3 $numBarsBotCol122 $barArea122 -$scoreColY $scoreColZ
-$scoreColY -$scoreColZ;# bottom layer reinforcement

};# end of fibersection definition
# -----
# for columns 123 and 124
set numBarsTotal123 12;      # number of longitudinal-reinforcement
bars in the column
        set numBarsTopCol123 4;# number of longitudinal-reinforcement
bars on top layer
set numBarsBotCol123 4;# number of longitudinal-reinforcement bars on
bottom layer

```

```

set numBarsIntCol123 2;# number of reinforcing bars on the
intermediate layers
set barAreaTotal123 40.70E-4; # total longitudinal-reinforcement bar
area
set barArea123 [expr $barAreaTotal123/$numBarsTotal123];#
longitudinal-reinforcement bar area
# Define the fiber section, rectangular section with one layer of
steel evenly distributed around the perimeter and a confined core.
section fiberSec 123 {
# Define the core patch
# PatchQuad:  matTag  NSIJ      NSJK      Iy      Iz      Jy      Jz
Ky      Kz      Ly      Lz
                patch quadr 1 $nfCoreColZ $nfCoreColY -$scoreColY
$scoreColZ -$scoreColY -$scoreColZ $scoreColY -$scoreColZ $scoreColY
$scoreColZ

# Define the four cover patches
                # PatchQuad:  matTag NSIJ  NSJK      Iy      Iz      Jy      Jz
Ky      Kz      Ly      Lz
patch quadr 2 2 $nfCoverColY -$coverColY $coverColZ -$scoreColY
$scoreColZ $scoreColY $scoreColZ $coverColY $coverColZ
patch quadr 2 2 $nfCoverColY -$scoreColY -$scoreColZ -$coverColY -
$coverColZ $coverColY -$coverColZ $scoreColY -$scoreColZ
patch quadr 2 $nfCoverColZ 2 -$coverColY $coverColZ -$coverColY -
$coverColZ -$scoreColY -$scoreColZ -$scoreColY $scoreColZ
patch quadr 2 $nfCoverColZ 2 $scoreColY $scoreColZ $scoreColY -$scoreColZ
$coverColY -$coverColZ $coverColY $coverColZ

# define reinforcing layers
                # LayerStraight :   matTag   numBar   areaBar   yStart
zStart   yEnd   zEnd
layer straight 3 $numBarsIntCol123 $barArea123 -$scoreColY $scoreColZ
$scoreColY $scoreColZ;      # intermediate skin reinf. +z
layer straight 3 $numBarsIntCol123 $barArea123 -$scoreColY -$scoreColZ
$scoreColY -$scoreColZ;# intermediate skin reinf. -z
layer straight 3 $numBarsTopCol123 $barArea123 $scoreColY $scoreColZ
$scoreColY -$scoreColZ;# top layer reinforcement

```

```

layer straight 3 $numBarsBotCol123 $barArea123 -$scoreColY $scoreColZ
-$scoreColY -$scoreColZ;# bottom layer reinforcement

};# end of fibersection definition
# -----
# for columns 131 and 136
set numBarsTotal131 12;          # number of longitudinal-reinforcement
bars in the column
      set numBarsTopCol131 4;# number of longitudinal-reinforcement
bars on top layer
set numBarsBotCol131 4;# number of longitudinal-reinforcement bars on
bottom layer
set numBarsIntCol131 2;# number of reinforcing bars on the
intermediate layers
set barAreaTotal131 30.5E-4; # total longitudinal-reinforcement bar
area
set barArea131 [expr $barAreaTotal131/$numBarsTotal131];#
longitudinal-reinforcement bar area
# Define the fiber section, rectangular section with one layer of
steel evenly distributed around the perimeter and a confined core.
section fiberSec 131 {
# Define the core patch
# PatchQuad:  matTag  NSIJ      NSJK      Iy      Iz      Jy      Jz
Ky      Kz      Ly      Lz
      patch quadr 1 $nfCoreColZ $nfCoreColY -$scoreColY
$scoreColZ -$scoreColY -$scoreColZ $scoreColY -$scoreColZ $scoreColY
$scoreColZ

# Define the four cover patches
      # PatchQuad:  matTag NSIJ  NSJK      Iy      Iz      Jy      Jz
Ky      Kz      Ly      Lz
patch quadr 2 2 $nfCoverColY -$coverColY $coverColZ -$scoreColY
$scoreColZ $scoreColY $scoreColZ $coverColY $coverColZ
patch quadr 2 2 $nfCoverColY -$scoreColY -$scoreColZ -$coverColY -
$coverColZ $coverColY -$coverColZ $scoreColY -$scoreColZ
patch quadr 2 $nfCoverColZ 2 -$coverColY $coverColZ -$coverColY -
$coverColZ -$scoreColY -$scoreColZ -$scoreColY $scoreColZ

```

```

patch quadr 2 $nfCoverColZ 2 $scoreColY $scoreColZ $scoreColY -$scoreColZ
$coverColY -$coverColZ $coverColY $coverColZ

# define reinforcing layers
      # LayerStraight :      matTag      numBar      areaBar      yStart
zStart      yEnd      zEnd
layer straight 3 $numBarsIntCol131 $barArea131 -$scoreColY $scoreColZ
$scoreColY $scoreColZ;      # intermediate skin reinf. +z
layer straight 3 $numBarsIntCol131 $barArea131 -$scoreColY -$scoreColZ
$scoreColY -$scoreColZ;# intermediate skin reinf. -z
layer straight 3 $numBarsTopCol131 $barArea131 $scoreColY $scoreColZ
$scoreColY -$scoreColZ;# top layer reinforcement
layer straight 3 $numBarsBotCol131 $barArea131 -$scoreColY $scoreColZ
-$scoreColY -$scoreColZ;# bottom layer reinforcement

};# end of fibersection definition
# -----
# for columns 132 and 135
set numBarsTotal132 12;      # number of longitudinal-reinforcement
bars in the column
      set numBarsTopCol132 4;# number of longitudinal-reinforcement
bars on top layer
set numBarsBotCol132 4;# number of longitudinal-reinforcement bars on
bottom layer
set numBarsIntCol132 2;# number of reinforcing bars on the
intermediate layers
set barAreaTotal132 38.23E-4; # total longitudinal-reinforcement bar
area
set barArea132 [expr $barAreaTotal132/$numBarsTotal132];#
longitudinal-reinforcement bar area
# Define the fiber section, rectangular section with one layer of
steel evenly distributed around the perimeter and a confined core.
section fiberSec 132 {
# Define the core patch
# PatchQuad:  matTag  NSIJ      NSJK      Iy      Iz      Jy      Jz
Ky      Kz      Ly      Lz

```

```

        patch quadr 1 $nfCoreColZ $nfCoreColY -$scoreColY
$scoreColZ -$scoreColY -$scoreColZ $scoreColY -$scoreColZ $scoreColY
$scoreColZ

# Define the four cover patches
        # PatchQuad:  matTag NSIJ  NSJK      Iy      Iz      Jy      Jz
Ky      Kz      Ly      Lz
patch quadr 2 2 $nfCoverColY -$coverColY $coverColZ -$scoreColY
$scoreColZ $scoreColY $scoreColZ $coverColY $coverColZ
patch quadr 2 2 $nfCoverColY -$scoreColY -$scoreColZ -$coverColY -
$coverColZ $coverColY -$coverColZ $scoreColY -$scoreColZ
patch quadr 2 $nfCoverColZ 2 -$coverColY $coverColZ -$coverColY -
$coverColZ -$scoreColY -$scoreColZ -$scoreColY $scoreColZ
patch quadr 2 $nfCoverColZ 2 $scoreColY $scoreColZ $scoreColY -$scoreColZ
$coverColY -$coverColZ $coverColY $coverColZ

# define reinforcing layers
        # LayerStraight :  matTag      numBar      areaBar      yStart
zStart      yEnd      zEnd
layer straight 3 $numBarsIntCol132 $barArea132 -$scoreColY $scoreColZ
$scoreColY $scoreColZ;      # intermediate skin reinf. +z
layer straight 3 $numBarsIntCol132 $barArea132 -$scoreColY -$scoreColZ
$scoreColY -$scoreColZ;# intermediate skin reinf. -z
layer straight 3 $numBarsTopCol132 $barArea132 $scoreColY $scoreColZ
$scoreColY -$scoreColZ;# top layer reinforcement
layer straight 3 $numBarsBotCol132 $barArea132 -$scoreColY $scoreColZ
-$scoreColY -$scoreColZ;# bottom layer reinforcement

};# end of fibersection definition
# -----
# for columns 133 and 134
set numBarsTotal133 12;      # number of longitudinal-reinforcement
bars in the column
        set numBarsTopCol133 4;# number of longitudinal-reinforcement
bars on top layer
set numBarsBotCol133 4;# number of longitudinal-reinforcement bars on
bottom layer

```



```

set numBarsIntCol133 2;# number of reinforcing bars on the
intermediate layers
set barAreaTotal133 37.20E-4; # total longitudinal-reinforcement bar
area
set barArea133 [expr $barAreaTotal133/$numBarsTotal133];#
longitudinal-reinforcement bar area
# Define the fiber section, rectangular section with one layer of
steel evenly distributed around the perimeter and a confined core.
section fiberSec 133 {
# Define the core patch
# PatchQuad:  matTag  NSIJ      NSJK      Iy      Iz      Jy      Jz
Ky      Kz      Ly      Lz
                patch quadr 1 $nfCoreColZ $nfCoreColY -$scoreColY
$scoreColZ -$scoreColY -$scoreColZ $scoreColY -$scoreColZ $scoreColY
$scoreColZ

# Define the four cover patches
                # PatchQuad:  matTag NSIJ  NSJK      Iy      Iz      Jy      Jz
Ky      Kz      Ly      Lz
patch quadr 2 2 $nfCoverColY -$coverColY $coverColZ -$scoreColY
$scoreColZ $scoreColY $scoreColZ $coverColY $coverColZ
patch quadr 2 2 $nfCoverColY -$scoreColY -$scoreColZ -$coverColY -
$coverColZ $coverColY -$coverColZ $scoreColY -$scoreColZ
patch quadr 2 $nfCoverColZ 2 -$coverColY $coverColZ -$coverColY -
$coverColZ -$scoreColY -$scoreColZ -$scoreColY $scoreColZ
patch quadr 2 $nfCoverColZ 2 $scoreColY $scoreColZ $scoreColY -$scoreColZ
$coverColY -$coverColZ $coverColY $coverColZ

# define reinforcing layers
                # LayerStraight :   matTag   numBar   areaBar   yStart
zStart   yEnd   zEnd
layer straight 3 $numBarsIntCol133 $barArea133 -$scoreColY $scoreColZ
$scoreColY $scoreColZ;          # intermediate skin reinf. +z
layer straight 3 $numBarsIntCol133 $barArea133 -$scoreColY -$scoreColZ
$scoreColY -$scoreColZ;# intermediate skin reinf. -z
layer straight 3 $numBarsTopCol133 $barArea133 $scoreColY $scoreColZ
$scoreColY -$scoreColZ;# top layer reinforcement

```

```

layer straight 3 $numBarsBotCol133 $barArea133 -$scoreColY $scoreColZ
-$scoreColY -$scoreColZ;# bottom layer reinforcement

};# end of fibersection definition
# -----
# for columns 141 and 146, 151-156
set numBarsTotal141 12;          # number of longitudinal-reinforcement
bars in the column
      set numBarsTopCol141 4;# number of longitudinal-reinforcement
bars on top layer
set numBarsBotCol141 4;# number of longitudinal-reinforcement bars on
bottom layer
set numBarsIntCol141 2;# number of reinforcing bars on the
intermediate layers
set barAreaTotal141 25E-4; # total longitudinal-reinforcement bar
area
set barArea141 [expr $barAreaTotal141/$numBarsTotal141];#
longitudinal-reinforcement bar area
# Define the fiber section, rectangular section with one layer of
steel evenly distributed around the perimeter and a confined core.
section fiberSec 141 {
# Define the core patch
# PatchQuad:  matTag  NSIJ      NSJK      Iy      Iz      Jy      Jz
Ky      Kz      Ly      Lz
      patch quadr 1 $nfCoreColZ $nfCoreColY -$scoreColY
$scoreColZ -$scoreColY -$scoreColZ $scoreColY -$scoreColZ $scoreColY
$scoreColZ

# Define the four cover patches
      # PatchQuad:  matTag NSIJ  NSJK      Iy      Iz      Jy      Jz
Ky      Kz      Ly      Lz
patch quadr 2 2 $nfCoverColY -$coverColY $coverColZ -$scoreColY
$scoreColZ $scoreColY $scoreColZ $coverColY $coverColZ
patch quadr 2 2 $nfCoverColY -$scoreColY -$scoreColZ -$coverColY -
$coverColZ $coverColY -$coverColZ $scoreColY -$scoreColZ
patch quadr 2 $nfCoverColZ 2 -$coverColY $coverColZ -$coverColY -
$coverColZ -$scoreColY -$scoreColZ -$scoreColY $scoreColZ

```

```

patch quadr 2 $nfCoverColZ 2 $scoreColY $scoreColZ $scoreColY -$scoreColZ
$coverColY -$coverColZ $coverColY $coverColZ

# define reinforcing layers
      # LayerStraight :      matTag      numBar      areaBar      yStart
zStart      yEnd      zEnd
layer straight 3 $numBarsIntCol141 $barArea141 -$scoreColY $scoreColZ
$scoreColY $scoreColZ;      # intermediate skin reinf. +z
layer straight 3 $numBarsIntCol141 $barArea141 -$scoreColY -$scoreColZ
$scoreColY -$scoreColZ;# intermediate skin reinf. -z
layer straight 3 $numBarsTopCol141 $barArea141 $scoreColY $scoreColZ
$scoreColY -$scoreColZ;# top layer reinforcement
layer straight 3 $numBarsBotCol141 $barArea141 -$scoreColY $scoreColZ
-$scoreColY -$scoreColZ;# bottom layer reinforcement

};# end of fibersection definition
# -----
# for columns 142 and 145
set numBarsTotal142 12;      # number of longitudinal-reinforcement
bars in the column
      set numBarsTopCol142 4;# number of longitudinal-reinforcement
bars on top layer
set numBarsBotCol142 4;# number of longitudinal-reinforcement bars on
bottom layer
set numBarsIntCol142 2;# number of reinforcing bars on the
intermediate layers
set barAreaTotal142 28.21E-4; # total longitudinal-reinforcement bar
area
set barArea142 [expr $barAreaTotal142/$numBarsTotal142];#
longitudinal-reinforcement bar area
# Define the fiber section, rectangular section with one layer of
steel evenly distributed around the perimeter and a confined core.
section fiberSec 142 {
# Define the core patch
# PatchQuad:      matTag      NSIJ      NSJK      Iy      Iz      Jy      Jz
Ky      Kz      Ly      Lz

```

```

        patch quadr 1 $nfCoreColZ $nfCoreColY -$scoreColY
$scoreColZ -$scoreColY -$scoreColZ $scoreColY -$scoreColZ $scoreColY
$scoreColZ

# Define the four cover patches
        # PatchQuad:  matTag NSIJ  NSJK      Iy      Iz      Jy      Jz
Ky      Kz      Ly      Lz
patch quadr 2 2 $nfCoverColY -$coverColY $coverColZ -$scoreColY
$scoreColZ $scoreColY $scoreColZ $coverColY $coverColZ
patch quadr 2 2 $nfCoverColY -$scoreColY -$scoreColZ -$coverColY -
$coverColZ $coverColY -$coverColZ $scoreColY -$scoreColZ
patch quadr 2 $nfCoverColZ 2 -$coverColY $coverColZ -$coverColY -
$coverColZ -$scoreColY -$scoreColZ -$scoreColY $scoreColZ
patch quadr 2 $nfCoverColZ 2 $scoreColY $scoreColZ $scoreColY -$scoreColZ
$coverColY -$coverColZ $coverColY $coverColZ

# define reinforcing layers
        # LayerStraight :  matTag      numBar      areaBar      yStart
zStart      yEnd      zEnd
layer straight 3 $numBarsIntColl42 $barArea142 -$scoreColY $scoreColZ
$scoreColY $scoreColZ;      # intermediate skin reinf. +z
layer straight 3 $numBarsIntColl42 $barArea142 -$scoreColY -$scoreColZ
$scoreColY -$scoreColZ;# intermediate skin reinf. -z
layer straight 3 $numBarsTopColl42 $barArea142 $scoreColY $scoreColZ
$scoreColY -$scoreColZ;# top layer reinforcement
layer straight 3 $numBarsBotColl42 $barArea142 -$scoreColY $scoreColZ
-$scoreColY -$scoreColZ;# bottom layer reinforcement

};# end of fibersection definition
# -----
# for columns 143 and 144
set numBarsTotal143 12;      # number of longitudinal-reinforcement
bars in the column
        set numBarsTopColl43 4;# number of longitudinal-reinforcement
bars on top layer
set numBarsBotColl43 4;# number of longitudinal-reinforcement bars on
bottom layer

```

```

set numBarsIntColl143 2;# number of reinforcing bars on the
intermediate layers
set barAreaTotal143 27.42E-4; # total longitudinal-reinforcement bar
area
set barArea143 [expr $barAreaTotal143/$numBarsTotal143];#
longitudinal-reinforcement bar area
# Define the fiber section, rectangular section with one layer of
steel evenly distributed around the perimeter and a confined core.
section fiberSec 143 {
# Define the core patch
# PatchQuad:  matTag  NSIJ      NSJK      Iy      Iz      Jy      Jz
Ky      Kz      Ly      Lz
                patch quadr 1 $nfCoreColZ $nfCoreColY -$scoreColY
$scoreColZ -$scoreColY -$scoreColZ $scoreColY -$scoreColZ $scoreColY
$scoreColZ

# Define the four cover patches
                # PatchQuad:  matTag NSIJ  NSJK      Iy      Iz      Jy      Jz
Ky      Kz      Ly      Lz
patch quadr 2 2 $nfCoverColY -$coverColY $coverColZ -$scoreColY
$scoreColZ $scoreColY $scoreColZ $coverColY $coverColZ
patch quadr 2 2 $nfCoverColY -$scoreColY -$scoreColZ -$coverColY -
$coverColZ $coverColY -$coverColZ $scoreColY -$scoreColZ
patch quadr 2 $nfCoverColZ 2 -$coverColY $coverColZ -$coverColY -
$coverColZ -$scoreColY -$scoreColZ -$scoreColY $scoreColZ
patch quadr 2 $nfCoverColZ 2 $scoreColY $scoreColZ $scoreColY -$scoreColZ
$coverColY -$coverColZ $coverColY $coverColZ

# define reinforcing layers
                # LayerStraight :   matTag   numBar   areaBar   yStart
zStart   yEnd   zEnd
layer straight 3 $numBarsIntColl143 $barArea143 -$scoreColY $scoreColZ
$scoreColY $scoreColZ;          # intermediate skin reinf. +z
layer straight 3 $numBarsIntColl143 $barArea143 -$scoreColY -$scoreColZ
$scoreColY -$scoreColZ;# intermediate skin reinf. -z
layer straight 3 $numBarsTopColl143 $barArea143 $scoreColY $scoreColZ
$scoreColY -$scoreColZ;# top layer reinforcement

```

```

layer straight 3 $numBarsBotCol143 $barArea143 -$scoreColY $scoreColZ
-$scoreColY -$scoreColZ;# bottom layer reinforcement

};# end of fibersection definition
# -----
# Beams
set HBeam 0.60; # Beam depth -- perpendicular to bending axis
(parallel to y-axis)
set BBeam 0.30; # Beam width -- parallel to bending axis (parallel to
z-axis)
set AgBeam [expr $HBeam*$BBeam]; # rectuangular-Beam
cross-sectional area
set CrackedBeam 1
set IzBeam [expr $CrackedBeam*1./12*$BBeam*pow($HBeam,3)];# about-
local-z Rect-Beam cracked moment of inertia

# FIBER SECTION properties
# Beam section geometry: 30x60, with fibers of 2cm
    set coverBeam 0.02; # rectangular-RC-Beam cover
    set nfCoreBeamY 30; #[expr $HBeam/0.02];# number of fibers in
the core patch in the y direction
set nfCoreBeamZ 15; #[expr $BBeam/0.02];# number of fibers in the
core patch in the z direction
set nfCoverBeamY 30; #[expr $HBeam/0.02];# number of fibers in the
cover patches with long sides in the y direction
set nfCoverBeamZ 15; #[expr $BBeam/0.02];# number of fibers in the
cover patches with long sides in the z direction

    set coverBeamY [expr $HBeam/2.0];# The distance from the
section z-axis to the edge of the cover concrete -- outer edge of
cover concrete
set coverBeamZ [expr $BBeam/2.0];# The distance from the section y-
axis to the edge of the cover concrete -- outer edge of cover
concrete
set coreBeamY [expr $coverBeamY-$coverBeam];# The distance from the
section z-axis to the edge of the core concrete -- edge of the core
concrete/inner edge of cover concrete

```

```

set coreBeamZ [expr $coverBeamZ-$coverBeam];# The distance from the
section y-axis to the edge of the core concrete -- edge of the core
concrete/inner edge of cover concrete
# 1st floor -----
# for beam 1021, i-end, 1021(0), 0 for i-end (same for the beam 1025)
set numBarsTopBeam10210 8;# number of longitudinal-reinforcement bars
on top layer
set numBarsBotBeam10210 8;# number of longitudinal-reinforcement bars
on bottom layer
set barAreaTopTotal10210 23.45E-4; # total top-longitudinal-
reinforcement bar area
set barAreaBotTotal10210 19.45E-4; # total bottom-longitudinal-
reinforcement bar area
    set barAreaTop10210 [expr
$barAreaTopTotal10210/$numBarsTopBeam10210];# 1 longitudinal-
reinforcement bar area, for top of the section
    set barAreaBot10210 [expr
$barAreaBotTotal10210/$numBarsBotBeam10210];# 1 longitudinal-
reinforcement bar area, for bottom of the section
# Define the fiber section, rectangular section with two layers of
steel on the top and bottom.
# element 1021(0), 0 for i-end
    section fiberSec 10210 {
# Define the core patch
# PatchQuad: matTag NSIJ      NSJK      Iy      Iz      Jy      Jz
Ky      Kz      Ly      Lz
        patch quadr 1 $nfCoreBeamZ $nfCoreBeamY -$coreBeamY
$coreBeamZ -$coreBeamY -$coreBeamZ $coreBeamY -$coreBeamZ $coreBeamY
$coreBeamZ
# Define the four cover patches
    # PatchQuad: matTag NSIJ NSJK      Iy      Iz      Jy      Jz
Ky      Kz      Ly      Lz
        patch quadr 2 2 $nfCoverBeamY -$coverBeamY $coverBeamZ -$coreBeamY
$coreBeamZ $coreBeamY $coreBeamZ $coverBeamY $coverBeamZ
        patch quadr 2 2 $nfCoverBeamY -$coreBeamY -$coreBeamZ -$coverBeamY -
$coreBeamZ $coverBeamY -$coverBeamZ $coreBeamY -$coreBeamZ
        patch quadr 2 $nfCoverBeamZ 2 -$coverBeamY $coverBeamZ -$coverBeamY -
$coreBeamZ -$coreBeamY -$coreBeamZ -$coreBeamY $coreBeamZ

```

```

patch quadr 2 $nfCoverBeamZ 2 $scoreBeamY $scoreBeamZ $scoreBeamY -
$scoreBeamZ $coverBeamY -$coverBeamZ $coverBeamY $coverBeamZ
# define reinforcing layers
      # LayerStraight :      matTag      numBar      areaBar      yStart
zStart      yEnd      zEnd
layer straight 3 $numBarsTopBeam10210 $barAreaTop10210 $scoreBeamY
$scoreBeamZ $scoreBeamY -$scoreBeamZ;# top layer reinforcement
layer straight 3 $numBarsBotBeam10210 $barAreaBot10210 -$scoreBeamY
$scoreBeamZ -$scoreBeamY -$scoreBeamZ;# bottom layer reinforcement
};

      # for beam 1021, j-end, 1021(1), 1 for j-end
set numBarsTopBeam10211 8;# number of longitudinal-reinforcement bars
on top layer
set numBarsBotBeam10211 8;# number of longitudinal-reinforcement bars
on bottom layer
set barAreaTopTotal10211 21.14E-4; # total top-longitudinal-
reinforcement bar area
set barAreaBotTotal10211 16.85E-4; # total bottom-longitudinal-
reinforcement bar area
      set barAreaTop10211 [expr
$barAreaTopTotal10211/$numBarsTopBeam10211];# 1 longitudinal-
reinforcement bar area, for top of the section
      set barAreaBot10211 [expr
$barAreaBotTotal10211/$numBarsBotBeam10211];# 1 longitudinal-
reinforcement bar area, for bottom of the section
# Define the fiber section, rectangular section with two layers of
steel on the top and bottom.
# element 1021(1), 1 for j-end
      section fiberSec 10211 {
# Define the core patch
# PatchQuad:  matTag  NSIJ      NSJK      Iy      Iz      Jy      Jz
Ky      Kz      Ly      Lz
      patch quadr 1 $nfCoreBeamZ $nfCoreBeamY -$scoreBeamY
$scoreBeamZ -$scoreBeamY -$scoreBeamZ $scoreBeamY -$scoreBeamZ $scoreBeamY
$scoreBeamZ
# Define the four cover patches
      # PatchQuad:  matTag NSIJ  NSJK      Iy      Iz      Jy      Jz
Ky      Kz      Ly      Lz

```



```

patch quadr 2 2 $nfCoverBeamY -$coverBeamY $coverBeamZ -$scoreBeamY
$scoreBeamZ $scoreBeamY $scoreBeamZ $coverBeamY $coverBeamZ
patch quadr 2 2 $nfCoverBeamY -$scoreBeamY -$scoreBeamZ -$coverBeamY -
$coverBeamZ $coverBeamY -$coverBeamZ $scoreBeamY -$scoreBeamZ
patch quadr 2 $nfCoverBeamZ 2 -$coverBeamY $coverBeamZ -$coverBeamY -
$coverBeamZ -$scoreBeamY -$scoreBeamZ -$scoreBeamY $scoreBeamZ
patch quadr 2 $nfCoverBeamZ 2 $scoreBeamY $scoreBeamZ $scoreBeamY -
$scoreBeamZ $coverBeamY -$coverBeamZ $coverBeamY $coverBeamZ
# define reinforcing layers
      # LayerStraight :      matTag      numBar      areaBar      yStart
zStart      yEnd      zEnd
layer straight 3 $numBarsTopBeam10211 $barAreaTop10211 $scoreBeamY
$scoreBeamZ $scoreBeamY -$scoreBeamZ;# top layer reinforcement
layer straight 3 $numBarsBotBeam10211 $barAreaBot10211 -$scoreBeamY
$scoreBeamZ -$scoreBeamY -$scoreBeamZ;# bottom layer reinforcement
};# end of fibersection definition
# -----
# for beam 1022, i-end, 1022(0), 0 for i-end (same for the beams 1023
and 1024)
set numBarsTopBeam10220 8;# number of longitudinal-reinforcement bars
on top layer
set numBarsBotBeam10220 8;# number of longitudinal-reinforcement bars
on bottom layer
set barAreaTopTotal10220 19.56E-4; # total top-longitudinal-
reinforcement bar area
set barAreaBotTotal10220 15.31E-4; # total bottom-longitudinal-
reinforcement bar area
      set barAreaTop10220 [expr
$barAreaTopTotal10220/$numBarsTopBeam10220];# 1 longitudinal-
reinforcement bar area, for top of the section
      set barAreaBot10220 [expr
$barAreaBotTotal10220/$numBarsBotBeam10220];# 1 longitudinal-
reinforcement bar area, for bottom of the section
# Define the fiber section, rectangular section with two layers of
steel on the top and bottom.
# element 1022(0), 0 for i-end
      section fiberSec 10220 {
# Define the core patch

```

```

# PatchQuad:  matTag  NSIJ      NSJK      Iy      Iz      Jy      Jz
Ky      Kz      Ly      Lz
      patch quadr 1 $nfCoreBeamZ $nfCoreBeamY -$scoreBeamY
$scoreBeamZ -$scoreBeamY -$scoreBeamZ $scoreBeamY -$scoreBeamZ $scoreBeamY
$scoreBeamZ
# Define the four cover patches
      # PatchQuad:  matTag NSIJ  NSJK      Iy      Iz      Jy      Jz
Ky      Kz      Ly      Lz
patch quadr 2 2 $nfCoverBeamY -$coverBeamY $coverBeamZ -$scoreBeamY
$scoreBeamZ $scoreBeamY $scoreBeamZ $coverBeamY $coverBeamZ
patch quadr 2 2 $nfCoverBeamY -$scoreBeamY -$scoreBeamZ -$coverBeamY -
$coverBeamZ $coverBeamY -$coverBeamZ $scoreBeamY -$scoreBeamZ
patch quadr 2 $nfCoverBeamZ 2 -$coverBeamY $coverBeamZ -$coverBeamY -
$coverBeamZ -$scoreBeamY -$scoreBeamZ -$scoreBeamY $scoreBeamZ
patch quadr 2 $nfCoverBeamZ 2 $scoreBeamY $scoreBeamZ $scoreBeamY -
$scoreBeamZ $coverBeamY -$coverBeamZ $coverBeamY $coverBeamZ
# define reinforcing layers
      # LayerStraight :  matTag      numBar      areaBar      yStart
zStart      yEnd      zEnd
layer straight 3 $numBarsTopBeam10220 $barAreaTop10220 $scoreBeamY
$scoreBeamZ $scoreBeamY -$scoreBeamZ;# top layer reinforcement
layer straight 3 $numBarsBotBeam10220 $barAreaBot10220 -$scoreBeamY
$scoreBeamZ -$scoreBeamY -$scoreBeamZ;# bottom layer reinforcement
};

      # for beam 1022, j-end, 1022(1), 1 for j-end
set numBarsTopBeam10221 8;# number of longitudinal-reinforcement bars
on top layer
set numBarsBotBeam10221 8;# number of longitudinal-reinforcement bars
on bottom layer
set barAreaTopTotal10221 19.71E-4; # total top-longitudinal-
reinforcement bar area
set barAreaBotTotal10221 15.48E-4; # total bottom-longitudinal-
reinforcement bar area
      set barAreaTop10221 [expr
$barAreaTopTotal10221/$numBarsTopBeam10221];# 1 longitudinal-
reinforcement bar area, for top of the section

```

```

        set barAreaBot10221 [expr
$barAreaBotTotal10221/$numBarsBotBeam10221];# 1 longitudinal-
reinforcement bar area, for bottom of the section
# Define the fiber section, rectangular section with two layers of
steel on the top and bottom.
# element 1022(1), 1 for j-end
        section fiberSec 10221 {
# Define the core patch
# PatchQuad:  matTag  NSIJ      NSJK      Iy      Iz      Jy      Jz
Ky      Kz      Ly      Lz
                patch quadr 1 $nfCoreBeamZ $nfCoreBeamY -$scoreBeamY
$scoreBeamZ -$scoreBeamY -$scoreBeamZ $scoreBeamY -$scoreBeamZ $scoreBeamY
$scoreBeamZ
# Define the four cover patches
        # PatchQuad:  matTag NSIJ  NSJK      Iy      Iz      Jy      Jz
Ky      Kz      Ly      Lz
patch quadr 2 2 $nfCoverBeamY -$coverBeamY $coverBeamZ -$scoreBeamY
$scoreBeamZ $scoreBeamY $scoreBeamZ $coverBeamY $coverBeamZ
patch quadr 2 2 $nfCoverBeamY -$scoreBeamY -$scoreBeamZ -$coverBeamY -
$coverBeamZ $coverBeamY -$coverBeamZ $scoreBeamY -$scoreBeamZ
patch quadr 2 $nfCoverBeamZ 2 -$coverBeamY $coverBeamZ -$coverBeamY -
$coverBeamZ -$scoreBeamY -$scoreBeamZ -$scoreBeamY $scoreBeamZ
patch quadr 2 $nfCoverBeamZ 2 $scoreBeamY $scoreBeamZ $scoreBeamY -
$scoreBeamZ $coverBeamY -$coverBeamZ $coverBeamY $coverBeamZ
# define reinforcing layers
        # LayerStraight :      matTag      numBar      areaBar      yStart
zStart      yEnd      zEnd
layer straight 3 $numBarsTopBeam10221 $barAreaTop10221 $scoreBeamY
$scoreBeamZ $scoreBeamY -$scoreBeamZ;# top layer reinforcement
layer straight 3 $numBarsBotBeam10221 $barAreaBot10221 -$scoreBeamY
$scoreBeamZ -$scoreBeamY -$scoreBeamZ;# bottom layer reinforcement
};# end of fibersection definition
# 2nd floor -----
# for beam 1031, i-end, 1031(0), 0 for i-end (same for the beam 1035)
set numBarsTopBeam10310 8;# number of longitudinal-reinforcement bars
on top layer
set numBarsBotBeam10310 8;# number of longitudinal-reinforcement bars
on bottom layer

```

```

set barAreaTopTotal10310 23.04E-4; # total top-longitudinal-
reinforcement bar area
set barAreaBotTotal10310 18.64E-4; # total bottom-longitudinal-
reinforcement bar area
    set barAreaTop10310 [expr
$barAreaTopTotal10310/$numBarsTopBeam10310];# 1 longitudinal-
reinforcement bar area, for top of the section
    set barAreaBot10310 [expr
$barAreaBotTotal10310/$numBarsBotBeam10310];# 1 longitudinal-
reinforcement bar area, for bottom of the section
# Define the fiber section, rectangular section with two layers of
steel on the top and bottom.
# element 1031(0), 0 for i-end
    section fiberSec 10310 {
# Define the core patch
# PatchQuad:  matTag  NSIJ      NSJK      Iy      Iz      Jy      Jz
Ky      Kz      Ly      Lz
        patch quadr 1 $nfCoreBeamZ $nfCoreBeamY -$scoreBeamY
$scoreBeamZ -$scoreBeamY -$scoreBeamZ $scoreBeamY -$scoreBeamZ $scoreBeamY
$scoreBeamZ
# Define the four cover patches
        # PatchQuad:  matTag NSIJ  NSJK      Iy      Iz      Jy      Jz
Ky      Kz      Ly      Lz
        patch quadr 2 2 $nfCoverBeamY -$coverBeamY $coverBeamZ -$scoreBeamY
$scoreBeamZ $scoreBeamY $scoreBeamZ $coverBeamY $coverBeamZ
        patch quadr 2 2 $nfCoverBeamY -$scoreBeamY -$scoreBeamZ -$coverBeamY -
$coverBeamZ $coverBeamY -$coverBeamZ $scoreBeamY -$scoreBeamZ
        patch quadr 2 $nfCoverBeamZ 2 -$coverBeamY $coverBeamZ -$coverBeamY -
$coverBeamZ -$scoreBeamY -$scoreBeamZ -$scoreBeamY $scoreBeamZ
        patch quadr 2 $nfCoverBeamZ 2 $scoreBeamY $scoreBeamZ $scoreBeamY -
$scoreBeamZ $coverBeamY -$coverBeamZ $coverBeamY $coverBeamZ
# define reinforcing layers
        # LayerStraight :  matTag  numBar  areaBar  yStart
zStart  yEnd  zEnd
        layer straight 3 $numBarsTopBeam10310 $barAreaTop10310  $scoreBeamY
$scoreBeamZ $scoreBeamY -$scoreBeamZ;# top layer reinforcement
        layer straight 3 $numBarsBotBeam10310 $barAreaBot10310  -$scoreBeamY
$scoreBeamZ -$scoreBeamY -$scoreBeamZ;# bottom layer reinforcement

```

```

};

    # for beam 1031, j-end, 1031(1), 1 for j-end
set numBarsTopBeam10311 8;# number of longitudinal-reinforcement bars
on top layer
set numBarsBotBeam10311 8;# number of longitudinal-reinforcement bars
on bottom layer
set barAreaTopTotal10311 20.69E-4; # total top-longitudinal-
reinforcement bar area
set barAreaBotTotal10311 16.76E-4; # total bottom-longitudinal-
reinforcement bar area

    set barAreaTop10311 [expr
$barAreaTopTotal10311/$numBarsTopBeam10311];# 1 longitudinal-
reinforcement bar area, for top of the section

    set barAreaBot10311 [expr
$barAreaBotTotal10311/$numBarsBotBeam10311];# 1 longitudinal-
reinforcement bar area, for bottom of the section
# Define the fiber section, rectangular section with two layers of
steel on the top and bottom.
# element 1031(1), 1 for j-end
    section fiberSec 10311 {
# Define the core patch
# PatchQuad:  matTag  NSIJ      NSJK      Iy      Iz      Jy      Jz
Ky      Kz      Ly      Lz

        patch quadr 1 $nfCoreBeamZ $nfCoreBeamY -$scoreBeamY
$scoreBeamZ -$scoreBeamY -$scoreBeamZ $scoreBeamY -$scoreBeamZ $scoreBeamY
$scoreBeamZ
# Define the four cover patches
        # PatchQuad:  matTag NSIJ  NSJK      Iy      Iz      Jy      Jz
Ky      Kz      Ly      Lz
        patch quadr 2 2 $nfCoverBeamY -$coverBeamY $coverBeamZ -$scoreBeamY
$scoreBeamZ $scoreBeamY $scoreBeamZ $coverBeamY $coverBeamZ
        patch quadr 2 2 $nfCoverBeamY -$scoreBeamY -$scoreBeamZ -$coverBeamY -
$coverBeamZ $coverBeamY -$coverBeamZ $scoreBeamY -$scoreBeamZ
        patch quadr 2 $nfCoverBeamZ 2 -$coverBeamY $coverBeamZ -$coverBeamY -
$coverBeamZ -$scoreBeamY -$scoreBeamZ -$scoreBeamY $scoreBeamZ
        patch quadr 2 $nfCoverBeamZ 2 $scoreBeamY $scoreBeamZ $scoreBeamY -
$scoreBeamZ $coverBeamY -$coverBeamZ $coverBeamY $coverBeamZ
# define reinforcing layers

```

```

# LayerStraight :    matTag    numBar    areaBar    yStart
zStart    yEnd    zEnd
layer straight 3 $numBarsTopBeam10311 $barAreaTop10311 $coreBeamY
$coreBeamZ $coreBeamY -$coreBeamZ;# top layer reinforcement
layer straight 3 $numBarsBotBeam10311 $barAreaBot10311 -$coreBeamY
$coreBeamZ -$coreBeamY -$coreBeamZ;# bottom layer reinforcement
};# end of fibersection definition
# -----
# for beam 1032, i-end, 1032(0), 0 for i-end (same for the beams 1033
and 1034)
set numBarsTopBeam10320 8;# number of longitudinal-reinforcement bars
on top layer
set numBarsBotBeam10320 8;# number of longitudinal-reinforcement bars
on bottom layer
set barAreaTopTotal10320 19.83E-4; # total top-longitudinal-
reinforcement bar area
set barAreaBotTotal10320 15.65E-4; # total bottom-longitudinal-
reinforcement bar area
    set barAreaTop10320 [expr
$barAreaTopTotal10320/$numBarsTopBeam10320];# 1 longitudinal-
reinforcement bar area, for top of the section
    set barAreaBot10320 [expr
$barAreaBotTotal10320/$numBarsBotBeam10320];# 1 longitudinal-
reinforcement bar area, for bottom of the section
# Define the fiber section, rectangular section with two layers of
steel on the top and bottom.
# element 1032(0), 0 for i-end
    section fiberSec 10320 {
# Define the core patch
# PatchQuad:  matTag  NSIJ      NSJK      Iy      Iz      Jy      Jz
Ky      Kz      Ly      Lz
        patch quadr 1 $nfCoreBeamZ $nfCoreBeamY -$coreBeamY
$coreBeamZ -$coreBeamY -$coreBeamZ $coreBeamY -$coreBeamZ $coreBeamY
$coreBeamZ
# Define the four cover patches
        # PatchQuad:  matTag NSIJ  NSJK      Iy      Iz      Jy      Jz
Ky      Kz      Ly      Lz

```

```

patch quadr 2 2 $nfCoverBeamY -$coverBeamY $coverBeamZ -$scoreBeamY
$scoreBeamZ $scoreBeamY $scoreBeamZ $coverBeamY $coverBeamZ
patch quadr 2 2 $nfCoverBeamY -$scoreBeamY -$scoreBeamZ -$coverBeamY -
$coverBeamZ $coverBeamY -$coverBeamZ $scoreBeamY -$scoreBeamZ
patch quadr 2 $nfCoverBeamZ 2 -$coverBeamY $coverBeamZ -$coverBeamY -
$coverBeamZ -$scoreBeamY -$scoreBeamZ -$scoreBeamY $scoreBeamZ
patch quadr 2 $nfCoverBeamZ 2 $scoreBeamY $scoreBeamZ $scoreBeamY -
$scoreBeamZ $coverBeamY -$coverBeamZ $coverBeamY $coverBeamZ
# define reinforcing layers
      # LayerStraight :      matTag      numBar      areaBar      yStart
zStart      yEnd      zEnd
layer straight 3 $numBarsTopBeam10320 $barAreaTop10320 $scoreBeamY
$scoreBeamZ $scoreBeamY -$scoreBeamZ;# top layer reinforcement
layer straight 3 $numBarsBotBeam10320 $barAreaBot10320 -$scoreBeamY
$scoreBeamZ -$scoreBeamY -$scoreBeamZ;# bottom layer reinforcement
};

      # for beam 1032, j-end, 1032(1), 1 for j-end
set numBarsTopBeam10321 8;# number of longitudinal-reinforcement bars
on top layer
set numBarsBotBeam10321 8;# number of longitudinal-reinforcement bars
on bottom layer
set barAreaTopTotal10321 19.95E-4; # total top-longitudinal-
reinforcement bar area
set barAreaBotTotal10321 15.68E-4; # total bottom-longitudinal-
reinforcement bar area
      set barAreaTop10321 [expr
$barAreaTopTotal10321/$numBarsTopBeam10321];# 1 longitudinal-
reinforcement bar area, for top of the section
      set barAreaBot10321 [expr
$barAreaBotTotal10321/$numBarsBotBeam10321];# 1 longitudinal-
reinforcement bar area, for bottom of the section
# Define the fiber section, rectangular section with two layers of
steel on the top and bottom.
# element 1032(1), 1 for j-end
      section fiberSec 10321 {
# Define the core patch
# PatchQuad:  matTag  NSIJ      NSJK      Iy      Iz      Jy      Jz
Ky      Kz      Ly      Lz

```

```

        patch quadr 1 $nfCoreBeamZ $nfCoreBeamY -$scoreBeamY
$scoreBeamZ -$scoreBeamY -$scoreBeamZ $scoreBeamY -$scoreBeamZ $scoreBeamY
$scoreBeamZ
# Define the four cover patches
        # PatchQuad:  matTag NSIJ  NSJK      Iy      Iz      Jy      Jz
Ky      Kz      Ly      Lz
patch quadr 2 2 $nfCoverBeamY -$coverBeamY $coverBeamZ -$scoreBeamY
$scoreBeamZ $scoreBeamY $scoreBeamZ $coverBeamY $coverBeamZ
patch quadr 2 2 $nfCoverBeamY -$scoreBeamY -$scoreBeamZ -$coverBeamY -
$coverBeamZ $coverBeamY -$coverBeamZ $scoreBeamY -$scoreBeamZ
patch quadr 2 $nfCoverBeamZ 2 -$coverBeamY $coverBeamZ -$coverBeamY -
$coverBeamZ -$scoreBeamY -$scoreBeamZ -$scoreBeamY $scoreBeamZ
patch quadr 2 $nfCoverBeamZ 2 $scoreBeamY $scoreBeamZ $scoreBeamY -
$scoreBeamZ $coverBeamY -$coverBeamZ $coverBeamY $coverBeamZ
# define reinforcing layers
        # LayerStraight :  matTag      numBar      areaBar      yStart
zStart      yEnd      zEnd
layer straight 3 $numBarsTopBeam10321 $barAreaTop10321 $scoreBeamY
$scoreBeamZ $scoreBeamY -$scoreBeamZ;# top layer reinforcement
layer straight 3 $numBarsBotBeam10321 $barAreaBot10321 -$scoreBeamY
$scoreBeamZ -$scoreBeamY -$scoreBeamZ;# bottom layer reinforcement
};# end of fibersection definition
# 3rd floor -----
# for beam 1041, i-end, 1041(0), 0 for i-end (same for the beam 1045)
set numBarsTopBeam10410 8;# number of longitudinal-reinforcement bars
on top layer
set numBarsBotBeam10410 8;# number of longitudinal-reinforcement bars
on bottom layer
set barAreaTopTotal10410 17.85E-4; # total top-longitudinal-
reinforcement bar area
set barAreaBotTotal10410 13.54E-4; # total bottom-longitudinal-
reinforcement bar area
        set barAreaTop10410 [expr
$barAreaTopTotal10410/$numBarsTopBeam10410];# 1 longitudinal-
reinforcement bar area, for top of the section
        set barAreaBot10410 [expr
$barAreaBotTotal10410/$numBarsBotBeam10410];# 1 longitudinal-
reinforcement bar area, for bottom of the section

```



```

# Define the fiber section, rectangular section with two layers of
steel on the top and bottom.
# element 1041(0), 0 for i-end
    section fiberSec 10410 {
# Define the core patch
# PatchQuad:  matTag  NSIJ      NSJK      Iy      Iz      Jy      Jz
Ky      Kz      Ly      Lz
        patch quadr 1 $nfCoreBeamZ $nfCoreBeamY -$scoreBeamY
$scoreBeamZ -$scoreBeamY -$scoreBeamZ $scoreBeamY -$scoreBeamZ $scoreBeamY
$scoreBeamZ
# Define the four cover patches
        # PatchQuad:  matTag NSIJ  NSJK      Iy      Iz      Jy      Jz
Ky      Kz      Ly      Lz
        patch quadr 2 2 $nfCoverBeamY -$coverBeamY $coverBeamZ -$scoreBeamY
$scoreBeamZ $scoreBeamY $scoreBeamZ $coverBeamY $coverBeamZ
        patch quadr 2 2 $nfCoverBeamY -$scoreBeamY -$scoreBeamZ -$coverBeamY -
$coverBeamZ $coverBeamY -$coverBeamZ $scoreBeamY -$scoreBeamZ
        patch quadr 2 $nfCoverBeamZ 2 -$coverBeamY $coverBeamZ -$coverBeamY -
$coverBeamZ -$scoreBeamY -$scoreBeamZ -$scoreBeamY $scoreBeamZ
        patch quadr 2 $nfCoverBeamZ 2 $scoreBeamY $scoreBeamZ $scoreBeamY -
$scoreBeamZ $coverBeamY -$coverBeamZ $coverBeamY $coverBeamZ
# define reinforcing layers
        # LayerStraight :    matTag    numBar    areaBar    yStart
zStart    yEnd    zEnd
        layer straight 3 $numBarsTopBeam10410 $barAreaTop10410    $scoreBeamY
$scoreBeamZ $scoreBeamY -$scoreBeamZ;# top layer reinforcement
        layer straight 3 $numBarsBotBeam10410 $barAreaBot10410    -$scoreBeamY
$scoreBeamZ    -$scoreBeamY -$scoreBeamZ;# bottom layer reinforcement
    };

    # for beam 1041, j-end, 1041(1), 1 for j-end
set numBarsTopBeam10411 8;# number of longitudinal-reinforcement bars
on top layer
set numBarsBotBeam10411 8;# number of longitudinal-reinforcement bars
on bottom layer
set barAreaTopTotal10411 15.83E-4; # total top-longitudinal-
reinforcement bar area
set barAreaBotTotal10411 12.39E-4; # total bottom-longitudinal-
reinforcement bar area

```

```

        set barAreaTop10411 [expr
$barAreaTopTotal10411/$numBarsTopBeam10411];# 1 longitudinal-
reinforcement bar area, for top of the section

        set barAreaBot10411 [expr
$barAreaBotTotal10411/$numBarsBotBeam10411];# 1 longitudinal-
reinforcement bar area, for bottom of the section
# Define the fiber section, rectangular section with two layers of
steel on the top and bottom.
# element 1041(1), 1 for j-end
        section fiberSec 10411 {
# Define the core patch
# PatchQuad:  matTag  NSIJ      NSJK      Iy      Iz      Jy      Jz
Ky      Kz      Ly      Lz
                patch quadr 1 $nfCoreBeamZ $nfCoreBeamY -$scoreBeamY
$scoreBeamZ -$scoreBeamY -$scoreBeamZ $scoreBeamY -$scoreBeamZ $scoreBeamY
$scoreBeamZ
# Define the four cover patches
                # PatchQuad:  matTag NSIJ  NSJK      Iy      Iz      Jy      Jz
Ky      Kz      Ly      Lz
patch quadr 2 2 $nfCoverBeamY -$coverBeamY $coverBeamZ -$scoreBeamY
$scoreBeamZ $scoreBeamY $scoreBeamZ $coverBeamY $coverBeamZ
patch quadr 2 2 $nfCoverBeamY -$scoreBeamY -$scoreBeamZ -$coverBeamY -
$coverBeamZ $coverBeamY -$coverBeamZ $scoreBeamY -$scoreBeamZ
patch quadr 2 $nfCoverBeamZ 2 -$coverBeamY $coverBeamZ -$coverBeamY -
$coverBeamZ -$scoreBeamY -$scoreBeamZ -$scoreBeamY $scoreBeamZ
patch quadr 2 $nfCoverBeamZ 2 $scoreBeamY $scoreBeamZ $scoreBeamY -
$scoreBeamZ $coverBeamY -$coverBeamZ $coverBeamY $coverBeamZ
# define reinforcing layers
                # LayerStraight :      matTag      numBar      areaBar      yStart
zStart      yEnd      zEnd
layer straight 3 $numBarsTopBeam10411 $barAreaTop10411      $scoreBeamY
$scoreBeamZ $scoreBeamY -$scoreBeamZ;# top layer reinforcement
layer straight 3 $numBarsBotBeam10411 $barAreaBot10411      -$scoreBeamY
$scoreBeamZ      -$scoreBeamY -$scoreBeamZ;# bottom layer reinforcement
};# end of fibersection definition
# -----
# for beam 1042, i-end, 1042(0), 0 for i-end (same for the beams 1043
and 1044)

```

```

set numBarsTopBeam10420 8;# number of longitudinal-reinforcement bars
on top layer
set numBarsBotBeam10420 8;# number of longitudinal-reinforcement bars
on bottom layer
set barAreaTopTotal10420 15.70E-4; # total top-longitudinal-
reinforcement bar area
set barAreaBotTotal10420 11.76E-4; # total bottom-longitudinal-
reinforcement bar area
    set barAreaTop10420 [expr
$barAreaTopTotal10420/$numBarsTopBeam10420];# 1 longitudinal-
reinforcement bar area, for top of the section
    set barAreaBot10420 [expr
$barAreaBotTotal10420/$numBarsBotBeam10420];# 1 longitudinal-
reinforcement bar area, for bottom of the section
# Define the fiber section, rectangular section with two layers of
steel on the top and bottom.
# element 1042(0), 0 for i-end
    section fiberSec 10420 {
# Define the core patch
# PatchQuad:  matTag  NSIJ      NSJK      Iy      Iz      Jy      Jz
Ky      Kz      Ly      Lz
        patch quadr 1 $nfCoreBeamZ $nfCoreBeamY -$coreBeamY
$coreBeamZ -$coreBeamY -$coreBeamZ $coreBeamY -$coreBeamZ $coreBeamY
$coreBeamZ
# Define the four cover patches
        # PatchQuad:  matTag NSIJ  NSJK      Iy      Iz      Jy      Jz
Ky      Kz      Ly      Lz
        patch quadr 2 2 $nfCoverBeamY -$coverBeamY $coverBeamZ -$coreBeamY
$coreBeamZ $coreBeamY $coreBeamZ $coverBeamY $coverBeamZ
        patch quadr 2 2 $nfCoverBeamY -$coreBeamY -$coreBeamZ -$coverBeamY -
$coreBeamZ $coverBeamY -$coverBeamZ $coreBeamY -$coreBeamZ
        patch quadr 2 $nfCoverBeamZ 2 -$coverBeamY $coverBeamZ -$coverBeamY -
$coreBeamZ -$coreBeamY -$coreBeamZ -$coreBeamY $coreBeamZ
        patch quadr 2 $nfCoverBeamZ 2 $coreBeamY $coreBeamZ $coreBeamY -
$coreBeamZ $coverBeamY -$coverBeamZ $coverBeamY $coverBeamZ
# define reinforcing layers
        # LayerStraight :      matTag      numBar      areaBar      yStart
zStart      yEnd      zEnd

```

```

layer straight 3 $numBarsTopBeam10420 $barAreaTop10420 $coreBeamY
$coreBeamZ $coreBeamY -$coreBeamZ;# top layer reinforcement
layer straight 3 $numBarsBotBeam10420 $barAreaBot10420 -$coreBeamY
$coreBeamZ -$coreBeamY -$coreBeamZ;# bottom layer reinforcement
};

# for beam 1042, j-end, 1042(1), 1 for j-end
set numBarsTopBeam10421 8;# number of longitudinal-reinforcement bars
on top layer
set numBarsBotBeam10421 8;# number of longitudinal-reinforcement bars
on bottom layer
set barAreaTopTotal10421 15.79E-4; # total top-longitudinal-
reinforcement bar area
set barAreaBotTotal10421 11.75E-4; # total bottom-longitudinal-
reinforcement bar area
set barAreaTop10421 [expr
$barAreaTopTotal10421/$numBarsTopBeam10421];# 1 longitudinal-
reinforcement bar area, for top of the section
set barAreaBot10421 [expr
$barAreaBotTotal10421/$numBarsBotBeam10421];# 1 longitudinal-
reinforcement bar area, for bottom of the section
# Define the fiber section, rectangular section with two layers of
steel on the top and bottom.
# element 1042(1), 1 for j-end
section fiberSec 10421 {
# Define the core patch
# PatchQuad: matTag NSIJ NSJK Iy Iz Jy Jz
Ky Kz Ly Lz
patch quadr 1 $nfCoreBeamZ $nfCoreBeamY -$coreBeamY
$coreBeamZ -$coreBeamY -$coreBeamZ $coreBeamY -$coreBeamZ $coreBeamY
$coreBeamZ
# Define the four cover patches
# PatchQuad: matTag NSIJ NSJK Iy Iz Jy Jz
Ky Kz Ly Lz
patch quadr 2 2 $nfCoverBeamY -$coverBeamY $coverBeamZ -$coreBeamY
$coreBeamZ $coreBeamY $coreBeamZ $coverBeamY $coverBeamZ
patch quadr 2 2 $nfCoverBeamY -$coreBeamY -$coreBeamZ -$coverBeamY -
$coverBeamZ $coverBeamY -$coverBeamZ $coreBeamY -$coreBeamZ

```

```

patch quadr 2 $nfCoverBeamZ 2 -$coverBeamY $coverBeamZ -$coverBeamY -
$coverBeamZ -$scoreBeamY -$scoreBeamZ -$scoreBeamY $scoreBeamZ
patch quadr 2 $nfCoverBeamZ 2 $scoreBeamY $scoreBeamZ $scoreBeamY -
$scoreBeamZ $coverBeamY -$coverBeamZ $coverBeamY $coverBeamZ
# define reinforcing layers
      # LayerStraight :      matTag      numBar      areaBar      yStart
zStart      yEnd      zEnd
layer straight 3 $numBarsTopBeam10421 $barAreaTop10421 $scoreBeamY
$scoreBeamZ $scoreBeamY -$scoreBeamZ;# top layer reinforcement
layer straight 3 $numBarsBotBeam10421 $barAreaBot10421 -$scoreBeamY
$scoreBeamZ -$scoreBeamY -$scoreBeamZ;# bottom layer reinforcement
};# end of fibersection definition
# 4th floor -----
# for beam 1051, i-end, 1051(0), 0 for i-end (same for the beam 1055)
set numBarsTopBeam10510 6;# number of longitudinal-reinforcement bars
on top layer
set numBarsBotBeam10510 6;# number of longitudinal-reinforcement bars
on bottom layer
set barAreaTopTotal10510 11.16E-4; # total top-longitudinal-
reinforcement bar area
set barAreaBotTotal10510 7.08E-4; # total bottom-longitudinal-
reinforcement bar area
      set barAreaTop10510 [expr
$barAreaTopTotal10510/$numBarsTopBeam10510];# 1 longitudinal-
reinforcement bar area, for top of the section
      set barAreaBot10510 [expr
$barAreaBotTotal10510/$numBarsBotBeam10510];# 1 longitudinal-
reinforcement bar area, for bottom of the section
# Define the fiber section, rectangular section with two layers of
steel on the top and bottom.
# element 1051(0), 0 for i-end
      section fiberSec 10510 {
# Define the core patch
# PatchQuad:  matTag  NSIJ      NSJK      Iy      Iz      Jy      Jz
Ky      Kz      Ly      Lz
      patch quadr 1 $nfCoreBeamZ $nfCoreBeamY -$scoreBeamY
$scoreBeamZ -$scoreBeamY -$scoreBeamZ $scoreBeamY -$scoreBeamZ $scoreBeamY
$scoreBeamZ

```

```

# Define the four cover patches
      # PatchQuad:  matTag NSIJ  NSJK      Iy      Iz      Jy      Jz
Ky      Kz      Ly      Lz
patch quadr 2 2 $nfCoverBeamY -$coverBeamY $coverBeamZ -$coreBeamY
$coreBeamZ $coreBeamY $coreBeamZ $coverBeamY $coverBeamZ
patch quadr 2 2 $nfCoverBeamY -$coreBeamY -$coreBeamZ -$coverBeamY -
$coreBeamZ $coverBeamY -$coverBeamZ $coreBeamY -$coreBeamZ
patch quadr 2 $nfCoverBeamZ 2 -$coverBeamY $coverBeamZ -$coverBeamY -
$coreBeamZ -$coreBeamY -$coreBeamZ -$coreBeamY $coreBeamZ
patch quadr 2 $nfCoverBeamZ 2 $coreBeamY $coreBeamZ $coreBeamY -
$coreBeamZ $coverBeamY -$coverBeamZ $coverBeamY $coverBeamZ
# define reinforcing layers
      # LayerStraight :      matTag      numBar      areaBar      yStart
zStart      yEnd      zEnd
layer straight 3 $numBarsTopBeam10510 $barAreaTop10510 $coreBeamY
$coreBeamZ $coreBeamY -$coreBeamZ;# top layer reinforcement
layer straight 3 $numBarsBotBeam10510 $barAreaBot10510 -$coreBeamY
$coreBeamZ -$coreBeamY -$coreBeamZ;# bottom layer reinforcement
};

      # for beam 1051, j-end, 1051(1), 1 for j-end
set numBarsTopBeam10511 6;# number of longitudinal-reinforcement bars
on top layer
set numBarsBotBeam10511 6;# number of longitudinal-reinforcement bars
on bottom layer
set barAreaTopTotal10511 9.81E-4; # total top-longitudinal-
reinforcement bar area
set barAreaBotTotal10511 6.72E-4; # total bottom-longitudinal-
reinforcement bar area
      set barAreaTop10511 [expr
$barAreaTopTotal10511/$numBarsTopBeam10511];# 1 longitudinal-
reinforcement bar area, for top of the section
      set barAreaBot10511 [expr
$barAreaBotTotal10511/$numBarsBotBeam10511];# 1 longitudinal-
reinforcement bar area, for bottom of the section
# Define the fiber section, rectangular section with two layers of
steel on the top and bottom.
# element 1051(1), 1 for j-end
      section fiberSec 10511 {

```

```

# Define the core patch
# PatchQuad:  matTag  NSIJ      NSJK      Iy      Iz      Jy      Jz
Ky      Kz      Ly      Lz
      patch quadr 1 $nfCoreBeamZ $nfCoreBeamY -$scoreBeamY
$scoreBeamZ -$scoreBeamY -$scoreBeamZ $scoreBeamY -$scoreBeamZ $scoreBeamY
$scoreBeamZ
# Define the four cover patches
      # PatchQuad:  matTag NSIJ  NSJK      Iy      Iz      Jy      Jz
Ky      Kz      Ly      Lz
patch quadr 2 2 $nfCoverBeamY -$coverBeamY $coverBeamZ -$scoreBeamY
$scoreBeamZ $scoreBeamY $scoreBeamZ $coverBeamY $coverBeamZ
patch quadr 2 2 $nfCoverBeamY -$scoreBeamY -$scoreBeamZ -$coverBeamY -
$coverBeamZ $coverBeamY -$coverBeamZ $scoreBeamY -$scoreBeamZ
patch quadr 2 $nfCoverBeamZ 2 -$coverBeamY $coverBeamZ -$coverBeamY -
$coverBeamZ -$scoreBeamY -$scoreBeamZ -$scoreBeamY $scoreBeamZ
patch quadr 2 $nfCoverBeamZ 2 $scoreBeamY $scoreBeamZ $scoreBeamY -
$scoreBeamZ $coverBeamY -$coverBeamZ $coverBeamY $coverBeamZ
# define reinforcing layers
      # LayerStraight :      matTag      numBar      areaBar      yStart
zStart      yEnd      zEnd
layer straight 3 $numBarsTopBeam10511 $barAreaTop10511      $scoreBeamY
$scoreBeamZ $scoreBeamY -$scoreBeamZ;# top layer reinforcement
layer straight 3 $numBarsBotBeam10511 $barAreaBot10511      -$scoreBeamY
$scoreBeamZ      -$scoreBeamY -$scoreBeamZ;# bottom layer reinforcement
};# end of fibersection definition
# -----
# for beam 1052, i-end, 1052(0), 0 for i-end (same for the beams 1053
and 1054)
set numBarsTopBeam10520 6;# number of longitudinal-reinforcement bars
on top layer
set numBarsBotBeam10520 6;# number of longitudinal-reinforcement bars
on bottom layer
set barAreaTopTotal10520 10.29E-4; # total top-longitudinal-
reinforcement bar area
set barAreaBotTotal10520 6.69E-4; # total bottom-longitudinal-
reinforcement bar area

```

```

        set barAreaTop10520 [expr
$barAreaTopTotal10520/$numBarsTopBeam10520];# 1 longitudinal-
reinforcement bar area, for top of the section

        set barAreaBot10520 [expr
$barAreaBotTotal10520/$numBarsBotBeam10520];# 1 longitudinal-
reinforcement bar area, for bottom of the section
# Define the fiber section, rectangular section with two layers of
steel on the top and bottom.
# element 1052(0), 0 for i-end
        section fiberSec 10520 {
# Define the core patch
# PatchQuad:  matTag  NSIJ      NSJK      Iy      Iz      Jy      Jz
Ky      Kz      Ly      Lz
                patch quadr 1 $nfCoreBeamZ $nfCoreBeamY -$coreBeamY
$coreBeamZ -$coreBeamY -$coreBeamZ $coreBeamY -$coreBeamZ $coreBeamY
$coreBeamZ
# Define the four cover patches
        # PatchQuad:  matTag NSIJ  NSJK      Iy      Iz      Jy      Jz
Ky      Kz      Ly      Lz
patch quadr 2 2 $nfCoverBeamY -$coverBeamY $coverBeamZ -$coreBeamY
$coreBeamZ $coreBeamY $coreBeamZ $coverBeamY $coverBeamZ
patch quadr 2 2 $nfCoverBeamY -$coreBeamY -$coreBeamZ -$coverBeamY -
$coreBeamZ $coverBeamY -$coverBeamZ $coreBeamY -$coreBeamZ
patch quadr 2 $nfCoverBeamZ 2 -$coverBeamY $coverBeamZ -$coverBeamY -
$coreBeamZ -$coreBeamY -$coreBeamZ -$coreBeamY $coreBeamZ
patch quadr 2 $nfCoverBeamZ 2 $coreBeamY $coreBeamZ $coreBeamY -
$coreBeamZ $coverBeamY -$coverBeamZ $coverBeamY $coverBeamZ
# define reinforcing layers
        # LayerStraight :  matTag  numBar  areaBar  yStart
zStart  yEnd  zEnd
layer straight 3 $numBarsTopBeam10520 $barAreaTop10520  $coreBeamY
$coreBeamZ $coreBeamY -$coreBeamZ;# top layer reinforcement
layer straight 3 $numBarsBotBeam10520 $barAreaBot10520  -$coreBeamY
$coreBeamZ -$coreBeamY -$coreBeamZ;# bottom layer reinforcement
};

        # for beam 1052, j-end, 1052(1), 1 for j-end
set numBarsTopBeam10521 6;# number of longitudinal-reinforcement bars
on top layer

```



```

set numBarsBotBeam10521 6;# number of longitudinal-reinforcement bars
on bottom layer
set barAreaTopTotal10521 10.37E-4; # total top-longitudinal-
reinforcement bar area
set barAreaBotTotal10521 6.57E-4; # total bottom-longitudinal-
reinforcement bar area
    set barAreaTop10521 [expr
$barAreaTopTotal10521/$numBarsTopBeam10521];# 1 longitudinal-
reinforcement bar area, for top of the section
    set barAreaBot10521 [expr
$barAreaBotTotal10521/$numBarsBotBeam10521];# 1 longitudinal-
reinforcement bar area, for bottom of the section
# Define the fiber section, rectangular section with two layers of
steel on the top and bottom.
# element 1052(1), 1 for j-end
    section fiberSec 10521 {
# Define the core patch
# PatchQuad:  matTag  NSIJ      NSJK      Iy      Iz      Jy      Jz
Ky      Kz      Ly      Lz
        patch quadr 1 $nfCoreBeamZ $nfCoreBeamY -$scoreBeamY
$scoreBeamZ -$scoreBeamY -$scoreBeamZ $scoreBeamY -$scoreBeamZ $scoreBeamY
$scoreBeamZ
# Define the four cover patches
        # PatchQuad:  matTag NSIJ  NSJK      Iy      Iz      Jy      Jz
Ky      Kz      Ly      Lz
        patch quadr 2 2 $nfCoverBeamY -$coverBeamY $coverBeamZ -$scoreBeamY
$scoreBeamZ $scoreBeamY $scoreBeamZ $coverBeamY $coverBeamZ
        patch quadr 2 2 $nfCoverBeamY -$scoreBeamY -$scoreBeamZ -$coverBeamY -
$coverBeamZ $coverBeamY -$coverBeamZ $scoreBeamY -$scoreBeamZ
        patch quadr 2 $nfCoverBeamZ 2 -$coverBeamY $coverBeamZ -$coverBeamY -
$coverBeamZ -$scoreBeamY -$scoreBeamZ -$scoreBeamY $scoreBeamZ
        patch quadr 2 $nfCoverBeamZ 2 $scoreBeamY $scoreBeamZ $scoreBeamY -
$scoreBeamZ $coverBeamY -$coverBeamZ $coverBeamY $coverBeamZ
# define reinforcing layers
        # LayerStraight :  matTag  numBar  areaBar  yStart
zStart  yEnd  zEnd
        layer straight 3 $numBarsTopBeam10521 $barAreaTop10521  $scoreBeamY
$scoreBeamZ $scoreBeamY -$scoreBeamZ;# top layer reinforcement

```

```

layer straight 3 $numBarsBotBeam10521 $barAreaBot10521 -$scoreBeamY
$scoreBeamZ -$scoreBeamY -$scoreBeamZ;# bottom layer reinforcement
};# end of fibersection definition
# 5th floor -----
# for beam 1061, i-end, 1061(0), 0 for i-end (same for the beam 1065)
set numBarsTopBeam10610 4;# number of longitudinal-reinforcement bars
on top layer
set numBarsBotBeam10610 3;# number of longitudinal-reinforcement bars
on bottom layer
set barAreaTopTotal10610 5.61E-4; # total top-longitudinal-
reinforcement bar area
set barAreaBotTotal10610 3.36E-4; # total bottom-longitudinal-
reinforcement bar area
      set barAreaTop10610 [expr
$barAreaTopTotal10610/$numBarsTopBeam10610];# 1 longitudinal-
reinforcement bar area, for top of the section
      set barAreaBot10610 [expr
$barAreaBotTotal10610/$numBarsBotBeam10610];# 1 longitudinal-
reinforcement bar area, for bottom of the section
# Define the fiber section, rectangular section with two layers of
steel on the top and bottom.
# element 1061(0), 0 for i-end
      section fiberSec 10610 {
# Define the core patch
# PatchQuad:  matTag  NSIJ      NSJK      Iy      Iz      Jy      Jz
Ky      Kz      Ly      Lz
      patch quadr 1 $nfCoreBeamZ $nfCoreBeamY -$scoreBeamY
$scoreBeamZ -$scoreBeamY -$scoreBeamZ $scoreBeamY -$scoreBeamZ $scoreBeamY
$scoreBeamZ
# Define the four cover patches
      # PatchQuad:  matTag NSIJ  NSJK      Iy      Iz      Jy      Jz
Ky      Kz      Ly      Lz
      patch quadr 2 2 $nfCoverBeamY -$coverBeamY $coverBeamZ -$scoreBeamY
$scoreBeamZ $scoreBeamY $scoreBeamZ $coverBeamY $coverBeamZ
      patch quadr 2 2 $nfCoverBeamY -$scoreBeamY -$scoreBeamZ -$coverBeamY -
$coverBeamZ $coverBeamY -$coverBeamZ $scoreBeamY -$scoreBeamZ
      patch quadr 2 $nfCoverBeamZ 2 -$coverBeamY $coverBeamZ -$coverBeamY -
$coverBeamZ -$scoreBeamY -$scoreBeamZ -$scoreBeamY $scoreBeamZ

```

```

patch quadr 2 $nfCoverBeamZ 2 $scoreBeamY $scoreBeamZ $scoreBeamY -
$scoreBeamZ $coverBeamY -$coverBeamZ $coverBeamY $coverBeamZ
# define reinforcing layers
      # LayerStraight :      matTag      numBar      areaBar      yStart
zStart      yEnd      zEnd
layer straight 3 $numBarsTopBeam10610 $barAreaTop10610 $scoreBeamY
$scoreBeamZ $scoreBeamY -$scoreBeamZ;# top layer reinforcement
layer straight 3 $numBarsBotBeam10610 $barAreaBot10610 -$scoreBeamY
$scoreBeamZ -$scoreBeamY -$scoreBeamZ;# bottom layer reinforcement
};

      # for beam 1061, j-end, 1061(1), 1 for j-end
set numBarsTopBeam10611 4;# number of longitudinal-reinforcement bars
on top layer
set numBarsBotBeam10611 3;# number of longitudinal-reinforcement bars
on bottom layer
set barAreaTopTotal10611 5.61E-4; # total top-longitudinal-
reinforcement bar area
set barAreaBotTotal10611 2.91E-4; # total bottom-longitudinal-
reinforcement bar area
      set barAreaTop10611 [expr
$barAreaTopTotal10611/$numBarsTopBeam10611];# 1 longitudinal-
reinforcement bar area, for top of the section
      set barAreaBot10611 [expr
$barAreaBotTotal10611/$numBarsBotBeam10611];# 1 longitudinal-
reinforcement bar area, for bottom of the section
# Define the fiber section, rectangular section with two layers of
steel on the top and bottom.
# element 1061(1), 1 for j-end
      section fiberSec 10611 {
# Define the core patch
# PatchQuad:  matTag  NSIJ      NSJK      Iy      Iz      Jy      Jz
Ky      Kz      Ly      Lz
      patch quadr 1 $nfCoreBeamZ $nfCoreBeamY -$scoreBeamY
$scoreBeamZ -$scoreBeamY -$scoreBeamZ $scoreBeamY -$scoreBeamZ $scoreBeamY
$scoreBeamZ
# Define the four cover patches
      # PatchQuad:  matTag NSIJ  NSJK      Iy      Iz      Jy      Jz
Ky      Kz      Ly      Lz

```

```

patch quadr 2 2 $nfCoverBeamY -$coverBeamY $coverBeamZ -$scoreBeamY
$scoreBeamZ $scoreBeamY $scoreBeamZ $coverBeamY $coverBeamZ
patch quadr 2 2 $nfCoverBeamY -$scoreBeamY -$scoreBeamZ -$coverBeamY -
$coverBeamZ $coverBeamY -$coverBeamZ $scoreBeamY -$scoreBeamZ
patch quadr 2 $nfCoverBeamZ 2 -$coverBeamY $coverBeamZ -$coverBeamY -
$coverBeamZ -$scoreBeamY -$scoreBeamZ -$scoreBeamY $scoreBeamZ
patch quadr 2 $nfCoverBeamZ 2 $scoreBeamY $scoreBeamZ $scoreBeamY -
$scoreBeamZ $coverBeamY -$coverBeamZ $coverBeamY $coverBeamZ
# define reinforcing layers
      # LayerStraight :      matTag      numBar      areaBar      yStart
zStart      yEnd      zEnd
layer straight 3 $numBarsTopBeam10611 $barAreaTop10611 $scoreBeamY
$scoreBeamZ $scoreBeamY -$scoreBeamZ;# top layer reinforcement
layer straight 3 $numBarsBotBeam10611 $barAreaBot10611 -$scoreBeamY
$scoreBeamZ -$scoreBeamY -$scoreBeamZ;# bottom layer reinforcement
};# end of fibersection definition
# -----
# for beam 1062, i-end, 1062(0), 0 for i-end (same for the beams 1063
and 1064)
set numBarsTopBeam10620 4;# number of longitudinal-reinforcement bars
on top layer
set numBarsBotBeam10620 3;# number of longitudinal-reinforcement bars
on bottom layer
set barAreaTopTotal10620 5.61E-4; # total top-longitudinal-
reinforcement bar area
set barAreaBotTotal10620 3.20E-4; # total bottom-longitudinal-
reinforcement bar area
      set barAreaTop10620 [expr
$barAreaTopTotal10620/$numBarsTopBeam10620];# 1 longitudinal-
reinforcement bar area, for top of the section
      set barAreaBot10620 [expr
$barAreaBotTotal10620/$numBarsBotBeam10620];# 1 longitudinal-
reinforcement bar area, for bottom of the section
# Define the fiber section, rectangular section with two layers of
steel on the top and bottom.
# element 1062(0), 0 for i-end
      section fiberSec 10620 {
# Define the core patch

```

```

# PatchQuad:  matTag  NSIJ      NSJK      Iy      Iz      Jy      Jz
Ky      Kz      Ly      Lz
      patch quadr 1 $nfCoreBeamZ $nfCoreBeamY -$scoreBeamY
$scoreBeamZ -$scoreBeamY -$scoreBeamZ $scoreBeamY -$scoreBeamZ $scoreBeamY
$scoreBeamZ
# Define the four cover patches
      # PatchQuad:  matTag NSIJ  NSJK      Iy      Iz      Jy      Jz
Ky      Kz      Ly      Lz
patch quadr 2 2 $nfCoverBeamY -$coverBeamY $coverBeamZ -$scoreBeamY
$scoreBeamZ $scoreBeamY $scoreBeamZ $coverBeamY $coverBeamZ
patch quadr 2 2 $nfCoverBeamY -$scoreBeamY -$scoreBeamZ -$coverBeamY -
$coverBeamZ $coverBeamY -$coverBeamZ $scoreBeamY -$scoreBeamZ
patch quadr 2 $nfCoverBeamZ 2 -$coverBeamY $coverBeamZ -$coverBeamY -
$coverBeamZ -$scoreBeamY -$scoreBeamZ -$scoreBeamY $scoreBeamZ
patch quadr 2 $nfCoverBeamZ 2 $scoreBeamY $scoreBeamZ $scoreBeamY -
$scoreBeamZ $coverBeamY -$coverBeamZ $coverBeamY $coverBeamZ
# define reinforcing layers
      # LayerStraight :  matTag      numBar      areaBar      yStart
zStart      yEnd      zEnd
layer straight 3 $numBarsTopBeam10620 $barAreaTop10620 $scoreBeamY
$scoreBeamZ $scoreBeamY -$scoreBeamZ;# top layer reinforcement
layer straight 3 $numBarsBotBeam10620 $barAreaBot10620 -$scoreBeamY
$scoreBeamZ -$scoreBeamY -$scoreBeamZ;# bottom layer reinforcement
};

      # for beam 1062, j-end, 1062(1), 1 for j-end
set numBarsTopBeam10621 4;# number of longitudinal-reinforcement bars
on top layer
set numBarsBotBeam10621 3;# number of longitudinal-reinforcement bars
on bottom layer
set barAreaTopTotal10621 5.61E-4; # total top-longitudinal-
reinforcement bar area
set barAreaBotTotal10621 3.23E-4; # total bottom-longitudinal-
reinforcement bar area
      set barAreaTop10621 [expr
$barAreaTopTotal10621/$numBarsTopBeam10621];# 1 longitudinal-
reinforcement bar area, for top of the section

```

```

        set barAreaBot10621 [expr
$barAreaBotTotal10621/$numBarsBotBeam10621];# 1 longitudinal-
reinforcement bar area, for bottom of the section
# Define the fiber section, rectangular section with two layers of
steel on the top and bottom.
# element 1062(1), 1 for j-end
        section fiberSec 10621 {
# Define the core patch
# PatchQuad:  matTag  NSIJ      NSJK      Iy      Iz      Jy      Jz
Ky      Kz      Ly      Lz
                patch quadr 1 $nfCoreBeamZ $nfCoreBeamY -$scoreBeamY
$scoreBeamZ -$scoreBeamY -$scoreBeamZ $scoreBeamY -$scoreBeamZ $scoreBeamY
$scoreBeamZ
# Define the four cover patches
        # PatchQuad:  matTag NSIJ  NSJK      Iy      Iz      Jy      Jz
Ky      Kz      Ly      Lz
patch quadr 2 2 $nfCoverBeamY -$coverBeamY $coverBeamZ -$scoreBeamY
$scoreBeamZ $scoreBeamY $scoreBeamZ $coverBeamY $coverBeamZ
patch quadr 2 2 $nfCoverBeamY -$scoreBeamY -$scoreBeamZ -$coverBeamY -
$coverBeamZ $coverBeamY -$coverBeamZ $scoreBeamY -$scoreBeamZ
patch quadr 2 $nfCoverBeamZ 2 -$coverBeamY $coverBeamZ -$coverBeamY -
$coverBeamZ -$scoreBeamY -$scoreBeamZ -$scoreBeamY $scoreBeamZ
patch quadr 2 $nfCoverBeamZ 2 $scoreBeamY $scoreBeamZ $scoreBeamY -
$scoreBeamZ $coverBeamY -$coverBeamZ $coverBeamY $coverBeamZ
# define reinforcing layers
        # LayerStraight :  matTag      numBar      areaBar      yStart
zStart      yEnd      zEnd
layer straight 3 $numBarsTopBeam10621 $barAreaTop10621 $scoreBeamY
$scoreBeamZ $scoreBeamY -$scoreBeamZ;# top layer reinforcement
layer straight 3 $numBarsBotBeam10621 $barAreaBot10621 -$scoreBeamY
$scoreBeamZ -$scoreBeamY -$scoreBeamZ;# bottom layer reinforcement
};# end of fibersection definition
# -----
# define ELEMENTS
# set up geometric transformations of element
# separate columns and beams, in case of P-Delta analysis for columns
set IDColTransf 1; # all columns
set IDBeamTransf 2; # all beams

```

```

geomTransf Linear $IDColTransf; # -jntOffset 0 0 0 -$HBeam; #only
columns can have PDelta effects (gravity effects)
geomTransf Linear $IDBeamTransf; # -jntOffset [expr $HCol/2] 0 [expr
-$HCol/2] 0 ;
# Define Beam-Column Elements
set np 5;# number of Gauss integration points for nonlinear curvature
distribution-- np=2 for linear distribution ok
# columns
set N0col 100;# column element numbers
set level 1; # 1st story
for {set pier 1} {$pier <= 6} {incr pier 5} {
set elemID [expr $N0col + $level*10 + $pier]
set nodeI [expr $level*10 + $pier]
set nodeJ [expr ($level+1)*10 + $pier]
element nonlinearBeamColumn $elemID $nodeI $nodeJ $np 111
$IDColTransf -iter 1000 1.0E-2;# columns 111 and 116
}
for {set pier 2} {$pier <= 5} {incr pier 3} {
set elemID [expr $N0col + $level*10 + $pier]
set nodeI [expr $level*10 + $pier]
set nodeJ [expr ($level+1)*10 + $pier]
element nonlinearBeamColumn $elemID $nodeI $nodeJ $np 112
$IDColTransf -iter 1000 1.0E-2; # columns 112 and 115
}
for {set pier 3} {$pier <= 4} {incr pier 1} {
set elemID [expr $N0col + $level*10 + $pier]
set nodeI [expr $level*10 + $pier]
set nodeJ [expr ($level+1)*10 + $pier]
element nonlinearBeamColumn $elemID $nodeI $nodeJ $np 113
$IDColTransf -iter 1000 1.0E-2;# columns 113 and 114
}
set level 2; # 2nd story
for {set pier 1} {$pier <= 6} {incr pier 5} {
set elemID [expr $N0col + $level*10 + $pier]
set nodeI [expr $level*10 + $pier]
set nodeJ [expr ($level+1)*10 + $pier]
element nonlinearBeamColumn $elemID $nodeI $nodeJ $np 121
$IDColTransf -iter 1000 1.0E-2;# columns 121 and 126

```

```

}
for {set pier 2} {$pier <= 5} {incr pier 3} {
set elemID [expr $N0col + $level*10 + $pier]
set nodeI [expr $level*10 + $pier]
set nodeJ [expr ($level+1)*10 + $pier]
element nonlinearBeamColumn $elemID $nodeI $nodeJ $np 122
$IDColTransf -iter 1000 1.0E-2;# columns 122 and 125
}
for {set pier 3} {$pier <= 4} {incr pier 1} {
set elemID [expr $N0col + $level*10 + $pier]
set nodeI [expr $level*10 + $pier]
set nodeJ [expr ($level+1)*10 + $pier]
element nonlinearBeamColumn $elemID $nodeI $nodeJ $np 123
$IDColTransf -iter 1000 1.0E-2;# columns 123 and 124
}
set level 3; # 3rd story
for {set pier 1} {$pier <= 6} {incr pier 5} {
set elemID [expr $N0col + $level*10 + $pier]
set nodeI [expr $level*10 + $pier]
set nodeJ [expr ($level+1)*10 + $pier]
element nonlinearBeamColumn $elemID $nodeI $nodeJ $np 131
$IDColTransf -iter 1000 1.0E-2;# columns 131 and 136
}
for {set pier 2} {$pier <= 5} {incr pier 3} {
set elemID [expr $N0col + $level*10 + $pier]
set nodeI [expr $level*10 + $pier]
set nodeJ [expr ($level+1)*10 + $pier]
element nonlinearBeamColumn $elemID $nodeI $nodeJ $np 132
$IDColTransf -iter 1000 1.0E-2;# columns 132 and 135
}
for {set pier 3} {$pier <= 4} {incr pier 1} {
set elemID [expr $N0col + $level*10 + $pier]
set nodeI [expr $level*10 + $pier]
set nodeJ [expr ($level+1)*10 + $pier]
element nonlinearBeamColumn $elemID $nodeI $nodeJ $np 133
$IDColTransf -iter 1000 1.0E-2;# columns 133 and 134
}
set level 4; # 4th story

```



```

for {set pier 1} {$pier <= 6} {incr pier 5} {
set elemID [expr $N0col + $level*10 + $pier]
set nodeI [expr $level*10 + $pier]
set nodeJ [expr ($level+1)*10 + $pier]
element nonlinearBeamColumn $elemID $nodeI $nodeJ $np 141
$IDColTransf -iter 1000 1.0E-2;# columns 141 and 146
}
for {set pier 2} {$pier <= 5} {incr pier 3} {
set elemID [expr $N0col + $level*10 + $pier]
set nodeI [expr $level*10 + $pier]
set nodeJ [expr ($level+1)*10 + $pier]
element nonlinearBeamColumn $elemID $nodeI $nodeJ $np 142
$IDColTransf -iter 1000 1.0E-2;# columns 142 and 145
}
for {set pier 3} {$pier <= 4} {incr pier 1} {
set elemID [expr $N0col + $level*10 + $pier]
set nodeI [expr $level*10 + $pier]
set nodeJ [expr ($level+1)*10 + $pier]
element nonlinearBeamColumn $elemID $nodeI $nodeJ $np 143
$IDColTransf -iter 1000 1.0E-2;# columns 143 and 144
}
set level 5; # 5th story
for {set pier 1} {$pier <= [expr $NBay+1]} {incr pier 1} {
set elemID [expr $N0col + $level*10 + $pier]
set nodeI [expr $level*10 + $pier]
set nodeJ [expr ($level+1)*10 + $pier]
element nonlinearBeamColumn $elemID $nodeI $nodeJ $np 141
$IDColTransf -iter 1000 1.0E-2;# columns, 5th story
}
# beams
set N0beam 1000;# beam element numbers
# 1st floor
element beamWithHinges 1021 21 22 10210 [expr $HBeam/2] 10211 [expr
$HBeam/2] $Ec $AgBeam $IzBeam $IDBeamTransf -iter 1000 1.0E-2;
element beamWithHinges 1022 22 23 10220 [expr $HBeam/2] 10221 [expr
$HBeam/2] $Ec $AgBeam $IzBeam $IDBeamTransf -iter 1000 1.0E-2;
element beamWithHinges 1023 23 24 10220 [expr $HBeam/2] 10221 [expr
$HBeam/2] $Ec $AgBeam $IzBeam $IDBeamTransf -iter 1000 1.0E-2;

```

```

element beamWithHinges 1024 24 25 10221 [expr $HBeam/2] 10220 [expr
$HBeam/2] $Ec $AgBeam $IzBeam $IDBeamTransf -iter 1000 1.0E-2;
element beamWithHinges 1025 25 26 10211 [expr $HBeam/2] 10210 [expr
$HBeam/2] $Ec $AgBeam $IzBeam $IDBeamTransf -iter 1000 1.0E-2;
# 2nd floor
element beamWithHinges 1031 31 32 10310 [expr $HBeam/2] 10311 [expr
$HBeam/2] $Ec $AgBeam $IzBeam $IDBeamTransf -iter 1000 1.0E-2;
element beamWithHinges 1032 32 33 10320 [expr $HBeam/2] 10321 [expr
$HBeam/2] $Ec $AgBeam $IzBeam $IDBeamTransf -iter 1000 1.0E-2;
element beamWithHinges 1033 33 34 10320 [expr $HBeam/2] 10321 [expr
$HBeam/2] $Ec $AgBeam $IzBeam $IDBeamTransf -iter 1000 1.0E-2;
element beamWithHinges 1034 34 35 10321 [expr $HBeam/2] 10320 [expr
$HBeam/2] $Ec $AgBeam $IzBeam $IDBeamTransf -iter 1000 1.0E-2;
element beamWithHinges 1035 35 36 10311 [expr $HBeam/2] 10310 [expr
$HBeam/2] $Ec $AgBeam $IzBeam $IDBeamTransf -iter 1000 1.0E-2;
#
# 3rd floor
element beamWithHinges 1041 41 42 10410 [expr $HBeam/2] 10411 [expr
$HBeam/2] $Ec $AgBeam $IzBeam $IDBeamTransf -iter 1000 1.0E-2;
element beamWithHinges 1042 42 43 10420 [expr $HBeam/2] 10421 [expr
$HBeam/2] $Ec $AgBeam $IzBeam $IDBeamTransf -iter 1000 1.0E-2;
element beamWithHinges 1043 43 44 10420 [expr $HBeam/2] 10421 [expr
$HBeam/2] $Ec $AgBeam $IzBeam $IDBeamTransf -iter 1000 1.0E-2;
element beamWithHinges 1044 44 45 10421 [expr $HBeam/2] 10420 [expr
$HBeam/2] $Ec $AgBeam $IzBeam $IDBeamTransf -iter 1000 1.0E-2;
element beamWithHinges 1045 45 46 10411 [expr $HBeam/2] 10410 [expr
$HBeam/2] $Ec $AgBeam $IzBeam $IDBeamTransf -iter 1000 1.0E-2;
#
# 4th floor
element beamWithHinges 1051 51 52 10510 [expr $HBeam/2] 10511 [expr
$HBeam/2] $Ec $AgBeam $IzBeam $IDBeamTransf -iter 1000 1.0E-2;
element beamWithHinges 1052 52 53 10520 [expr $HBeam/2] 10521 [expr
$HBeam/2] $Ec $AgBeam $IzBeam $IDBeamTransf -iter 1000 1.0E-2;
element beamWithHinges 1053 53 54 10520 [expr $HBeam/2] 10521 [expr
$HBeam/2] $Ec $AgBeam $IzBeam $IDBeamTransf -iter 1000 1.0E-2;
element beamWithHinges 1054 54 55 10521 [expr $HBeam/2] 10520 [expr
$HBeam/2] $Ec $AgBeam $IzBeam $IDBeamTransf -iter 1000 1.0E-2;

```

```

element beamWithHinges 1055 55 56 10511 [expr $HBeam/2] 10510 [expr
$HBeam/2] $Ec $AgBeam $IzBeam $IDBeamTransf -iter 1000 1.0E-2;
#
# 5th floor
element beamWithHinges 1061 61 62 10610 [expr $HBeam/2] 10611 [expr
$HBeam/2] $Ec $AgBeam $IzBeam $IDBeamTransf -iter 1000 1.0E-2;
element beamWithHinges 1062 62 63 10620 [expr $HBeam/2] 10621 [expr
$HBeam/2] $Ec $AgBeam $IzBeam $IDBeamTransf -iter 1000 1.0E-2;
element beamWithHinges 1063 63 64 10620 [expr $HBeam/2] 10621 [expr
$HBeam/2] $Ec $AgBeam $IzBeam $IDBeamTransf -iter 1000 1.0E-2;
element beamWithHinges 1064 64 65 10621 [expr $HBeam/2] 10620 [expr
$HBeam/2] $Ec $AgBeam $IzBeam $IDBeamTransf -iter 1000 1.0E-2;
element beamWithHinges 1065 65 66 10611 [expr $HBeam/2] 10610 [expr
$HBeam/2] $Ec $AgBeam $IzBeam $IDBeamTransf -iter 1000 1.0E-2;
# -----
source Recorders.tcl
# -----
# Recorders.tcl
# Define RECORDERS -----
recorder Drift -file Drift.out -time -iNode 11 21 31 41 51 -jNode 21
31 41 51 61 -dof 1 -perpDirn 2;# lateral drift
recorder Node -file FloorDisp.out -time -node 21 31 41 51 61 -dof 1
disp; # displacements of free node
recorder Node -file FloorAcc.out -time -node 21 31 41 51 61 -dof 1
accel; # accelerations of free node
recorder Node -file FloorVel.out -time -node 21 31 41 51 61 -dof 1
vel; # velocities of free node
recorder Node -file BaseReact.out -time -node 11 12 13 14 15 16 -dof
1 reaction; # base node reactions
#
recorder Element -file SideColumns_PlasticRot.out -time -ele 111 121
131 141 151 plasticRotation
recorder Element -file MidColumns_PlasticRot.out -time -ele 113 123
133 143 153 plasticRotation
recorder Element -file SideBeams_PlasticRot.out -time -ele 1021 1031
1041 1051 1061 plasticRotation
recorder Element -file MidBeams_PlasticRot.out -time -ele 1023 1033
1043 1053 1063 plasticRotation

```

```

#
recorder Element -file SideColumns_LocalForce.out -time -ele 111 121
131 141 151 localForce; # element forces in local coordinates
recorder Element -file MidColumns_LocalForce.out -time -ele 113 123
133 143 153 localForce; # element forces in local coordinates
#recorder Element -file SideColumns_GlobalForce.out -time -ele 111
121 131 141 151 globalForce; # element forces in local coordinates
recorder Element -file SideBeams_LocalForce.out -time -ele 1021 1031
1041 1051 1061 localForce; # element forces in local coordinates
#recorder Element -file SideBeams_GlobalForce.out -time -ele 1021
1031 1041 1051 1061 globalForce; # element forces in local
coordinates
recorder Element -file MidBeams_LocalForce.out -time -ele 1023 1033
1043 1053 1063 localForce; # element forces in local coordinates
# End of recorder generation
# -----
# GRAVITY LOADS
# define gravity load applied to beams and columns -- eleLoad applies
loads in local coordinate axis
# uniform span loads on the beams
# G=14.60kN/m, Q=4.82kN/m, G+0.3Q=16.05kN/m, for normal stories
# G=10.75kN/m, Q=5.02kN/m, G+0.3Q=12.26kN/m, for top story
# point loads on top of the columns from tribuatriy areas
# G=36.5kN, Q=6.5kN, G+0.3Q=38.45kN, for corner columns, normal
stories
# G=51kN, Q=12.05kN, G+0.3Q=54.62kN, for interior columns, normal
stories
# G=26.87kN, Q=7.02kN, G+0.3Q=28.98kN, for corner columns, top story
# G=41.37kN, Q=12.54kN, G+0.3Q=45.13kN, for interior columns,top
story
#
set QdlCol [expr 25*$BCol*$HCol]; # self-weight of Column, weight per
length (25kN/m3 concrete density)
pattern Plain 101 Linear {
    for {set level 1} {$level <= $NStory} {incr level 1} {
for {set pier 1} {$pier <= [expr $NBay+1]} {incr pier 1} {
set elemID [expr $N0col + $level*10 + $pier]

```

```

eleLoad -ele $elemID -type -beamUniform 0 -$QdlCol; # Columns self-
weight uniformly distributed along the length of the column
}
}

    for {set level 2} {$level <=[expr $NStory]} {incr level 1} {
for {set pier 1} {$pier <= [expr $NBay+1]} {incr pier 5} {
    set nodeID [expr $level*10+$pier]
    load $nodeID 0. -38.45 0.;# Corner Columns, normal stories
}

    }

    set level [expr $NStory+1]
for {set pier 1} {$pier <= [expr $NBay+1]} {incr pier 5} {
    set nodeID [expr $level*10+$pier]
    load $nodeID 0. -28.98 0.;# Corner Columns, top story
}

    for {set level 2} {$level <=[expr $NStory]} {incr level 1} {
for {set pier 2} {$pier <= [expr $NBay]} {incr pier 1} {
    set nodeID [expr $level*10+$pier]
    load $nodeID 0. -54.62 0.;# Interior Columns, normal stories
}

    }

    set level [expr $NStory+1]
for {set pier 2} {$pier <= [expr $NBay]} {incr pier 1} {
    set nodeID [expr $level*10+$pier]
    load $nodeID 0. -45.13 0.;# Interior Columns, top story
}

    for {set level 2} {$level <=[expr $NStory]} {incr level 1} {
for {set bay 1} {$bay <= $NBay} {incr bay 1} {
set elemID [expr $N0beam + $level*10 +$bay]
eleLoad -ele $elemID -type -beamUniform -16.05; # BEAMS, normal
stories
}
}

    set level [expr $NStory+1]
for {set bay 1} {$bay <= $NBay} {incr bay 1} {
set elemID [expr $N0beam + $level*10 +$bay]
eleLoad -ele $elemID -type -beamUniform -12.26; # BEAMS, top story
}

```

```

}
# Gravity-analysis parameters - load-controlled static analysis
set Tol 1.0E-7;# convergence tolerance for test
variable constraintsTypeGravity Plain;# default;
constraints $constraintsTypeGravity ;      # how it handles boundary
conditions
numberer RCM;# renumber dof's to minimize band-width (optimization),
if you want to
system BandGeneral ;# how to store and solve the system of equations
in the analysis (large model: try UmfPack)
test NormDispIncr $Tol 7 ; # determine if convergence has been
achieved at the end of an iteration step
algorithm Newton;# use Newton's solution algorithm: updates tangent
stiffness at every iteration
set NstepGravity 10; # apply gravity in 10 steps
set DGravity [expr 1./$NstepGravity]; # first load increment;
integrator LoadControl $DGravity;# determine the next time step for
an analysis
analysis Static;# define type of analysis static or transient
analyze $NstepGravity;# apply gravity
# -----
loadConst -time 0.0; # maintain constant gravity loads and reset time
to zero

source DynamicAnalysis.tcl
# -----
# DynamicAnalysis.tcl
# calculating the fundamental vibration PERIOD
set nEigenI 1;# mode 1
set nEigenJ 3;# mode 3
set lambdaN [eigen [expr $nEigenJ]];# eigenvalue analysis for nEigenJ
modes
set lambdaI [lindex $lambdaN [expr $nEigenI-1]]; # eigenvalue mode i
set lambdaJ [lindex $lambdaN [expr $nEigenJ-1]]; # eigenvalue mode j
set omegaI [expr pow($lambdaI,0.5)];
set omegaJ [expr pow($lambdaJ,0.5)];
puts "Eigenvalues for 3 modes: $lambdaN"
set T1 [expr 2*$PI/$omegaI]; # period (sec.)

```

```

puts "1st Mode Period of the Building: $T1"
set period [open period.txt w]
puts $period "$T1";
# -----
# define & apply DAMPING
# RAYLEIGH damping parameters, Where to put M/K-prop damping
#  $D = \alpha_M M + \beta_K K_{curr} + \beta_K K_{init} + \beta_K K_{comm}$ 
set xDamp 0.05;# damping ratio
set MpropSwitch 1.0;
set KcurrSwitch 0.0;
set KinitSwitch 0.0;
set KcommSwitch 1.0;
set alphaM [expr
$MpropSwitch*$xDamp*(2*$omegaI*$omegaJ)/($omegaI+$omegaJ)];# M-prop.
damping; D = alphaM*M
set betaKcurr [expr $KcurrSwitch*2.*$xDamp/($omegaI+$omegaJ)];
# current-K;      +betaKcurr*KCurrent
set betaKinit [expr $KinitSwitch*2.*$xDamp/($omegaI+$omegaJ)];
# initial-K;      +betaKinit*Kinit
set betaKcomm [expr $KcommSwitch*2.*$xDamp/($omegaI+$omegaJ)]; #
last-committed K;  +betaKcomm*KlastCommitt
rayleigh $alphaM $betaKcurr $betaKinit $betaKcomm; # RAYLEIGH damping
# -----
# Define earthquake excitation
# -----
# set up ground-motion-analysis parameters
set dt 0.005; # time increment in ground motion file
set DtAnalysis $dt;# time-step Dt for time-history analysis
set TmaxAnalysis 25;          # maximum duration of ground-motion
analysis
# set up analysis parameters
# CONSTRAINTS handler
constraints Transformation
# DOF NUMBERER
numberer RCM
# SYSTEM- Create the system of equation storage and solver

```

```

variable systemTypeDynamic BandGeneral;# try UmfPack for large
problems
system $systemTypeDynamic
# TEST-convergence test
test EnergyIncr 1.e-6 1000 0;
# Solution ALGORITHM- Iterate from the last time step to the current
algorithm Newton;
# Transient INTEGRATOR- determine the next time step for an analysis
including inertial effects
variable NewmarkGamma 0.5;# Newmark-integrator gamma parameter (also
HHT)
variable NewmarkBeta 0.25;# Newmark-integrator beta parameter
variable integratorTypeDynamic Newmark;
integrator $integratorTypeDynamic $NewmarkGamma $NewmarkBeta
# ANALYSIS- defines what type of analysis is to be performed
analysis Transient;
# ----- perform Dynamic Ground-Motion
Analysis
# the following commands are unique to the Uniform Earthquake
excitation
set IDloadTag 400;# for uniformSupport excitation
# Uniform EXCITATION: acceleration input
set AccelSeries "Series -dt $dt -filePath ACC.DAT -factor [expr
$Gravity]";# time series information
pattern UniformExcitation $IDloadTag 1 -accel $AccelSeries ;#
create Uniform excitation
set Nsteps [expr int($TmaxAnalysis/$DtAnalysis)]; # total time steps
8000
analyze $Nsteps $DtAnalysis;# actually perform analysis
puts "Ground Motion Done. End Time: [getTime]"

set AnalysisTime [open AnalysisTime.txt w]
puts $AnalysisTime "[getTime]";

```